2011

Risk Assessment of Human-induced Accelerated Soil Erosion Processes in the Intermountain Watersheds of Central Italy.

A Case Study of the Upper Turano Watershed (Latium-Abruzzi)

Pasquale Borrelli

Freie Universität Berlin

Berlin
7/13/2011

Department of Earth Sciences
Institute for Geographic Sciences
Physical Geography

Dissertation to obtain Degree
Dr. rer. nat.

Risk Assessment of Human-induced Accelerated Soil Erosion Processes in the Intermountain Watersheds of Central Italy.

A Case Study of the Upper Turano Watershed (Latium-Abruzzi).

Pasquale Borrelli

Supervisors:

Univ. Prof. Dr. Brigitta Schütt - Freie Universität Berlin
Univ. Prof. Dr. Karl Tilman Rost - Freie Universität Berlin

Date of defence: 13.07.2011

Acknowledgements

The successful completion of this thesis became possible only because of the unrestricted accessibility, meaningful and result-driven guidance and always encouraging nature of my principal supervisor Prof. Dr. Brigitta Schütt. Therefore, I would like to express my sincere gratitude to Prof. Dr. Brigitta Schütt for making it possible for me to gain this academical experience and for her excellent supervision. My sincere gratitude also addresses my co-supervisor, Prof. Dr. Karl Tilman Rost for his valuable guidance and support. Particularly, I would like to acknowledge Dr. Philipp Holzmann who offered an invaluable human and technical support during my stay at the Freie Universität Berlin. Furthermore, I would like to thank the academic and general staff members of the Freie Universität Berlin for their technical and administrative support.

I am also grateful that various institutions and people provided material and shared their valuable data and experiences with me thereby contributing to the completion of this dissertation.

Pasquale Borrelli
Berlin

'Water knawels at the mountains and fills the valleys.
If it could it would reduce the earth to a perfect sphere'
(Leonardo Da Vinci)

Table of Contents

List of figures ..... **x**
List of tables ..... **xv**
List of appendices ..... **xviii**
List of symbols ..... **xix**
List of abbreviations and acronyms ..... **xx**
Abstract ..... **xxi**
Zusammenfassung ..... **xxiii**

1. **Introduction** **2**
1.1. Overall aim 3
1.2. Objectives 3
1.3. Main research questions 4

2. State of the art **6**
2.1. Soil erosion by water 6
2.2. Academic approaches to the problem 7
2.3. The physical process 10
2.4. Factors influencing soil erosion 12
2.5. Is soil erosion a new threat for our landscapes? 13
2.6. Present scenario on soil erosion studies, an 'exclusive' problem of the agricultural areas 15
2.7. Soil erosion in forested mountain watersheds 18
2.7.1. Causes of soil erosion in forested mountain watersheds 19
2.7.2. Effects of soil erosion in forested mountain watersheds 21

3. Study area **26**
3.1. Localization of study area 26
3.2. Geology 27
3.2.1. Geological-structural setting of the turano watershed in the apennine context 27
3.2.2. Lithologic distribution and characteristics 31
3.2.3. Hydrogeological patterns 35
3.3. Morphometry and Geomorphology 36
3.4. Land use 45
3.4.1. Settlement dynamics and socio-economic characters 45
3.4.2. Land cover units 47
3.4.3. Distribution of natural vegetation 50
3.5. Soils 51

4. Analysis of the climatic conditions of the Turano watershed 56
4.1. Climate dynamics at large- and meso-scale 56
4.2. Climate dynamics at watershed scale 57
4.2.1. Temperature 57
4.2.2. Rainfall 61
4.2.3. Snowfall 67
4.2.4. Bioclimates and soil moisture regimes 68

5. Spatially distributed modeling of soil erosion at watershed scale 72
5.1. METHODOLOGY 72
5.1.1. Revised Universal Soil Loss Equation Model 72
5.1.2. Unit Stream Power Erosion Deposition Model 84
5.1.3. Validation of the models 86
5.2. RESULTS 91
5.2.1. Rusle model 91
5.2.2. Usped model 104
5.2.3. model intercomparison 113
5.2.4. validation of the models 114
5.3. DISCUSSIONS 119
5.3.1. Results of the Turano watershed case study in the panorama of soil erosion modeling based on rusle in italy 120
5.3.2. Factors conditioning soil erosion modeling in the Turano watershed 123
5.3.3. Soil erosion rates in croplands and environmental risk 124
5.3.4. Validation of model results 125

6. Sediment yield prediction for the Turano watershed 130
6.1. METHODOLOGY 130
6.1.1. Model description 130
6.1.2. Extrapolation of Turano drainage network and sub-watershed 131
6.1.3. Statistical analysis 131
6.2. RESULTS 132
6.2.1. Turano drainage network classification and sub-watershed division 132
6.2.2. Tu index 133
6.2.3. Statistical analysis 134
6.3. DISCUSSIONS 135

7. Measurement of soil erosion at hillslope-scale: field monitoring 142
7.1. STUDY SITES DESCRIPTION 142
7.2. METHODOLOGY 144

7.2.1. Fieldwork activities 144
7.2.2. Laboratory soil samples analysis 150
7.2.3. Gis operations 151
7.3. RESULTS 152
7.3.1. Geomorphological survey 152
7.3.2. Physical-chemical characteristics of the soil 158
7.3.3. GIS processing of the analytic data 162
7.3.4. Measurements in plot of water and sediment yields 164
7.3.5. Hydraulic conductivity and the factors influencing its variability in the ex-01 watershed 166
7.3.6. Soil erosion response 168
7.3.7. Soil erosion modeling 173
7.4. DISCUSSIONS 177
7.4.1. Erosion susceptibility of the experimental site 177
7.4.2. Hillslope morphoevolution 180
7.4.3. Comparing multiple methods 182

8. Past and present dynamics of human-induced soil erosion in a sensitive area of the Turano watershed 186
8.1. STUDY SITE 186
8.2. METHODOLOGY 188
8.2.1. Geomorphological and morphometrical analyses 188
8.3. RESULTS 190
8.3.1. Landform and present-day morphodynamics in the FDS watershed 190
8.3.2. Sedimentological results 194
8.4. DISCUSSIONS 205
8.4.1. present day uplands erosional processes 205
8.4.2. FDR watershed evolution 205

9. Summary and conclusions 216
9.1. SUMMARY 216
9.2. CONCLUSIONS 219
9.3. FUTURE RESEARCH 221

10. References 223

11. Appendices 258

12. Erklärung 278

List of figures

Fig. 2.1: Fundamental factor categories influencing the process of soil degradation by erosion. 6

Fig. 2.2: Factors controlling hydric soil erosion based on Symeonakis (2001) with modification of the author. 13

Fig. 3.1: Tiber drainage basin and study site in the Latium-Abruzzi border, Italy. 26

Fig. 3.2: Turano watershed. 27

Fig. 3.3: Turano watershed geological map derived from the geological map of Central Apennine according to Cavinato and De Celles, 1999. The insert shows the location of the map of the Central Apennine and the location of the Apennine subduction front. 28

Fig. 3.4: Map of the main Quaternary faults in the Apennine area around the Turano watershed (a) according to Galadini and Messina (2004). In maps 'b' and 'c' the 3D location of the Turano fault and its position in the cross-profile is shown. 30

Fig. 3.5: Detailed lithological map of the Turano watershed. 31

Fig. 3.6: Landscape characteristics in the Pelagic and transitional lithological sector (June, 2009). 32

Fig. 3.7: Landscape characteristics in the carbonat and synorogenic turbiditic sequences of the carbonate-platform domain (April, 2009). 33

Fig. 3.8: Quaternary deposits (April and June, 2009). 34

Fig. 3.9: Hydrogeological patterns of the Turano watershed. 35

Fig. 3.10: Ipsographic curve of the Turano watershed. 37

Fig. 3.11: Hypsometric curves of the Turano watershed (CalHypso – Pérez, 2009). 37

Fig. 3.12: Digital elevation model of the Turano watershed. 38

Fig. 3.13: Distribution of altitude classes of the Turano watershed. 38

Fig. 3.14: Slope gradient map of the Turano watershed. 39

Fig. 3.15: Distribution of slope gradient classes of the Turano watershed. 39

Fig. 3.16: Frequency distribution of mean slope angle (b) with respect to aspect (a). 40

Fig. 3.17: Distribution of slope aspect classes of the Turano watershed. 41

Fig. 3.18: Longitudinal profile of the Fosso Fioio and Turano River. 43

Fig. 3.19: Azimuthal distribution of the ordered streams (Strahler, 1957) 43

Fig. 3.20: Land use map made by visual interpretation of orthophotos (2001 and 2005). 48
Fig. 3.21: Forest-harvesting activities from 1997 to 2005 in the Turano watershed. 49
Fig. 3.22: Forest hervasted near Carsoli (December, 2009). 50
Fig. 3.23: Classification of the vegetation in the Turano watershed. 51
Fig. 3.24: Soils texture classes of the Turano watershed. 52
Fig. 4.1: Italian pluviometric regime types. 57
Fig. 4.2: Location of the thermometric stations in the research area. 58
Fig. 4.3: Annual temperature range of the region 59
Fig. 4.4: Monthly and seasonal thermometric characteristic for the stations of Subiaco, Posticciola and Carsoli. 60
Fig. 4.5: Monthly temperature range. 60
Fig. 4.6: Location of the pluviometric/pluviographic stations. 62
Fig. 4.7: Monthly average precipitation versus elevation. 63
Fig. 4.8: Computed annual (a) and seasonal precipitation (b,c,d and e). 64
Fig. 4.9: Mean monthly precipitation distribution 65
Fig. 4.10: Mean of the monthly precipitation and number of rainy days. The dotted lines indicate the minimum and maximum values in the period 1961–1990. a) Posticciola; b) Subiaco; c) Carsoli; d) Pereto; e) Tubione; f) Tagliacozzo; g) Licenza; h) Rosciolo. 66
Fig. 4.11: Snow days versus elevation (n=5; R^2=0.999; α<0.01). 67
Fig. 4.12: Meteorological data of study site, expressed by Bagnouls-Gaussen diagrams, referred to the mean annual rainfall 1961-1990. 69
Fig. 5.1: Digital elevation model: a) Turano (10 m); b) Ovito (3 m). 79
Fig. 5.2: Flowchart for creating the seasonal C-factor. 83
Fig. 5.3: Relief and river network of the Ovito. 89
Fig. 5.4: Land-use map of the Ovito. 90
Fig. 5.5: Distribution of the RUSLE factors in the Turano watershed: a) rainfall erosivity ‘R-factor’ b) soil erodibility ‘K-factor’, c) topographic factor ‘LS-factor’, d) cover-management factor ‘C-factor’. 92
Fig. 5.6: Flowchart for creating a RUSLE-based soil erosion prediction. 93
Fig. 5.7: Predicted average annual soil erosion for the Turano watershed (1997–2005). 95
Fig. 5.8: Predicted average seasonal soil erosion for the Turano watershed (1997–2005). 96

Fig. 5.9: Potential soil erosion risk in the Turano watershed. 97
Fig. 5.10: Digital elevation model of the Turano watershed. 97
Fig. 5.11: Monthly variation of soil loss from October 1997 to September 2005 in the Turano watershed..... 100
Fig. 5.12: Soil loss in the areas under coppicing silvicultural activities divided by year. 101
Fig. 5.13: Soil loss in the undisturbed forested areas divided by year. For the year 1997 and 2005 only the periods from October to December and from January to September are considered, respectively. 102
Fig. 5.14: Predicted average annual soil erosion in harvested forested area of the Ovito sub-watershed. 103
Fig. 5.15: Predicted average annual soil erosion for the no-harvesting scenario in the Ovito sub-watershed. 103
Fig. 5.16: Predicted average annual soil erosion for the Turano watershed (1997-2005). 105
Fig. 5.17: Predicted average seasonal soil erosion for the Turano watershed (1997–2005). 106
Fig. 5.18: Potential soil erosion risk in the Turano watershed..... 107
Fig. 5.19: Digital elevation model of the Turano watershed. 107
Fig. 5.20: Monthly variation of gross soil loss from October 1997 to September 2005 in the Turano watershed..... 109
Fig. 5.21: Soil loss in the areas under coppicing silvicultural activities divided by year. 110
Fig. 5.22: Soil loss in the undisturbed forested areas divided by year. For the year 1997 and 2005 only the periods from October to December and from January to September are considered, respectively. 111
Fig. 5.23: Predicted average annual soil erosion in harvested forested area of the Ovito sub-watershed. 112
Fig. 5.24 Predicted average annual soil erosion for the no-harvesting scenario in the Ovito sub-watershed. 112
Fig. 5.25: Box plots of the predicted soil erosion value..... 113
Fig. 5.26: Difference between RUSLE and USPED models. 113
Fig. 5.27: Endorheic areas in the Turano watershed ‘a’, endorheic areas mask on the RUSLE output ‘b’ and endorheic areas mask on the USPED output ‘c’. 114
Fig. 5.28: Scheme of the semi-qualitative validation procedure for the Ovito sub-watershed. 116
Fig. 5.29: Ovito sub-watershed classification according to the erosion features mapped during field survey and by remote sensing. 117

Fig. 5.30: Predicted average annual soil erosion for the Turano watershed (1998–2009). 117
Fig. 5.31: Result of the comparison between the erosion features map and the predicted soil erosion. 118
Fig. 6.1: Turano drainage network. 132
Fig. 6.2: Turano without endorheic areas. 132
Fig. 6.3: Map of the erosion index for the Turano sub-watershed. 134
Fig. 7.1: Study sites. 143
Fig. 7.2: Destribution of the metallic stakes across the experimental watersheds. 146
Fig. 7.3: Some stakes before to be placed. 146
Fig. 7.4: Some stakes of Plot-01. 146
Fig. 7.5: Soil sampling locations. 147
Fig. 7.6: Hydro-plot locations. 149
Fig. 7.7: Erosion features. a) Area shortly after the trees-harvesting still presenting a good ground litter cover. b) Area under combined effect of inter-rill and rill erosion processes. c) Area washed by concentrated run-off. d) Minute morphological detail of an area where an erosion of the soil higher than 1 cm occurred. 153
Fig. 7.8: Geomorphological map EX-01 watershed. 154
Fig. 7.9: Longitudinal profile of the EX-01 watershed drainageway. 154
Fig. 7.10: Geomorphological map EX-02 watershed. 155
Fig. 7.11: Longitudinal profile of the EX-01 watershed drainageway. 155
Fig. 7.12: Photo of the EX-01 watershed (January 2009). 157
Fig. 7.13: Valley EX-01 cross-profiles A-D. 157
Fig. 7.14: Soil horizons. 158
Fig. 7.15: Grain size distribution curves derived by the average of the soil samples for three watershed elevation levels (a.low; b. medium; c.high). 159
Fig. 7.16: Soil texture classes of the EX-01 samples according to the USDA (2010) soil texture triangle. 160
Fig. 7.17: Spatial variation of skeleton fraction. 162
Fig. 7.18: Spatial variation of sand fraction. 162
Fig. 7.19: Spatial variation of silt fraction. 163
Fig. 7.20: Spatial variation of clay fraction. 163
Fig. 7.21: Spatial variation of TOC. 163
Fig. 7.22: Spatial variation of TIC. 163
Fig. 7.23: Plot rainfall-run-off measurements. 164

Fig. 7.24: Relationship between rainfall and run-off: a) HPlot-01; b) HPlot-02. 166
Fig. 7.26: Areal solar radiation' for the years 2009. 167
Fig. 7.27: TWI index with the infiltration test sites. 167
Fig. 7.28: Soil surface in the Plot-01 during August 2008. 170
Fig. 7.29: Soil surface in the Plot-01 during January 2010. 171
Fig. 7.30: Soil surface difference in the Plot-01. 171
Fig. 7.31: Some stakes of the Plot-01. 172
Fig. 7.32: Surface changes in the station profile P-1 and profile P-2. 172
Fig. 7.33: Modeled soil loss from 1st September 2008 to 8th January 2010: a) RUSLE soil erosion map; b) USPED soil erosion/deposition map. 174
Fig. 7.34: Modeled surface change in centimeters from 1st September 2008 to 8th January 2010: a) RUSLE soil erosion map; b) USPED soil erosion/deposition map. 175
Fig. 7.35: Relationship between soil loss measured by stakes and the soil loss modeled by the USPED (a) and RUSLE (b) models in the EX-01 watershed. 175
Fig. 8.1: The study site. 186
Fig. 8.2: Drilling core locations in the FDR watershed. Ortophoto: Lazio Region 2005. 188
Fig. 8.3: Geomorphological map of FDR. 191
Fig. 8.4: Drainage network FDR sub-watershed 2005. 192
Fig. 8.5: Drainage network FDR sub-watershed 2010. 192
Fig. 8.6: Gully incision on the rock basement. 193
Fig. 8.7: Gully confluence with the mainstream. 193
Fig. 8.8: Paths in the FDR watershed. 193
Fig. 8.9: Drilling core PS-04 location. 194
Fig. 8.10: Core PS-04 stratigraphy. 195
Fig. 8.11: Organic (a) and inorganic (b) carbon content in core PS-04. 196
Fig. 8.12: Drilling core PS-01 location. 197
Fig. 8.13: Core PS-01 stratigraphy. 198
Fig. 8.14: Organic (a) and inorganic (b) carbon content in core PS-01. 199
Fig. 8.15: Drilling core PS-11 location. 200
Fig. 8.16: Core PS-11 stratigraphy. 201
Fig. 8.17: Organic (a) and inorganic (b) carbon content in core PS-11. 202
Fig. 8.18: Magnetic susceptibility of the core PS-11. 203
Fig. 8.19: Age model of the core PS-11. 204

List of tables

Table 2.1: Erosion and sediment transport models adapted from Merrit et al. 2003 and Saavedra 2005. 9

Table 2.2: Plot erosion rates for different land uses in the Mediterranean Region (Cerdan et al., 2006). 16

Table 2.3: Plot erosion rates for different land uses in the other regions (Europe) (Cerdan et al., 2006). 17

Table 2.4: Impacts of forest management practices on water balance processes. 22

Table 2.5: Impact of forest management practices on erosion processes. 23

Table 3.1: Morphometric characteristics of the Turano watershed. 44

Table 3.2: Soils types of the Turano watershed. 54

Table 4.1: Thermometric characteristics in the research area (1991-2000). 57

Table 4.2: Descriptive statistic of the extreme thermal events. 61

Table 4.3: Descriptive statistic of the annual precipitation for the thirty years 1961–1990. 62

Table 4.4: Characteristics of the maximum intensity precipitations (1h, 2hrs and 6hrs). 66

Table 4.5: Climate indices of the Turano watershed. 68

Table 5.1: Equations tested for rainfall erosivity calculations (R= monthly R-factor; Mo=monthly precipitation; P=yearly precipitation). * These equitations estimate the annual R values and the determination coefficient and were obtained through correlation 120 monthly values. In contrast, the equations based on yearly data are based on 8 years (the equation proposed by Diodato (2004) on only 5 years). 76

Table 5.2: C-Factor for the Turano watershed 82

Table 5.3: Soil losses by different land-use and land-cover types at Turano watershed. 95

Table 5.4: Soil loss according to land-use and land cover units. 99

Table 5.5: Soil loss according to land use and land-cover units divided by slope inclination. 99

Table 5.6: Soil loss in the undisturbed forested areas (1997–2005). 101

Table 5.7: Soil loss in the areas under coppicing activities divided by slope inclination (1997-2005). 101

Table 5.8: Soil loss in the undisturbed forested areas (1997–2005). 102

Table 5.9: Soil loss in the undisturbed forested areas divided by slope inclination. 102

Table 5.10: Soil losses by different land use and land-cover type at Turano watershed. 105
Table 5.11: Soil gross erosion according to land-cover units..... 108
Table 5.12: Soil gross erosion according to land use and land-cover units divided by slope inclination. 108
Table 5.13: Soil gross erosion in the areas under coppicing silvicultural activities (1997–2005). 110
Table 5.14: Soil gross erosion in the areas under coppicing silvicultural activities divided by slope inclination (1997–2005)..... 110
Table 5.15: Soil loss in the undisturbed forested areas (1997–2005). 111
Table 5.16: Soil loss in the undisturbed forested areas divided by slope inclination (1997–2005)..... 111
Table 5.17: Areas under erosion divided by intensity classes. 113
Table 5.18: Grain size classification of Turano Lake sediments according to ENEL/E-ON. Mass refers to sediments smaller 2 mm. 115
Table 5.19: Level of agreement between the RUSLE model erosion outputs with the soil erosion features mapped..... 118
Table 5.20: RUSLE and USPED models applications in Italy (m.d., missing data; * estimated value)..... 121
Table 5.21: Comparison between different techniques for R-factor estimation..... 122
Table 6.1: Characteristics of the drainage network of the Turano watershed. 132
Table 6.2: Characteristics of the Turano drainage network without the endorheic areas. 132
Table 6.3: Geomorphic parameters of the drainage network within the Turano sub-watershed. 133
Table 6.4: Main characteristics of 41 Italia watersheds. 137
Table 6.5: Characteristics of the watershed used by van Rompaey (2005). 140
Table 7.1: Characteristics of the study sites..... 143
Table 7.2: Monitoring stations. 145
Table 7.3: Rainfall events. 148
Table 7.4: The characteristics of the sampled area. 149
Table 7.5: Characteristics of the soil profile in EX-02. 158
Table 7.6: Main statistics of the soil samples. 159
Table 7.7: Averages of organic and inorganic carbon for 35 samples at 0–10cm depth. 161

Table 7.8: Averages of electric conductivity for 12 samples at 0–10 cm depth..... 161
Table 7.9: Average pH values for 12 samples at 0– 10 cm depth. 161
Table 7.10: Bulk density of 8 samples at 6 cm depth. 162
Table 7.11: Liquid yield values for individual storm event in the two plots [* all the 19 storms]..... 165
Table 7.12: Plot sediment yield values of the three storm events observed..... 165
Table 7.13: Temperature measurements25th July 2009..... 168
Table 7.14: Hydraulic conductivityEx-01 [*measuring made in the vegetated area]..... 168
Table 7.15: Statistics of soil surface changes for the undisturbed and harvested slopes of the experimental watersheds. The period from 8th September 2008 to 5th January 2010 is reported because more stakes were in place. 169
Table 7.16: Min. and max. surface level variation measured during the experimental period from 8th September 2008 to 5th January 2010. 169
Table 7.17: Bulk density of the soil mineral fraction. 173
Table 7.18: Comparison between soil loss measured by stakes and the soil loss modeled by the RUSLE and USPED models in the EX-01 watershed. 176
Table 8.1: Climate characteristics of the study site (data from Fredi and Pugliese, 1994). 187
Table 8.2: PS-04 core characteristics. 194
Table 8.3: Ps-01 core characteristics..... 197
Table 8.4: PS-11 core characteristics. 200
Table 8.5: 14C dates of the FDR. 204

List of appendices

Appendix A: Lithotypes present in the Turano watershed 258

Appendix B: Geomorphological units 259

Appendix C: Regional climate 260

Appendix D: Analysis of the climate anomalies 262

Appendix E: C-factor test 267

Appendix F: USPED scheme 269

Appendix G: Rainfall erosivity 270

Appendix H: Measured and predicted Area-specific sediment yield (SSY in t ha^{-1} yr^{-1}) for 21 Italian drainage basins 272

Appendix J: Calibrated date 276

Appendix K: Soil erosion risk classes and geomorphometric characteristics of the Turano sub-watersheds……..CD

Appendix L: Average annual soil loss maps (RUSLE and USPED models, period 1997-2005)……..CD

List of symbols

A	Average annual soil loss
α	Slope length
Ac	Upslope contributing area
β	Slope angle
Bd	Soil bulk density
CC	Canopy-cover
C	Cover-management factor
Cf	Sub-continental climate
Δa	Hierarchical anomaly index
Dd	Drainage density
Dg	Geometric mean particle diameter
E	Kinetic energy
EC	Electrical Conductivity
$ED_{(r)}$	Net erosion/deposition rate
EI_{30}	Erosivity index for 30 minutes rainfall intensity
F	Fournier index
$ƒi$	Primary particle size
ga	Density of hierarchical anomaly
I	Precipitation intensity
IC	Infiltration capacity
I30	Maximum 30-min intensity
K	Soil erodibility factor
Kh	Hydraulic conductivity
LDS	Laser Direct Structuring method (grain size analysis)
LS	Length-slope factor
LS(r)	Modified slope length factor
M	Millions
Mi	arithmetic mean of the particle size
MJ	Megajoule
Mo	Monthly rainfall
Ø	Particle size diameter
OM	Organic matter
P	Support practice factor
PLU	Prior land use
Po	Annual rainfall
Q	Overland flow
$q_{(r)}$	Water flow
$qs_{(r)}$	Sediment flow rate
R	Rainfall intensity
R^2	Goodness of fit or coefficient of determination
SC	Surface-cover
SY	Sediment yield
SYe	Estimated sediment yield
SLR	Soil-loss-ratio
SM	Soil-moisture
SR	Surface-roughness
SSY	Suspended sediment yield
T(r)	Transport capacity

List of abbreviations and acronyms

AD	Anno domini
a.s.l.	Above sea level
ARSAA	Agenzia Regionale Per i Servizi di Sviluppo (Regional Agency for the Development Services)
BC	Before Christ
BP	Before present
CARG	Cartografia Geologica e Geotematica (Geologic and geothematic map)
CN	Curve number
DEM	Digital elevation model
DGPS	Differential Global Positioning System
EEA	European Environmental Agency
e.g.	Exempli gratia (for example)
ENEL	Nazionale Energia Elettrica (National Electricity Authority)
EU	European Union
FAO	Food and Agriculture Organization
FDR	Fosso delle Rosce (Turano sub-watershed)
GIS	Geographic information system
GDP	Gross domestic product
i.e.	Id est (that is)
IGMI	Istituto Geografico Militare Italiano (Italian Military Geographic Institute)
ITCZ	Intertropical Convergence Zone
ISE	Institute for environment and sustainability
ISTAT	Istituto Nazionale di Statistica (National Institute of Statistics)
NDVI	Normalized Difference Vegetation Index
NRCS	Natural Resources Conservation Service
PCN	Portale Cartografico Nazionale (National Cartographic Portal)
PESERA	Pan European Soil Erosion Risk Assessment
RUSLE	Revised Universal Soil Loss Equation
SD	Standard deviation
SDR	Sediment delivery ratio
SIMN	National Hydrographic and Oceanographic Service
SRTM	Shuttle Radar Topography Mission
TC	Total carbon
TIC	Total inorganic carbon content
TOC	Total organic carbon content
UN	United Nations
UNCCD	United Nations Convention to Combat Desertification
UNCED	United Nations Conference on Environment and Development
UNFCC	United Nations Framework Convention on Climate Change
UNFCD	United Nations Framework Convention to Combat Desertification
US	United States of America
USDA	United States Department of Agriculture
USLE	Universal Soil Loss Equation
USPED	Unit Stream Power - based Erosion Deposition
USDA	United States Department of Agriculture
UTM	Universal Transverse Mercator coordinates system
WEPP	Water Erosion Prediction Project

Abstract

This study investigates the spatio-temporal pattern and dynamic changes of the risk of soil erosion in a semi-forested mountainous area. The selected physiographic unit is the watershed of the Upper Turano River, a middle-scale watershed located in the Central Apennine chain, approximately 58 km northeastern of Rome. The watershed cover around 466.7 km² where the intramountain basin Conca di Oricola, which constitutes its central sector, is spatially limited by the reliefs belonging to the Carseolani (N-E), Simbruini (S) and Sabini (N-W) mountain chains. The landscape within the study area is typical for the intermountain Apennine watersheds, showing an evident heterogeneity of the geological, geomorphological as well as climatic and vegetation patterns. Although not densely populated, the area is still affected by human activities which give rise to relevant environmental impacts. Large sectors of the study area are exploited for farming, grazing and wood supply.

In carrying out this study particular attention has been paid to the human-induced accelerated soil erosion processes in harvested forested areas. Two spatially distributed soil erosion models (RUSLE, USPED) were applied to predict the potential spatial distribution of soil erosion processes for the whole Turano watershed. The models were both qualitatively and quantitatively validated. With the aim to gain a better understanding of and to quantify the hillslope soil erosion in the selected forested Turano sub-watersheds that had recently been harvested, field observations and measurements were performed. In doing so, the relationships between indirectly estimated erosion rates at the watershed scale and field measurements data at the hillslope scale were analyzed.

The main conclusions of this research project are as follows: 1) Soil erosion processes are very active in the Turano watershed. 38% of the total study area (466.7 km²) has been estimated as belonging to the high erosion class (soil loss > 5 t ha^{-1} yr^{-1}). 2) The measured annual sediment yield is 1.33 M t^{-1} yr^{-1}, which is equal to an area-specific sediment yield of 32.35 t ha^{-1} yr^{-1}. Hence, the Turano watershed is among the Italian watersheds with the highest sediment discharge. 3) According to the application of soil erosion prediction models, the forest sectors involved in tree harvesting activities experience severe erosion rates. Compared to the undisturbed forest area (270 km²) for which a mobilized amount of sediments equal to 79,218 t yr^{-1} was estimated, the 19 km² of disturbed forest area could potentially produce an amount of mobilized sediment equal to 36,516 t yr^{-1} which is almost 46% of the sediments mobilized in the undisturbed forest. 4) Field observations and measurements of the soil erosion dynamics in harvested and undisturbed forested areas confirmed the different severities of erosion predicted by the models. From the soil surface changes measured by the erosion stakes, erosion rates equal to 2.3 t ha^{-1} yr^{-1} for the

undisturbed forested hillslopes and 49 t ha^{-1} yr^{-1} for the harvested hillslopes were estimated. 5) Evidence of a past phase of human-induced accelerated soil erosion processes starting between the 1st and 2nd century BC was acquired through sedimentological analyses of alluvial sediments.

Zusammenfassung

Die vorliegende Arbeit erforscht raum-zeitliche Muster und Veränderungen des Bodenerosionsrisikos eines in weiten Teilen forstwirtschaftlich genutzten Untersuchungsgebietes. Forschungsobjekt dieser Arbeit ist das 466,7 km² große italienische Einzugsgebiet des Oberen Turano, 58 km nord-östlich von Rom. Dieses zentral in den Apeninnen gelegene Einzugsgebiet erstreckt sich hauptsächlich über das intermontane Conca di Oricola Becken und wird räumlich durch die Höhenzüge der Carseolani Berge (N-E), Simbruini Berge (S) und Sabiner Berge (N-W) begrenzt. Die heterogenen geologischen, geomorphologischen und klimatischen Strukturen sowie die Vegetationsmuster des Einzugsgebiets sind charakteristisch für intermontane Landschaft wie die des Apennins. Obwohl das Gebiet dünn besiedelte ist, zeigen sich dennoch erhebliche Anzeichen land- und forstwirtschaftlicher Nutzung.

Der Fokus dieser Arbeit liegt auf der anthropogen-induzierten Beschleunigung von Bodenerosionsprozesse in den bewaldeten Gebieten.

Zur Berechnung der räumlich differenzierten Bodenerosion des Einzugsgebiets werden zwei Bodenerosionsmodelle (RUSLE, USPED) verwendet. Beide Modelle werden quantitativ sowie qualitativ validiert. Für ein besseres Verständnis der ablaufenden Bodenerosionsprozesse werden Geländebeobachtungen und Messdaten verwendet. Zur Quantifizierung der Bodenerosion auf der Mikroskale werden Hänge in einem kürzlich aufgeforsteten Teileinzugsgebiet eingemessen. Damit lassen sich die Zusammenhänge zwischen der indirekten Schätzung der Erosionsraten auf der Einzugsgebietsebene und den vor Ort erhobenen Messdaten auf der Hangebene analysieren.

Zusammenfassend lassen sich folgende Forschungsergebnisse nennen: 1) Im Turano Einzugsgebiet sind die Bodenerosionsprozesse sehr aktiv. 38% der betrachteten Gesamtfläche (466,7 km²) des Einzugsgebiet werden nach Modellschätzungen als hochgradig erosionsgefährdet_klassifiziert (Bodenverlust > 5 t ha^{-1} a^{-1}). 2) Mit einer gemessenen jährlichen Sedimentfracht von 1,33 M t^{-1} a^{-1}, was einer gebietsspezifischen Sedimentgesamtfracht von 32,35 t ha^{-1} a^{-1} entspricht, gehört das Turano Einzugsgebiet zu den italienischen Einzugsgebiet mit der höchsten Sedimentfracht. 3) Für die von Rodungsaktivitäten betroffenen Gebiete, berechnen die verwendeten Bodenerosionsmodelle hohe Erosionsraten. Verglichen mit den ungestörten Waldgebiet des Einzugsgebiet (270 km²), für die eine Sedimentfracht von 79.218 t a^{-1} geschätzt wurde, resultiert aus der Modellschätzung für die gerodeten Forstflächen (19 km²) eine geschätzte Sedimentfracht von 36.516 t a^{-1}, was etwa 46% der transportierten Sedimente der ungestörten Waldflächen entspricht. 4) Geländebeobachtungen und -messungen

bestätigen den unterschiedlichen Grad des Bodenerosionsrisikos zwischen den gerodeten und ungestörten Waldflächen, der durch die Bodenerosionsmodelle berechnet wird. Veränderungen in der Höhe der Bodenoberfläche wurden durch Metallstäbe gemessen. Aus diesen Messungen ergeben sich Erosionsraten von 2,3 t ha^{-1} a^{-1} für die nicht abgeforsteten Hänge und 49 t ha^{-1} a^{-1} für die gerodeten Hangflächen. 5) Sedimentologische Analysen der alluvialen Sedimente geben Hinweise auf eine anthropogen-induzierte, Beschleunigung der Bodenerosionsprozesse, deren Beginn in den Zeitraum zwischen dem ersten und zweiten Jahrhundert vor Christus datieren werden kann.

Chapter 1

Introduction

1. INTRODUCTION

This study focuses on the analysis of land degradation caused by soil erosion. The soil erosion is a natural geomorphologic process of landscape development which is accelerated under the influence of unwise land-use (Felix-Henningsen et al., 1997). It is defined as 'the wearing away of the land surface by physical forces such as rainfall, flowing water, wind, ice, temperature change, gravity or other natural or anthropogenic agents that abrade, detach and remove soil or geological material from one point on the earth's surface to be deposited elsewhere' (Soil Science Society of America, 2001; Jones et al., 2006). Despite numerous forms of soil erosion, erosion by water is the most widespread type (Lal, 2003) globally affecting an estimated area of about 1094 million ha (Mha) (Oldeman, 1994). Although it is a natural process that, from a geological perspective, has contributed to creating and shaping the present landscape, when accelerated or induced by humans it may constitute a serious threat for the environment. In fact, the aggravation of erosion processes by human activity (e.g., agriculture, grazing, forest management, building and mining), which large parts of the landscape are presently being subjected to, is one of the most destructive phenomena related to natural resources in the world (Reich et al., 2000).

Regarding the Mediterranean regions, the increasing pressure of anthropogenic environmental changes together with long dry periods followed by heavy bursts of intensive and erosive rainfall especially when falling on steep slopes with fragile soils (van der Knijff et al., 1999) drive the landscapes of some areas towards a stage of irremediable perturbations (Scheffer et al., 2001). According to the APAT (Italian Agency for Environmental Protection and Technical Services, 2009), two-thirds of the soil in Italy is affected by degradation problems. Soil degradation in Italian landscapes is linked to the alarming increase in soil erosion by water that has occurred in the last few decades (Boardman and Poesen, 2006). Recent studies by the JRC-IES (Joint Research Centre-Institute for Environment and Sustainability – European Commission) (Gobin et al., 1999; Grimm et al., 2002) have shown that approximately 30% of the Italian soil shows indications of a water erosion risk above the tolerable threshold.

The current situation of accelerated soil erosion processes in Italy might further worsen if the predicted changes in climatic conditions (IPCC, 2000), more precisely, the increase in rainfall in the Western Mediterranean sector (Oljienink, 1988) prove true. For Italy, Rodolfi and Zanchi (2002) posited that it is already possible to note a progressive lengthening of the dry season with a concentration of (high intensity) precipitation at sporadic events.

Given these serious concerns, the aim of this thesis is to integrate the state of the art of accelerated soil erosion processes for Italian forested mountain watersheds. In particular,

a watershed of the Central Apennine Mountains where so far no study has been carried out on the topic was chosen. The selected watershed is located in the upper Turano River drainage basin. Notably, the absence of research publications for this area cannot be attributed to the irrelevance of soil erosion risk in this location. Instead, the lack of an efficient network for monitoring soil erosion in these environments is more likely to be the reason. In fact, this Apennine region does not provide any control stations for the measurement of both, liquid and solid river discharges. Despite these unfavorable circumstances the identified gap in research called for an in-depth investigation of the area containing evidence of a high soil erosion risk potential. Thus, several means have been developed to substitute for the lack of measurement data and technical equipment.

The selected physiographic unit is a middle scale watershed that shows the typical conformation of the Central Apennine region. There are two sizable geological sectors with semi-impermeable terrigenous lithotypes incised by a dense river network within the watershed. Moreover, intensive forest harvesting is carried out in these sectors. The hydrological characteristics of the lithological substratum (Bono and Capelli, 1994), together with the removal of the protective effect of the vegetation for the soil, makes these areas potentially prone to continued, severe soil erosion.

1.1. OVERALL AIM

The overall aim of this research is to investigate the spatio-temporal pattern and dynamic changes of soil erosion risk within the selected physiographic unit by means of a spatially distributed approach. In addition, this thesis will observe the environmental impact that results from the silviculture activities in the area, i.e., cyclical forest harvesting (coppicing).

1.2. OBJECTIVES

To achieve the overall aim, sub-objectives have been formulated for this research:

1) Analysis of the climatic conditions of the Turano watershed.
2) Indirect evaluation of soil erosion rates:
    a. Prediction of both, gross and net erosion rates using distributed soil erosion models.
    b. Prediction of accelerated soil erosion due to forest harvesting applying distributed soil erosion models.
    c. Sediment yield (SY) prediction for the Turano watershed.
    d. Qualitative and quantitative assessment of the effectiveness of the models to predict soil erosion in the study environment.
3) Direct evaluation of soil erosion rates:

a. Measurement of soil erosion at hillslope-scale. Field monitoring in experimental watersheds (EX-01 and EX-02 first-order watersheds).

4) Evaluation of the past and present anthropogenic influence on soil erosion processes in the Ovito sub-watershed through fieldwork activities.

1.3. MAIN RESEARCH QUESTIONS

Do researchers underestimate soil erosion rates on hillslopes of forested, mountainous watersheds as well as the suspended sediment yields in the drainage networks?

Can areas in the Central Apennine that are subject to coppicing activities be hotspots of soil erosion?

Chapter 2

State of the Art

2. STATE OF THE ART

2.1. SOIL EROSION BY WATER

Soil erosion by water, also known as hydric soil erosion, is the ongoing geomorphic process of soil degradation studied most in the Mediterranean region (Kosmas et al., 1997; Boardman and Poesen, 2006) and most likely also on a global scale. The scientific community recognizes it as a principal form of land degradation (Bordman 2006). The majority of the publications on soil erosion agree when identifying this phenomenon as one of the most pressing environmental problems, since it is argued to potentially result in a degradation of the ecosystem function (Kirkby et al., 2000), decrease of agricultural productivity (Boardman and Poesen, 2006) and the displacement of human populations (Opie, 2000). The scope and in some cases the speed of this soil degradation process led national as well as international organizations to deal with it, e.g., FAO (1976; 1993), UN (UNCED, 1992; UNCCD, 1994; UNFCD, 1996; UNFCC, 1997), EU (EEA-CORINE, 1992; USLE, 1996; PESERA, 1999; INRA, 2001).

This study uses the term soil erosion by water to refer to a natural process that has existed since before the impact on the environment of human beings (Castiglioni, 1986). It results from the detachment and transportation of soil materials by the erosive effect of the water (Foster and Meyer, 1972). Today, it occurs either naturally as part of the geological evolution of the landscape or due to the intervention of human beings in the environment (Morgan, 1996). On the one hand, natural erosion (also called geologic erosion) of the soil is an inevitable process (Castiglioni, 1986) which in most cases does not have a strong degradation impact (Lal, 1990) and is therefore tolerated by the environment. On the other hand, in locations where the anthropogenic activities disturb the natural landscape balance, predominantly causing changes in vegetation cover and soil character, a strong erosive response may result (Lal, 2001). In conceptual terms, soil erosion shifts from a natural geomorphological process to a human-accelerated geomorphological process. Thus, the intensity of the process directly depends on a series of biophysical natural factors and also on those which are under direct human influence. Accordingly, the soil degradation by erosion may be described as the result of the interaction between three fundamental factor categories (Morgan, 1996) and the anthropogenic influence on them, as illustrated in Figure 2.1.

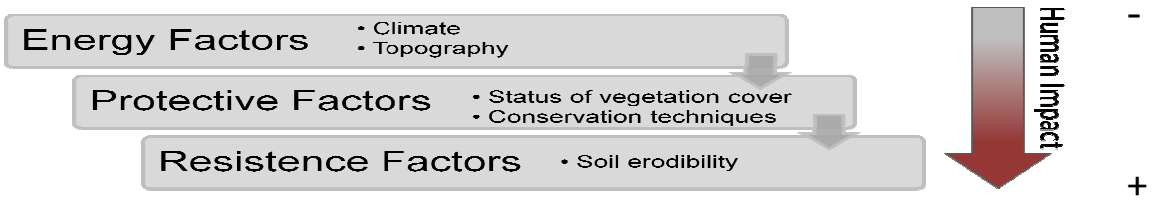

Fig. 2.1 – Fundamental factor categories influencing the process of soil degradation by erosion.

With regard to the extent of soil erosion, the statistics most widely used are those proposed by Oldeman (1991,1994). According to Oldeman (1991,1994), in the 90s about 1094 million hectares (M ha) were subject to hydric erosive phenomena of the soils, out of which around 751 M ha were severely affected. The continent most affected by severe water erosion was Asia (317 M ha), followed by Africa (169 M ha), Europe (93 M ha), South America (77 M ha) and North America (46 M ha) (Oldman, 1994; Scherr, 1999, cited in Lal, 2003). More recent studies pointed out that from the total 1094 M ha affected by hydric soil erosion, about 43% is due to deforestation, 29% result from overgrazing, 24% are due to the absence of conservative management of agricultural land and the last 4% can be attributed to over-exploitation of natural vegetation (Walling and Fang, 2003). Beyond this, further processes of land degradation can be directly or indirectly influenced by soil erosion, as in the case of soil salinity (Herrero and Pérez-Coveta, 2005), desertification (Stringer, 2008) and the decrease of aquatic resources quality (Ochumba, 1990).

2.2. ACADEMIC APPROACHES TO THE PROBLEM

The scientific community has been dealing with this environmental problem for a long time (Knapen et al., 2007). Research into geomorphologic processes that are behind soil erosion benefits from cognitive contributions of neighboring disciplines, i.e., geography, soil science, engineering, physics as well as human sciences and economics. The numerous approaches presented so far with the intention of gaining a better understanding of this phenomenon vary in terms of temporal and spatial scales, methodologies and research goals (Boardman, 2006). Qualitative and quantitative descriptions of hydric soil erosion have been directly performed through field observations (Wischmeier and Smith, 1978; Boardman and Poesen, 2006; Cerdan et al., 2007; Verheijen et al., 2009; Bagarello et al., 2011) and laboratory experiments (Ellison, 1945; Dennis et al., 1982; Bryan and Poesen, 1989; Torri and Poesen, 1992; Bryan, 2000). In contrast, indirect estimations of the erosion processes for large areas (global, regional and watershed scale) have generally been carried out estimating the sediments accumulated in artificial lakes, reservoirs and check–dams or using rivers suspended sediment yield data (Ciccacci et al., 1983; Ciccacci et al., 1986; Bazzoffi et al., 1996; van Rompeay, 2003; Romero-Díaz et al., 2004; Romero-Díaz 2007; de Vente and Poesen, 2005). In addition, the use of remote–sensing techniques to perform qualitative assessment of soil erosion has increased (Vrieling, 2006). By applying these techniques, information about the phenomenon is acquired from sensing devices housed in airplanes or satellites. With a ground resolution ranging from 10 cm (aerial photos 1:2000 scale) to 30 m (Landsat ETM+) erosion forms

can be mapped in large areas, choosing the data that best fits the scale and the specific processes.

However, in the last few decades most studies have focused on the development and application of models able to indirectly predict the magnitude, frequency, scope as well as temporal spacing of soil erosion (USLE – Wischmeier and Smith, 1978; SWAT – Arnold and Williams, 1995; WEPP – Nearing et al., 1989; Lisem – De Roo et al., 1996; RUSLE – Renard et al., 1997; USPED – Mitas and Mitasova, 1998; EUROSEM – Morgan et al., 1998). As stated in several review papers (e.g., Aksoy and Kavvas, 2005; Jetten and Favis-Mortlock, 2006; Boardman 2006), a large number of models have been proposed, ranging from very simplistic expressions to highly complex ones able to consider a large number of factors as well as the physical relationships that link them. In general, based on the criteria, the models fall into three main categories: empirical, conceptual and physical based models (Aksoy and Kavvas, 2005). The main diffused erosion and sediment transport models are listed in Table 2.1.

Table 2.1 – Erosion and sediment transport models adapted from Merrit et al. 2003 and Saavedra 2005.

Model	Type	Spatial scale	Temporal scale	Outputs	Wischmeier and Smith, (1978)
USLE	Empirical	Hillslope	Annual	Erosion	Mitasova et al. (1996)
RUSLE	Empirical	Hillslope	Annual	Erosion	Renard et al. (1997)
RUSLE-3D	Empirical/conceptual	Watershed	Annual	Erosion	Mitasova et al. (2009)
USPED	Empirical/conceptual	Watershed	Event/ Annual	Erosion/deposition	Mitas and Mitasova,(1998)
AGNPS	Conceptual	Small watershed	Event/continuous	Run-off, peak rate, erosion, sediment yield	Young et al. (1989)
LASCAM	Conceptual	Watershed	Continuous	Run-off, sediments	Viney and Sivapalan,(1999)
ANSWERS	Physical	Small watershed	Event/continuous	Run-off, peak rate, erosion, sediment yield	Beasley et al. (1980)
LISEM	Physical	Small watershed	Event	Run-off, sediment	De Roo et al. (1996)
CREAMS	Physical	Plot/field	Event/continuous	Erosion, deposition	Foster et al. (1981)
WEPP	Physical	Hillslope/watershed	Continuous	Run-off, sediment yield, soil loss	Nearing et al. (1989)
EUROSEM	Physical	Small watershed	Event	Run-off, erosion, sediment	Morgan et al. (1998)
KINEROS	Physical	Hillslope/small watershed	Event	Run-off, peak rate, erosion, sediment	Smith, (1981)
SWAT	Conceptual	Watershed	Continuous	Run-off, peak rate, erosion,sediment yield	Arnold and Williams, (1995)
AGWA	Conceptual/physical	Watershed/basin	Continuous	Run-off, peak rate, erosion,sediment yield	
GUEST	Physical	Plot/field	Continuous	Run-off, sediment concentration	Yu et al. (1997)
EMSS	Conceptual	Watershed	Continuous	Run-off, sediment loads	Vertessey et al. (2001)
HSPF	Conceptual	Watershed	Continuous	Run-off, flow rate, sediment load	Johanson et al. (1980)
PERFECT	Physical	Plot/field	Continuous	Run-off, erosion	Littleboy et al. (1992)
SEDNET	Conceptual/empirical	Watershed/basin	Annual/continuous	Suspended sediment, relative contribution from overland flow, gully and bank erosion processes	Prosser et al. (2001)
T0POG	Physical	Hillslope		Erosion hazard	Haskins and Davey (1991)
EROSION-3D	Physical	Watershed	Event	Run-off, erosion, sediment	Schmidt et al. (1996)
MMMF	Empirical/conceptual	Hillslope/watershed	Annual	Run-off, erosion	Morgan et al. (1984)
THORNES	Conceptual/empirical	Hillslope/watershed	Annual	Run-off, erosion	Thornes (1990)
EPIC	Physical	Hillslope/watershed	Continuous	Erosion	Williams et al. (1984)
SEDEM/WaTEM	Conceptual	Watershed	Annual	Erosion	van Rompaey et al. (2001)
MIKE-11	Physical	Watershed	Continuous	Sediment yield, run-off	Hanley et al. (1998)
SHETRAN	Physical	Watershed	Event	Run-off, peak rate, sediment yield, sediment	Ewen et al. (2000)
SEAGIS	Empirical/conceptual	Watershed	Annual	Erosion, sediment yield	
PESERA	Physical	Hillslope/regional	Continuous	Run-off, erosion, sediments	Gobin et al. (1999)
SPL	Empirical/conceptual	Watershed/river	Annual	Fluvial erosion, river incision	Stock and Montgomery, (1999)

2.3. THE PHYSICAL PROCESS

Soil erosion by water can be described as a dynamic process that can be divided into three stages: detachment, transportation and deposition of eroded particles (Morgan, 1996). Water unfolds its erosive power on the soil surface in two ways: Firstly, through the raindrop impact (rainsplash) and secondly by means of overland flow (run-off) (Bryan, 2000). The detachment and transport processes of soil particles occur when the rainsplash and overland flow exceed the interstitial forces holding the soil particles together (Harmon and Doe, 2001). Through the washing out of erosive agents, insoluble and soluble materials are removed from the soil surface (Norton et al., 1999). This means that a dual process takes place: the first due to the physical erosion, while the second can be attributed to chemical erosion. The products of the detachment are transported from their original locations to lower hypsometric levels where the quantities and the dynamics of the soil particles are governed by many local conditions, such as soil properties, topography, rock lithology, morphology, climate, vegetation and anthropogenic activity (Morgan et al,. 1996).

The erosive forms of soil resulting from the single or combined action of the erosive agents are numerous. Usually, the hydric erosion forms are conceptually subdivided into inter-rills, rills and gullies (Bryan, 2000). The occurrence of these three processes depends on the stage of the erosion cycle and on the specific location in the landscape (Harmon and Doe, 2001). As a consequence, following a general convention watersheds are frequently divided into two sectors based on the predominant geomorphic processes (Harmon and Doe, 2001), hillslopes (or upland areas) and channels (or drainage system).

The rainsplash erosion represents the first stage of the process of soil erosion by water (Ellison, 1945; van Dijk et al., 2002). It is considered to be the most important detaching agent in the erosive process (Morgan and Davidson, 1986; Lal, 1990) and has been found to be the main cause of erosion risk in the temperate areas (Teklehaimanot, 2003). Studying soil erosion processes in disturbed forested areas of southern Italy, van Asch (1983, cited in Falace, 2007) stated that the rainsplash effect is responsible for between 30% and 95% of soil particles dethatched during the erosion process.

The second step of the soil erosion phenomenon is due to the action of the overland flow. After a short-term ponding on the ground surface the rainfall water normally infiltrates the soil (Kirkby, 1985). In specific cases parts of the water cannot infiltrate the soil. Consequently, an overland flow appears in the form of infiltration excess overland flow (also called Hortonian run-off, after Robert Horton (1933)) or as saturation excess overland flow (Dunne, 1978). For the former, overland flow occurs when the rainfall intensity exceeds the infiltration capacity and the depression storage capacity of the soil (Horton,

1933). The generation of this type of overland flow is typical for bare soil areas where the raindrop impact rearranges the soil surface particles thereby reducing its porosity, sealing the macrospores and occasionally forming a superficial crust (Cerdan, 2002). In contrast, in densely vegetated areas the Hortonian run-off is usually rather rare because of the high infiltration capacities (Knapp, 1978), the hydraulic conductivities that characterize the soils of these areas (Dunne, 1978) as well as the effect canopy cover interception (Salsotto and Dama, 1980). The latter, i.e. saturation excess overland flow, occurs when the incoming rainfall hits saturated or almost saturated soil (Beven, 2001). Thus, the main factor affecting this overland flow process is the level of antecedent soil moisture (Dunne, 1978). As a result, this kind of flow tends to be located in specific watershed places, such as valley bottoms and convergence topography areas (Beven, 2001). Yet, the generations of the infiltration and saturation excess mechanisms are not mutually exclusive in a watershed (Walter et al., 2003). Instead, both may occur in the same watershed although in different locations or at different moments in time.

Detachment as well as transport of soil particles may occur in the inter-rill, rill areas and gullies (Hudson, 1995). In the inter-rill areas the downslope moving flow has a little detachment and transport capacity. According to Foster (1982) for inter-rill erosion the detachment by shallow flow by itself can be neglected. In fact, the shear stress of the flow itself is in the order of pascals, while the soil tensile strength could reach an order of kilopascals (Sharma, 1996). Nevertheless, the detachment and entrainment capacity of this flow together with the raindrop impact (Torri and Poesen, 1992) has a high potential erosive power (De Ploey, 1971; Walker et al., 1978; Kinnell, 1985; Guy et al., 1987; Moss, 1988). Moving downslope, in some parts of the hillslope the direction of the laminar sheet flow typical for the inter-rill areas converges towards preferential flows and therefore becomes more concentrated (Poesen et al., 2003). In these areas the run-off is sufficient to form a shallow channel, the so-called rill (Harmon and Doe, 2001). The transition from inter-rill to rill processes is critical for both, erosion rates and the geomorphic evolution of hillslopes (Bryan, 2000). In fact, in the rills the depth of flow, velocity of the flow and shear stress on the soil surface are, in general, greatly enhanced by flow concentration (Knapen, 2007) resulting in an improved ability of the flowing water to erode and transport soil particles (Gatto et al., 2001). Rill conversion may result in mega-rill or gully formation (Poesen et al., 2003).

Furthermore, if somewhere along the water flow path the velocity is decreased (on the hillslope or in the channels) parts of the soil particles carried by the flow can be deposited because of the reduced transport capacity (Haan et al., 1994). Still, the soil particles not deposited continue floating downstream until they reach the watershed outlet (Nichols and

Renard, 1999). This part of the eroded soil particles is called the sediment yield (SY) (de Vente et al., 2007). The ratio between the sediment yield at a specific location in the stream system (net erosion) and the gross erosion from the drainage area above that point is defined as the sediment delivery ratio (SDR) (Maner, 1958*).* This ratio varies widely with the area size, steepness, density of the drainage network and further factors (van Rompaey, 2001) that remain ambiguous for researchers.

The transport capacity can be described as the maximum amount of sediment that a given flow can carry without net deposition (Morgan, 1996). Furthermore, detachment and transport capacity are interconnected. More precisely, their interaction controls the magnitudes and patterns of both, erosion and deposition dynamics (Hudson, 1995). Conditions where one of these two factors exceeds the others are denoted as detachment-limited or transport-limited erosion, respectively (Foster, 1982). Detachment-limited erosion appears when the quantity and characteristics of the overland flow are greater than the available soil particles detached by the raindrop impact and overland flow. As a consequence, the magnitude of soil erosion is limited by the low detachment capacity. On the other hand, transport-limited erosion occurs where the quantity or energy of the overland flow is insufficient to wash away the soil detached by the erosive agents.

2.4. FACTORS INFLUENCING SOIL EROSION

The raindrop impact and the shearing action of the overland flow tend to break down the soil structure and wash away the soil particles (Ellison, 1945). However, this is counteracted by the tensile strength of the soils commonly termed soil erodibility (Wischmeier and Smith, 1978). The effectiveness with which the soil resists the erosive agents is related to its physical and chemical characteristics (Renard et al., 1997; Torri et al., 1997; Morgan et al., 1996). These characteristics, in turn, define the aggregate stability of the soil which ranges from coherent to non-coherent conditions of the soil. Specifically, the aggregate stability is influenced by primary soil properties such as texture, content of organic carbon, exchangeable sodium percentage, bulk density and minerals content (Lal and Elliot, 1994, Knapen et al., 2007). In addition, soil roughness and some time-dependent parameters such as soil-moisture content (Le Bissonnais et al., 1995), evapotranspiration (Kort et al., 1998) and the formation of seasonal soil crusts (Bissonnais and Singer, 1992; Govers et al., 2004; Valentin et al., 2004) play important roles.

However, beyond the dependence of soil erosion on the rainfall erosivity and soil erodibility, it is also related to other factors. These are considered as spatial variables (Symeonakis, 2001) able to alter the denudational processes. Figure 2.2 shows the main factors controlling the process of hydric erosion based on Symeonakis (2001):

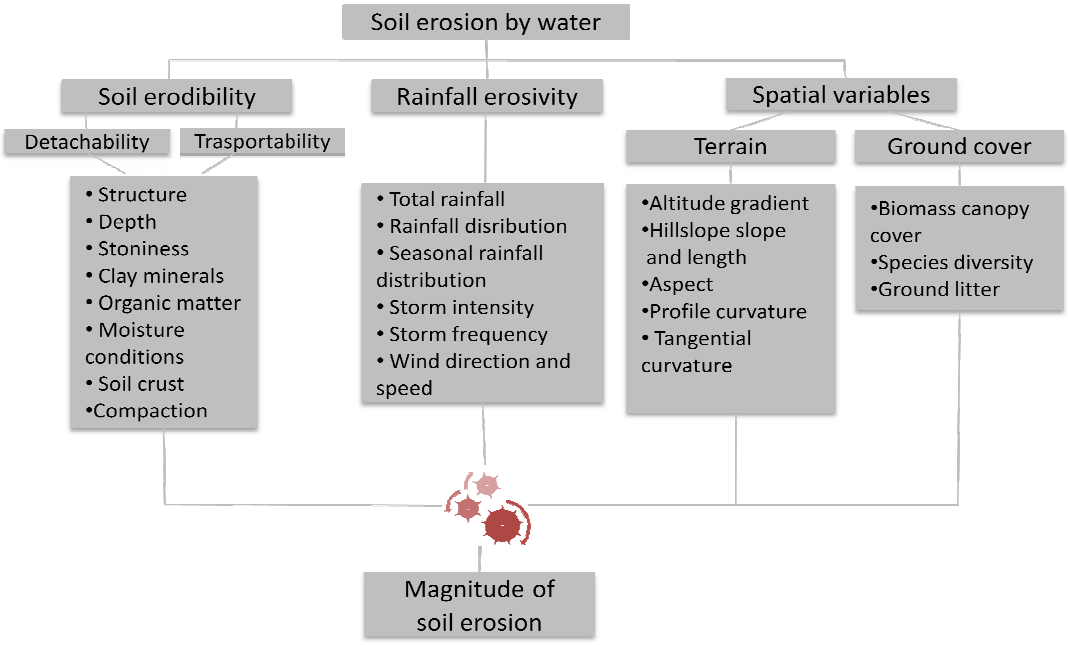

Fig. 2.2 – Factors controlling hydric soil erosion based on Symeonakis (2001) with modification of the author.

2.5. IS SOIL EROSION A NEW THREAT FOR OUR LANDSCAPES?

Following the insights provided by the state of the art, accelerated rates of soil erosion induced by anthropogenic activities similar to those observable at present have to be assumed for the past. Several studies in European landscapes found evidence of erosion features and sediments related to past land use (Bell and Boardman, 1992; Lang and Bork, 2006; Dotterweich, 2008). According to Lang and Bork (2006), in many European landscapes the observation of the present-day soil clearly shows evidence of a past phase of landscape stability characterized by soil formation which was followed by a phase of land use and soil erosion. Among others, deeply truncated soils on the slopes, ancient rills and gullies, colluvial deposits on the lower slopes and clastic deposits in floodplains and lakes (Rommens et al., 2005) are examples for the instable phase.

The dynamics and intensity of the accelerated soil erosion in the past can only be estimated by studying their cumulative effect (Rommens et al., 2005). During the last few decades many studies focused on the past climatic and anthropogenic impacts on the soil erosion have pointed in this direction. Most of them were carried out in areas considered as geoarchives (Dotterweich, 2008) such as lake sediments (Zolitschka, 1998; Ramrath, 1999; Ramrath, 2000; Schütt, 2000; Sadori et al., 2004), colluvial deposits (Lang and Hönscheidt, 1999; Foster et al., 2000; Lang et al., 2003), alluvial sediment (Mäcklin et al., 1991; Taylor et al., 2000; Mäckel et al., 2003; Hoffmann et al., 2007) and small catchments sediment storages (Walling et al., 2002; Rommens et al., 2005; Rommens et al., 2006).

Most of the studies presented, mainly in the Central Europe, identified a strong anthropogenic impact on the past soil erosion processes, namely the Neolithic revolution around 7500 years ago (Lüning, 1996, cited in Dotterweich, 2008). In the Mediterranean region the effects of changed land use have even been assumed to have more ancient origins of around 9000 years ago (Lang and Bork, 2006). Regarding North Europe, severe soil erosion occurred between 2000 BC and 200 AD as a repercussion of the permanent clearance of woodlands and the intensification of agriculture (Favis-Mortlock et al., 1997).

The main cause of accelerated erosion of the past was detected during field work for agricultural purposes (Meeus et al., 1988). According to Lang and Bork (2006), the anthropogenic influence on the soil erosion phenomenon can be related back to the first agricultural activities during the Neolithic period. In his review paper about past soil erosion studies in Central Europe, Dotterweich (2008) emphasized that during the Neolithic period a weak, but diffused, hillslope erosion must have taken place in Central Europe. Publications developed for Central Europe observed a considerable increase in soil erosion during the Iron Age (Dotterweich, 2008) and the Roman period (Mäckel et al., 2001, 2002, 2003) and attributed this to the extension of settlements (villages, rural estates and military camps), higher technical standards and intensified agricultural land use as well as mining and woodlands clearance. During these periods wide deforestation exposed huge areas where previously the geomorphic processes had greatly been hindered by natural vegetation, thus resulting in accelerated soil erosion (Williams, 2000).

Although studies of past soil erosion in Italy are rare, some high soil erosion rates attributable to the past anthropogenic activities were also found in central Italy. Ramrath et al. (2000) and Sadori et al. (2004) found a massive occurrence of turbidites dated at 1300 calibrated yr BC in lake sediments. The significant decrease of tree pollen concentration values in the sediments related to the turbidites observed in the analysis of the lake sediments was considered an indicator of forest vegetation cover disturbances (Ramrath et al., 2000). Many historical sources described an active forest harvesting in Italy during the Roman period (Livy, cited in Hughes and Thirgood, 1982; Pliny the Elder, cited in Sciò et al., 2000; Lucretius, cited in Williams, 2000; Ovid, cited in Maialetti, 2001).

Dotterweich's literature review paper (2008) identified the highest historical impact of soil erosion during the Middle Ages, a period of high land-use intensity and rapid climate change. In this period, land-use intensity reached a very high level and up to 80% of Central Europe's surface was used as fields and grassland Dotterweich (2008). According to Dotterweich (2008) in more than 50% of the investigated sites in Central Europe traces of soil erosion were detected. The good data quality of some studies during this time allowed for quantitative estimations of the erosive processes. In the High Middle Ages, and

with a lesser extent in the Roman period, severe soil erosion rates that greatly influenced the floodplain sedimentation dynamics in Europe were found (de Moor et al., 2008). In this period the sediment production was 40 times higher than during the early and middle Holocene (de Moor et al., 2008). Soil losses 10 to 100 times higher than before were estimated with erosion rates up to 48 t ha^{-1} yr^{-1} typically calculated in loess areas (Dotterweich, 2008).

As shown in several studies, for instance, carried out in Germany, England, Belgium, Poland and Finland, accelerated soil erosion phenomena have affected European soils since human beings shifted from the more transitory nomadic hunting-and-gathering existence to a more permanent, settled and intensive plant-and-animal-farming system (Boardman and Poesen, 2006). The anthropogenic impacts are positively related to the population and technological knowledge development. The erosive phenomena, when followed by irreversible degradation of the soils, could result in a forced cessation of the agriculture in specific places (Lal, 1990). In the most severe cases a massive degradation of agricultural fields could have even led to the fall of entire civilizations (Olson, 1981; Sanders, 1992).

Moreover, in some locations the phenomenon of past soil erosion has unfolded long-term consequences that affected the landscapes until today (Hughes and Thirgood, 1982). Rozanov et al. (1990) noted that most likely during the past 10,000 years the more productive soil has been irreversibly lost.

2.6. PRESENT SCENARIO ON SOIL EROSION STUDIES, AN 'EXCLUSIVE' PROBLEM OF THE AGRICULTURAL AREAS

Historically, the most severe and visible effects of soil erosion have been observed in agricultural areas. Already beginning in the last century some studies recognized the close relationship between the loss of topsoil due to hydric erosion and agricultural and pasture land activities (Chapline, 1929). These studies also noticed the resulting fertility decreases of the fields (USDA, 1928) and hence the reduction of cultivable surfaces (Ayres, 1936). This link caused an increasing interest among the international scientific community to focus on the erosion processes in agricultural areas. This academic trend gave rise to experimental studies (Held and Clawson, 1965; USDA: Wischmeier and Smith, 1978; Flanagan and Livingston, 1995; Renard et al., 1997; Kosmas et al., 1997; Boardman and Poesen, 2006; Cerdan et al., 2010) that enhanced the cognitive level of erosion processes in such environments. The dependence of the soil erosion magnitude on factors like climate, type of soils, topography and type of agricultural practices has been examined and broadly described in literature (Wischmeier and Smith, 1978; Morgan, 1996). Particularly,

the insights gained led researchers to understand the essential role of soil conservation practices in order to develop strategies to reduce the soil erosion phenomenon (Agassi, 1995).

The publication 'Soil erosion in Europe: Major processes, causes and consequences', edited by Boardman and Poesen (2006), is probably the most complete work about soil erosion in Europe. This collection of scientific findings in 33 European countries about soil erosion evidently shows the high polarization of soil erosion studies in agricultural environments. This has resulted in a significant displacement of studies on non-agricultural environments, although they can also be subject to severe denudation processes.

The vast amount of publications based on agricultural environments can firstly be amenable to economic reasons since approximately 40.5% of the territory of the European Union (22 countries) is used for agricultural production, covering between 7.3% (Finland) and 73.3% (Ireland) of the countries' area (Eurostat, 2009).

The second reason is mostly linked to the magnitude of soil erosion. In fact, in agricultural areas in Europe, especially in the Mediterranean region, individual rainstorms can result in 20 to 40 t ha^{-1} gross erosion (Morgan, 1992) with measured peaks of losses of more than 100 t ha^{-1} in extreme events (Morgan, 1992). Remarkably, extreme values up to 200 t ha^{-1} per rainfall event have been recorded in the southwest of France (Le Bissonnais et al., 2003).

According to the data collected by Cerdan et al. (2006) for 57 experimental sites spread across 13 countries, representing a total of 2162 plot-years, experiments in forested areas cover only about 2.5% of the total observations (see Table 2.2 and Table 2.3). Although this publication does not contain all of the studies performed in Europe, it still it offers a good idea about the forestlands that have been neglected.

Table 2.2 – Plot erosion rates for different land uses in the Mediterranean Region (Cerdan et al., 2006).

Land-use	No. of entries	Equivalent plot-year	Mean area	Mean slope length	Mean slope	Mean rainfall	Mean run-off	Mean erosion
	[-]	[-]	[m^2]	[m]	[%]	[mm yr^{-1}]	[mm yr^{-1}]	[t ha^{-1} yr^{-1}]
Bare soil	23	246	113.9	21	18	559	90.6	31.62
Vineyard	6	101	99.4	32.2	16.4	640	116.4	16.64
Vineyard + grass	2	6	100.0	41.8	23.5	582	33.3	1.92
Post-fire	8	112	1859.	11.3	28.7	466	40.2	1.54
Forage	9	192	500.2	34.7	17.3	661	27.6	1.35
Cereal	18	244	222.6	22.8	13.8	520	24.7	0.66
Shrubs	31	275	70.1	17	22.1	375	9.4	0.54
Grassland	11	142	180.8	22.9	15.6	564	16.9	0.42
Forest	4	46	65	13.8	19.9	334	8.6	0.15
Orchard	1	18	30	10	19	467	0.7	0.05
Total/Mean	113	1382	281.2	21.7	18.7	500	39.8	7.87

Table 2.3 – Plot erosion rates for different land uses in the other regions (Europe) (Cerdan et al., 2006).

Land-use	No. of entries	Equivalent plot-year	Mean area	Mean slope length	Mean slope	Mean rainfall	Mean run-off	Mean erosion
	[-]	[-]	[m²]	[m]	[%]	[mm yr^{-1}]	[mm yr^{-1}]	[t ha^{-1} yr^{-1}]
Vineyard	4	12	105	82.5	23.8	612	21.4	24.96
Bare soil	31	317	21.7	10.1	14.4	760	93.2	17.3
Maize	6	27	38.1	12.9	9.9	676	63.7	13.95
Spring crop	13	62	375.8	43.4	11	749	16.1	10.64
Cereal	18	91	3059.	52.6	11.6	739	11.6	3.53
Maiz + cover	3	21	21.2	10.9	8.7	560	19.9	2.65
Arable crop	6	139	16	8	10.8	862	42.2	0.53
Barley + cover	1	3	66.3	22.1	10	665	-	0.28
Shrubs	3	8	16	8	-	780	10.8	0.13
Vineyard + grass	3	6	105	76.7	24.3	608	1	0.02
Grassland	5	89	176.7	50.4	16.3	751	0.7	0.01
Forest	2	5	16	8	-	780	0.7	0.003
Total/Mean	95	780	691.8	30.1	13.4	738	43	9.83

With regard to Italian conditions, they do not significantly differ from the general European soil erosion research context. According to Rodolfi (2006), the process of soil erosion in Italy has been subject to scientific investigations since the 1930s, a time when the progressive reduction of cultivable surfaces for agricultural purposes was recognized. Since that time, the studies about soil erosion in agricultural areas have increased rapidly (Zanchi, 1993). This can be attributed to the crucial role that the high-quality agricultural production 'Made in Italy' plays in the economy of the country (Pratesi, 2007).

In non-agricultural Italian areas, a large emphasis was given to the most evident erosive forms in Italy. These are the badlands, typical geomorphological environments of the post-orogenic formations outcropping between the Apennine ridges (Castiglioni, 1986). The poor resistance of such environments to the morphogenetic agents and their rapid evolution has aroused strong interest in the major Italian geomorphology research groups. This situation has resulted in a vast amount of literature about the evolution dynamics of the badlands, locally called 'calanchi' and 'biancane', starting with the studies of Stefanini (1927), Castiglioni (1933), Passerini (1937) until the most recent studies of Torri and Bryan (1997), Moretti and Rodolfi (2000), Farifteh and Soeters (2006) and Della Seta et al. (2009).

So far, only a few studies have been developed for the Italian forested areas. Hence, research has only developed a rough understanding of soil erosion processes and their impacts for these areas. In fact, this situation is critical because about 23% (ISTAT, 2002) of the Italian territory is covered by forest vegetation and is highly exploited by silviculture and pastures practices (Ciancio and Corona, 2000). The Italian forests are 60% privately owned and about 53% is managed as coppice (ISTAT, 2002). The number of studies on

soil erosion in Italian forested mountainous areas is almost exclusively limited to a few studies carry out by the National Research Council (CNR) in some experimental sites of southern Italy (Iovino and Puglisi, 1991; Sorriso-Valvo et al., 1995; Porto et al., 2005; Garfì et al., 2006; Porto et al., 2009). The most recent research about soil erosion by water on a national scope funded by the Ministry of Public Education (project PRIN/COFIN 2002–2006) has involved seven academic research groups to evaluate the soil erosion risk in several Italian locations. However, none of these studies has focused on the accelerated soil erosion processes due to forest harvesting in forested areas. Moreover, most projects lacked direct measurements of soil erosion rates, preferring the application of GIS techniques and models for the indirect estimation of soil erosion.

2.7. SOIL EROSION IN FORESTED MOUNTAIN WATERSHEDS

The forested mountain areas play a very important role in the ecological cycle. Besides absorbing the CO_2 from the atmosphere and producing O_2 through the photosynthesis process, these types of ecosystems fulfill essential hydrological functions. They act as important sources of water supply and regulators of floods (Ferrari et al., 2004; Viviroli and R. Weingartner, 2004), providing high-quality water important for the integrity of the natural ecosystem and human beings (Foster, 1995). On a global scale, mountain areas covered by vegetation are considered to be the most important sources of drinking-water supply (Gomi et al., 2005). This is also the case for Italy, where many intra-mountainous watersheds are exploited not only for drinking water but also for hydropower, agriculture, industry and other purposes (Fanelli, 2000). Moreover, the forests regulate the time of concentration of the watersheds and the river water regimes through the reduction of overland flow (Bosch and Hewlett, 1982). This, in turn, facilitates the reduction of flooding (Anderson et al., 1997) and reduces the effects of erosion agents on the soils (Iovino and Marchetti, 2010).

Generally, it is assumed that forested mountain areas are rather unaffected by severe impacts of the soil erosion phenomena (Swanston, 1991). However, this is only partly true, inasmuch that this situation dramatically changes with regard to forest management practices (Stott et al., 2001). Using the erosion rates of 18 undisturbed forested watersheds of the USA, in his review study Patrick (1976) found values of erosion rates between 0.02 and 0.04 t ha^{-1} $year^{-1}$. Concerning Italy, Bazzoffi (1996, cited in van Rompaey et al., 2005) analyzed the annual sediment delivery of 40 Italian watersheds and reported annual sediment delivery values ranging from 0.1 to 5.6 t ha^{-1} yr^{-1} in semi-natural watersheds, without arable lands. These low erosion rates observed in undisturbed watersheds are justified because such mountain environments tend to be little affected by

soil erosion processes (Iovino and Marchetti, 2010). In support of this, soil erosion rates ranging from 1–5 t ha^{-1} yr^{-1} have been considered typical for the mountainous regions with normal vegetation cover (Patric, 2002) whereas sporadic mass movements (e.g., creep, mudflow and landslides) and the presence of areas poorly vegetated are the main cause of SY fluctuations (Swanston, 1991; van Rompaey et al., 2005).

In contrast, inappropriate forest management practices in mountainous watersheds can normally induce severe erosion processes with strong negative impacts on the environment (Stott et al., 2001). In the south of Italy, in the disturbed mountainous areas of Calabria, high erosion rates ranging from 100 to 150 t ha^{-1} yr^{-1} were observed during an experimental investigation by the National Research Council of Italy (CNR) (Sorriso-Valvo et al., 1995). Further studies carried out in Calabria's mountain areas by the CNR reported high erosion rates in poorly vegetated sectors (Porto et al., 2005; Porto et al., 2009) and apparent run-off increases in the first two years following the tree clearance (Callegari et al., 2001). As a positive effect researchers also observed a reduction of the erosion rates in areas under afforestation practices (Porto et al., 2009).

2.7.1. CAUSES OF SOIL EROSION IN FORESTED MOUNTAIN WATERSHEDS

According to Garcìa-Ruiz et al. (2005), the main risks for forested mountain watersheds are linked to the modern demographic growth that together with the socio-economic expansion are imposing fast changes to the land use and land cover in the landscape. These changes increasingly affect mountain environments where the modifications of forest management practices influence their main ecological and hydrological functions (Harden, 2001).

The most pressing impacts of anthropogenic origin for such areas origin from activities such as deforestation (Bosch and Hewlett, 1982), wildfires (Campo et al., 2006; Smith and Dragovich, 2008), forest road construction (Arnàez et al., 2004) and overgrazing (Strunk, 2003). Particularly, the clearance of trees is considered the main cause of accelerated soil erosion processes and the resulting landscape degradation (Walling and Fang, 2003). In fact, the key role the vegetative cover effect plays in natural environments for controlling hydric erosion has largely been documented (Bochet et al., 2006). In addition, researchers have observed unfavorable effects of the forest harvesting, coppicing and other silvicultural practices (Robichaud and Waldrop, 1994; Shaoshan An et al., 2008; Iovino and Marchetti, 2010).

Increases of the soil erosion rates associated with forest harvesting were found in several areas of the world including USA, New Zealand, England, Italy, Japan and Southeast Asia among others (Stott et al., 2001).

The factors that mostly determine the impacts of forest-harvesting activities are listed below:

– Forest harvesting strategy: Harvesting activities influence erosion processes in various ways. Firstly, the area management approach (Iovino and Veltri, 2004) and the specific methods of clear-cutting (Iovino, 2009) have a fundamental impact on the erosion process. Indeed, it has been shown that the erosion rates in clear-cut areas vary strongly with the application of either traditional or mechanized harvesting techniques (Murphy and Jackson, 1989; Marchi and Piegai, 2001), with the pattern of remaining trees *(*single or group) (Ciancio et al., 2006) and also with the structure formed by the discarded tree branches left on the hillslopes (Cantore et al., 1994). Secondly, independent of the applied harvesting technique the absence of vegetation cover exposes the forest soils which are often poorly covered by grass vegetation to the direct rainfall impact. In doing so, the vegetation removal alters the water balance (Table 2.4, Chapter 2.7.2) and the magnitude of the erosion (Table 2.5, chapter 2.7.2) processes in forests.

– Forest road construction: In general, a rather dense road network in the areas subject to forest harvesting allows for the movement of trucks and harvesting machines and the transport of the lumber. Several European (Arnáez et al., 2004; Jordán and Martínez-Zavala, 2008) and American studies (Swanson and Dyrness, 1975; Reid and Dunne, 1984; Megahan et al., 1986; Anderson and Potts, 1987; Baihua Fu et al., 2010) emphasized the negative effects of these with respect to water quality and threats of soil erosion. The forest roads, also if unpaved, may cause substantial changes in the local soil properties and the hydrogeomorphic behavior of the hillslopes (Gucinski et al., 2001). This can result in hydrological changes like the disruption of natural dynamics of the surface and subsurface flows (Tague and Band, 2001; Wemple et al., 1996). This involves a general increment of the overland flow that in turn can increase the sediment yield in the watersheds (Swanson and Dyrness, 1975; Wemple et al., 2001). In addition, the complex topography of the mountainous areas challenges the upward transportation of the necessary harvesting machinery. In order to deal with this, soils as well as unaltered rocks are excavated to provide solid paths for the lumberman and the harvesting machinery. Their size and specific forms depend on the type of harvest system. In the case of mechanized harvesting systems their amplitude can be about 2.5 m (observed during field surveys), resulting in a removal of about 4.5 m² of material (soil and rock) for every linear meter of paths. Both, the removed material as well as the paths themselves can become a major source of eroded sediments that may highly increase the SY in the drainage network of the watersheds involved in harvesting operations.

2.7.2. EFFECTS OF SOIL EROSION IN FORESTED MOUNTAIN WATERSHEDS

The increase of the erosion rate in forested mountain areas may result in in-site and off-site impacts. As in-site impacts, researchers have stated the general soil degradation (APAT, 2002), landscape aesthetic damages (Ceccarelli et al., 2006), breakdown of soil structure (Bryan, 2000), decline in nutrients and organic matter in the soil (Hornbeck, 1975), loss of biodiversity (Ciancio and Nocentini, 2004) and the alteration of niches for animals as well as biodiversity (Pimentel and Kounang, 1998). Further in-site impacts are the reduction of infiltration and water storage capacities (Iovino et al., 2009b), the possible formation of soil superficial crusts with consequent compaction of the soil (Moore and Singer, 1990) and significant run-off increases (Bosch and Hewlett, 1982). In contrast, off-site effects due to increased soil erosion on the hillslopes can result in ecological disorders on the river network (Marks and Rutt, 1997), increased suspended sediment concentrations (Stott et al., 1986), increased bedload transport (Newson, 1980), higher rates of channel bank erosion (Stott et al., 1997) and problems of fluvial eutrophication due to a higher amount of incoming nutrients (Sibbesen, 1995). Beyond that, sediments floating downstream into the drainage network can cause an infilling of the artificial lakes (Ciccacci et al., 1983) and reservoirs (Bazzoffi, 1996; A. Romero-Díaz et al., 2007). This accumulation of terrigenous material in the water reserve areas reduces their drinking water storage capacity, diminishes the function of the hydro-electricity dams (Fanelli, 2000) and can cause problems of channel instability (Poesen and Hooke, 1997). Especially in mountainous areas where the energy and river discharges can be very high, a reduced capacity of the drainage network retention may significantly increase the risk of flooding (Boardman et al., 1994) and muddy floods (Verstraeten and Poesen, 1999) with severe threats to human beings (Frattini et al., 2004).

Table 2.4 – Impacts of forest management practices on water balance processes.

Water balance processes	Impact due to forested area management	References
Precipitation	No effects	-
Evapotranspiration	Directly dependent on vegetation. Decreases as vegetation decreases.	Bosch and Hewlett (1982); Roberts (1983); Fritschen and Simpson (1985); Murakami et al. (2000); Borghetti and Magnani (2009).
Interception	Reduced by vegetative cover removal. Directly dependent on the vegetation type and density.	Grah and Wilson (1944); Teklehaimanot et al. (1991); Guidi and Manetti (1994); Wallace (1997); Baumler and Zech (1997); Iovino et al. (2009).
Infiltration	Generally high in the forested areas. Reduced by soil compaction due to forest harvesting activities and post-fire hydrophobicity.	Arend (1942), cited in Susmel (1968); Susmel (1968); Hover (1967), cited in Iovino et al. (2009); De Philippis (1970); Johnson and Beschta (1980); Croke et al. (2001).
Water storage and moisture content of soil	The natural dynamics are altered by vegetation reduction and exposure of bare soil. The increase of evaporation decrease the soil moisture.	Llorens and Gallas (2000);Beven (2001); Levia and Herwitz (2005).
Sub-surface flow	Alteration of the sub-surface flow dynamics. Decreases due to soil compaction and preferential flow paths occlusion.	Wemple et al (1996); Huang et al. (1996); Tague and Band (2001).
Overland flow	Overland flow usually increases in disturbed forested areas as a result of the changes in the above listed factors.	Hewlett and Hibbert (1961); Bosch and Hewlett (1982); Burch et al. (2007); Beven (2001); Stoneman (1993); Cantore et al. (1994); Callegari et al. (2001).
Channel flow	Generally increases of peak and river discharge occur.	Hewlett and Hibbert (1961); Hornbeck (1975); Bosch and Hewlett (1982); Stednick (1996); Brown et al. (2005); Iovino et al. (2009).

Table 2.5 – Impact of forest management practices on erosion processes.

Erosion processes	Impact due to forested area management	References
Detachment by rain splash erosion	Increased by a reduced vegetative cover.	Morgan (1978); Dissmeyer and Foster (1984); Ciampalini and Torri (1998); Teklehaimanot (2003); Novotny (1994);
Detachment by overland flow	Increased by an increase of overland flow volume. Both inter-rill and rill processes are involved.	Wischmeier and Smith (1978); Foster (1982); Rose et al. (1983); Kinnell (1990); Sorriso-Valvo et al. (1995); Bryan (2000).
Detachment in river network	Increased channel bank erosion rates due to increased discharge and water turbidity.	Stott et al. (1997b); Stott (1999); Green (1999).
Hillslope transport and deposition	The transport is increased by increased overland flow volume and flow turbulence due to raindrop impact on it and the hillslope characteristics. Decreased by increased hydraulic roughness resulting by increased slash deposition.	Wischmeier and Smith (1978); Bryan (2000); Sorriso-Valvo et al. (1995); Avolio et al. (1980); Edeso et al. (1999); Porto et al. (2009); Keim and Shoenholtz (1999).
Transport and deposition in the river network	The sediment transport is increased by increased detachment and transport on the hillslopes. Increased by channel erosion induced by increased channel flow. At the same time, the deposition is increased due the increased sediment delivery from hillslopes.	Stott (1997b); Newson (1980); Green (1999); Bazzoffi (1996); Cornish (2001); Iovino et al. (2009); Anderson (1976); Green et al. (1999); Ciccacci (1983).

Chapter 3

Study Area

3. STUDY AREA

This chapter introduces the major characteristics of the area chosen in order to perform soil erosion risk analyses in an Apennine environment. More precisely, the geological-structural setting, geomorphological and morphometrical features, the anthropogenic influence on the territory, land-use units as well as soil characteristics are presented.

3.1. LOCALIZATION OF STUDY AREA

The study site is located in the Upper Turano River Watershed, approximately 58 km northeastern of the city of Rome in central Italy. It is a tributary of the Velino River which in turn is the major sub-tributary of the Tiber River. The total surface of the area is about 466.7 km², situated between 41° 55' 20" to 42° 14' 60" north latitude and 12° 53' 36" to 13° 20' 20" west latitude (WGS-84). With an elongated and irregular shape, the watershed stretches in north-west/south-east direction for 47.3 km from its northernmost to its southernmost tip across the Latium-Abruzzi border. Furthermore, it is included in a mountain area of the Central Apennine. The intramountain basin (Conca di Oricola) that constitutes its central sector is spatially limited by the reliefs belonging to the Carseolani (N-E), Simbruini (S) and Sabini (N-W) mountain chains. The landscape within the study area is typical for the intermountain Apennine watersheds showing an evident heterogeneity of the geological, geomorphological as well as climatic and vegetation patterns.

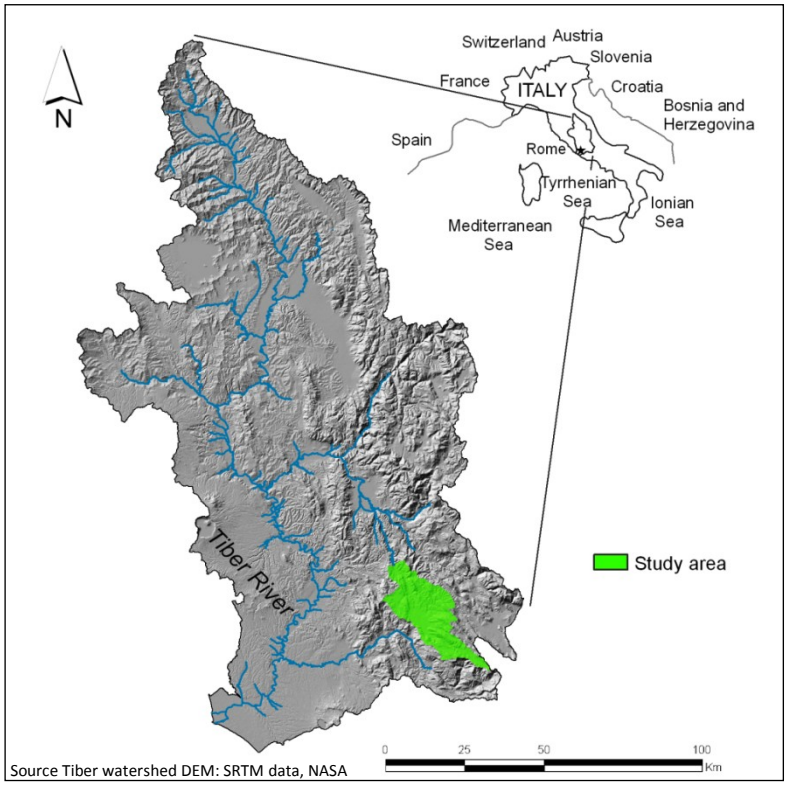

Fig. 3.1 – Tiber drainage basin and study site in the Latium-Abruzzi border, Italy.

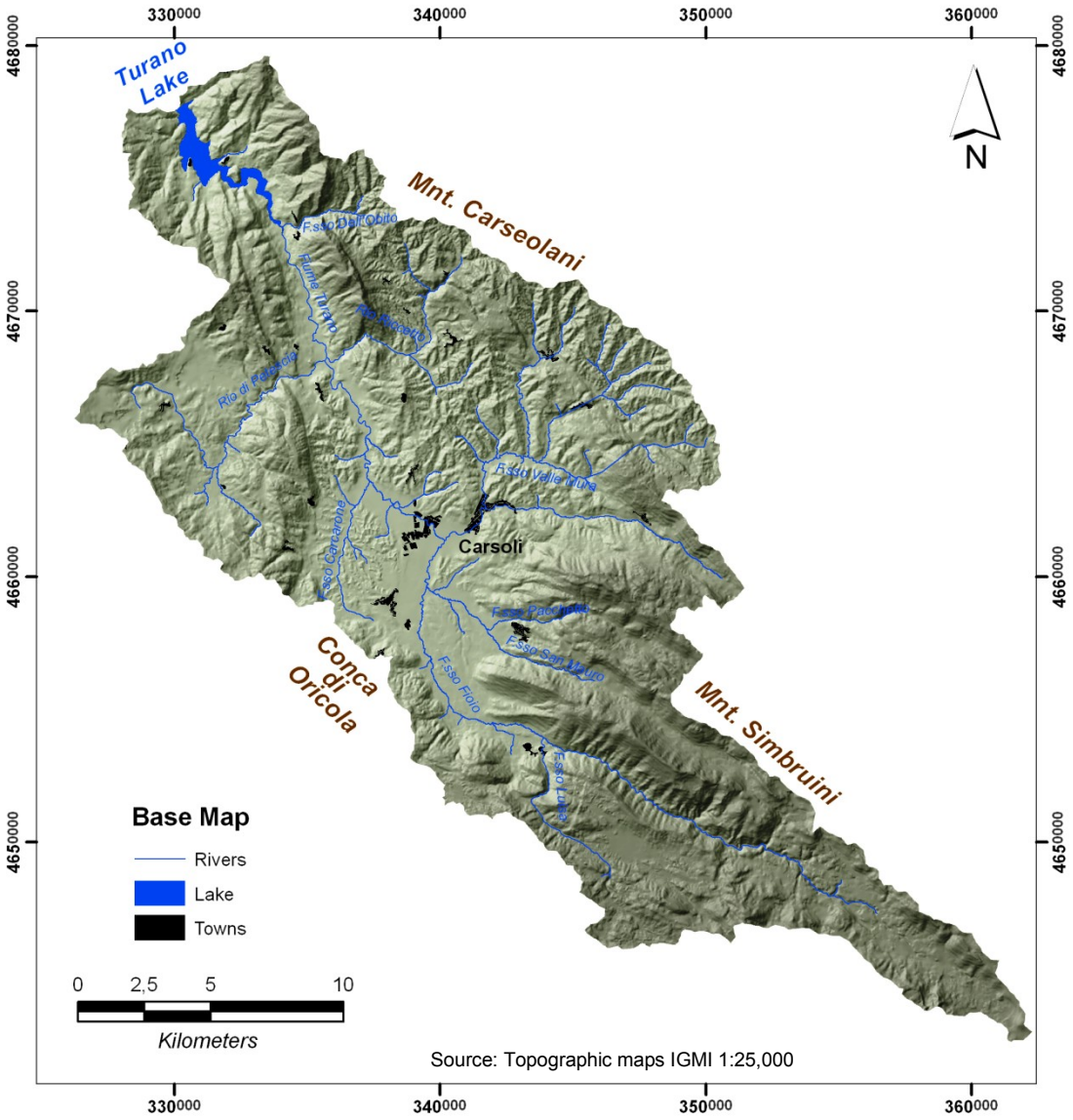

Fig. 3.2 – Turano watershed.

3.2. GEOLOGY

3.2.1. GEOLOGICAL-STRUCTURAL SETTING OF THE TURANO WATERSHED IN THE APENNINE CONTEXT

The drainage basin of the Turano River is located in the Apennines fold-and-thrust belt. It is a late-Oligocene-to-Present mountain belt relatable to the west-direction subduction of the Adriatic plate under the European plate (Doglioni, 1991). The mountain belt can be subdivided into three domains based on the differing structural styles, the central, the northern and the southern sector (Bigi and Costa Pisani, 2005). During the Neogene deformation of the area, lower-middle Miocene carbonate platforms widely crop out, particularly in the central and southern sectors (Corda and Brandano, 2003). In the central sector, where the Turano watershed is situated, one of this Miocene carbonate platforms together with the Sabina-Umbria-Marche basin succession form the two main

paleogeographic domains of the area (Accordi et al., 1988). This carbonate platform, called Latium-Abruzzi, consists of a 5000–6000 m thick pile of shallow-water carbonates, developed on a subsiding platform from the late Triassic to the late Miocene period (Bigi and Costa Pisani, 2005). A further characteristic of the described sector are the widespread siliciclastic turbidities that origin from the deposition processes during the foredeep stage of the platform evolution (Carminati et al., 2007). In contrast, the Sabina-Umbria-Marche domain is a Liassic to Eocene basin succession consisting of pelagic limestones, marls and siliceous rocks with an average thickness of 3000 m (Bigi and Costa Pisani, 2005).

According to the simplified geological map of the Central Apennine elaborated by Cavinato and De Celles (1999) (Fig. 3.3), the Turano watershed directly stretches across a contact zone between the two paleogeographic domains, i.e., where the Olevano-Antrodoco tectonic line crossing the northwest sector of the watershed defines the tectonic-stratigraphic limit (Martino et al., 2004). Based on this geological map the watershed can be divided into four main geological units:

- Carbonate-platform domains, Latium-Abruzzi Platform (Triassic-Miocene),
- Hemipelagites and synorogenic turbiditic sequences (Tortonian-Pliocene),
- Pelagic and transitional domains (Liassic-Miocene),
- Marine and continental deposits (Pliocene-Quaternary).

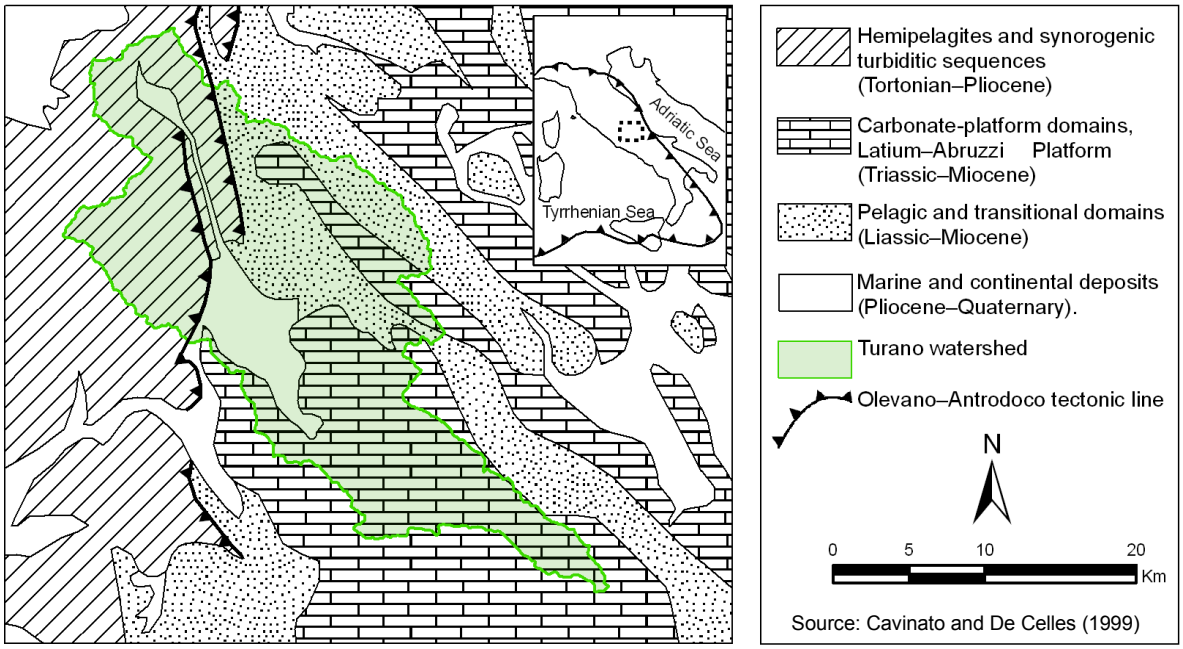

Fig. 3.3 – Turano watershed geological map derived from the geological map of Central Apennine according to Cavinato and De Celles, 1999. The insert shows the location of the map of the Central Apennine and the location of the Apennine subduction front.

At present, the area is complex in both, the morphology and its relief distribution. This is the result of recent tectonic movements, which are still responsible for diffuse crustal seismic activity and intense morphodynamic processes in the area (Martino et al., 2004).

The structural setting of the Turano watershed and the wider landscape of the Central Apennine is a consequence of two deformation events (Galadini et al., 2003) that modeled a Latium-Abruzzi paleogeographic unit which had already been divided into blocks in the upper Cretaceous period (Bono and Capelli, 1994). The first event, a compressive phase, lasted from the Miocene to the upper part of early Pliocene period whereas the second, an extensional phase, was initiated during the late-Pliocene and continued into the Pleistocene (Bigi et al., 1996). During the late-Miocene compressive phase, also known as translational phase, the area suffered a general shortening. As a result, the lithotypes of the marine facies present in the area became orogenetically elevated, folded and ruptured during this phase. This phenomenon becomes visible through the doublings of series present in the area. Moreover, it is evident from the overthrust located on the North-Oriental border, where carbonate structural highs overthrust the synorogenic terrigenous deposits (Bono and Capelli, 1994). The superimposition of the extensional tectonics phase (with a general uplift of the Apennine region) following the compressive period is due to the east-northeastward migration of the deformation fronts and the related foredeeps (Ricci Lucchi, 1986, cited in Carminati, 2007). This eastward migration of the Apennines fold-and-thrust belt was accompanied by extensional tectonics in the hinterland, leading to the progressive opening of younger back-arc basins. This back-arc basin system contains the Provencal (Gueguen et al., 1998), the Tyrrhenian and Tuscany basins and several intermountain basins along the Italian peninsula, among others the Turano basin (Bartole et al., 1995 Cavinato and De Celles, 1999).

In the specific case of the Turano watershed, the morphological formation of the area was conditioned by the activity of a normal fault situated on the northeast broadside of Turano Valley (Melchiorri, 1987; Galadini et al., 2003) (Fig.3.4b). The mentioned fault belongs to a NW-SE-oriented normal fault system (southwest dipping) that initiated the formation of several intramountain valleys (Salto, Liri, Turano, Aterno) and basins (Sulmona, Rieti, Fucino) in the vicinity (Cavinato and De Celles, 1999) (Fig.3.4a). In this way, this Apennine region is characterized by alternating NW-SE ridges (peaks over 2000 m a.s.l.) and valleys, of which the Turano watershed is a representative expression (Fig. 3.4c).

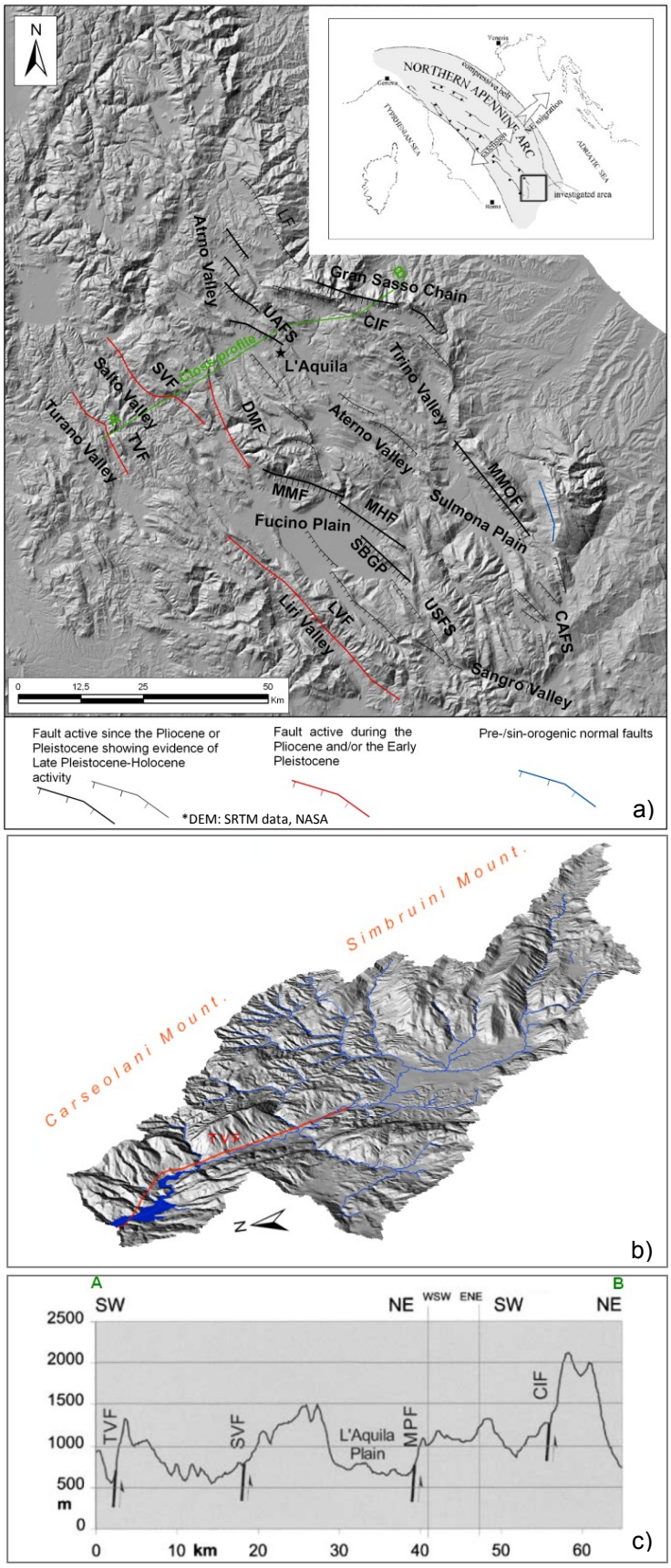

Fig. 3.4 – Map of the main Quaternary faults in the Apennine area around the Turano watershed (a) according to Galadini and Messina (2004). In maps 'b' and 'c' the 3D location of the Turano fault and its position in the cross-profile is shown.

3.2.2. LITHOLOGIC DISTRIBUTION AND CHARACTERISTICS

More detailed information about the lithotypes outcropping within the investigated area was taken from the geological maps (357, 358, 366, 367 and 376), scaled 1:50,000, which was provided by the CARG project (CARtografia Geologica). Figure 3.5, was created using ArcMap 9.3 and shows the distribution of the lithological substratum fit with the watershed scale.

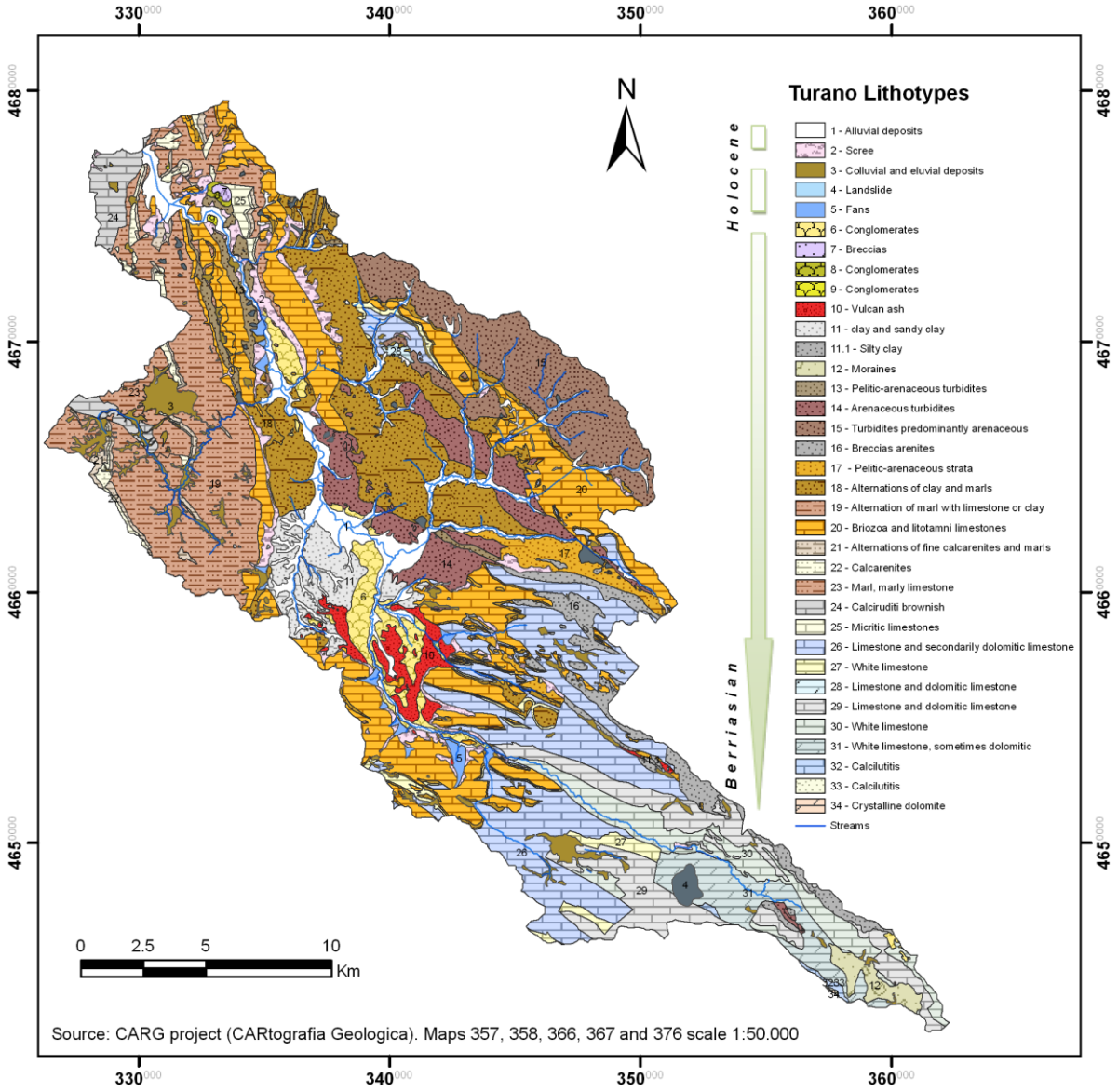

Fig. 3.5 – Detailed lithological map of the Turano watershed.

The geological maps reveal a significant heterogeneity and complexity of the lithology types. The stratigraphic series distinguishes several rock types covering the period from Berriasian to Holocene. Here, the fundamental units of the watershed are grouped based on their lithological characteristics: carbonate, arenaceous, marly and Quaternary deposits (complete list, Appendix A). These units differ in their mineral and petrographic

characteristics (Bertolani et al., 1994; Moscatelli et al., 2004), their hydrological behavior (Bono and Capelli, 1994), their response to the erosive agents (Angelucci et al., 1959) as well as the vegetation cover patterns (Abbate et al., 1994).

Pelagic and transitional domains

In the northwest sector of the watershed lithology types such as, marls, calcareous marls, clayey marls and subordinately calciruditic calcarenites and calcarenites (Mesozoic Era – Paleogene Period 65–23 million of years) can be found on the surface in a predominant way. Marl represents the wider lithologic type in this sector, where it adopts a greyish color and a thickness of about 450 m. It covers about 52 km^2 of a mountain sector ranging between 480 and 1400 m a.s.l. In contrast, calcarenites is the least-diffused rock in the area, appearing as thin lineations stretching from a S-W to N-E direction and covers about 8 km^2. The sector is, moreover, marked by Quaternary colluvial-eluvial deposits, mainly made of silts and sands.

Marlstone substratum sector Calcarenite substratum sector

Fig. 3.6 – Landscape characteristics in the Pelagic and transitional lithological sector (June, 2009).

Carbonate-platform domains, Latium-Abruzzi Platform

The sector that geologically belongs to the Latium-Abruzzi platform domain is the largest in the watershed. The Cretaceous (145–65 million years) carbonate formation shows indication of limestone, calcirudite and to some extent dolomitic limestones and dolomite that dominate the southeast sector of the watershed. The Miocene formations (Langhian-Serravallian 13.65–11.6 million years), in contrast, reveal litofacies of bryozoa and lithotamnium limestones of neritic formation (Accordi and Carbone, 1986) that sparsely outcrop in the central and northern sectors of the watershed. These formations cover an area of about 170 km^2, mainly within the contour lines of 1000 to 1900 m a.s.l. In this way, the limestone characterizes the higher ridges within the watershed.

The siliciclastic turbidites (mainly pelitic-arenaceous formations of the middle Miocene, Tortonian-Messinian 11.6–5.3 million years) cover an extended area of the central-eastern sector of the watershed. These units reach a thickness of about 800 m and originate from depositions during the foredeep stage of the platform evolution (Carminati et al., 2007). The elevation range of the pelitic-arenaceous lithotypes mainly ranges from 600 to 1000 m a.s.l. It constitutes a mountain area largely drained by rivers and with a comparably smooth relief with respect to the other mountain sectors within the Turano watershed. One can moreover observe another typical formation of the Latium-Abruzzi stratigraphic series, the Orbulina emipelagites marls (Serravalliano-Tortoniano 13.8–11.6 million years) between the siliciclastic turbidities and the bryozoa and lithotamnium limestones. The thickness of this sedimentary unit ranges from 50 to 80 m.

Carbonate reliefs in bryozoa and lithotamnium litofacies

Karst area of Monte Piano

Pelitic-arenaceous sector near the town of Nespolo

Pelitic-arenaceous outcrop near Pietrasecca

Fig. 3.7 – Landscape characteristics in the carbonat and synorogenic turbiditic sequences of the carbonate-platform domain (April, 2009).

The Quaternary deposits are largely composed of slope deposits related to gravitational movements, washout processes and torrential transport (APAT, 2008 – geomorphological

map 367). The valley bottoms near the sandy turbidities relief are generally filled by abundant Pleistocene and Holocene alluvial deposits (Colica et al., 1993; Barbieri et al., 1998). In certain areas post-orogenic lacustrine sediments of continental deposition outcrop. According to Colica et al. (1993), these units occupy a sizable sector of Turano Valley (next by Oricola). Covered by alluvial deposits these units are barely visible on the surface. Referring to Raffy (1982) and Colica et al. (1993), they are chronologically dated as middle Pleistocene. In contrast, Corda et al. (1986) dated these lacustrine formations as Plio-Pleistocene. Correctly dating these deposits is important in order to identify the lacustrine phases of the area as this, in turn, enables suitable evidence to be found to date the chain uplift (Galadini and Messina, 2004).

Landscape overview of the Conca di Oricola

Flat plain near the low Turano valley

Alluvial terrace reworked by gully erosion (Pietrasecca)

Colluvial deposit (Pietrasecca)

Fig. 3.8 – Quaternary deposits (April and June, 2009).

3.2.3. HYDROGEOLOGICAL PATTERNS

Figure 3.9 shows an approximation of the permeability patterns within the Turano watershed based on the lithological substrate characteristics. This map has been created to apply the permeability classes, which resulted from the hydrological study carried out by Agritec (2004) targeted at the enlargement of the Monti Cervia e Navegna Nature Reserve (northeast sector of the watershed), to all lithologies of the Turano watershed. According to the Agritec (2004) the lithologies were subdivided into six hydrogeological classes. The pelitic-arenaceous and marly rocks turned out to be the ones with the highest partial impermeability, with estimated hydraulic conductivity (Kh) values of about 0.00001 > Kh > 0.000001 cm s^{-1} and 0.003 > Kh > 0.000001 cm s^{-1}, respectively. The low permeability of the pelitic-arenaceous sector of the Turano found is consistent with the findings of Bono and Capelli (1994) carried out in the Carseolani Mountains.

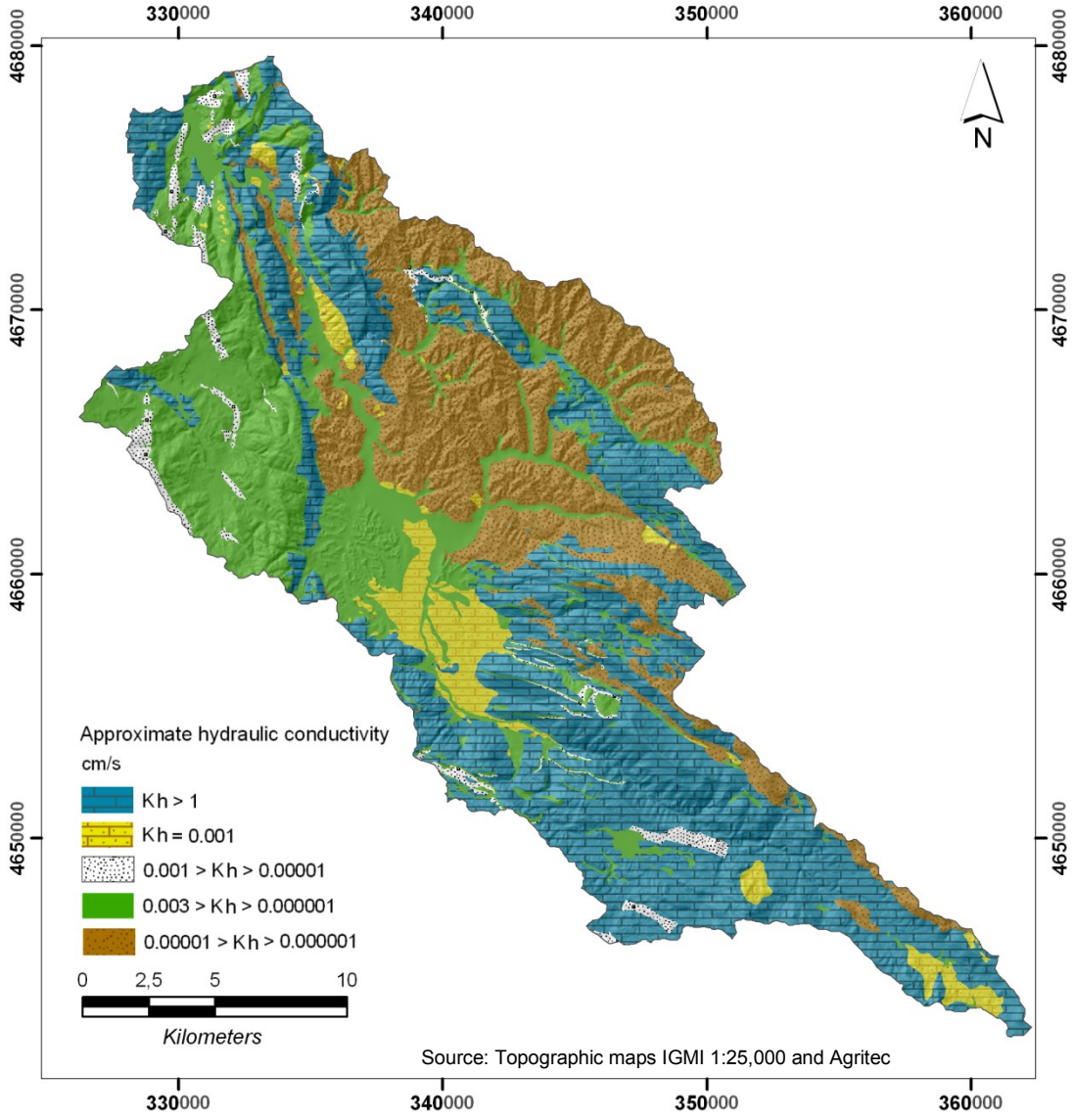

Fig. 3.9 – Hydrogeological patterns of the Turano watershed.

3.3. MORPHOMETRY AND GEOMORPHOLOGY

Physiographically, the watershed configures a long and narrow intermountain valley that stretches along SE-NW direction. The morphometry across the watershed highly differs, which is attributable to both the tectonic and lithological complexity of the area.

The territorial characteristics of the Turano watershed have been examined using a digital elevation model (DEM) generated from topographical maps (1:25,000 IGMI) with 10x10 m spatial resolution. According to the DEM, the relief distribution shows varying structures with the elevation ranging from 536 m a.s.l. at the lowest point (Turano Lake) up to 1907 m a.s.l. at the highest point (Monte Tarino). The average elevation, derived from the ipsographic curve, equals 983 m a.s.l. (Fig. 3.10). The hypsometric curve (Strahler, 1957) shows the trend of a watershed that has developed up to the point where it reaches the characteristics of the fluvial cycle of erosion in an advanced phase (Fig. 3.11). This is also confirmed by its hypsometric integral that equals 0.33. In addition, the convexity of the curve in its upper part raises the assumption of certain inhomogeneity within the watershed. A sub-watershed analysis also supported this inhomogeneity which was furthermore found by Avena and Palmieri (1969) in the adjacent Liri watershed. The north-central sector of the watershed is mainly included between the 450 m and 800 m a.s.l. isolines. In this sector of the watershed only 9% of the surface lies above 1000 m a.s.l., mainly situated in the carbonate heights of the mountains Cervia (1438 m a.s.l.), Navegna (1508 m a.s.l.) and Monte Piano (1118 m a.s.l.). Moving in a southeast direction the situation notably changes. Here, the relief stretches almost totally between 1200 m and 1600 m a.s.l., frequently overcoming the elevation of 1600 m a.s.l. consistent with the peaks of the Simbruini chain.

The relative relief (ratio of vertical difference in elevation between the highest and the lowest point and the drainage basin length) for the entire length of the Turano is 0.042 (Fig. 3.18). However, along the length profile the river shows different relative relief sections with values ranging from 0.017 to 0.032.

From the DEM the distribution of altitude levels, slope gradient and slope aspect derivatives were generated. In Figure 3.12 the elevation map is shown, while the chart provided in Figure 3.13 illustrates the distribution of altitude classes and its cumulative values.

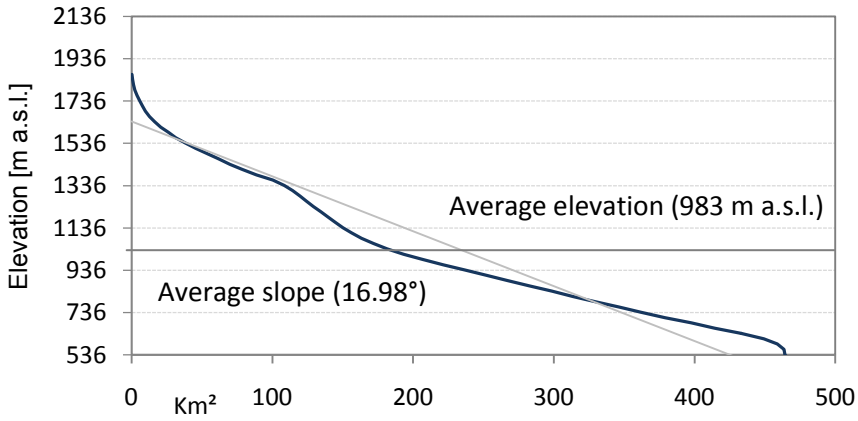

Fig. 3.10 – Ipsographic curve of the Turano watershed.

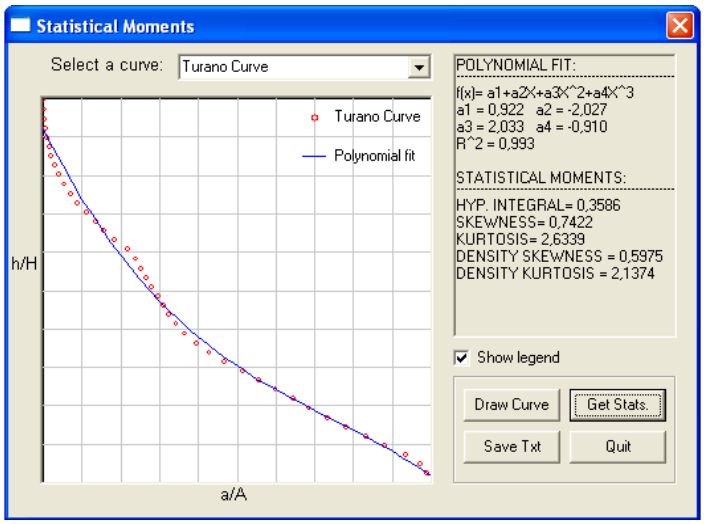

Fig. 3.11 – Hypsometric curves of the Turano watershed (CalHypso – Pérez, 2009).

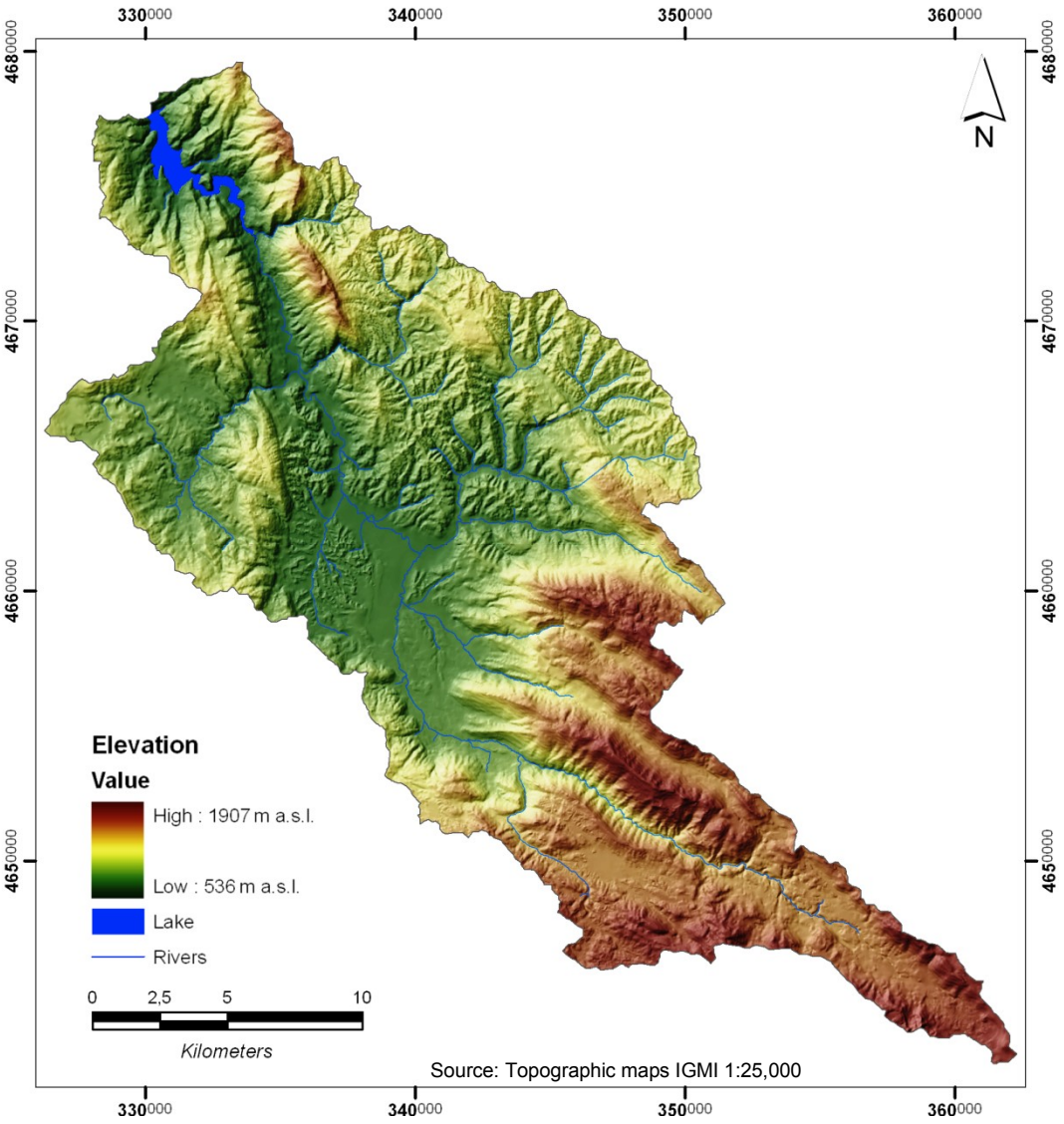

Fig. 3.12 – Digital elevation model of the Turano watershed.

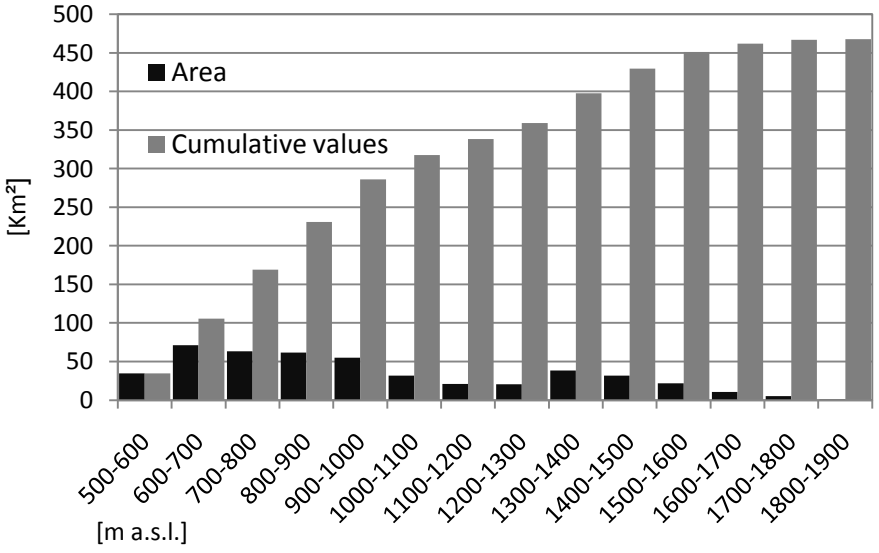

Fig. 3.13 – Distribution of altitude classes of the Turano watershed.

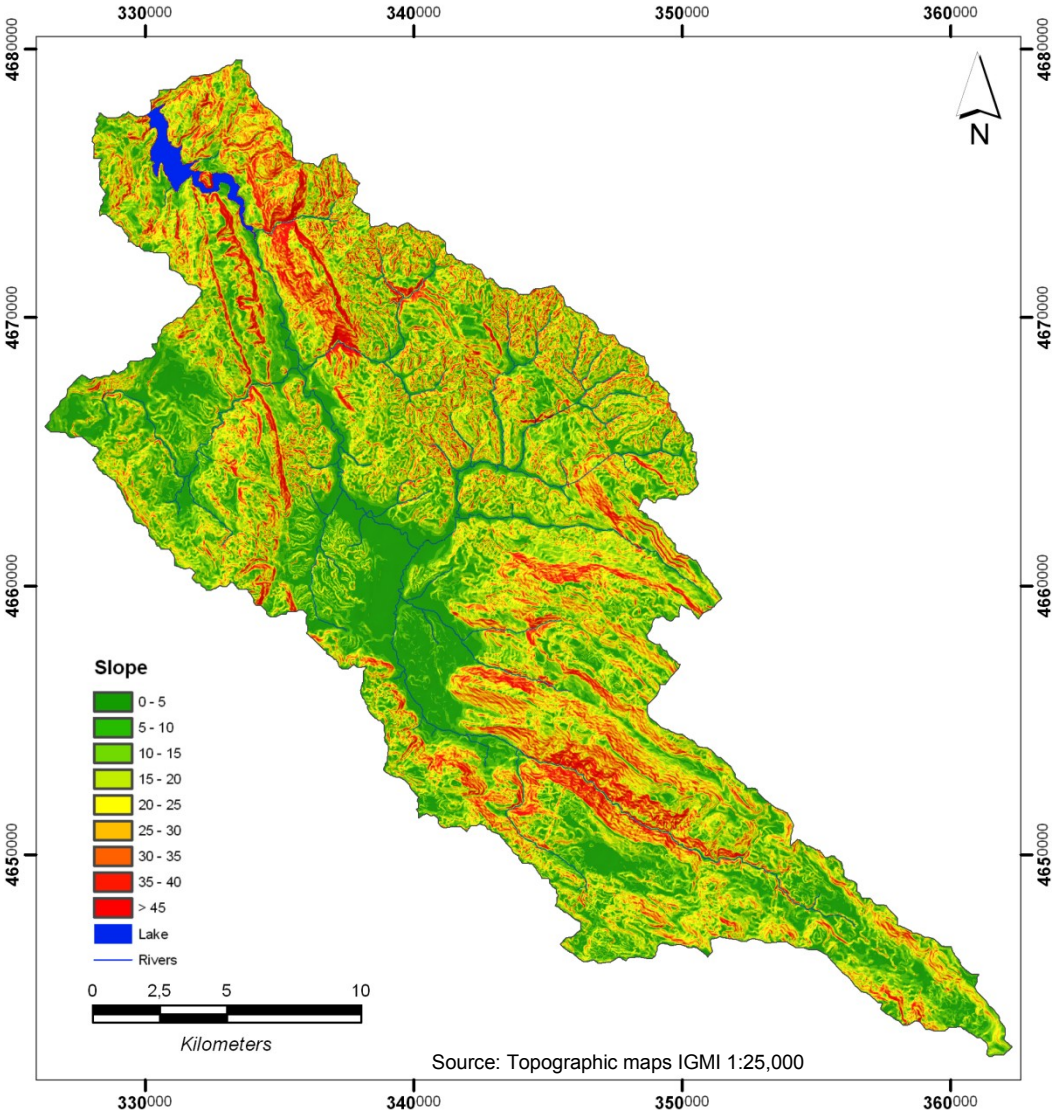

Fig. 3.14 – Slope gradient map of the Turano watershed.

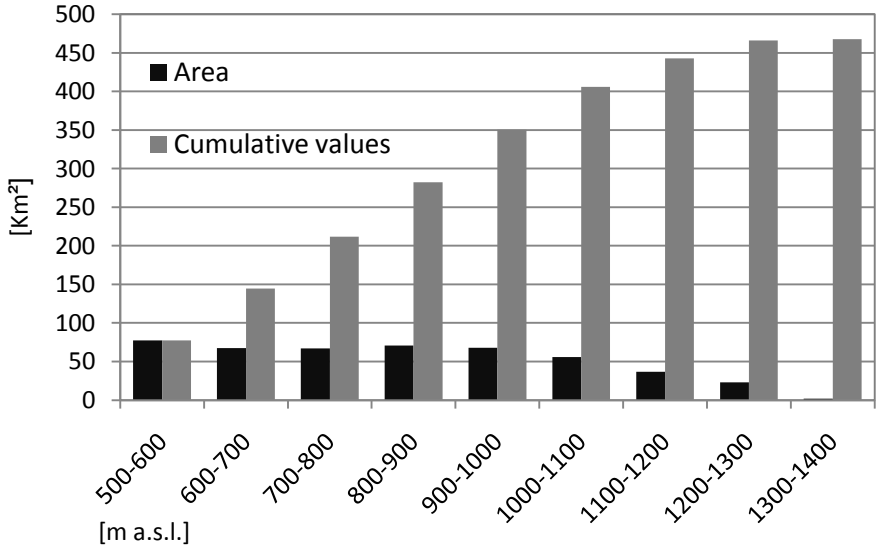

Fig. 3.15 – Distribution of slope gradient classes of the Turano watershed.

The slope gradient map (Fig. 3.14) provides information about how the steepness of the slopes follows the relief distribution and the geological background in the Turano watershed. About 64% of the area can be classified as moderate slopes with inclinations between 10° and 35°. Approximately 5% of the area shows slopes with an inclination higher than 35°. These areas with a high slope gradient are exclusively in places where the highest carbonatic ridges are located. The areas with a slope inclination lower than 10° cover 31% of the watershed surface. These low slope gradient values are typical for the valley bottom filled by Quaternary alluvial deposits. Spatially, numerous deposits of alluvial origin can be identified. They can reach remarkable dimensions which is particularly true in the proximity of the watershed sectors formed by sandy turbidities lithological substrate. Furthermore, the biggest physiographical unit of the Turano watershed with slope values lower than 10° is the intermountain basin of Oricola. It is situated among the towns of Oricola (W), Carsoli (N-E) and Rocca di Botte (SW). Notably, as previously mentioned this unit is a typical intermountain basin of the Central Apennine composed of fluvial and lacustrine Plio-Holocene sediments. It is approximately 34 km² in size which equals 7.3% of the watershed surface. The area shows fluvial accumulation terraces that surround the Turano River drainageway that can also be observed in the proximity of its main tributaries. In this sector of the watershed the alluvial terraces reach a high thickness and complexity as described by Colica et al. (1993). Excluding the Quaternary deposits due to their low inclination (up to 10°), considerable slopes of the watershed can be classified as morphologically mature.

The slope aspect exposure of the Turano watershed slopes is distributed in a rather homogeneous way with respect to the four cardinal points (Fig. 3.16a). The northwest-exposed slopes are the most frequent (17.5%). Contrarily, slopes exposed in a south and southeast direction are less frequent (8.5 – 10%). Both, slope aspect exposure (Fig. 3.17) and the frequency distribution of the average slope angles (Fig. 3.16b) confirm the structural conditioning of the area that shows the characteristic SE-NW-oriented trend of the Apennine sectors and is consistent with Centamore et al. (1996).

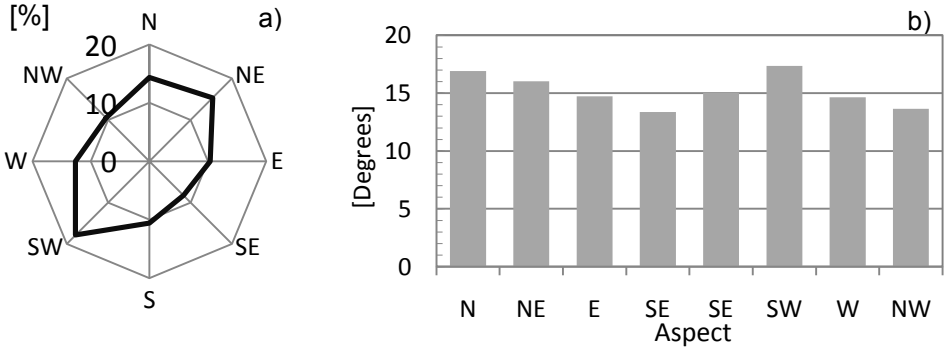

Fig. 3.16 – Frequency distribution of mean slope angle (b) with respect to aspect (a).

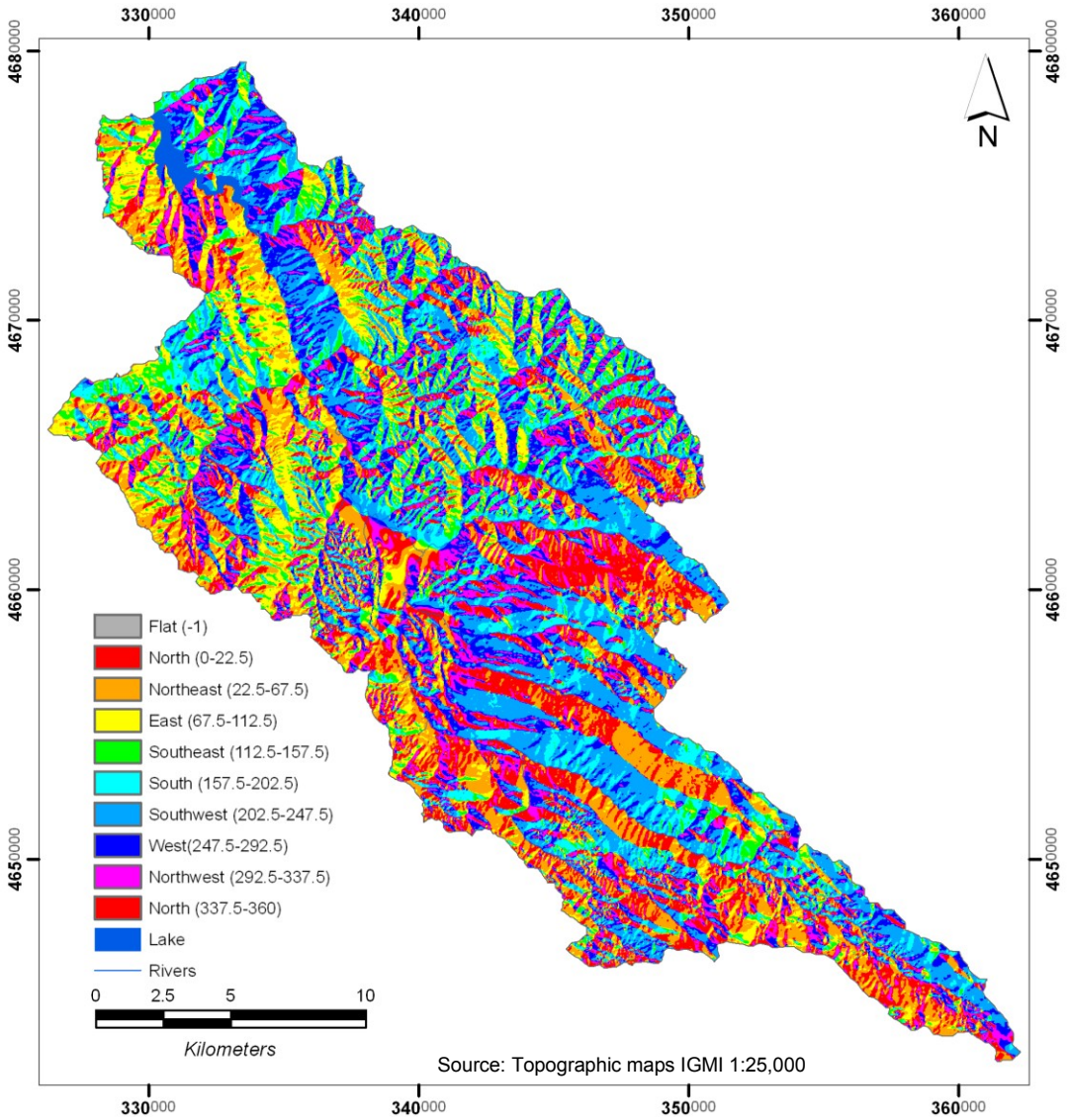

Fig. 3.17 – Distribution of slope aspect classes of the Turano watershed.

The lithological factor, intended as the response of the rocks to the exogenous agents, can be identified as the main driver of the different conformations of the morphology within the study area. Different inclination patterns of the relief slopes composed of siliciclastic turbidites, limestones and marlstone can be observed. The chemical and petrographic characteristics of the rocks have a great impact on the relief, its local slope gradients and the type and location of the Quaternary deposits. Due to its geomorphological landforms, the turbidite lithological sector, in particular, shows poor resistance to weathering processes. Here, a dense system of elongated and narrow valleys, often of considerable steepness, characterizes the area. Some sporadic slopes in the areas where the layers are more pelitic indicate the typical rapid morphological evolution of the badlands of the Pliocene clay (Stefanini, 1921). To a limited extent, these forms can be observed in the proximity of the towns Tufo and Pietrasecca. Similar morphological conditions appear in

the northwestern sector the watershed mainly composed of marlstone substrata. This area is primarily modeled by fluvio-denudational geomorphological processes. Here, gravitational processes related to earth flow mass movement in the presence of the rocks with higher clay content can be identified. According to the ISPRA database (2010), in this watershed sector the highest concentration of mass movement occurs, while these movements have minor impacts in the rest of the investigated area. In contrast, the limestone sector generally shows a more compact structure. The erosive effects of the rainfall and the overland flow are significantly lower. This situation is amenable to the higher cohesion and infiltration capacity of these lithological formations. As a consequence, these rocks result considerably less incise by the concentrated surface overland flow. However, this sector is characterized by epigean karst. Several dolines and poljes are present in karst territories, such as Monte Piano, Colle delle Pagliere, Prato di Camposecco and Tre Confini. In addition, a highly evolved hypogeal karst system characterizes both, the Miocene as well as the Cretaceous carbonate formations of the area (Bono and Capelli, 1994; Agostini and Rossi, 1986; Angelucci et al., 1959). Finally, broad slope deposits in conformation of talus pile can be found close to the bryozoa and lithothamnium limestone formation being more concentrated at the eastern slopes.

With regard to the drainage network, it has a main stream of 7th order flowing in a SE-NW direction. This stream has a length of about 57.8 km starting from an elevation of 1.390 m a.s.l. in the Simbruini Mountains (Monna di Campo Ceraso) ending in Turano Lake at about 536 m a.s.l. The average slope of the stream is low, being about 0.91° (Fig. 3.18). In addition, the drainage density (Dd, Horton, 1945) of the whole watershed is not particularly elevated. With a value equal to 4.17 km/km² the Turano shows the pattern of a watershed moderately drained. Yet, the situation changes significantly if the Dd values of the different lithological sectors of the watershed are considered. In correspondence with the turbidite sector, a higher Dd value equal to 6.4 can be found. Contrarily, in the other lithological sectors of the watershed the Dd values range between 1.6 for the calcarenite and 3.2 for marl. The stream frequency (Horton, 1945) and drainage texture (Smith, 1950) calculations provide values of 14.9 and 62.1, respectively.

Moreover, the drainage system generally shows a dendritic pattern. Examined in greater detail, it also shows local variation of the pattern types. In the headwaters of the watershed morphological structures different from the dendritic type are particularly evident. Here, the Cretaceous carbonate lithology is dominant and parallel, sub-parallel and sometimes rectangular patterns can be observed. Furthermore, considering the azimuthal trend of the higher hierarchic order streams (Strahler, 1957), they generally follow the typical SE-NW Apennine direction or SW-NE anti-Apennine direction. In fact, that means that the

development of this kind of stream depended and still depends on the influence of the tectonic and the faults system of the area. This fact is emphasized by the analysis of the azimuthal distribution frequency of the fluvial streams (Fig.3.19).

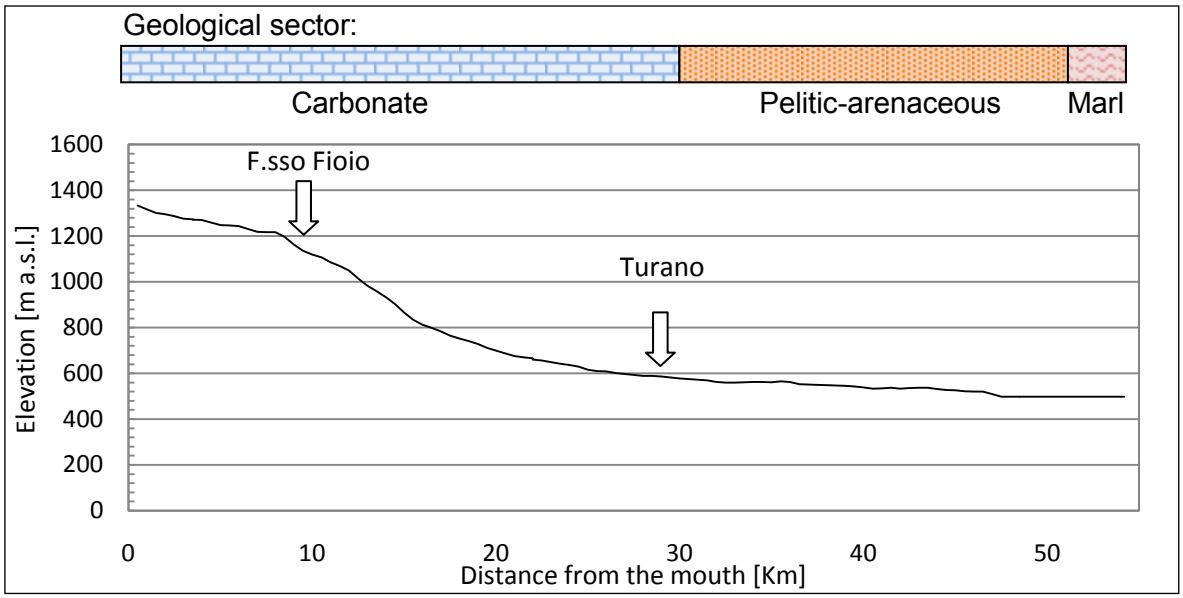

Fig. 3.18 – Longitudinal profile of the Fosso Fioio and Turano River.

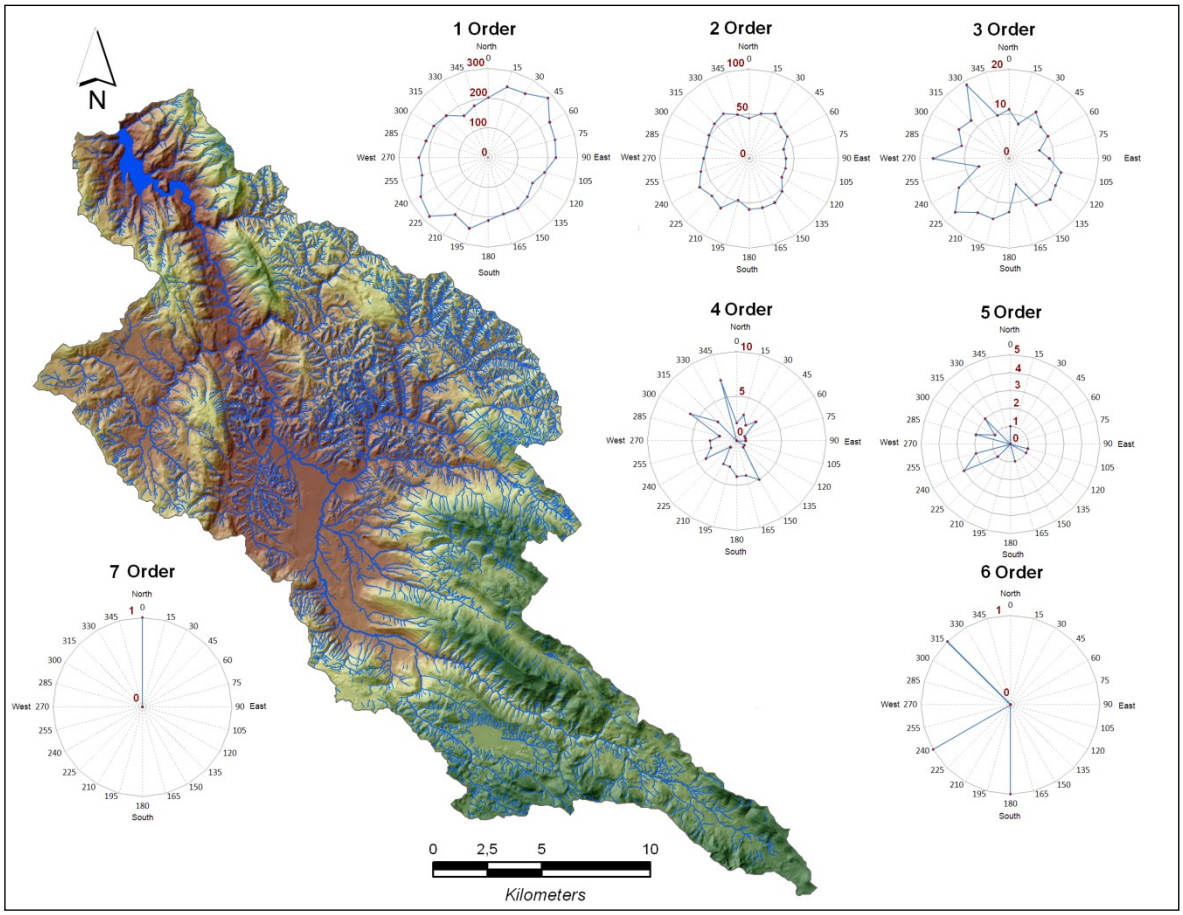

Fig. 3.19 – Azimuthal distribution of the ordered streams (Strahler, 1957).

The final section of the river is made up by Turano Lake, an artificial reservoir resulting from a dam built in 1939. The surface area amounts to 3.27 km² while the elevation level of the water (dam level) oscillates from 495 to 540 m a.s.l. The maximum depth of the lake is about 60 m.

Finally, Table 3.1 sums up various morphmetric characteristics of the Turano watershed. As an addition, Appendix K deals with the morphmetric characteristics of each individual sub-watershed. Appendix B shows the map of the geomorphological units (APAT, 2008) with modifications by the author.

Table 3.1 – Morphometric characteristics of the Turano watershed.

Properies	Values	References
Basin area, [km²]	466.7	-
Basin perimeter, [km]	148.7	-
Basin length, [Km]	47.3	-
Highest point, [m a.s.l.]	1907	-
Lowest point, [m a.s.l.]	536	-
Mean elevation, [m a.s.l.]	976	-
Basin relif, [m a.s.l.]	1371	Hadley and Schumm (1961)
Relief ratio	0.042	Schumm (1963)
Turano lake area, [Km²]	3.27	-
Area with slope < 10° [Km²]	144.4(lake excluded)	-
Area with slope > 10° < 30° [Km²]	284.7	-
Area with slop > 30° [Km²]	33.4	-
Number of streams	6944	-
Main stream length, [Km²]	57.8	-
Main stream slope, [Degree]	0.91°	-
Drainage density, [km/km²]	4.17	Horton (1945)
Stream frequency	14.9	Horton (1945)
Drainage intensity	3.57	Faniran (1968)
Drainage texture	62.1	Smith (1950)
Form factor	0.21	Horton (1945)
Elongation ratio	0.52	Schumm (1956)
Basin circularity ratio	0.27	Strahler (1964)
Gravelius index	1.92	Gravelius (1914)

3.4. LAND USE

3.4.1. SETTLEMENT DYNAMICS AND SOCIO-ECONOMIC CHARACTERS

The study site has been affected by anthropogenic activities ever since the ancient period. There is evidence of human activity during the Classical, Middle Ages and Modern periods in the area (Sciò et al., 2000). In the Turano Valley, several structures built during the Roman period, such as roads and villas as well as a temple, are still visible. The city of Carsoli itself, known by the Romans formally as Castum Soils, testifies the Roman presence in the area (Sommella, 1988). According to Cato (cited in Carrozoni, 1986), there were already settlements of ancient Italian populations in this area during the VIII century BC, assumingly the Sabines (Strabo, V book) and Aequi (Grossi, 1991).

The present settlement dynamics are still strongly linked to the historic ones. In the past, beginning from the III century BC, the spatial distribution of the villages initially followed the Roman pattern of rural settlement. During this time the areas selected for settlements were primarily located in the proximity of rivers along the main Roman roads (Cristallini et al., 2002). After the foundation of Carsoli in 303 BC (Livy, 59 BC – AD 17, cited in Giovannoni, 2003), the alluvial plain of the Turano area, characterized by a flat surface with good water resources and also close to an important Roman consular road, Via Tiburtina, offered an optimal environment for settlements. Thus, the valley sector of the Turano watershed was widely inhabited. Castum Soils could have been the main settlement of the area given its strategic location next to the Piana del Cavaliere (sector of the Oricola intermountain basin). This Piana, a secluded valley on the eastern side only accessible from the western side, offered a naturally well-protected location for the Roman military outpost in battles against hostile populations of the Italian Peninsula hinterland (Maialetti, 2001). This Roman rural settlement type, characteristic for the area until the X century AD (Cristallini et al., 2002), gradually shifted to a model based on hill fortresses. This settlement technique, known as encastellation (Cristallini et al., 2002), significantly and enduringly changed the landscape of the Sabine territory during the Middle Ages (De Meo, 2006). According to literature sources, the encastellation process of the Turano watershed mostly occurred between the X and XI century BC conducted by powerful local noble families (Cristallini et al., 2002). During this morphological evolution stage of the settlements in the area some ancient Roman towns were further fortified (as Carsoli) while others were built ex-novo in areas not easily accessible and hitherto uninhabited (Toubert, 1993). In this historical phase, the fortresses were secure shelters for the people and became important centers of attraction for the rural population scattered across the countryside (Toubert, 1993). Today, the larger towns of the Turano watershed are the result of the fortresses of the Middle Ages, e.g., Carsoli, Castel di Tora, Collalto, Rocca di Botte, and Pereto.

Today, the relatively low number of inhabitants in the area amounts to about 13,500 (I.S.T.A.T. 2005 – National Institute of Statistics) thereof 5841 registered in the municipality of Carsoli. The population density in Carsoli equals 61.5 inhabitants per km² compared to 28 inhabitants per km² in the entire Turano watershed. The low population in the area can be attributed to the economic difficulties that the Italian Apennines mountain areas have historically been confronted with (De Vecchis, 2004). Moreover, starting in the 1960s, the Turano population, like many other populations of the Apennines intermountain areas, suffered from a strong demographic decline caused by an emigration of the local population to the bigger cities. For the Rieti Province (2002), a population decline of about 40% with local emigration peaks of 80% (city of Paganico) has been recorded for the second half of the twentieth century. The downsizing of the population has led to an abandonment of traditional family farms. Yet, there has been an increase in the land controlled by agricultural companies resulting in increased monocultures. At the same time, the land left uncultivated has been recolonized by forest vegetation as described by Abbate et al. (1994) in some places near the town of Pietrasecca.

However, although the area is not intensively inhabited at present, the landscape clearly reflects the influence of human activities over the centuries. The Quaternary deposits of the valley bottoms with weak slope gradients have traditionally represented the best places within the watershed for the agricultural production. Columella and Pliny the Elder in I century AD (E. Pais, 1923, cited in Sciò et al., 2000) described the fertility of these areas. Ovid (43 BC – AD 18, cited in Maialetti, 2001) mentioned the cold autumn-winter climate, inappropriate for the olive farming but optimal for the wheat production (during summer). During past centuries, the hilly areas ranging from 500 to 700 m a.s.l. in the vicinity of the inhabited areas have been exploited for agricultural purposes, as well as for grazing. In order to enable this, Avesani (2009) argued that large deforestation and terracing activities must have been carried out during different historical periods, especially in the Early Middle Ages.

Today, the flat areas of the valley bottoms are the watershed sectors used mostly for farming, to cultivate the crops of traditional Italian farming such as tomatoes, corn, eggplant, zucchini and several other vegetables. Notably, on the one hand some agricultural sectors in the flat plains were equipped with irrigation systems and exploited by intensive farming. However, on the other hand, the hilly agricultural production decreased. Most of the hilly areas in the past used for farming have today been recolonized by natural vegetation. The sunny hill slopes, as the only exception, are occasionally used for olive-tree plantations or grazing.

The medium-elevation forested areas (800–1000 m a.s.l.) are also included in the economic system of the area by using them for silvicultural practices. Passing through the forest roads in the north-central sector of the watershed, several areas are regularly cut to keep them clear of low vegetation in order to facilitate the collection of truffles and chestnuts. Moreover, several coppice tree areas in this elevation range are exploited for both firewood and charcoal production. From the ancient time on, forest harvesting of the coppice trees has traditionally been practiced in the area. These past activities of loggers, as well as the collection of the other forest products (mushrooms, truffles, chestnuts etc.), have been confirmed by historical documents and maps of the footpath network of the area (Avesani, 2009). Additional evidence of logger activities in the area is stated in the epigraphies (C.I.L, IX; 4008, 4071, cited in Sciò et al., 2000) where the presence of *fabri tignari* (carpenters) and *dentrophori* (lambermen) was mentioned. The intense and prolonged use of the forested areas also implied that undisturbed forests have only remained in places of secondary importance. In other words, the natural wood coverage has not been subject to human alteration only in the most impervious and difficult-to-access areas of the watershed.

3.4.2. LAND COVER UNITS

At present, according to the map of land use and vegetation created for this study (Fig. 3.20) the Turano watershed is mainly covered by forested vegetation. In diverse forms the forested surface covers about 288.7 km² (61.7%), leaving mainly valley areas uncovered. Agricultural fields cover a total surface of 59.2 km² (12.64%) spatially concentrated, as mentioned above, in the areas with favorable geographical characteristics. Based on the types of agricultural use the farm fields can be classified into permanently irrigated land (58.1%), non-irrigated arable land (29%), complex cultivation patterns (0.1%) and agriculture with natural vegetation (12.8%). Furthermore, other agricultural areas have been classified into olive trees (0.72%), vineyards (0.01%) and fruit trees (0.04 %). Other types of semi-natural vegetation areas used for grazing comprise to 9.9% of the study area. Both continuous and discontinuous urban settlements stretch over a surface of about 5.8 km², equivalent to 1.2%.

The spatial distribution of the towns and population are particularly concentrated in the Oricola intermountain basin. Furthermore, rather evenly distributed towns can be found in the north-central sector of the watershed whereas the south-eastern mountain sector shows only sporadically isolated buildings. Yet, the road system appears to be quite dense, stretching over a total length of about 1200 km. Approximately 0.6 km² of principal roads, 2.3 km² of paved roads and 3.9 km² of unpaved roads have been estimated.

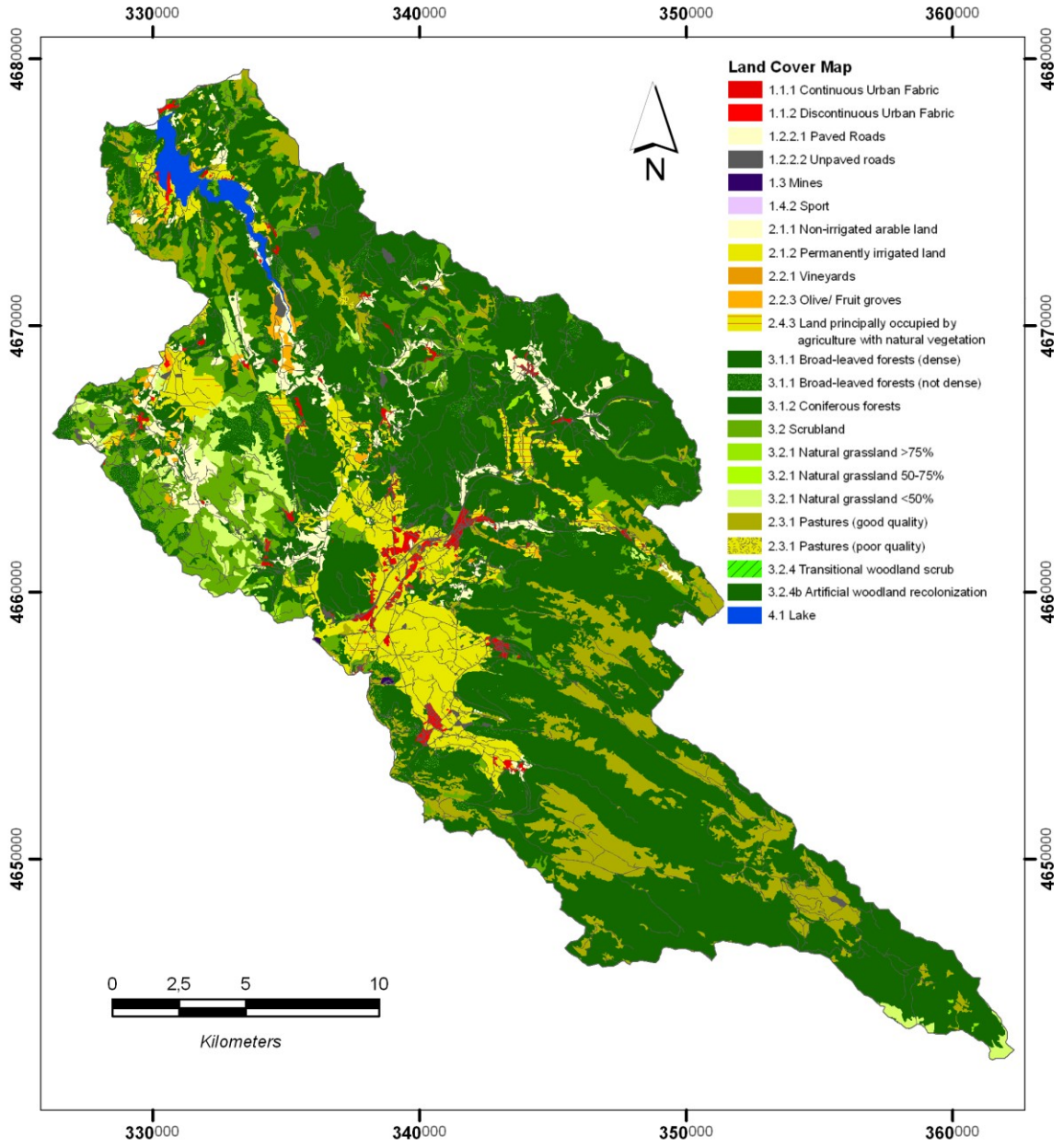

Fig. 3.20 – Land use map made by visual interpretation of orthophotos (2001 and 2005).

As the coppice woodland has largely been harvested in the area, for the purpose of a quantitative and qualitative classification of this silvicultural practice a map of coppice harvesting during the period of 1997–2005 was created. This was realized through visual interpretation of aerial orthophotos and supervised classification of Landsat satellite images.

According to this map (Fig. 3.21), within the Turano watershed the forested sector exploited by timber production covered about 19.4 km², mainly composed of Quercus *cerris*, *Ostya carpinifolia* and *Quercus pubescens* trees and to a lesser extent of *Castanea Sativa* trees. Most of the harvested trees were located on hillslopes with slope gradients ranging from 15 to 25°, which equals 38.4% of the total clear-cut surface. In contrast, the

figure for harvesting activities that focused on forested areas with an inclination greater than 35° was about 5.7%.

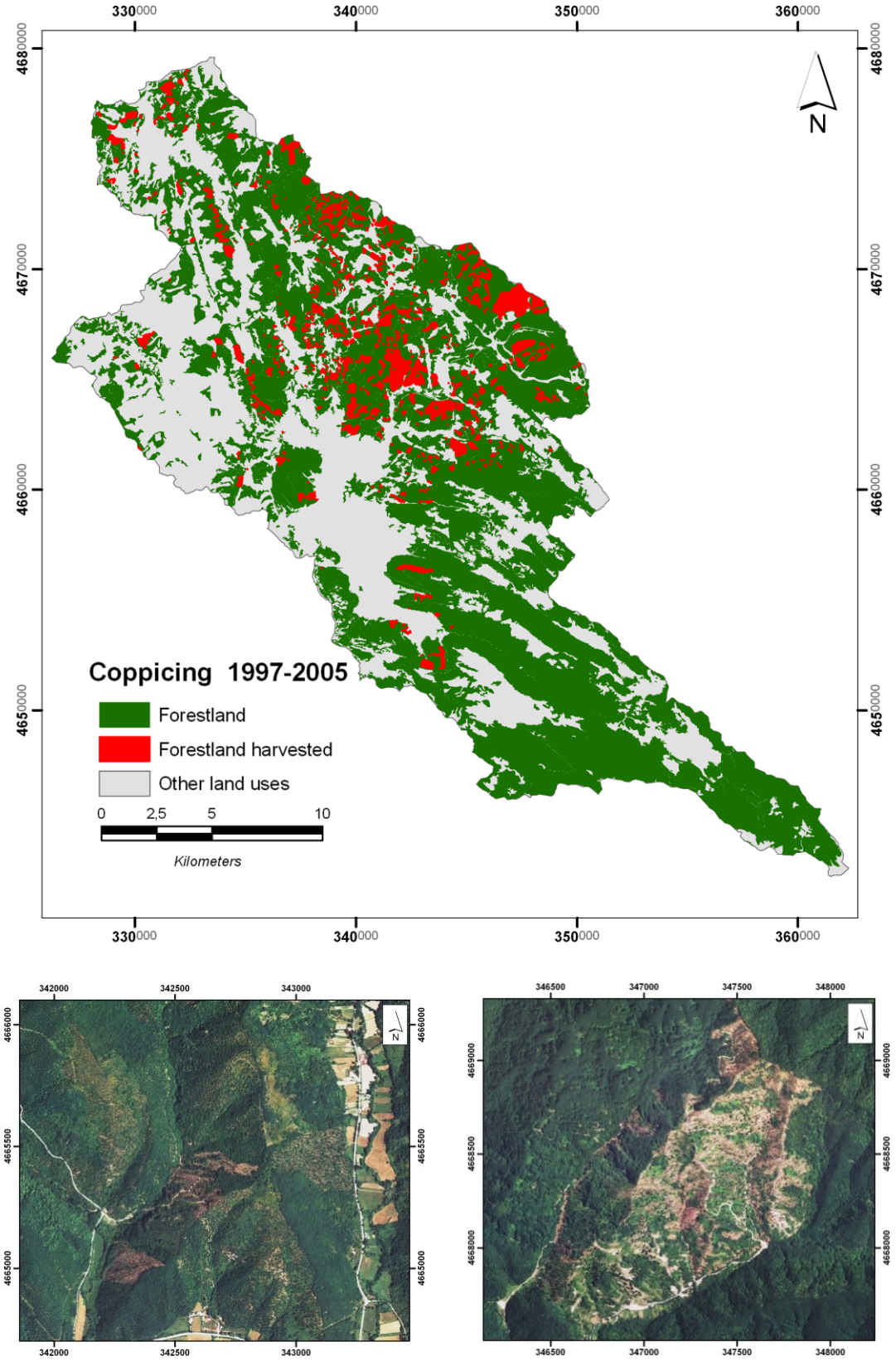

Fig. 3.21 – Forest-harvesting activities from 1997 to 2005 in the Turano watershed.

Fig. 3.22 – Forest hervasted near Carsoli (December, 2009).

3.4.3. DISTRIBUTION OF NATURAL VEGETATION

The natural vegetation of the Turano watershed follows the typical features of the landscape in the Central Apennine chain. Coherently with the relief morphology, it is predominantly covered by mountain and sub-mountain woodlands (Tonelli, 2007). As a matter of fact, the land-cover map (Fig. 3.20) indicates that forested area dominates the watershed with an extension of about 288.7 km² ranging from 600 to 1700 m a.s.l.

Furthermore, with respect to the maps of topographic and vegetation types the most widespread forest plants at low to medium elevation, 600–1000 m, are the *Quercus cerris* and the *Ostya carpinifolia*. These types of mesophile forests, which are also to a lesser degree complemented by Acers and *Carpinus betulus*, populate the shadowy hillslopes and the land with more acid rocks (Tonelli, 2007). Contrarily, the lower elevations particularly on the sunny calcareous slopes are mostly populated by *Quercus pubescens* and others thermophilous oaks. Yet, wide sectors of mesophile forest have been replaced by *Castanea sativa* by means of human intervention (Province of Rieti, 2002). In the areas at higher elevations, the population of *Quercus cerris* and *Ostya carpinifolia* rarefies until it disappears, leaving the area dominated by the population of *Fagus sylvatica*. *Fagus sylvatica* represents the elevation limit for the Turano forest. They populate the greatest part of the watershed area above the level of 1100 m a.s.l.

All kinds of tree populations present in the different sectors of the watershed belong to the family of deciduous plants. More precisely, such plants lose their mantle leaves during the adverse climatic season. The *Pinophyta* constitutes an exception in the area, as it does not seasonally lose its leaves. However, the *Pinophyta* covers only 0.4% of the forest region. According to Abbate et al. (1994), this great prevalence of the deciduous vegetation in the area is due to the fact that the biggest part of the watershed (also in modest elevation of 750–1000 m a.s.l.) is situated within the mesaxeric - cold axeric region (hypomesaxeric

and cold-temperate subregion) and the mesaxeric region (hypomesaxeric subregion). Within such climatic contexts with abundant rainfall, little or completely absent summer aridity and cold stress from autumn until spring (high during winter) offers a good environment for the growth of mesophile broad-leaved trees (Blasi, 1993).

Other non-forest vegetation species present in the area are mainly composed of shrub. A widespread presence of *Cytisus scoparius* and *Spartium junceum* can be detected within the boundaries of the forests. Presumably, juniper shrubs may represent a pre-forest stadium of the *Ostrya carpinifolia* in areas previously exploited by humans (Abbate et al., 1994; Monti Cervia and Navegna Nature Reserve, 2010). Finally, except for the high-mountain pastureland, all areas covered by grassy vegetation are a result of human management practices rather than a consequence of the accomplishment of vegetation climax.

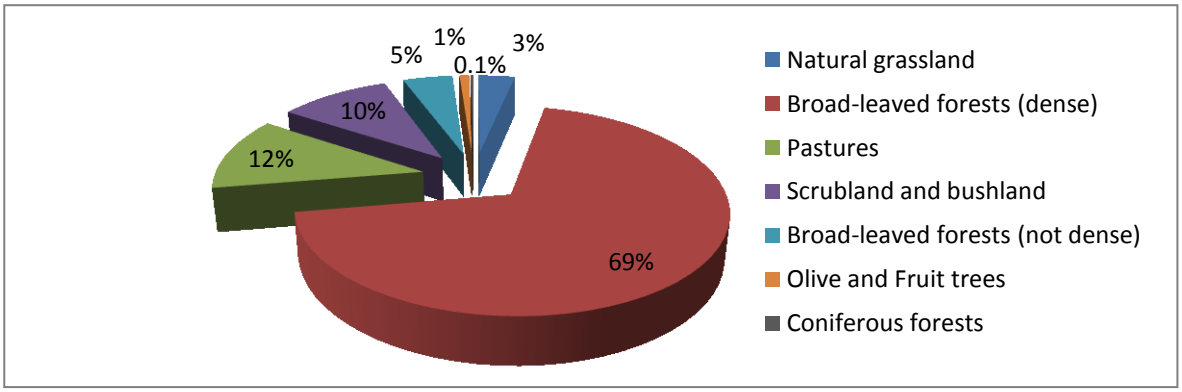

Fig. 3.23 – Classification of the vegetation in the Turano watershed.

3.5. SOILS

According to the Italian soil region database (1:5,000,000 scale), the Turano drainage basin is located within pedological region 16.4, called the 'Soil region of the Apennine reliefs on limestone and intra-mountain plains' (Righini et al., 2001). With a surface area of about 15.288 km² it covers 5% of the Italian territory. It includes the main carbonate chains of the Central Apennine, including Carseolani, Gran Sasso, Simbruini, Sabini and Velino among others. As a consequence of the alternation of ridges and valleys it is characterized by a high elevation range, with the elevations ranging from 100 up to 2912 m a.s.l. for the Corno Grande pick (Gran Sasso).

According to the ARSAA (2006), soil region 16.4 includes 14 systems, 49 sub-systems and 367 types of soils.

With reference to the watershed under study, the heterogeneous spatial distribution highlighted in the previous paragraphs regarding geological, climate, vegetation and

geomorphological patterns, are subsequently the cause of the heterogeneous and complex distribution of the soils within the studied watershed. According to the data for the development of the ecopedological maps of Italy (1:250,000 scale) provided by the Regione Abruzzo (ARSAA, 2006) and the Regione Lazio (PCN, 2010) 6 systems of soils, 9 sub-systems and 22 types of soils can be defined within the Turano watershed (ARSAA, 2006).

The ecopedological maps together with the data acquired during a soil survey and further studies about soils carried out in the area (Lorenzoni et al., 1995; Colica et al., 1993; ARSAA; Agritec, 2004; Domdey, 2009, personal communication; Holzmann, 2009, personal communication) were used to create a detailed soil map of the studied area (Fig. 2.24). The major soil types present in the area are listed in Table 2.2.

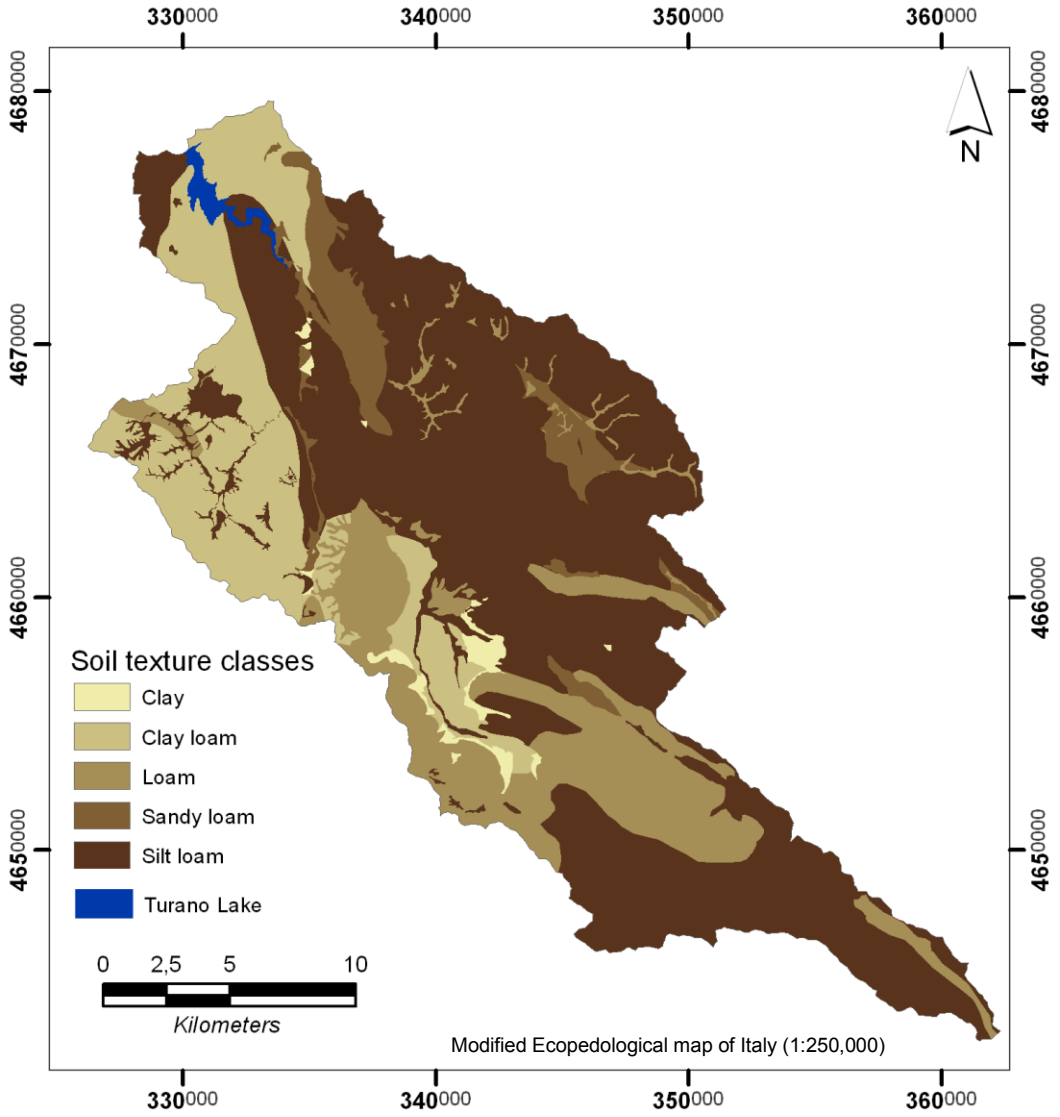

Fig. 3.24 – Soils texture classes of the Turano watershed.

On the Pleistocene-Holocene terraces in the lower altitudes of the watershed, several deep soils can be found (Lorenzoni et al., 1995). The soils of the actual fluvial plain are mainly Calcaric Fluvisols, Mollic Fluvisols and Eutric Fluvisols, and to a lesser extent Eutric Cambisols. All these soils belong to the great soil group of the Udifluvents, i.e., alluvial soils characterized by an udic moisture regime. The soils in this sector show evidence of actual or past hydromorphism. Here, they generally have only an A-C profile morphology and the primary elements of differentiation are the soil taxonomy and the calcium carbonate content. Soils with silt-loamy and loamy texture prevail on the surface resulting in a good drainage capacity. On the alluvial fans, which are currently inactive, some more evolved soils attributable to Eutric Cambisols are present. The drainage capacity of these soils is increased by the surface stoniness that ranges from 3 to 15%. At the Conca di Oricola location where the Pleistocene fluvio-lacustrine terraces reach the surface, soils classifiable as Mollic Fluvisols, Haplic Luvisols and Dystric Regosols are present. The top layer (≤30 cm) of these soils is composed of fine material and poor skeleton. The result is a low drainage capacity, especially on the inclined surface where the clay content is high (Haplic Luvisol).

On the low mountain reliefs the occurrence of different soil types is related to lithological substratum. The round shaped mountain relief, with a pelitic-arenaceous substratum, gives rise to a predominant way of Calcaric Cambisols and Calcari Leptic Cambisols. On the steep slopes of the V-shaped valleys soils less developed such as Eutri Calcaric Leptosols, Endolepti Calcaric Cambisols and Haplic Calcisols can mainly be distinguished. In general, these soils display the horizon sequence A-Bw-C-R (Chicchiarelli, 2006). The link between the parent material and the pedogenetic profile becomes highly visible. The superficial stoniness is higher in the upper part of the slopes while it decreases downslope. In addition, at the lower part of the slopes thicker colluvial deposits that border the alluvial flat plains exist. Here, the soil reaches its maximum thickness, which is generally higher than 1.5 meters. The soils of the siliciclastic turbidites lithological sector show a silt-loamy particle composition and are characterized by a low drainage capacity. The marly lithological sector frequently gives rise to Calcaric Endoleptic Regosols, Gleyic Calcisols and Heplic Calcisols. Gleyic Calcisols are more typical for the slopes with low inclination whereas in the steep slopes soils belonging to the types mentioned above occur. The particle sizes of the top layer of these soils are generally loamy and silt-loamy. In the case of Calcaric Endoleptic Regosols they are predominantly coarse-loamy.

The soils that have developed on mountain carbonatic slopes between 800 and 1800 m a.s.l. are characterized by poor to very poor depth. In this sector of the investigated watershed the most representative soils are Calcari Endoleptic Phaeozems, Episkeleti

Calcaric and Leptic Phaeozems, Dystri Leptic Cambisols and Chromi Endoleptic Luvisols. These are OH-A-Bw-C or OH-A-Bw-C-R (Chicchiarelli, 2006) soils where the topsoil generally shows high surface stoniness. The grain size of the topsoil ranges from silty to sandy-skeletal. Pyroclastic materials derived from the Latium volcanism that are mixed into the soil can be found. In addition, further pyroclastic materials are also present such as deep soil layers in areas that have been affected by morpho-evolutional processes. Moreover, a high drainage capacity of both, soils as well as lithological substratum distinguishes the area.

Bare rock outcrops are mainly concentrated in the calcareous sector of the watershed and characterize its higher ridges. In contrast, bare rock outcrops can rarely be observed in the presence of siliciclastic turbidites and marly lithological substrata. Here, due to the fast weathering of these rocks a coarse thin soil (10–20 cm) is almost always existent.

Table 3.2 **–** Soils types of the Turano watershed.

Soil type (WRB 98)	Soil Taxonomy (98)	Topsoil composition	
		Soil texture	Stoniness
Mollic Fluvisols	Fluventic Hapludolls	Silt loam	Low
Haplic Luvisols	Mollic Hapludalfs	Clay loam	Frequent
Calcaric Fluvisols	Typic Udifluvents	Silt loam	Absent
Mollic Fluvisols	Mollic Udifluvents	Clay loam	Frequent
Eutric Fluvisols	Aquic Udifluvents	Loam	Absent
Eutric Cambisols	Dystric Eutrochrepts	Loam	Absent
Eutric Cambisols	Fluventic Eutrochrepts	Clay	Low
Dystric Regosols	Vitrandic Udorthents	Loam	Absent
Calcaric Cambisols	Typic Eutrudepts	Silt loam	Absent
Calcari Leptic Cambisols	Typic Eutrudepts	Silt loam	Absent
Haplic Calcisols	Typic Eutrudepts	Silt loam	Low
Eutri Calcaric Leptosols	Lithic Eutrudepts	Sandy loam	Frequent
Endolepti Calcaric Cambisols	Typic Eutrudepts	Silt loam	Frequent
Gleyic Calcisols	Fluvaquentic Eutrudepts	Silt loam	Absent
Calcaric Endoleptic Regosols	Typic Udorthents	Sandy	Low
Heplic Calcisols	Fluventic Calciudolls	Silt loam	Absent
Calcari Endoleptic Phaeozems	Typic Haprendolls	Sandy loam	Frequent
Dystri Leptic Cambisols	Lithic Dystrudepts	Clay loam	Low
Episkeleti Calcaric Phaeozems	Typic Haprendolls	Loam	Frequent
Leptic Phaeozems	Typic Hapludolls	Silt loam	Frequent
Leptic Phaeozems	Lithic Hapludolls	Loam	Very high
Chromi Endoleptic Luvisols	Lithic Argiudolls	Silt loam	High

Chapter 4

Analysis of the Climatic Conditions of the Turano Watershed

4. ANALYSIS OF THE CLIMATIC CONDITIONS OF THE TURANO WATERSHED

According to the climate classification system by Köppen (AIA, 2010), the Turano watershed is located in a sector of the Central Apennine with a temperate sub-continental climate (Cf).The climate characteristics of the specific watershed are determined by the peculiar combination of the large-, meso- and local-scale atmospheric circulation patterns and the geographical factors of the watershed, resulting in strong spatial and temporal variations of both air temperature and precipitation.

4.1. CLIMATE DYNAMICS AT LARGE- AND MESO-SCALE

The general meteorological aspects of the area are linked to the large-scale atmospheric circulation dynamics of the Mediterranean area, which manifest in a strong seasonality of temperature and precipitation. According to Bernacca (1972), the climate situation of Italy can be classified into:

- Winter season – During winter, the Mediterranean area is located between the rather weak high atmospheric pressure system of the Azores and the cold gravitating system of the Asian continent. The cold and wet winter climate unfolds its effect beginning in autumn with the setting in of the general cooling period in the northern hemisphere of the atmosphere. The effect results from the contraction of the Azores High, allowing for the low-pressure systems originating in the North Atlantic to access the Mediterranean region. As a consequence, the contrast between the temperature of the northwestern winds and the relatively higher temperature of the Mediterranean surface determines conditions of instability that lead to frequent frontal and orographic precipitation events.

- Summer season – In summer, because of the increased solar thermal impact, the system, described above, results shifted to the north. In this context, the Intertropical Convergence Zone (ITCZ) shifts northwards on the African continent up to the latitudes of the Tropic of Cancer. This simultaneously causes the strengthened northward moves of the Azores High towards the Mediterranean basin. The Westerlies are pressured in an eastern direction at latitudes above 50°. This leads to hot and dry weather in the Mediterranean area.

Notably, the meso-scale atmospheric circulations dynamics are responsible for the presence of different termo-pluviometric patterns along the Italian Peninsula. Five meso-scale pluviometric areas are distinguishable in Italy (Ciabbatti, 1982) (Fig. 4.1). In the case of the Apennines sector where the Turano watershed is located, the pluviometric regime is similar to the one shown in Figure 4.1 (4).

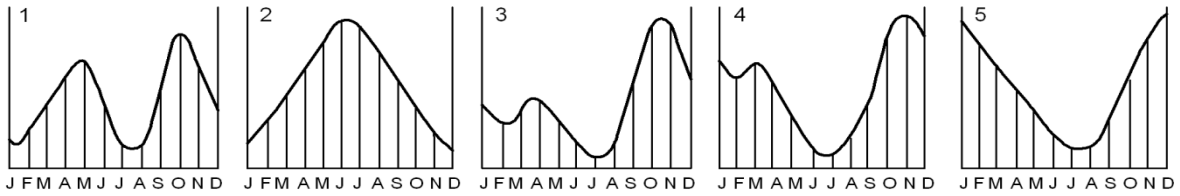

Fig. 4.1 – Italian pluviometric regime types.

In addition, downscaling of the topoclimate and microclimate patterns are influenced by local geographical factors such as elevation, slope exposure, wind, insolation and vegetation coverage (Caporali and Tartaglia, 2002). In order to develop an as precise-as-possible analysis of the soil erosion risk, it is important to consider the distribution of the space-temporal characteristics of temperature and rainfall. This is even more true for the investigation of a geographically and orographically highly complex territory like the Apenninic one. More specifically, according to the phytoclimatic map of Blasi (1996) the phenomenon of climatic heterogeneity can already be traced within small- to medium-scale watersheds of the Apenninic territory.

4.2. CLIMATE DYNAMICS AT WATERSHED SCALE

4.2.1. TEMPERATURE

The spatial and temporal distribution of the temperature characteristics of the area was analyzed using daily and monthly temperature data recorded by 8 meteorological stations belonging to the 'National Hydrographic and Oceanographic Service' (SIMN) (Fig. 4.2). The analyzed data correspond to the decade lasting from 1991 to 2000 (in the case of the temporal distribution the thirty-year period 1961–1990 was considered). The meteorological stations considered were Carsoli (640 m a.s.l.), Filettino (1062 m a.s.l.), Rocca di Mezzo (1329 m a.s.l.), Posticciola (540 m a.s.l.), Rosciolo (903 m a.s.l.) Subiaco (378 m a.s.l.), Tagliacozzo (740 m a.s.l.) and Tubione (865 m a.s.l.). Unfortunately, only the Carsoli and Posticciola stations are located inside the watershed, while the remaining stations are situated in the immediate vicinity, ranging from 1.5 to 15 km in distance.

Table 4.1 – Thermometric characteristics in the research area (1991-2000).

Station	Altitude	Annual Tmean	Monthly Tmax	Monthly Tmin
	[m a.s.l.]	[°C]	[°C]	[°C]
Subiaco Scolastica	378	13.4	26.4	4.2
Posticciola	540	13.3	24	3.2
Carsoli	640	11.4	24.6	-1
Tagliacozzo	740	10.8	23.1	2.7
Tubione	865	10.6	23.7	-1.9
Rosciolo	903	10.1	23.4	-2.7
Filettino	1062	10	20.3	0.6
Rocca di Mezzo	1329	7.4	20.7	-3.8

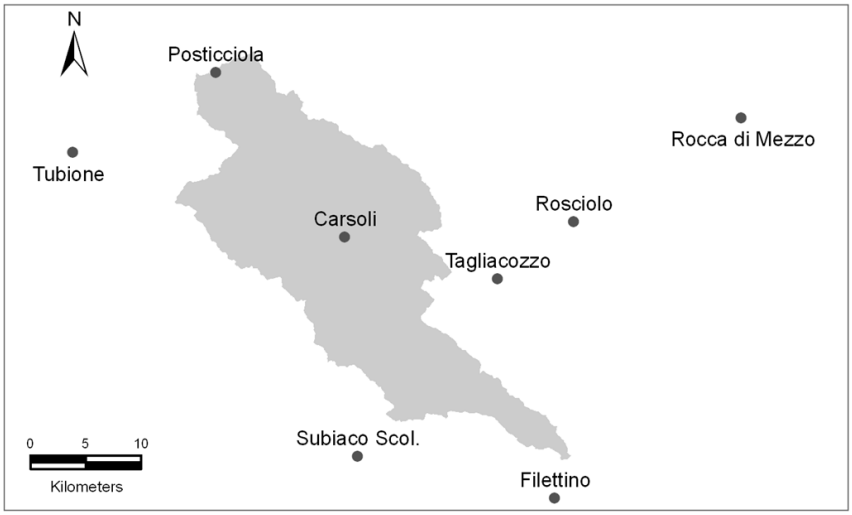

Fig. 4.2 – Location of the thermometric stations in the research area.

4.2.1.1. SPATIAL DISTRIBUTION OF THE TEMPERATURE

In the decade under consideration, the monthly average temperatures range from a minimum value of -0.3°C (February) recorded by Rocca di Mezzo to a maximum value of 23°C (August) recorded by Posticciola. Except for the Rocca di Mezzo meteorological station (1329 m a.s.l.), all stations recorded monthly average temperatures above zero. The warmest month was generally August, during which the average temperatures were attested to be around 20°C or higher. The temperature as well as the temperature range predominantly depend on the elevation. The relationship between elevation and annual average temperatures was quantified by calculating the vertical temperature gradient through linear regression analysis. To obtain the vertical temperature gradient, the database was enlarged using data from other 5 meteorological stations located around the study area (Aquila, 735 m a.s.l.; Leonessa, 974 m a.s.l.; Posta, 721 m a.s.l.; Rieti, 402 m a.s.l. and Terminillo, 1875 m a.s.l.). The calculated vertical temperature gradient is equal to -0.50°C/100 m. This value is both, supported by a highly significant determination coefficient ($n=13$; $R=0.974$; $\alpha<0.01$) and confirmed by the values calculated by other studies in the Tyrrhenian (-0.50 °C, Ducci, 1999) and Adriatic (-0.55°C, Fazzini 1997) sectors of the Apennines. It was therefore assumed as being highly valid.

Figure 4.3 shows the distribution of the annual average temperatures in the Turano watershed. According to the map, the highest average temperature of approximately 12.8°C is found near Turano Lake, which represents the lowest sector of the watershed. Relatively high average temperatures of around 10°C are typical of a wide part of the center-northern sector between Turano Valley and the intramountain basin of Oricola. In contrast, moving toward the southwest sector of the watershed the temperature conditions

change rapidly. Here, where the Sinbruini Mountains reach up to 1900 m a.s.l., the annual average temperature drops down to 5.6°C.

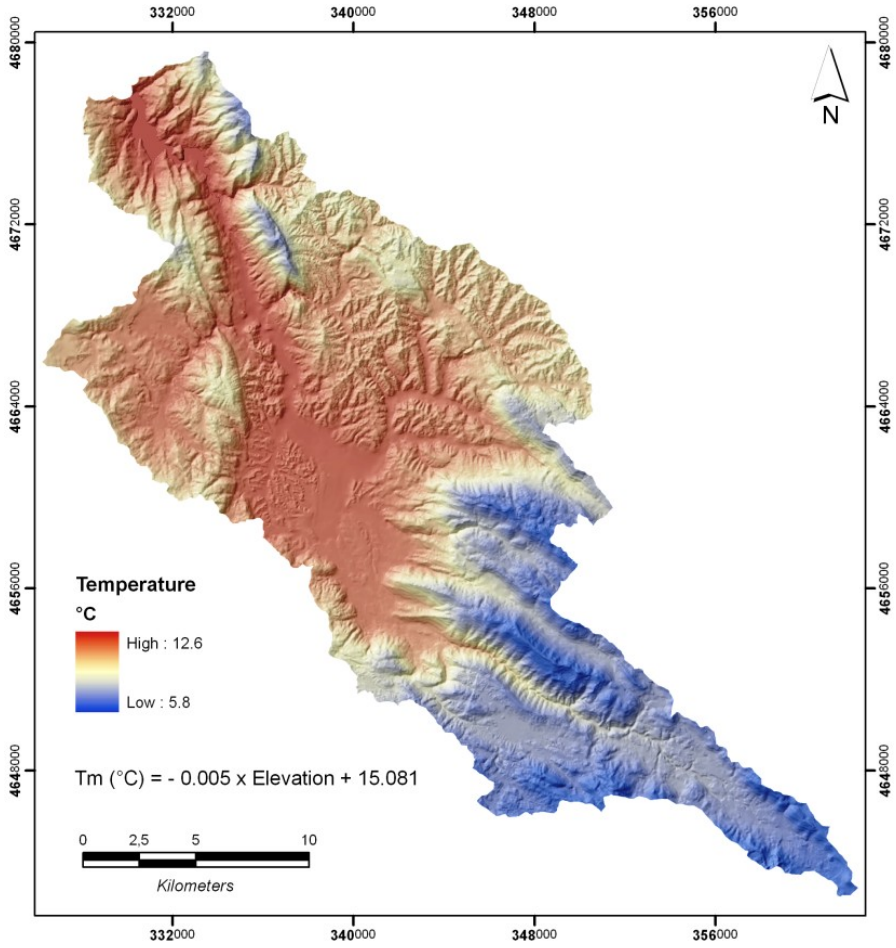

Fig. 4.3 – Annual temperature range of the region

4.2.1.2. TEMPORAL DISTRIBUTION OF THE TEMPERATURES

The temporal variations of the temperatures were observed using the temperature values recorded by meteorological stations Posticciola, Carsoli and Subiaco. These stations are located in the north, center and south of the watershed, respectively. In the thirty-year period considered (1961–1990), the annual average temperatures measured at Carsoli, Subiaco and Posticciola were 11.4 °C, 12.3 °C and 12.5 °C, respectively, with a variation between the coldest and the warmest year from the 2.1°C (Subiaco) to the 3°C (Posticciola). For Carsoli, Subiaco and Posticciola, the monthly average temperatures of the warmest (August) and coldest (January) months were equal to 19.9, 20.8, 21.7 and 3.9, 4.9, 4.3, respectively. Both, the monthly and annual temperature range rises with an increase in elevation. In the case of the annual temperature range the measured values were 13.8 °C for Subiaco, 15.8 °C for Posticciola and 17.4 °C for Carsoli. The monthly temperature ranges are given in figure 4.5 (period 1961–1990).

The observation of seasonal temperatures in terms of mean, minimum and maximum shows similar patterns (Fig. 4.4). The monthly and seasonal average temperatures show a gradual increase from January to April, then climb rapidly to the maximum values in the summer months. After having touched the maximum temperature in August, from September on, the temperature decreases until reaching its winter values.

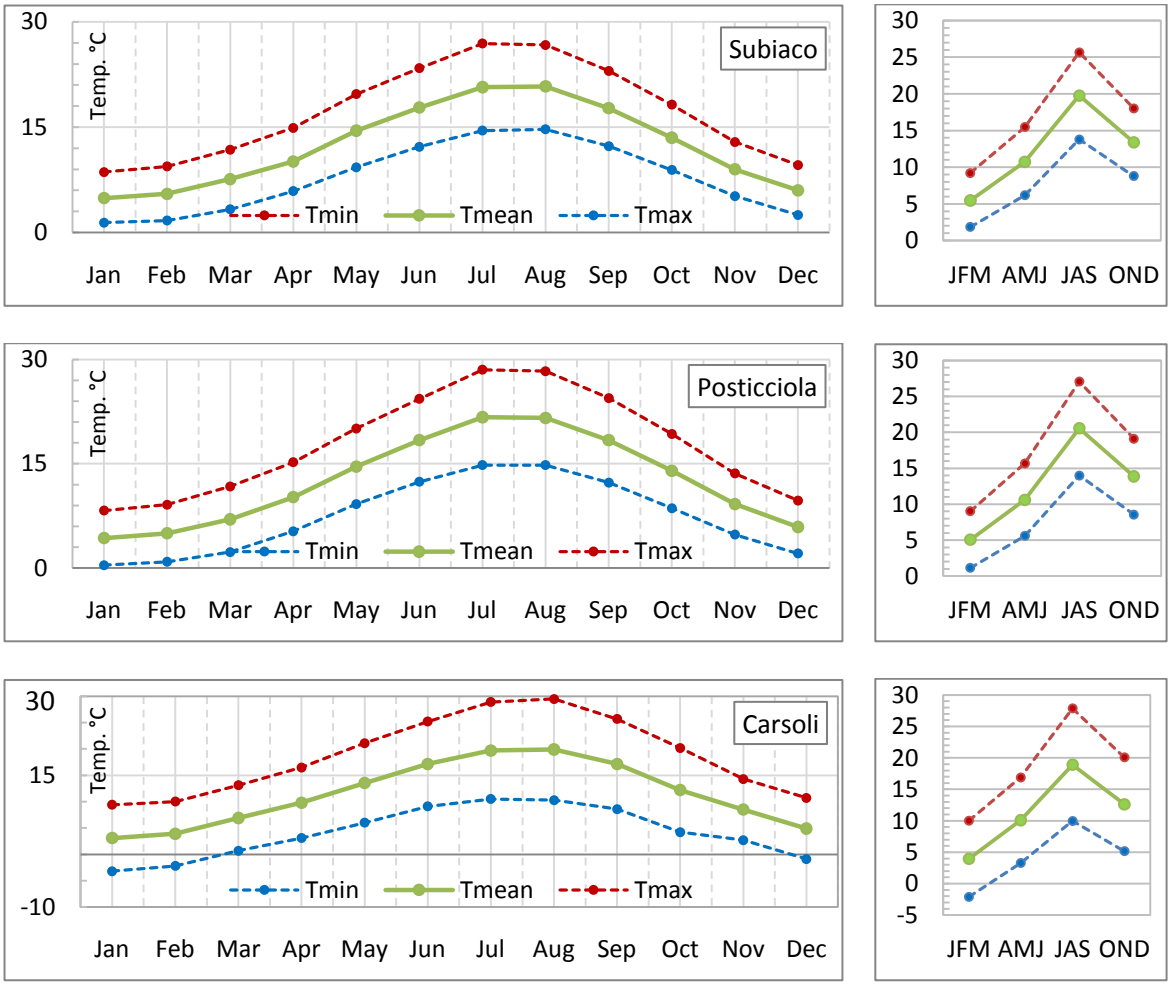

Fig. 4.4 – Monthly and seasonal thermometric characteristic for the stations of Subiaco, Posticciola and Carsoli.

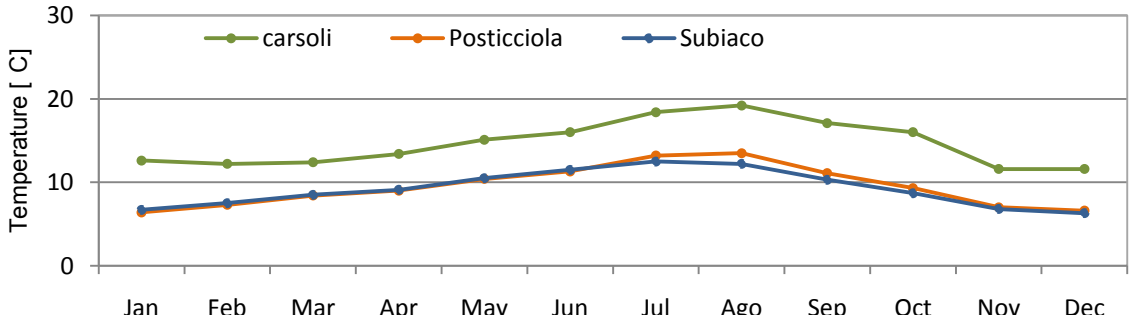

Fig. 4.5 – Monthly temperature range.

With regard to the temporal occurrence of extreme temperature events, both winter and summer events were accessed using minimum, maximum and mean daily temperature data. During winter, the number of 'days with frost' ($T_{min} \leq 0°C$) and 'days of frost' ($T_{max} \leq 0°C$), whereas in summer the number of 'tropical days' ($T_{max} \geq 30°C$) and days with $T_{max} \geq 35°C$ were observed. Table 4.2 shows the annual distribution of the extreme temperature events recorded by the three meteorological stations. The comparison of the temperature data recorded by the stations denotes that the 'days of frost' are negligible. The amount of 'days with frost' depends on the elevation. The distribution of 'tropical days' concentrates on the period from June to September. Extreme values of the period from 1951 to 2009 of -22°C (February 1956, Carsoli) and 40°C (August 1998, Carsoli) were recorded. Finally, the freezing point in the area ranges from approximately 1360 m a.s.l. in January to 4530 m a.s.l. in August.

Table 4.2 – Descriptive statistic of the extreme thermal events.

Subiaco	Jan	Feb	Mar	Apr	May	Jun	Jul	Ago	Sep	Oct	Nov	Dec
n° days with frost	9.1	9.2	3.4	0.3	-	-	-	-	-	-	1.2	5.5
n° days of frost	-	-	-	-	-	-	-	-	-	-	-	-
n° days TMax >30	-	-	-	-	-	3.4	11	14.8	0.5	-	-	-
n° days TMax >35	-	-	-	-	-	-	-	-	-	-	-	-

Posticiola	Jan	Feb	Mar	Apr	May	Jun	Jul	Aug	Sep	Oct	Nov	Dec
n° days with frost	13.8	14.9	7.2	1.4	-	-	-	-	-	-	3	9.2
n° days of frost	0.1	0.1	-	-	-	-	-	-	-	-	0.1	-
n° days TMax >30	-	-	-	-	0.4	3.9	14.8	21.1	3.1	-	-	-
n° days TMax >35	-	-	-	-	-	-	-	-	-	-	-	-

Carsoli *8 years	Jan	Feb	Mar	Apr	May	Jun	Jul	Aug	Sep	Oct	Nov	Dec
n° days with frost	24.4	22.5	17.7	9.9	2.1	0.1	-	-	1.5	5	13	19
n° days of frost	1	-	-	-	-	-	-	-	-	-	-	0.3
n° days TMax >30	-	-	-	-	-	2.9	9.7	14.6	2	-	-	-
n° days TMax >35	-	-	-	-	-	-	-	-	-	-	-	-

4.2.2. RAINFALL

Similar to the analysis of temperatures, the analysis of the rainfall precipitation data was collected from the Hydrological Year Books of the SIMN. The rainfall data relating to the 12 selected meteorological stations are summarized in Table 4.3. Three of these stations are situated within the watershed, while the remaining are located in its close proximity. The distribution of precipitation was analyzed seasonally, monthly and daily. For some stations the availability sub-hourly rainfall data even allowed for an analysis of individual rainstorms, as in the case of the data of the Posticciola and Arsoli stations.

Table 4.3 – Descriptive statistic of the annual precipitation for the thirty years 1961–1990.

n°	Station	Elevation	PoMean	PoMin	PoMax	SD	CV	Annual rainy days	Yrs
		[m a.s.l.]	[mm yr^{-1}]	[mm yr^{-1}]	[mm yr^{-1}]	[mm]	[-]		[-]
1	Abbazia di farfa	192	1036	712	1407	185.5	0.18	89	30
2	Licenza	478	1641	1174	2367	303.3	0.18	98	29
3	Posticciola	540	978	536	1386	225.7	0.23	92	29
4	Carsoli	640	1136	1571	846	197.4	0.17	99	29
5	Tagliacozzo	740	936	546	1368	210.8	0.23	108	30
6	Subiaco Scol.	511	1229	842	1857	259.1	0.21	105	29
7	Pereto	800	1105	850	1450	179.4	0.16	83	29
8	Verrecchie	1019	1306	885	1923	298.2	0.23	77	26
9	Tubione	865	978	632	1566	231.4	0.24	98	27
10	Rosciolo	903	847	536	1571	343.1	0.41	96	30
11	Tornimparte	780	1097	678	1564	186.4	0.17	104	28
12	Filettino	1329	977	536	1571	329.7	0.34	-	26

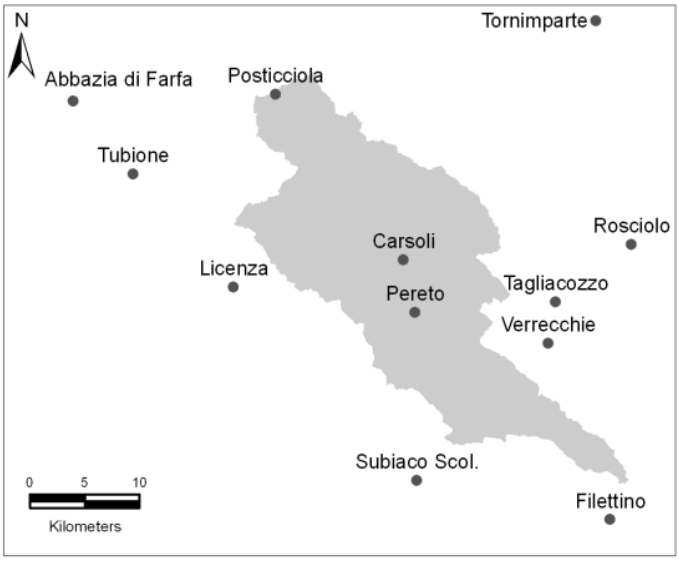

Fig. 4.6 – Location of the pluviometric/pluviographic stations.

4.2.2.1. SPATIAL DISTRIBUTION OF RAINFALL PRECIPITATIONS

A thirty-year period (1961–1990) was considered. The annual average precipitations were above the national average (970 mm yr^{-1}) for all stations except Rosciolo and Tagliacozzo. The highest rainfall annual average was recorded by Licenza (1641 mm yr^{-1}), while the lowest was measured by Rosciolo (847 mm yr^{-1}). The annual rainfall peak was indicated by Licenza in 1979 as 2367 mm yr^{-1}. Moreover, the rainfall intensity values ranged from 8.7 mm day^{-1} in Tagliaccozzo to 16.7 mm day^{-1} in Licenza.

The spatial patterns of annual precipitation essentially show a heterogeneous distribution. Thus, no direct evidence of a relationship between the rainfall values and altitude can be found. The correlation analysis of annual average rainfall and elevation delivers a 'no correlation' (n=13; R^2= -0.07; insignificant). However, the results obtained from the correlation based on monthly data differed significantly. More precisely, during the warm

months the rainfall seems to be much more influenced by altitude, particularly in June (n=13; R^2=0.365; insignificant), August (n=13; R^2=0.463; insignificant), September (n=13; R^2=388; insignificant) and October (n=13; R^2=0.317; insignificant). For the other months lower determination coefficients were found, ranging from R^2=0.008 to R^2=0.250 (insignificant). Moreover, at regional scale, although the higher annual average precipitation rates are more clearly concentrated in the mountainous compared to the coastal and pericoastal sectors, no straightforward dependence was found to explain a relation to the elevation (R^2 = 0.497; $\alpha < 0.01$; regional climate Appendix C). From the derived evidence, it may be assumed that the influence of the elevation on the recorded rainfall values is strongly conditioned by other geographical factors. Unfortunately, there have not been any studies on this issue in the described area or its close vicinity. However, Goovaerts (2000) investigating the Mediterranean mountainous area of Portugal, showed that the rainfall spatial variability in such an upland environment is strongly influenced not only by the elevation but also by other factors that he considered as secondary variables. Prudhomme (1998) observed in the mountainous regions of Scotland and suggested as secondary variables, factors such as direction and distance of moisture, slope gradient, slope orientation, relief obstructions and surface roughness. For the Turano watershed, multiple regression analyses were performed using the above-mentioned variables. However, no significant improvements of the weak correlation between annual precipitation rate and elevation were found.

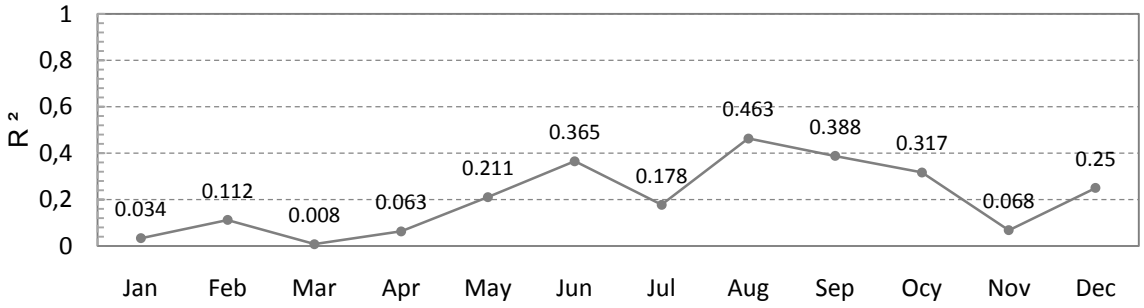

Fig. 4.7 – Monthly average precipitation versus elevation.

The spatial variability of the annual average precipitation within the Turano watershed is shown in Figure 4.8 (a), created using spline interpolation methods in ArcMap 9.3 (weight: 0.1; points: 12). The same procedure was used to make the seasonal average precipitation maps given in Figure 4.8 (b,c,d and e). Both, annual and seasonal precipitations are notably higher in two specific sectors of the watershed, namely, the southern and central-western areas of the watershed where the annual average lies between 1400 and 1600 mm yr^{-1}. In contrast, for the regions in the proximity of Turano Lake and around the intermountain basin of Oricola the precipitation values are lower,

ranging from 950 to 1200 mm yr⁻¹. With an annual average precipitation volume of about 583.4 ·10^6 m³ km⁻² yr⁻¹, spatially ranging from about 0.95 ·10^6 m³ km⁻² yr⁻¹ to 1.6 ·10^6 m³ km⁻² yr⁻¹, the overall area of the Turano watershed is clearly threatened by a high erosive potential of the rain.

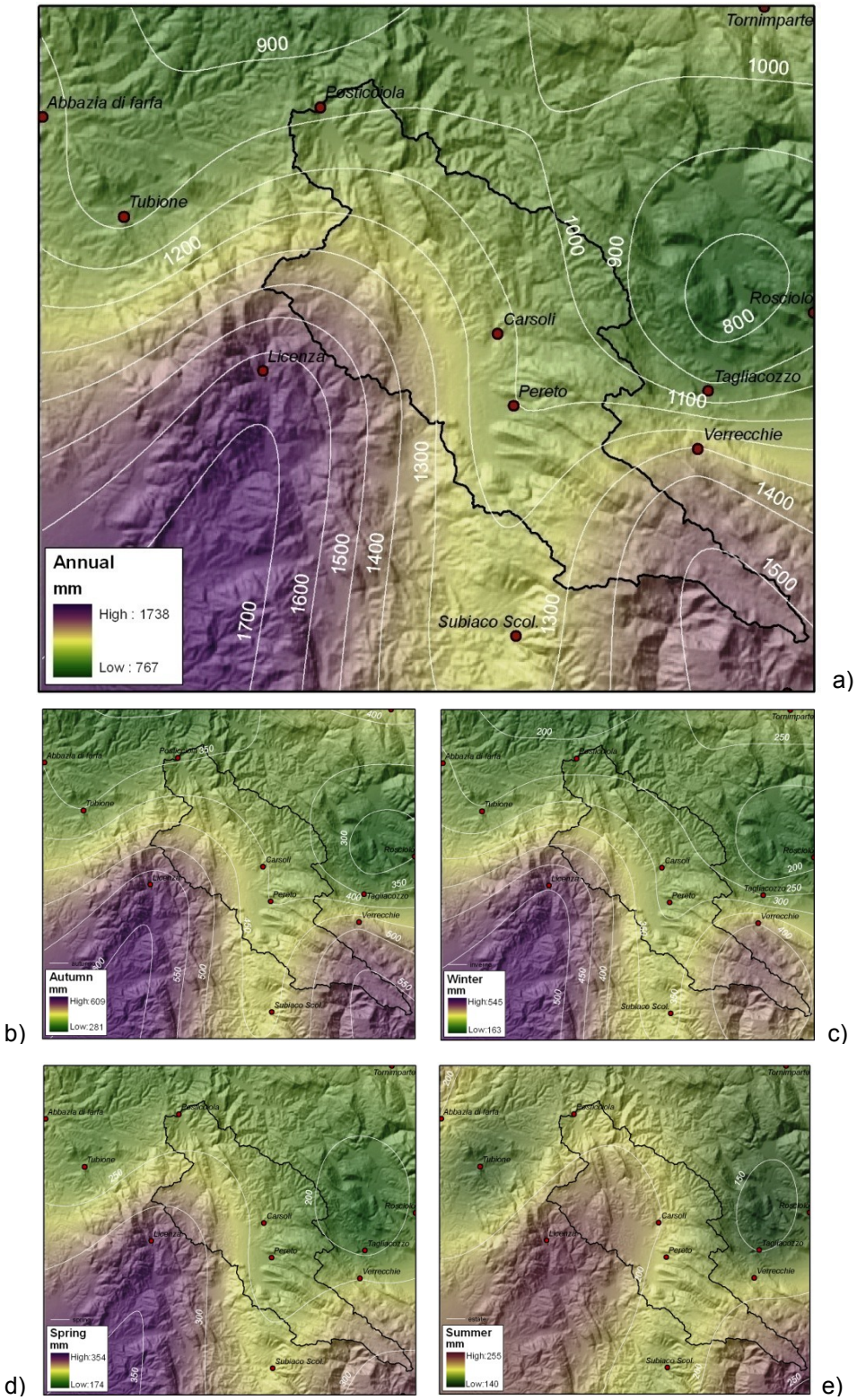

Fig. 4.8 – Computed annual (a) and seasonal precipitation (b,c,d and e).

4.2.2.2. TEMPORAL DISTRIBUTION OF RAINFALL PRECIPITATIONS

The rainfall distribution across the year shows itself to be of a slightly bimodal type (Fig. 4.9). The monthly rainfall in the area is heavy during October, November and December, with maximum values occurring in November. Then, the pluviometric regime decreases during the spring months, hitting the minimum values in July. According to the temporal distribution of the precipitations the annual pattern can be distinguished as follows:

- Main rainy season – from October to December
- Secondary rainy season – from January to April
- Dry season – July and August

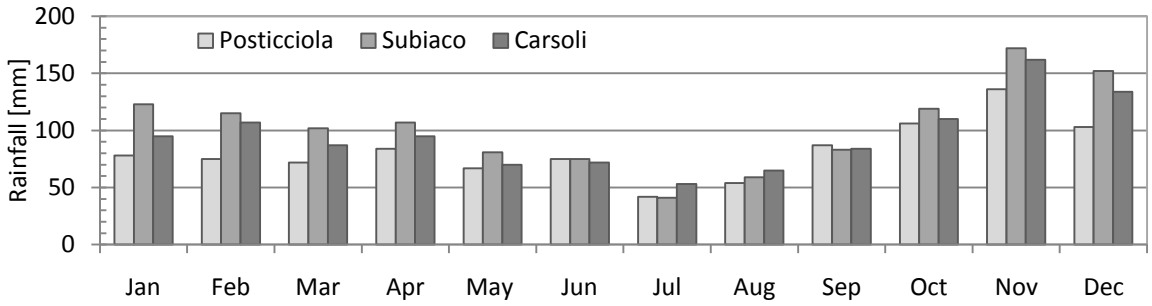

Fig. 4.9 – Mean monthly precipitation distribution

The precipitations recorded by the considered stations were subdivided into an annual average of rainy days ranging from 77 in Verrecchie to 108 in Tagliacozzo. An average of about 95 rainy days characterizes the investigated watershed. The rainfall intensity resulting from dividing the monthly rainfall by the monthly rainy days for all the 12 meteorological stations considered showed an effect of seasonality, with maximum values reached in the quarter from September to November (Table 4.4). In the annual consideration the variability of the monthly rainfall intensity is about 35% between the minimum and maximum values.

From the daily data of Posticciola (north of the watershed) and Subiaco (south of the watershed) the maximum precipitation with durations of 1,2,3,4 and 5 days, as well as their seasonal distribution (1961–1990 with few missing data) were analyzed. These types of rainfall events are temporally concentrated in the winter and autumn months. The greatest number of consecutive days of rain was recorded in October. In the area, the maximum precipitation with durations from one to five days can reach up to 246.8 mm, as occurred in Posticciola between 2nd and 6th September, 1965. Vice versa, the maximum intensity precipitations (1h, 2hrs and 6hrs) show different temporal patterns (Table 4.4). In fact, these types of events are mostly concentrated during the warm months, particularly during

August and September. The heaviest 1h rainfall event occurred in August 1982 with 54 mm (Posticciola).

The rainfall erosivity has been computed following the prescribed procedure of Wischmeier and Smith (1978). This is an integral part of the Revised Universal Soil Loss Equation (RUSLE) and will be described and discussed in Chapter 5.1.2.1 about soil erosion modeling.

Table 4.4 – Characteristics of the maximum intensity precipitations (1h, 2hrs and 6hrs).

		Posticciola			Subiaco		
		1 h	2 hrs	6hrs	1 h	2 hrs	6 hrs
[mm]	Mean	31.8	39.6	49.2	28.3	39.1	47.4
	Min	16	28	31.4	14	26	32.4
	Max	54.6	84.6	85.2	54.2	69.6	69.6
[%]	Autumn	11.1	16.7	27.8	16.7	50	66.7
	Winter	0	0	0	0	4.2	4.2
	Summer	77.8	55.6	38.9	66.7	33.3	25
	Spring	11.1	27.8	33.3	16.7	12.5	4.2

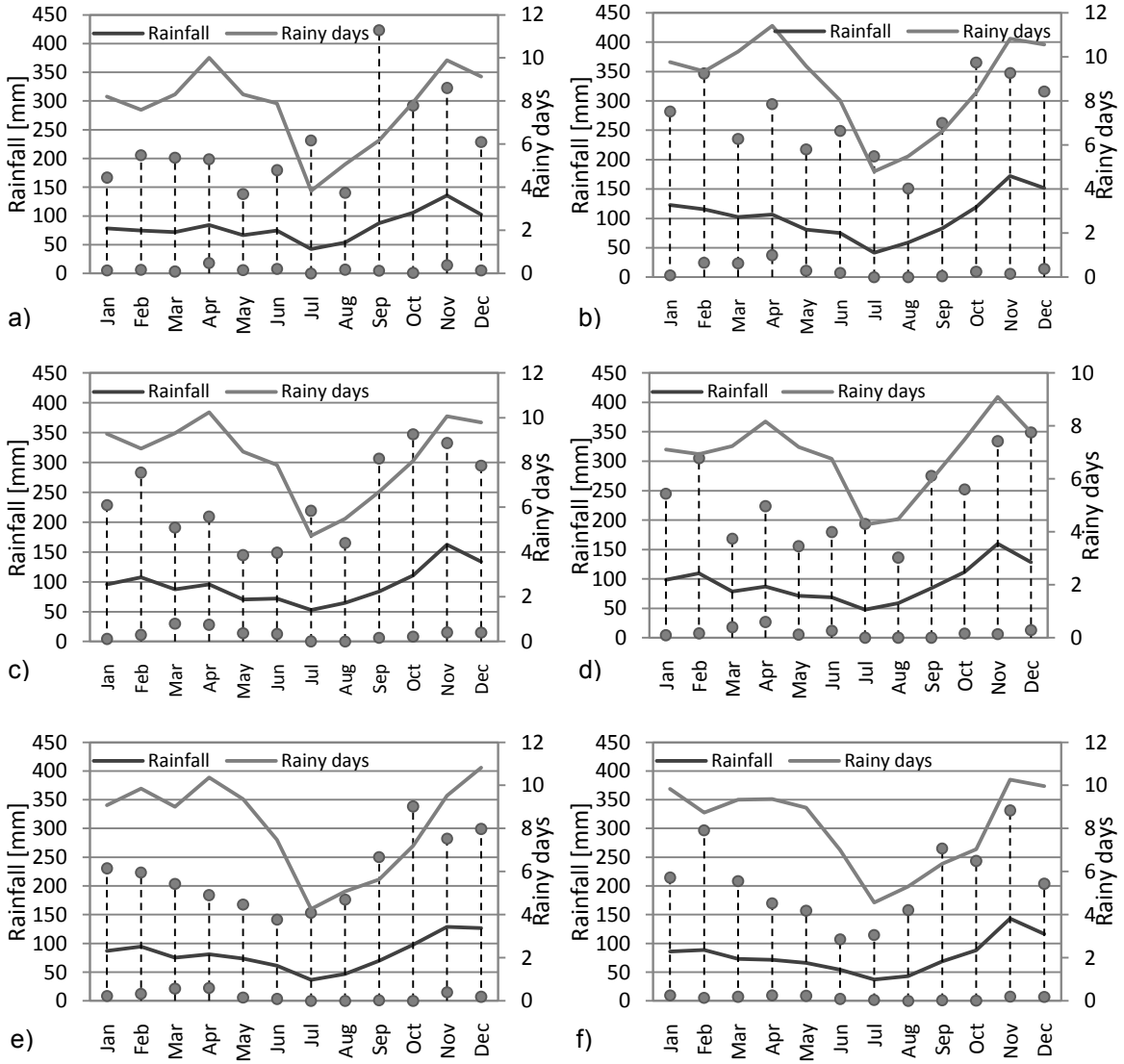

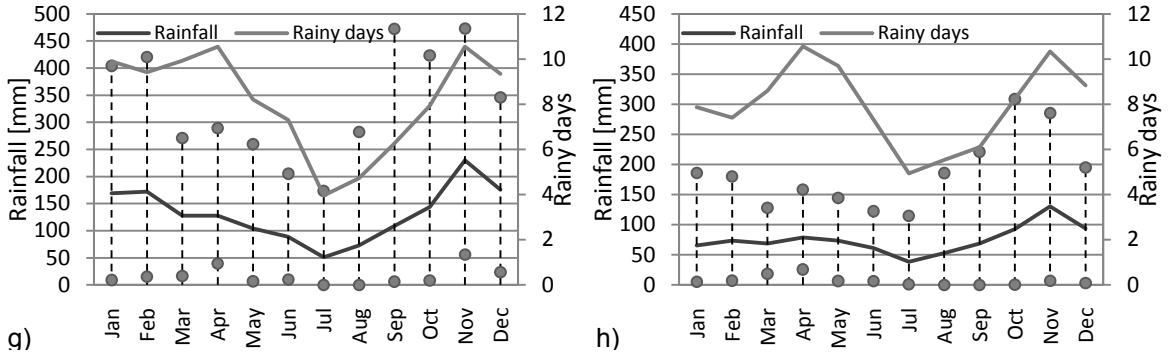

Fig. 4.10 – Mean of the monthly precipitation and number of rainy days. The dotted lines indicate the minimum and maximum values in the period 1961–1990. a) Posticciola; b) Subiaco; c) Carsoli; d) Pereto; e) Tubione; f) Tagliacozzo; g) Licenza; h) Rosciolo.

4.2.3. SNOWFALL

Both, spatial and temporal distributions of the snowfall measurements are strongly linked to the topography of the region. Based on the analysis of the snowfall recorded by 5 selected stations (i.e., Posticciola, 540 m a.s.l.; Carsoli, 640 m a.s.l.; Leonessa, 974 m a.s.l.; Rocca di Mezzo, 1329 m a.s.l. and Terminillo, 1750 m. a.s.l.) of the SIMN, the 'snow line' was found to be at about 900 m a.s.l., which means that snowfall events crossing the line upward occur almost every year. Above this altitude both snowfall days and snow amount increase linearly. At the same time, the days with permanently snow-covered ground increase with the elevation as well.

The months with snowfall events in the area are December, January, February, and to a lesser extent also March and November. At the Terminillo station (1875 m a.s.l.) a permanent snow cover of the ground lasted from December to February. Furthermore, during the coldest years with recorded snowfalls still in March, the permanence ground snow coverage can remain until April.

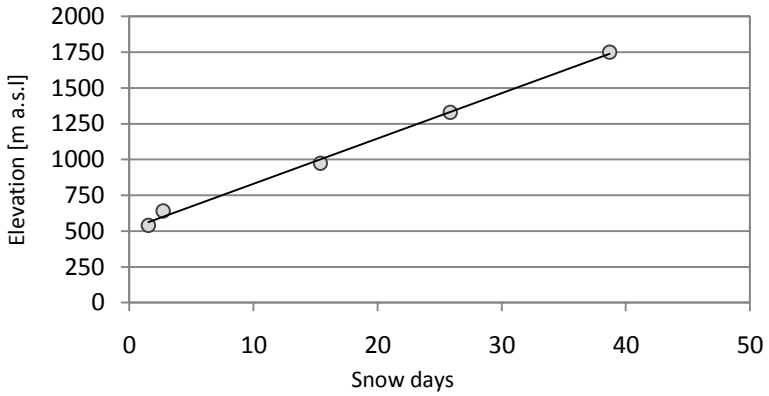

Fig. 4.11 – Snow days versus elevation (n=5; R^2=0.999; α<0.01).

4.2.4. BIOCLIMATES AND SOIL MOISTURE REGIMES

The description of spatial and temporal variability of the climate parameters carried out so far confirmed the climate heterogeneity indicated by Blasi (1996). The temperature and pluviometric regimes recognized within the watershed highlight different isobioclimate classes according to the bioclimatic indices of Rives-Martines (2004) and Blasi (1996). Consequently, Figure 4.12 shows the bioclimate map of the Turano watershed derived by an interpolation of the values of the continentaly index (Ic), the index of thermicity (It) and the ombrothermic index of the summer quarter. In the Turano watershed three different termotypes and three ombrotypes are present, resulting in nine isobioclimates. Furthermore, Figure 4.12 also provides the Gagnouls-Gaussen (1953) diagrams for the considered termo-pluviometric stations. These diagrams highlight a period of meteorological drought in the Turano watershed temporally concentrated in July and August, while water surplus occurs during the autumn and subordinately during the winter.

Finally, Appendix D provides the carried-out trend analyses of climatic parameters, i.e., annual and seasonal temperature (min, max, mean), annual temperature range, annual and seasonal rainfall and rainfall intensity.

Table 4.5 – Climate indices of the Turano watershed.

Bioclimate	Macroclimate	Thermicity index	Ombrotype
1	Temperate region	Mountain thermotype	Hyperhumid
2	Temperate region	Mountain thermotype	Humid
3	Temperate region	Mountain thermotype	Subhumid
4	Temperate region	Orotemperate thermotype	Hyperhumid
5	Temperate region	Orotemperate thermotype	Humid
6	Temperate region	Orotemperate thermotype	Subhumid
7	Temperate region	Supratemperate thermotype	Hyperhumid
8	Temperate region	Supratemperate thermotype	Subhumid
9	Temperate region	Supratemperate thermotype	Humid

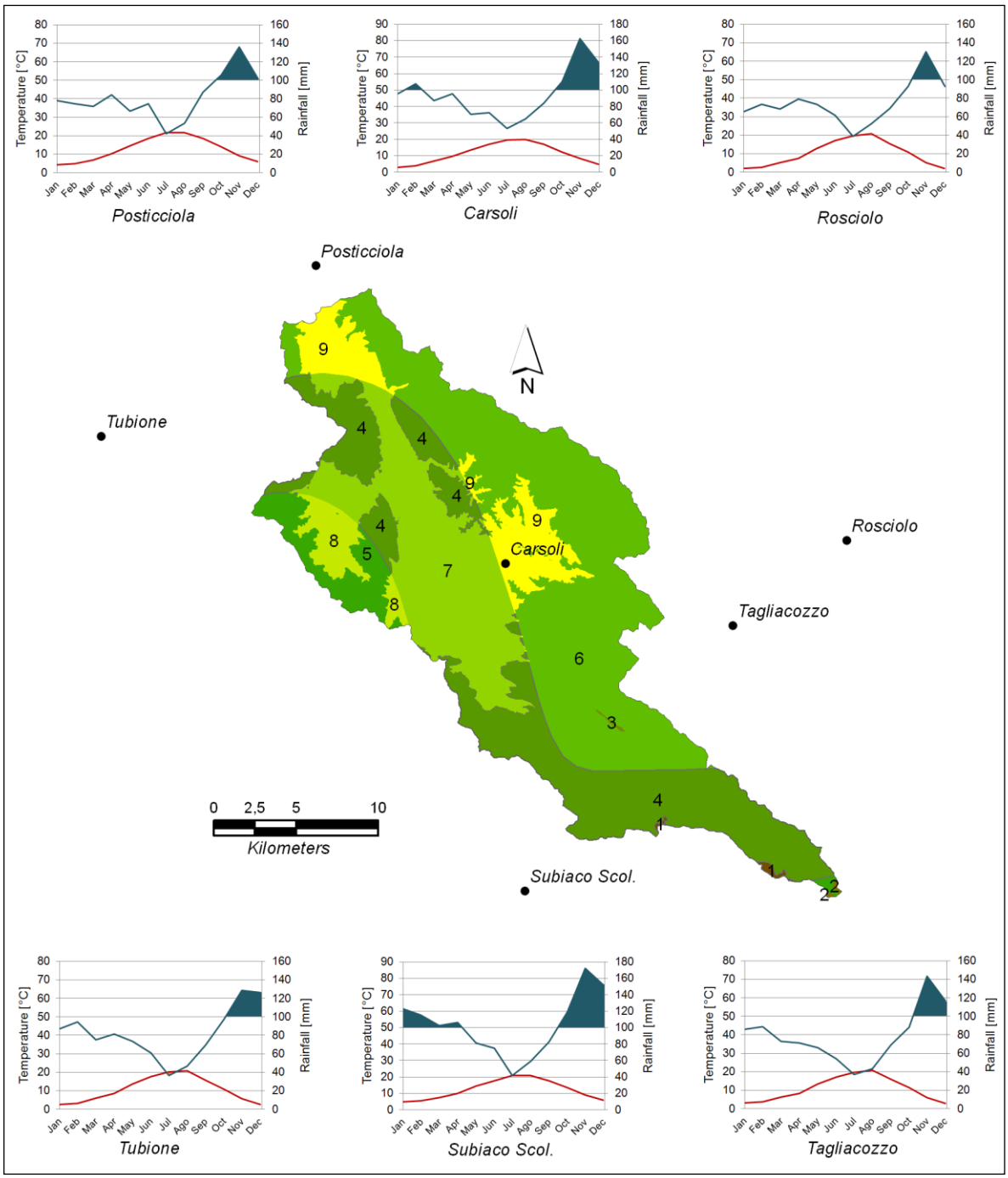

Fig. 4.12 – Meteorological data of study site, expressed by Bagnouls-Gaussen diagrams, referred to the mean annual rainfall 1961-1990.

Chapter 5

Spatially Distributed Modeling of Soil Erosion at Watershed Scale

5. SPATIALLY DISTRIBUTED MODELING OF SOIL EROSION AT WATERSHED SCALE

In the previous chapters, the socio-environmental conditions across the study area, as well as the presence of physical characteristics and anthropogenic activities that affect soil erosion processes were described. This chapter deals with the identification of a possible present scenario for soil erosion in the Turano watershed. The soil erosion models RUSLE (Renard et al., 1997) and USPED (Mitasova et al., 1996) are applied. Basic concepts of the selected soil erosion prediction methods are introduced. Furthermore, specific procedures for the model application are presented.

The input parameters of the models were derived from data acquired during the initial activity in the area. Fieldwork surveys, remote-sensing operations on aerial photographs and spatial satellite data as well as climate data manipulation and GIS analyses were performed for this purpose. After processing, the data collected were used to archive the three major goals this part of the thesis focuses on. The first goal deals with the application of the selected soil erosion prediction methods. Secondly, the impact of tree harvesting activities was estimated. As the final target, the reliability of the predictive capacity of the soil erosion models for the area under investigation are evaluated by application of both, quantitative and semi-quantitative validation methods.

5.1. METHODOLOGY

5.1.1. REVISED UNIVERSAL SOIL LOSS EQUATION MODEL

5.1.1.1. MODEL DESCRIPTION

The Universal Soil Loss Equation (USLE) is a mathematical model used to describe soil erosion processes. The USLE was first implemented by the USDA-Soil Conservation Service in the early 1960s (Wischmeier and Smith, 1960). The USLE has evolved through time and its application has greatly expanded from that in the early 1970s by the 1980s (Wischmeier and Smith, 1978).

At the end of the 1980s the U.S. Department of Agriculture (USDA) decided to revise the USLE soil erosion model (Renard et al., 1991). Following experimentation and an accurate validation, Renard et al. (1997) introduced the Revised Universal Soil Loss Equation (RUSLE). This empirical model, similar to the USLE, is based on experimental data that allows for an estimate of soil loss (t $acre^{-1}$ yr^{-1} or t ha^{-1} yr^{-1}) due to inter-rill and rill erosion processes. Although this model still builds on the basic structure of the USLE equation, it has several improvements in its determining factors (Renard et al., 1997). With the advent of Geographical Information Systems (GIS) and remote-sensing technology the RUSLE has been widely used during the last two decades with further improvements by contribution of several studies carried out across the world (Mitasova and Mitas, 1999).

Today, it is widely accepted in the international scientific society. Its simple but comprehensive structure provides a very good compromise between applicability and reliability of the soil loss estimation. Furthermore, unlike the physical based models RUSLE can be used for soil erosion predictions of large spatial scale. It is highly useful for environmental planning (e.g., Institute for Environment and Sustainability (IES) in Europe and Natural Resources Conservation Service (NRCS) in USA). Owing to the recent modifications (Foster et al., 2003) this model, originally developed to predict long-term annual average soil erosion, can also be used for short-term and single storm events. However, despite refinements and revisions RUSLE is not free from criticism. The rather low effectiveness in applications for non-agricultural areas has widely been put forward. Compared to more than 10,000 field plot-years of data (Kinnell, 2007) in farmland, the model has been applied to non-agricultural areas to a significantly lower extent. Further criticism relates to its applicability to watershed scale. The enhanced knowledge about the physical sub-processes behind the soil erosion phenomenon acquired during the last few years shed new light on the complexity of the entire process. This raises doubts about the reliability of RUSLE when used in complex environments. Nonetheless, it is still the most experimented-whit and applied soil erosion prediction model in various environments around the world. This is due to the fact that the more recently presented water soil erosion models place greater emphasis on the physical processes responsible for erosion but do not perform better in mountainous environments (Cernusca et al., 1998) and other geomorphological complex environments (van Rompaey et al., 2003a,b). Regarding Italy, both USLE and RUSLE have been largely applied. Nevertheless, validation operations to check the performance of the models in the Italian landscapes were carried out only in a few cases (Chisci, 1986).

From a technical point of view, RUSLE belongs to the detachment capacity-limited models. In other words, the flow can theoretically transport an infinite quantity of sediment but the amount of sediment actually available to be transported is limited by the soil detachment capacity given by the rainfall erosivity factor of the model. The influence of the terrain on the erosion process is given by a topographical factor. Additional parameters influencing the erosion process such as soil properties, land cover and soil conservation operations are also considered in the RUSLE model. The average soil loss (A) is predicted according to Renard et al. (1997) by the following multiplicative equation:

$$A = R \cdot K \cdot L \cdot S \cdot C \cdot P \qquad \text{(Eq. 5.1)}$$

Where:

A [t ha^{-1} yr^{-1}] is the annual average soil loss,

R [MJ mm h^{-1} ha^{-1} yr^{-1}] is the rainfall intensity factor,

K [t ha^{-1} per unit *R*] is the soil erodibility factor,

L [dimensionless] is the slope length factor,

S [dimensionless] is the slope steepness factor,

C [dimensionless] is the land cover factor,

P [dimensionless] is the soil conservation or prevention practices factor.

5.1.1.2. RUSLE MODEL APPLICATION USING GIS

In order to facilitate the elaboration of the landscape data necessary to prepare the model parameters, the RUSLE model was employed on a GIS platform (ArcGIS 9.3). The input parameters of the model, as well as the output maps of soil loss distribution were prepared in a raster format. Their calculation and manipulation was performed via a raster calculator tool with the methods described below. At the end of the process, the annual average soil loss (A) was calculated for each of the 4,667,412 individual cells (10x10 m cell size) the Turano watershed is subdivided into.

5.1.1.2.1. RAINFALL EROSIVITY COMPUTATION

The RUSLE R-factor, also known as rainfall erosivity index (EI_{30}), is a numerical descriptor of the rainfall's ability to erode soil (Wischmeier, 1958). According to Wischmeier and Smith (1978), the rainfall erosivity value of a rainstorm event is the product of the storm kinetic energy (E) and the maximum 30 min intensity of it (I_{30}):

$$EI30raistorm = E \cdot I30 \quad \text{(Eq. 5.2)}$$

The energy of a rainstorm event is a function of the amount of rain and the rainstorm's intensity components. Brown and Foster (1987) recommended the following equation for calculating the unit energy:

$$E = 0.29 \cdot \left[1 - 0.72e^{(-0.05Ir)}\right] \quad \text{(Eq. 5.3)}$$

Where E denotes the rainfall kinetic energy of 1 mm of the rain expressed in MJ ha^{-1} mm^{-1} and Ir as the rainfall intensity expressed in mm h^{-1}. Therefore, the total annual R-factor is the sum of the individual EI30-rainstorm events as given in Eq. 5.4. In the same way, the monthly or seasonal R-factor is the sum of the individual $EI_{30\text{-rainstorm}}$ events based on monthly or seasonal data.

$$\text{R annual} = \sum_{j=1}^{J} (\text{EI30rainstorm})j \quad \text{(Eq. 5.4)}$$

Where $EI_{30\text{-rainstorm}}$ (MJ mm ha^{-1} h^{-1}) is the erosion index for storm j, and *J* is the number of rainstorms during the year.

To calculate annual R-factor values using Eq. 5.4 according to the instructions in the RUSLE handbook (Renard et al., 1997) continuous sub-hourly pluviograph data (15- or 30-minute interval) are needed. As mentioned in the paragraph on climatic characteristics (Chapter 4.2.2) there are 12 meteorological stations available around the Turano area, out of which only two provide sub-hourly rainfall data for the considered period (Posticciola [1998–2007] and Arsoli [2000–2003]). With respect to the scope of the investigated watershed and the spatial heterogeneity of the precipitation pattern observed in the study area, in this thesis the use of a unique R-factor value derived from the Posticciola station data for the entire area was not believed to be representative. Thus, various methods, described below, were tested to calculate both monthly and annual R values.

As a first step, Eq. 5.2 was used to calculate the $R_{monthly}$ values using the data from the meteorological stations of Posticciola and Arsoli. In the case of Posticciola, a record length of 120 months (1998–2007) consisting of 454 recorded storms was analyzed on a 30 minutes interval basis. At the Arsoli station 125 storms were processed. All rainfall events in this series are greater than 10 mm, which is the lowest rainstorm depth that produce measurable run-off and soil loss in the Mediterranean environment (Loureiro and Coutinho, 2001; Capolongo et al., 2008). Each rainfall event was separated in time by at least six hours from the previous or the subsequent event following Foster et al. (1981). The rainstorm erosivity was calculated by the application of Eq. 5.2 for all 579 erosive storms through a spreadsheet technique.

After calculating the $R_{monthly}$ values for Posticciola and Arsoli following the RUSLE handbook (Renard et al., 1997), twelve methods presented in literature to estimate the monthly and annual rainfall erosivity were applied for the remaining meteorological stations. The results from the thirteen equations used (Table 5.1) were compared with the rainstorms based on $R_{monthly}$ values calculated following Renard et al. (1997) and validated by R^2 and root mean square error (RMSE). As a result any of these methods were found to be applicable in the Turano area. Except for the equation proposed by Diodato (2004), they all provided poor results in the rainfall erosivity prediction. Due to the unavailability of the maximum annual 60 min rainfall values for most of the considered climatic stations the equation proposed by Diodato (2004) could not be used.

As a consequence of the limitation of the equations listed in Table 5.1, in estimating the monthly and annual rainfall erosivity values from the rainfall data of the remaining Turano meteorological stations, a method based on linear regression analysis was used. The Posticciola and Arsoli $EI_{30\text{-rainstorms}}$ aggregated to $R_{monthly}$ values were correlated with

their respective total monthly rainfall data. In order to do so, a database composed of 168 R-monthly values of Posticciola and Arsoli was split into two datasets. The first composed of 120 R-monthly values computed by Posticciola data was used as the calibration dataset while the other consisting of 48 R-monthly computed using Arsoli data served as the validation dataset. After validation, four equations based on linear regression relationships (Eq. 5.5, 5.6, 5.7, 5.8) able to predict reliable monthly R-factor values in the Turano area were derived and calibrated (α<0.01). These rainfall erosivity equations were applied to the monthly rainfall series of 18 stations around the Turano watershed yielding time series of monthly rainfall erosivity for all of the period 1995–2007. The four equations are:

Nov, Dec and Jan	$Ei_{30} = 1283 \cdot$ Monthly Rainfall – 37.001	R^2=0.928	(Eq. 5.5)
Feb, Mar and Apr	$Ei_{30} = 1226 \cdot$ Monthly Rainfall – 20.303	R^2=0.838	(Eq. 5.6)
May, Jun and Jul	$Ei_{30} = 2377 \cdot$ Monthly Rainfall + 0.104	R^2=0.790	(Eq. 5.7)
Aug, Sep and Oct	$Ei_{30} = 3815 \cdot$ Monthly Rainfall – 93.842	R^2=0.883	(Eq. 5.8)

Table 5.1 – Equations tested for rainfall erosivity calculations (R= monthly R-factor; Mo=monthly precipitation; P=yearly precipitation). * These equitations estimate the annual R values and the determination coefficient and were obtained through correlation 120 monthly values. In contrast, the equations based on yearly data are based on 8 years (the equation proposed by Diodato (2004) on only 5 years).

	Equation for monthly R-factor estimation	Author(s)	R^2	RMSE (MJ mm ha^{-1} h^{-1})
1	$*R = (0.66 \cdot Mo) + 8.88$	Oliveira (1988)	0.497 (α<0.01)	1562.8
2	$*R = 19.55 + (4.20 \cdot Mo)$	Rufino et al. (1993)	0.497 (α<0.01)	2613.3
3	$*R = 0.13 \cdot Mo^{1.24}$	Leprun (1981)	0.500 (α<0.01)	1894.5
4	$*R = 68.73 \cdot \left(\frac{Mo^2}{P}\right)^{0.841}$	Lombardi et al. (1992)	0.500 (α<0.01)	3314
	Equation for annual R-factor estimation			
5	$R = 12.142 \cdot (\text{abc})^{0.6446}$	Diodato (2004)	0.978 (α<0.05)	183.5
6	$R = 0.0483 \cdot P^{1.61}$ P<850 $R = 587.8 - 1.219\,P + 0.004105 \cdot P^2$ P>850	Renard and Freimund (1994)	0.378	2216.6
7	$R = (0.302 \cdot F)^{1.93}$	Arnoldus, (1977)	0.354	1962.6
8	$R = (4.17 \cdot F) - 152$	Arnoldus, (1980)	0.383	1955.7
9	$R = (4.0112 \cdot P) - 965.53$	Ferrari et al. (2005)	0.406	1410.1
10	$R = (0.092 \cdot P^{1.4969})$	Ferrari et al. (2005)	0.393	1305.7
11	$R = a \cdot Pj$	van der Knijff (1999)	0.406	1108.1
12	$R = 38.46 + (3.48 \cdot Y)$	Lo et al. (1985)	0.406	1731.5

In a next step, precipitation and thus monthly R-factor values were regionalized in a GIS environment by using the spline interpolation method (weight: 0.1; points; 15–18) and

raster-calculated operations. 96 raster units (cellsize 10x10 m) containing spatial-distributed R-monthly (estimated by Eq. 5.5, 5.6, 5.7 and 5.8) values for the period from September 1997 to October 2005 were created. Finally, from the winter months R-factor rasters, i.e., given snow coverage, their erosivity values were filtered by a reduction of 50%. The snowy precipitations were identified using the data reported within the Hydrological Year Books, by observation of the Landsat (U.S Geological Survey) images and via temperature analysis.

5.1.1.2.2. SOIL ERODIBILITY COMPUTATION

The soil erodibility K-factor is an empirical parameter based on the measurements of specific soil erodibility. This parameter is generally measured based on some intrinsic soil properties, such as texture, organic matter, structure and permeability of the soil profile (Wischmeier and Mannering, 1969; Torri et al., 1997). Wischmeier and Smith (1978) proposed a nomograph method to estimate the K-factor of a soil in the USLE manual. This methodology has been largely used in the U.S. However, it seems to be less accurate when applied in locations that do not conform with the ones for which the nomograph has originally calibrated (Römkens etal., 1986).

In the RUSLE (Renard et al., 1997) the K-factor is calculated through an equation that takes into account the soil grain size. The equation proposed by Renard et al. (1997) has a bigger applicability in comparison to the one proposed by Wischmeier and Smith (1978). Consequently, the former equation was developed with global data of measured K-factor values obtained from 225 soil classes with a determination coefficient of R^2=0.983. Thus, the K-factor is expressed by the equation:

$$K = \left\{0.0034 + 0.0405\ exp\left[-\frac{1}{2}\left(\frac{\log\ (\mathrm{Dg}) + 1.659}{0.7101}\right)^2\right]\right\}$$

(Eq. 5.9)

Where Dg is:

$$Dg\ (mm) = \exp\left(0.01 \sum f_i\ \ln \mathrm{m_i}\right)$$

(Eq. 5.10)

D_g is the geometric mean particle diameter following Shirazi and Boersma (1984); f_i is the primary particle size fraction in percent; m_i is the arithmetic mean of the particle size limits of that size.

The soil K-factor (in t h MJ^{-1} mm^{-1}) for the Turano watershed was calculated based on Eq. 5.9 (Renard et al., 1997) using the soil texture information derived from the eco-pedological maps of Italy (1:250,000) as a first data source. Later it was subsequently

improved using 50 top-soil samples collected in this study (10 cm depth), alluvional and colluvial sediments data (Hoelzman, 2009, personal communication), 16 soil samples from Conca di Oricola (Lorenzoni et al., 1995), soil data derived by the activities of diploma students (Domdey, 2009, personal communication) as well as soil data provided by the ARSAA (2006). In addition to CARG geological maps, further information about Quaternary deposits were acquired. Grain size classification was performed according to the USDA (2010) classification system. The modified Eco-pedological map was converted from a polygon shapefile into a raster 10x10 m cellsize. Finally, the K-factor raster was computed applying Eq. 5.9 on the modified Eco-pedological map through raster calculator operations.

5.1.1.2.3. LENGTH-SLOPE FACTOR COMPUTATION

The LS-factor parameter, also called the topographic factor, represents the influence of the terrain topography on the sediment transport capacity of the overland flow. It was originally proposed by Wischmeier and Smith (1978) in the USLE model, where it reflected the effects of the slope length (L) and the slope steepness (S) on sheet and rill erosion.

In the RUSLE model the parameter was improved through the incorporation of the profile convexity and concavity influence using segmentation of irregular slopes (Renard et al., 1997). Owing to the DEM manipulating ability of GIS software, the topographic factor has been further revisited in various studies and the impact of the flow convergence was incorporated into the LS-factor computation (Moore and Burch 1986, Mitasova et al., 1996; Desmet and Govers, 1996; Engel, 1999). In one of the latest modifications of RUSLE, the RUSLE-3D, Mitasova et al. (1999) proposed the replacement of the slope-length factor (*L*×*S*) with a factor that captures the upslope contributing area per unit of contour. Thus, referring to Mitasova et al. (1999) the modified $LS_{(r)}$ factor at a specific point on a hillslope is given by the following relation:

$$LS_{(r)} = (m+1)\left[\frac{Ac}{\alpha_0}\right]^m \left[\frac{sin\beta}{\beta_0}\right]^n \quad \text{(Eq. 5.11)}$$

Where A_c (m²) is the upslope contributing area per unit of width (Flow Accumulation); β is the slope angle (degree); α_0 is the length (72.6 ft, equals to 22.13 m) and β_0 is the angle of the standard terrain parcel (9%, equals to 5.16 degree slope) of USLE. Finally, m and n are exponent parameters depending of the specific prevailing type of flow.

For the Turano watershed the LS-factor was computed using Eq. 5.11 since it was considered more accurate that the equations proposed in the USLE and RUSLE consistent

with the method applied in most recent publications (Saavedra, 2005; Agnesi et al., 2006; Märker et al., 2008; Pelacari et al., 2008; Terranova et al., 2009). The topographic parameters were outlined from a DEM based on contour lines of a 1:25,000-scale topographical map (IGMI cartography, 1994) and enriched with additional elevation points. The Turano DEM with a resolution of 10 m was delineated using the Topogrid sub-module of ArcInfo 9.3 (Hutchinson, 1989). It is illustrated together with the Ovito sub-watershed DEM in Figure 5.1 that was generated with the same procedure but using a 1:5000-scale topographical maps (Carta Tecnica Regionale Abruzzo). The Acc value was derived from filled DEMs according to the method for flow accumulation of O'Callaghan and Mark (1984). The Ovito sub-watershed DEM with 3 m resolution was used to test the influence of the DEM resolution on the RUSLE soil loss prediction.

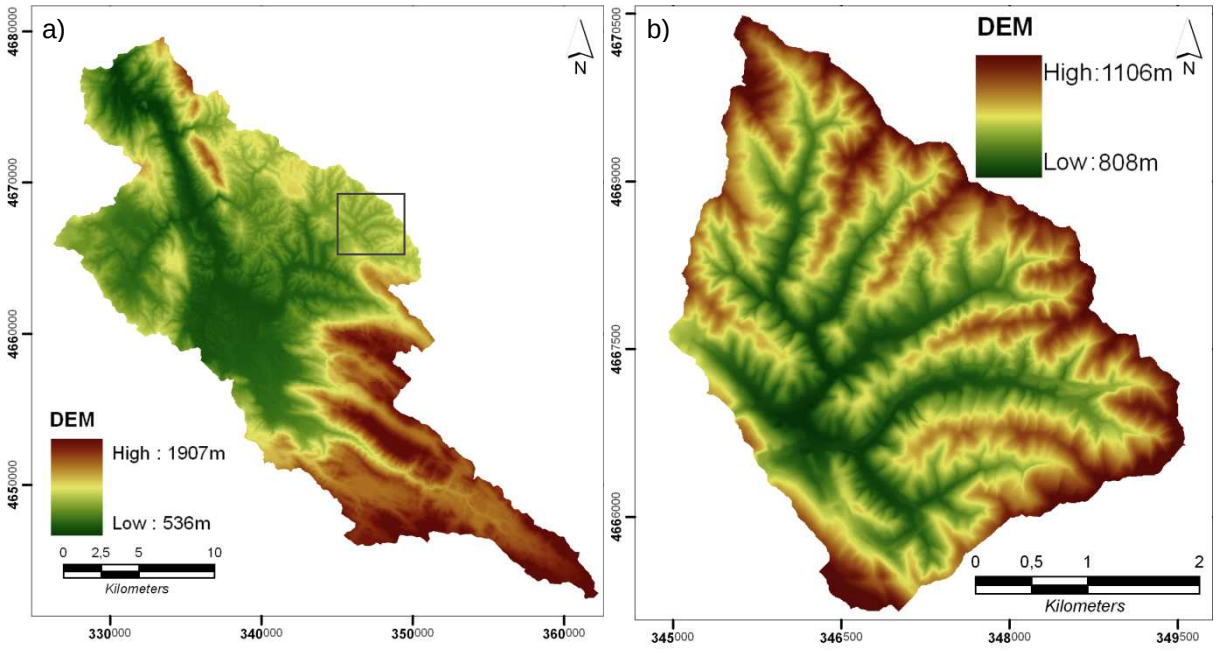

Fig. 5.1 – Digital elevation model: a) Turano (10 m); b) Ovito (3 m).

5.1.1.2.4. COVER-MANAGEMENT FACTOR COMPUTATION

According to Wischmeier and Smith (1978), the C-factor describes the cover and management factor that measures the combined effect of all the interrelated cover and management variables. In the RUSLE model (Renard et al., 1997) this C-factor has largely been improved compared to the one proposed by Wischmeier and Smith (1978). The C-factor results from the weighted average of the soil loss ratio:

$$SLR = PLU \cdot CC \cdot SC \cdot SR \cdot SM \quad \text{(Eq. 5.12)}$$

where the soil-loss ratio SLR is the multiplication of the sub-factors prior-land-use (PLU), canopy-cover (CC), surface-cover (SC), surface-roughness (SR) and soil-moisture (SM).

The C-value may range from 0 to 1 depending on the ground cover. Generally, values close to zero are typical for forested areas where the ground cover can reach up to 100% while values close to one are typical of bare soil areas (Pierce et al., 1986). According to Renard and Ferreira (1993), this factor is very important for the soil erosion estimation as it represents the only condition that may be regulated through management practices targeted to reduce the erosion in act.

The evaluation of the C-factor normally calls for long-term experiments and occasionally field plots soil loss measures are necessary. However, the estimation of the C-factor consistent with the Agricultural Handbook 537 (Renard et al., 1997) for large, topographically complex areas with heterogeneous vegetation patterns is not easily executable. Thus, in the last two decades several studies have developed alternative methodologies to extract the C-factor values in a simplified way compared to the strict methodology suggested by Renard et al. (1997). For agricultural areas in several studies the C-values are assigned to the land-use units according to available literature values derived by fieldwork experiments. This is made possible owing to the worldwide database resulting from the large RUSLE application in agricultural areas. Contrariwise, to estimate C-values for non-agricultural areas a heterogeneous scenario of methods is present in literature. For non-agricultural areas C-factor values are often assigned following the land-use classification, calculated with methods based on Curve Number (CN) (Øverland, 1990), remote-sensing operations (de Jong et al., 1998; van der Kniff et al., 1999; Singh et al., 2004; Warren et al., 2005) or methods involving remote-sensing and field observations (de Asis and Omasa, 2007, Zhou et al., 2008).

For the Turano watershed, after reviewing the methods presented in literature and pre-testing a few of them in one of its sub-catchments (the Ovito watershed), the C-factor was estimated with a method specifically created for this research. It is based on a spatial-distributed weighted overlap of C-factors assigned to the Turano basin land-use units according to the values proposed in literature (Zanchi and Giordani, 1995; Grimm et al., 2003; Garfi, 2006; Märker, 2008; Chisci and Bazzoffi, 1995) and C-factors estimated by a NDVI technique (de Jong, 1998).

This approach emerged after testing and comparing the results of a selected simplified methodology for C-value (de Jong et al., 1998; van der Kniff et al., 1999; Øverland, 1990) estimation with C-values calculated after field survey in the sixth-order Ovito sub-watershed according to Eq. 5.12. From the pre-testing procedure three insights have been gained to estimate the C-factor in a modified way.

Firstly, the method proposed by Renard et al. (1997) in the Agricultural Handbook 537 is not applicable in areas with environmental characteristics such as the Turano watershed and is highly time consuming. As a second aspect, a relevant overestimation of the C-factor calculated by equations based on NDVI data was observed. Applying such methods based on NDVI images means insufficient attention given to the areas unaffected by soil erosion, i.e., urban districts, paved roads and further any other properties. In sum, a considerable overestimation in the soil erosion modeling is very likely due to the described error, which is in fact avoidable, so that this approach was considered as inapplicable without adequate modifications. Last but not least, as expected although methods based on NDVI data seem to perform rather poorly in low or unvegetated areas, this does not hold for the forested areas. In the latter areas the C-factor derived by the NDVI technique, although overestimated compared to the reference value (Eq. 5.12), represents the tree density as well as their canopy cover status well. It follows that using NDVI-derived C-values the seasonal variations of the vegetation cover for high-vegetated areas often characterized by heterogeneous patterns can be considered.

Based on the pretest performed in the Ovito sub-watershed (detailed description see Appendix E) the 24 land cover units (land-use map 1:10,000 scaled, Fig. 3.20 Chapter 3.4.2) within the Turano watershed have been split into two groups. The first group includes farmland units (i.e. irrigated land, non-irrigated arable land, complex cultivation, principally agriculture with natural vegetation, olive trees, vineyards and fruit trees) and unvegetated (i.e., continuous urban fabric, discontinuous urban fabric, paver roads, unpaved roads, mines, sport, lake) or poorly vegetated areas (i.e., harvested forest, scrubland, natural grassland pastures, transitional woodland scrub). Highly vegetated areas (i.e., broad-leaved forest and coniferous forest) were assigned to the second. For the first group C-values derived exclusively from literature were considered. Table 5.2 visualizes these land-cover classes and the attributed C-factor values. In contrast, for the vegetated land-cover areas, within a first step C-values allocated according to literature values, have subsequently been crossed with C-values derived from NDVI data (de Jong, 1998). This procedure was developed in a GIS environment by the aforementioned weighted-overlap operations attributing weights equal to 90% for literature values and 10% for NDVI C-values.

Figure 5.2 provides the methodology employed to derive the final C-factor raster for the Turano case of study. For the period under investigation (1997–2005), apart from forested areas, no changes in the land-use for the Turano watershed were considered. The farmland and pastureland areas were considered unchanged, while for the forested area both seasonal variations of the canopy cover and coppicing activities were considered.

The seasonal variation of forested areas was given by using different Landsat images to estimate the NDVI C-factor, i.e., October 2000, January 2002, April 2003, and June 2003. These NDVI images were used for all eight years in which RUSLE was applied. In doing so, a similar annual vegetation cycle for the considered time step was assumed.

Furthermore, woodland sectors affected by forest-harvesting activities (1997–2005) that have been identified by orthophoto visual interpretation as well as LANDSAT supervised classification (Richards, 1992) were integrated into the C-values raster. The C-values for the areas after harvesting were taken from Garfì et al. (2006), who conducted their research in Italy under similar conditions. The values range from 0.25 in the 1st half year after trees-harvesting to 0.0030 in the 2nd half of the 4th year after trees-harvesting.

Table 5.2 – C-Factor for the Turano watershed

Land use and land cover	RUSLE C-factor	Area km²
Continuous urban fabric	0.0003	2.4
Discontinuous urban fabric	0.002	3.4
Paved roads	0	3
Unpaved roads	0.0003	3.9
Mines	0.36	0.2
Sports	0.003	0.001
Non-irrigated arable lands	0.12	17.2
Permanently irrigated arable lands	0.14	34.4
Vineyards	0.451	0.1
Olive	0.3	3.4
Lands principally occupied by	0.1	7.6
Broad-leaved forest (dense)	0.003	260.2
Broad-leaved forest (not dense)	0.005	17.6
Coniferous forest	0.003	1.1
Scrublands	0.014	39.5
Natural grassland > 75%	0.035	1.5
Natural grassland 50-75%	0.04	32.9
Natural grassland > 50%	0.045	11.3
Pastures (good quality)	0.15	12.9
Pastures (poor quality)	0.4	0.7
Transitional woodland scrub	0.003	8.7
Artificial woodland recolonization	0.003	0.1
Lake	0	4.7

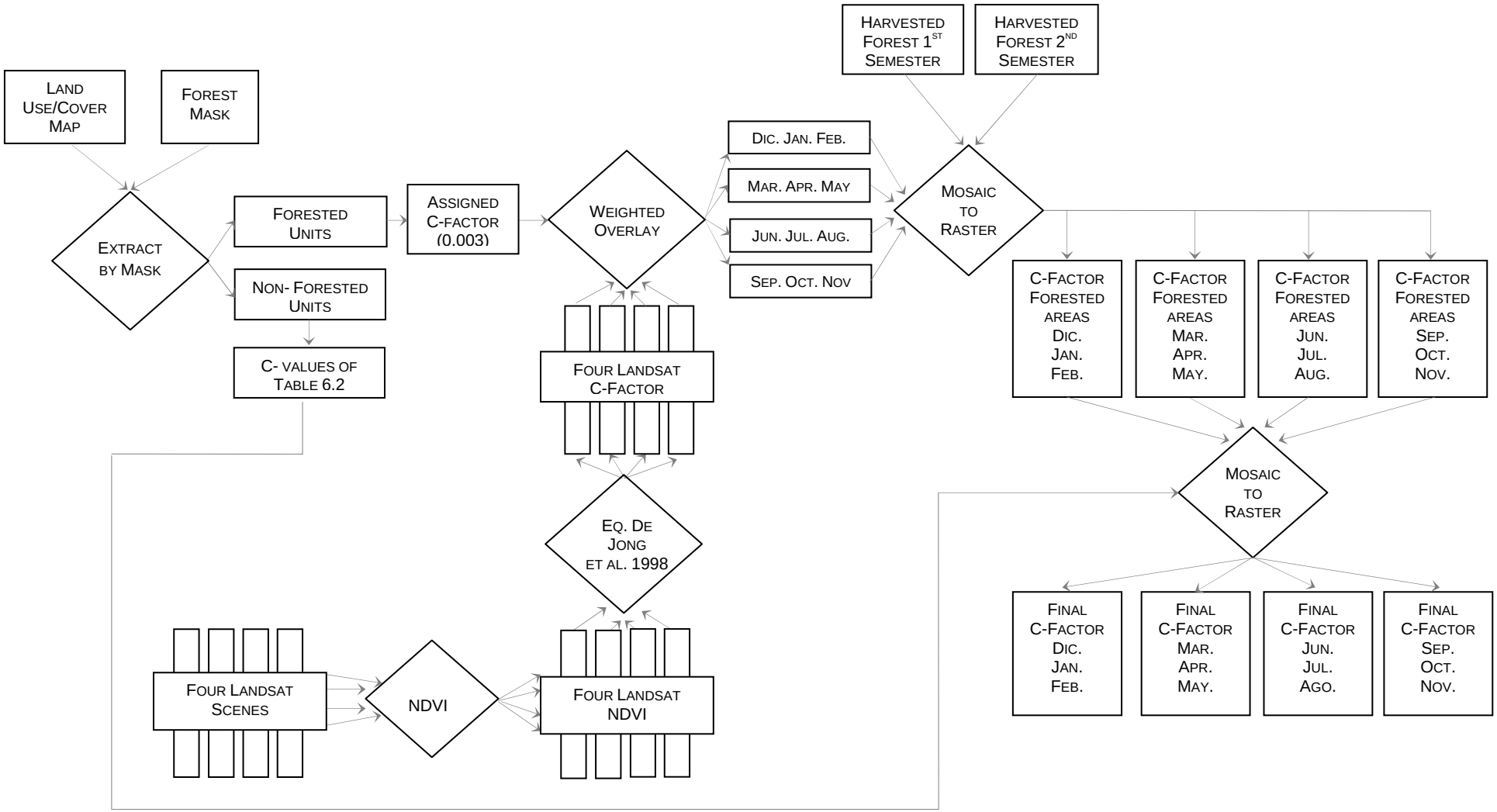

Fig. 5.2 – Flowchart for creating the seasonal C-factor.

5.1.1.2.5. SUPPORT PRACTICE FACTOR

The P-factor reflects the effects of contouring (tillage and planting on or close to the contours), stripcropping, terracing and subsurface drainage. For the area under investigation, the support practice P-factor has not been considered in this study and has thus been assumed to be a constant (equal to 1, i.e., no erosion practices according to Wischmeier and Smith, 1978). Keeping the value of this factor equal to 1 is used largely in the present literature contributions. A constant value is used in the absence of soil conservation practices (the case of the Turano area as confirmed during field survey) or when information about soil conservation practices is unavailable. Furthermore, the method to estimate the P-factor based on slope gradients, for instance, proposed for the USLE P-factor by Wener (1981) was considered not necessary due to the high concentration of agricultural activities in the flat plain.

5.1.1.2.6. RUN THE RUSLE EQUATION

The estimation of RUSLE predicted annual soil loss (gross erosion) values of the Turano watershed was carried out by applying Eq. 5.13, where the A-monthly values were computed for each month for the period between September 1997 and October 2005 applying Eq. 5.14. In doing so, the temporal variation of R-factor (monthly) and the C-factor (seasonal) across the year were considered while the K-, LS- and P-factor were taken as constants.

$$A = \sum_{j=1}^{J=12} (A_{monthly})j$$

(Eq. 5.13)

$$A_{monthly} = R_{monthly} \cdot K \cdot LS \cdot C_{seasonal} \cdot P$$

(Eq. 5.14)

Finally, the total loss of soil for the period stretching from September 1997 to October 2005 is given by the sum of the annual A-values. To get these values, 96 A-monthly rasters were computed.

5.1.2. UNIT STREAM POWER EROSION DEPOSITION MODEL

5.1.2.1. MODEL DESCRIPTION

The second soil erosion prediction model applied is the Unit Stream Power Erosion Deposition model (USPED). This is an empirical-conceptual model with moderate input requirements. It can be described as a three-dimensional enhancement of the RUSLE

(Warren et. 2005) due to the fact that its application requires some RUSLE parameters (Mitasova, 1997).

According to Mitasova (1999), this is 'a simple model which predicts the spatial distribution of erosion and deposition rates for a steady-state overland flow with uniform rainfall excess conditions for transport capacity limited case of erosion process'. The final version of this model (Mitasova, 1999) is based on the theory originally outlined by Moore and Burch (1986) and got improved by various authors (Desmet and Govers, 1995; Mitas and Mitasova, 1998; Mitasova et al., 1996). Basically, the innovative idea proposed by the authors of USPED is that the erosion-deposit rate does not only depend on the flow transport capacity but rather on its variation from one point to the other. Thus, erosion occurs where there is an increase of transport capacity of the running flow and, vice versa, deposition of the sediments takes place where there is a reduction of flow transport capacity. Whereas RUSLE can only estimate gross erosion and lacks the ability to compute sediment deposition occurring on the hillslopes, the USPED model is able to deliver the deposition rate. Consistent with the authors this model can also be used in conditions of complex topographic areas where the erosion is limited by the capacity of overland flow to transport sediment.

In USPED to represent the transport capacity a dimensionless index $T_{(r)}$ and a topographical index $ED_{(r)}$ (representing the change in the transport capacity in the flow direction) are used to estimate the spatial distribution of erosion-deposition processes. The $T_{(r)}$ parameter is derived from the unit stream power theory (Moore and Burch, 1986). The upslope contributing area is used as a proxy for the water flux at a given location or grid cell. The index $ED_{(r)}$ is positive for areas with topographical potential for deposition and negative for areas with an erosion potential. The sediment flow rate $q_{s\,(r)}$ at the sediment transport capacity $T_{(r)}$ (Julien and Simmons, 1985) is described by:

$$\left|q_{s\,(r)}\right| = T_{(r)} K_{t\,(r)} \left|q_{(r)}\right|^{m} \sin\beta_{(r)}^{n} \qquad \text{(Eq. 5.15)}$$

Where $q_{(r)}$ is the water flow, $K_{t\,(r)}$ is the soil transportability coefficient, and *m* and *n* are constants depending on the type of flow and soil properties.

According to the 2D flow formulation proposed by Mitas and Mitasova (1998), water and sediment flows are represented as bivariate vector fields $q_{(r)} = q_{(x,y)}$, $qs_{(r)} = qs_{(x,y)}$ and the net erosion and deposition rate $ED_{(r)}$ is estimated as the divergence of the sediment flow, as shown in the following equation:

$$ED_{(r)} = div\ q_{s\,(r)} = K_t\{[grad\ h_{(r)}] \cdot s_{(r)} \sin b_{(r)} - h_{(r)}\,[k_{p(r)} + Kt_{(r)}]\}$$

(Eq. 5.16)

Where $s_{(r)}$ is the unit vector in the steepest slope direction, $h_{(r)}$ (m) is the uniform rainfall intensity, $kp_{(r)}$ is the profile curvature or curvature in the direction of the steepest slope, and $kt_{(r)}$ is the tangential curvature or curvature in the direction perpendicular to the gradient.

Moreover, to apply the USPED model Mitasova (1997) proposed to use the RUSLE parameters to incorporate the impact of rainfall, soil and land cover to obtain a relative estimate of net erosion and deposition. Accordingly, USPED builds on the assumption that the sediment flow at sediment transport capacity can be estimated as:

$$T_{(r)} = R \cdot K \cdot C \cdot P \cdot A^m (\sin \beta)^n$$

(Eq. 5.17)

Where $R{\sim}i^m$, $K \cdot C \cdot P{\sim}Kt$, $LS = A^m sin\beta^n$ and m=1 n=1 for prevailing sheet erosion; while for prevailing rill erosion *m*=1.6, *n*=1.3 can be used.

Finally, the net erosion-deposition $ED_{(r)}$ is estimated as the change in the sediment flow rate expressed by a divergence in sediment flow:

$$ED_{(r)} = div(T_{(r)} \cdot s) = \frac{d(T_{(r)} \cdot cos\alpha)}{dx} + \frac{d(T_{(r)} \cdot sin\alpha)}{dy}$$

(Eq. 5.18)

Where α $[degree]$ is the aspect of the terrain surface.

5.1.2.2. USPED MODEL APPLICATION USING GIS

The USPED model was run for the Turano watershed according to the methodology proposed by Mitasova et al. (1999). The RUSLE parameters used for the USPED application were the same as those already described above. The K- and P-factors were taken as constant across the years while for the R- and C-factor monthly and seasonally variations were considered, respectively. Eq. 5.17 was carried out by applying raster-calculation operations following the scheme proposed by Mitasova et al. (1999) (Appendix F).

5.1.3. VALIDATION OF THE MODELS

Several studies accept as reliable the outputs of their application of the soil erosion prediction models without further consideration of the validity. This, however, is critical for both, the reliability of the results derived from the model application as well as for the development of future models themselves. To assess the effectiveness of the models on

soil erosion rate prediction a validation is necessary. Several methods to validate the results of the soil erosion models have so far been applied in literature, such as, fieldwork mapping (van Oost, 2005; Thiemann, 2006), plots experiments (Vittorini, 1977 Jetten et al., 1999; Del Monte, 2002; Bagarello and Ferro, 2010), radioactive isotopes (Walling et al., 1990; Porto et al., 2003; Porto et al., 2009), remote-sensing (Hill and Schütt, 2000; Gobin and Govers, 2003; Märker et al., 2008), monitoring of the sediment load in rivers (Ciccacci, 1983) and reservoir siltation measurements (Cicacci et al., 1992; Romero-Diaz, 2004; de Vente and Poesen, 2005 van Rompaey, 2005). However, most of the proposed methods are costly and time consuming so that many soil erosion studies neglect validation or apply controversial methods (Boardman, 2006). Given research-budget restrictions, this study utilizes two low-cost but well-tested and proven methods to validate model results for research on soil erosion:

1) Indirect quantitative validation through lake sediment deposition (5.1.3.1)
2) Semi-qualitatively validation through remote-sensing and field-mapping (5.1.3.2)

5.1.3.1. INDIRECT QUANTITATIVE VALIDATION

Quantitative information about erosion processes in the Turano watershed was obtained through an analysis of the sediments accumulated in Turano Lake. The volume of sediment accumulated at the lake bottom was estimated by the management of the dam (ENEL/E-ON, 2009, personal communication) by differencing bathymetric surveys taken in September 1997 and October 2005. The work was carried out under the supervision of C.I.P.E. (Interministerial Committee for Economic Planning). During the considered period no sediment dredging was performed in the lake, so that the dam sediment retention measured is equal to the total sedimentation.

The area-specific sediment yield (m^{-3} ha^{-1} yr^{-1}) was derived by dividing the lake siltation value by the watershed surface. This operation was performed after excluding the endorheic areas from the research watershed surface area. All areas that did not contribute to the outlet liquid and solid discharges were considered as endorheic. Consequently, some Turano sub-watershed and karst areas in the carbonate sector of the watershed, e.g., dolines, endorheic sub-watersheds, sinkholes, polje, and endorheic streams were removed after geomorphological analysis based on remote-sensing and GIS operations. The precipitation in these areas seems to contribute via a well-developed hypogenic karst system to the regional ground water system (Bono and Capelli, 1994). The water flow reaches the surface through resurgences only in a few cases.

The sediment volumes were converted to mass volume using a mean bulk density of 0.865 t m^{-3} conforming to analysis on sedimentary profiles performed by van Rompaey (2005) for Italian reservoirs.

Finally, the mean annual sediment yield (t ha^{-1} yr^{-1}) of the Turano watershed derived from the lake sediments was compared to the annual soil loss estimated by the applied models. For both models the eroded sediments caused by gully erosion (not detected in farmlands and only observed in sectors under intense coppicing activities during fieldwork surveys) and river channels erosion remained unconsidered. For RUSLE, the estimated sediment load (SYe) for Turano Lake was obtained as the sum of monthly soil loss (Eq. 5.14) in the considered period (1997–2005) multiply by the sediment delivery ratio (SDR). For SDR two methods were employed, the first based on observations of American watersheds by the United States Department of Agriculture (USDA, 1975 – Eq. 5.19) and the second derived from investigations in southern Italy by Bagarello et al., (1991 – Eq. 5.20). These are:

$$SDR = 0.5656 \cdot S^{-0.11} \quad \text{(Eq. 5.19)}$$

$$SRD = 5.37 \cdot S^{-0.69} \quad \text{(Eq. 5.20)}$$

Where S is the watershed area. The constants have been derived by the USDA (1975, Eq. 5.19) and Bagarello et al. (1991, Eq. 5.20).

Cooke and Doornkamp (1974) assumed that the suspended sediment yield (SSY) represents the erosion rate in humid climates (about 90% of the total erosion). This assumption combined with the fact that the fine grain size of the siltation in Turano Lake (ENEL/E-ON) leads to the hypothesis that a major share (in this study assumed to be 100%) of the hillslope net erosion reaching the stream channel network predicted by USPED is transported downstream to the lake.

5.1.3.2. SEMI-QUALITATIVELY VALIDATION

The second method to validate the model outcomes was carried out semi-qualitatively, based on a comparison of the soil erosion prediction maps of RUSLE with a soil erosion damage map. The location selected for the semi-qualitatively validation was part of the Ovito sub-watershed, also studied for other aspects of this thesis (Chapter 8, analysis of past and present dynamics of human-induced soil erosion in a sensitive area). This area was selected because of its geological (Bono and Capelli, 1994) and pedological (Bucci, 1978) characteristics that make it highly prone to soil erosion processes. In addition, widespread forest-harvesting activities are accomplished here.

The assessment of the actual erosion was conducted by stereoscopic observation of aerial photos as well as through fieldwork mapping. The aerial photos under consideration refer

to the years 2001, 2005 and 2007. Between April 2008 and September 2010 four fieldwork campaigns were performed in the Ovito area. During these activities a 1:10,000 scale map including information about erosion damages due to inter-rill, rill and gully processes was developed. In order to enlarge the time span to capture the soil erosion forms information acquired from the ISPRA geomorphological map (Foglio n° 367, Tagliacozzo) was integrated. In addition, also the modeled period have been enlarged from 1998 to 2009.

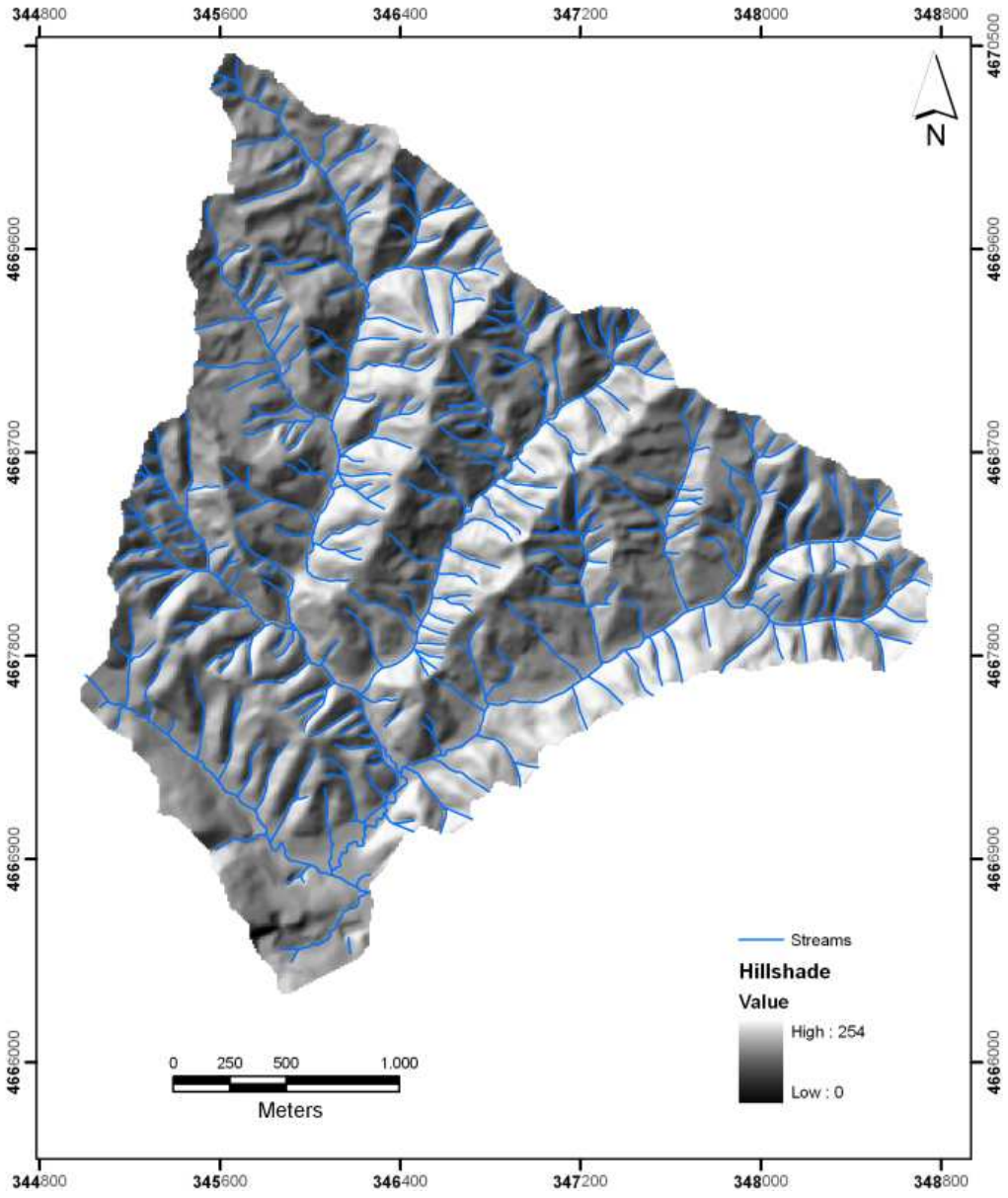

Fig. 5.3 – Relief and river network of the Ovito.

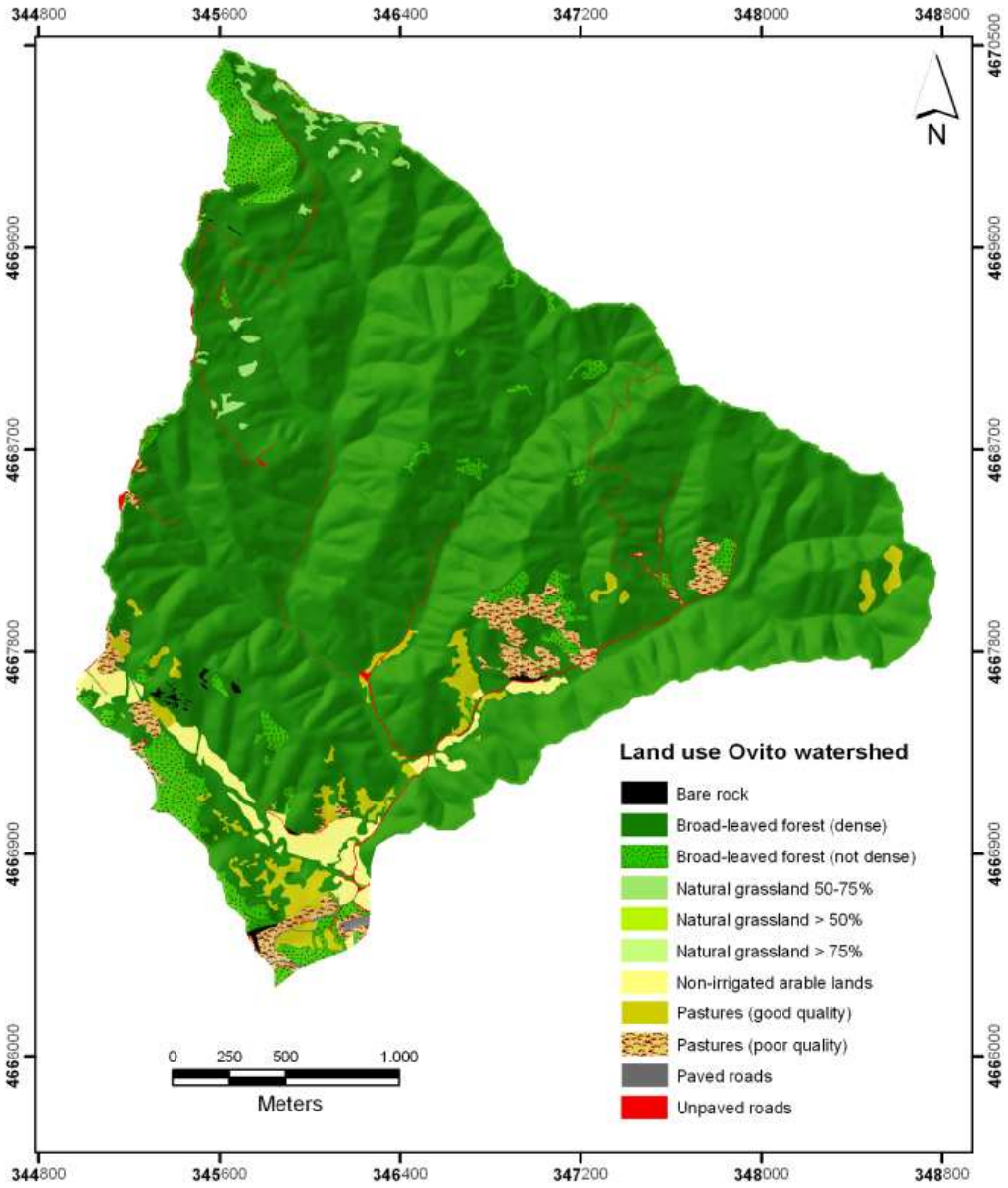

Fig. 5.4 – Land-use map of the Ovito.

5.2. RESULTS

The application of the RUSLE and USPED soil erosion models provides information on potential monthly and annual average soil erosion for the period from October 1997 to September 2005 in the Turano watershed. The selected period of time is representative of the current conditions of climate and land use in the watershed. In this way, information about the potential soil erosion (and deposition for USPED) dynamics of the investigated area as well as their spatial distribution was derived. Monthly variations of the rainfall erosivity as well as seasonal variations of the canopy cover of the forested areas were considered in the prediction of soil erosion. Moreover, the models were run taking into account the forest-harvesting in order to calculate the potential impact of this silvicultural activity in the mountainous areas. Finally, the models were run considering a hypothetical scenario where there is no coppice forest-harvesting for comparison.

5.2.1. RUSLE MODEL

5.2.1.1. INPUT PARAMETERS

The Turano watershed is mostly covered by forestlands (61.7% of the total watershed), of which 19.4 km² (6.8% of forestland) were harvested between 1997 and 2005. The forest predominantly consists of a coppice mix in the north-central sector of the watershed whereas the southern sector is covered by *Fagus sylvatica* trees. Of the remaining watershed area about 13.4% is used for agricultural production and 9.9% of the area remains permanently without arboreal cover (grassland and pastures). The C-factor in the watershed (Fig. 5.5a) varies from a maximum value assigned to vineyard (0.451) and a minimum calculated for densely vegetated forests (0.003). For all paved roads identified within the area a null C-factor value was assigned.

The analysis of the nature of the terrain showed a prevalence of areas classified as moderate slopes, with inclinations between 10° and 35°. In accordance with this the topographic LS-factor of the Turano watershed (Fig. 5.5b), which increases proportionally with respect to the slope, assumes a rather high average value equal to 10.05 (STD=9.44). The minimum LS-factor values are typical of the *displuvio* lines. In contrast, the spatial distributions of high values clearly display the structure of the Turano drainage network reaching values up to 68.6.

The K-factor, calculated according to the characteristics of the Turano soils, ranges from 0.017 t h MJ^{-1} mm^{-1} in the torbiditic sector of the watershed mainly covered by Endolepti Calcaric Cambisols to 0.038 t h MJ^{-1} mm^{-1} in the carbonatic sector which is predominantly covered by Dystri Leptic Cambisols (Fig. 5.5c).

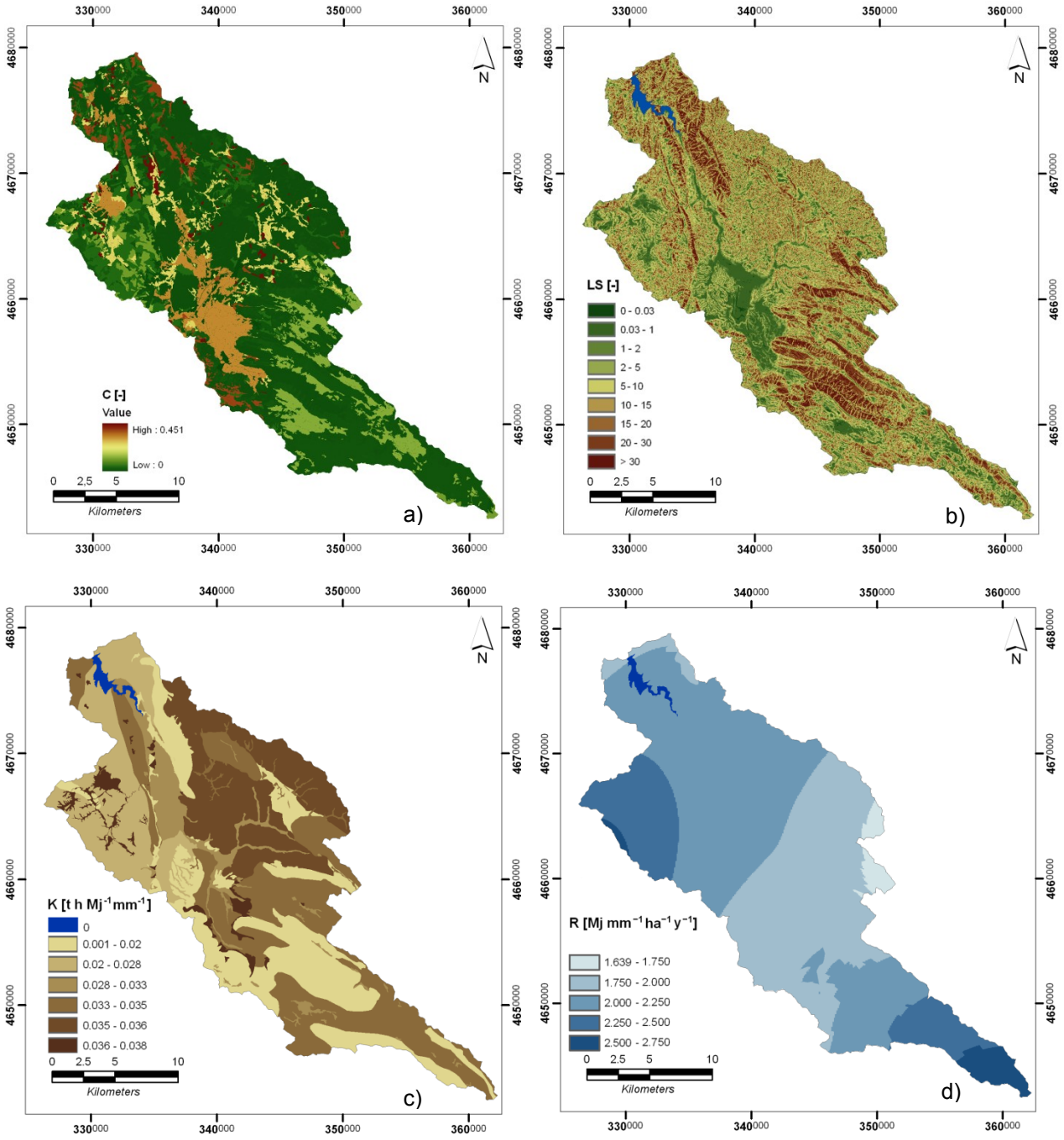

Fig. 5.5 – Distribution of the RUSLE factors in the Turano watershed: a) rainfall erosivity 'R-factor' b) soil erodibility 'K-factor', c) topographic factor 'LS-factor', d) cover-management factor 'C-factor'.

The annual average erosivity factor (Fig. 5.5d) computed for the studied watershed equals to 1942 MJ mm ha^{-1} h^{-1} yr^{-1} for the period studied. Observing the spatial distribution of the annual average rainfall erosivity within the area, the high variability between the lowest at 1552 MJ mm ha^{-1} h^{-1} yr^{-1} and the highest at 2415 MJ mm ha^{-1} h^{-1} yr^{-1} which is equal to a 36% difference, becomes evident. The temporal variability across the year showed high values of rainfall erosivity during the autumn period and during the second half of spring. In contrast, the rainfall erosivity is lower in summer and winter (for more information see in

Appendix G). In the observed period the highest yearly rainfall erosivity was recorded during 1998 (2338 MJ mm ha^{-1} h^{-1} yr^{-1}). According to the monthly data, the month with the strongest rainfall erosivity value (698 MJ mm ha^{-1} h^{-1}) was in September 1998, whereas the maximum single rainstorm erosivity was found in August 2005. Here, 60 mm of rainfall in 3.5 hours produced a rainfall erosivity value of 1064.42 MJ mm ha^{-1} h^{-1} (value excluded from the Eq. 5.8 (R-factor) calculation).

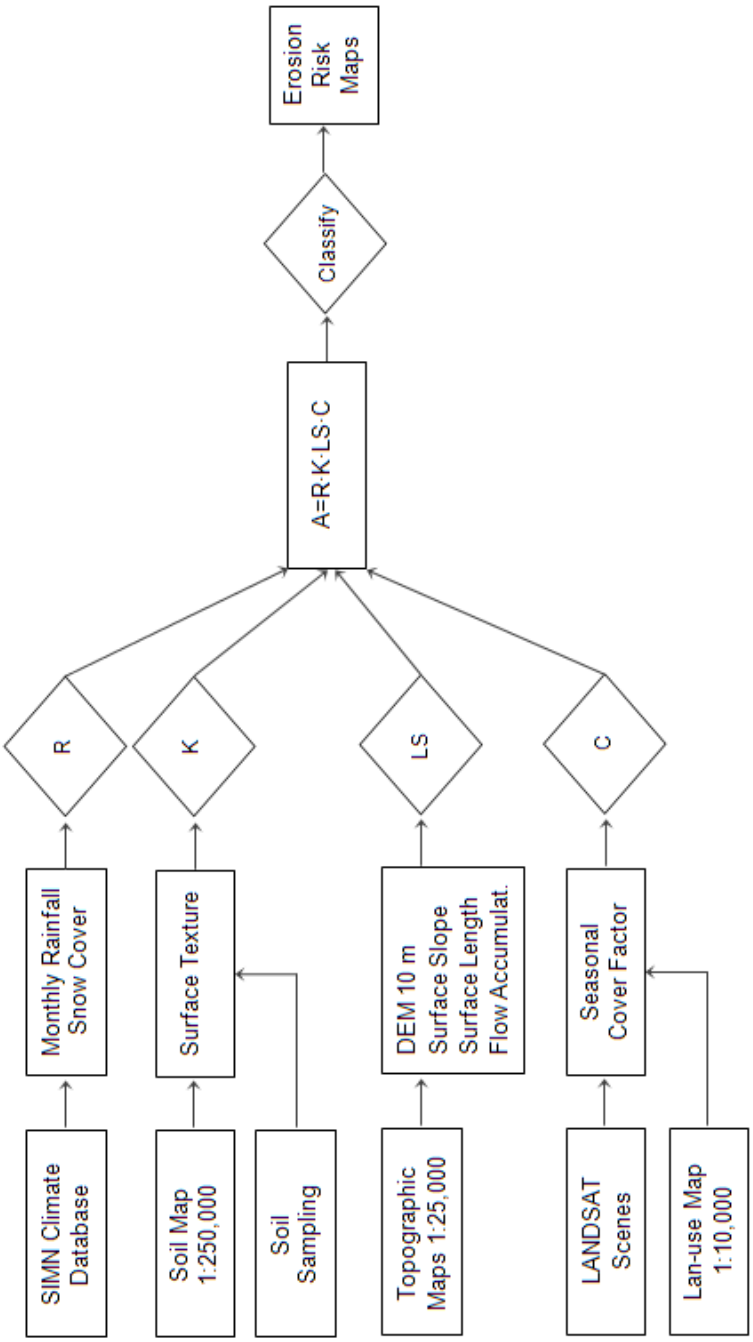

Fig. 5.6 – Flowchart for creating a RUSLE-based soil erosion prediction.

5.2.1.2. SOIL LOSS PREDICTION

The modeling approach provided erosion rate values for each of the 4,667,412 10x10 m cells into which the watershed was subdivided. The average soil loss predicted by RUSLE for the Turano watershed under the considered land use is equal to 513,458.69 t yr^{-1} with an average area-specific soil loss of 11 t ha^{-1} yr^{-1}. The predicted spatial patterns of gross soil erosion, shown in Figure 5.7, were divided into seven classes according to the European Soil Bureau classification (van der Knijff et al., 1999; van der Knijff et al., 2002; Grimm et al., 2003). The classes were: Class 1, very low erosion (0–1 t ha^{-1} yr^{-1}); Class 2, low erosion (1–3 t ha^{-1} yr^{-1}); Class 3, moderate erosion (3–5 t ha^{-1} yr^{-1}); Class 4, high erosion (5–10 t ha^{-1} yr^{-1}); Class 5, severe erosion (10–20 t ha^{-1} yr^{-1}); Class 6, very severe erosion (20-40 t ha^{-1} yr^{-1}); Class 7, extreme severe erosion (>40 t ha^{-1} yr^{-1}).

By means of statistical operations for the 466.7 km^2 area of the Turano watershed approximately 20.4% of it experience very low erosion rates. Further, 24.5% and 17.2% of the watershed are characterized by low and moderate erosion rates respectively, whereas 16.5% refer to high erosion. The portions of the watershed experiencing severe and very severe erosion rates account for 8.7% and 6.5%, respectively. Finally, about 6.2% of the investigated area is prone to extreme severe erosion.

Considering the amount of soil loss and the type of land cover average values corresponding to 25.94 t ha^{-1} yr^{-1} for croplands, 65.02 t ha^{-1} yr^{-1} for pastureland and 3.9 t ha^{-1} yr^{-1} for forestlands (2.93 t ha^{-1} yr^{-1} if only undisturbed forest is considered) were observed. The soil loss values show a high standard deviation within each land-cover group (Table 5.3). In the case of the agricultural fields low values ranging from 3 to 11 t ha^{-1} yr^{-1} are typical for the low-inclined flood plains. Contrarily, when the hillslope inclination raises a strong increase in the erosion rate occurs. In steep farmland slopes the average of annual soil loss reaches up to 106 t ha^{-1} yr^{-1}. Additional information about soil loss and hillslope gradients divided by land use is given in Table 5.5. Yet, the parts of the watershed in which the soil is severely threatened by erosion are the ones characterized by low vegetation cover combined with elevated LS-factor values. Locally high LS-factors may also explain the high erosion rate of the sparsely vegetated macchia (average = 7.98 t ha^{-1} yr^{-1}) obtained in the northwestern sector of the watershed. According to the RUSLE output, the hilly sectors of the Turano watersheds cultivated with olive plantation account for the highest average of annual specific soil loss (130 t ha^{-1} yr^{-1}).

Table 5.3 – Soil losses by different land-use and land-cover types at Turano watershed.

Land use type	Surface erosion		Soil loss		
	Area	Soil loss percent	Total	Mean	SD
	[km²]	[%]	[t yr⁻¹]	[t ha⁻¹ yr⁻¹]	[t ha⁻¹ yr⁻¹]
Urban and built-up areas	5.8	0.01	32.9	0.06	0.1
Cropland	59.2	29.9	153,486.0	25.94	33.1
Pasture land	13.7	17.3	88,953.9	65.02	70.2
Forest land	288.7	21.9	112,520.6	3.90	5.8
Rangeland	45.7	14.9	76,683.0	16.77	17.2
Macchia	39.5	6.1	31,486.3	7.98	6.9
Olive + vineyard	3.4	9.1	46,924.0	137.28	112.8
Others	10.8	0.7	3,372.1	3.11	23.8

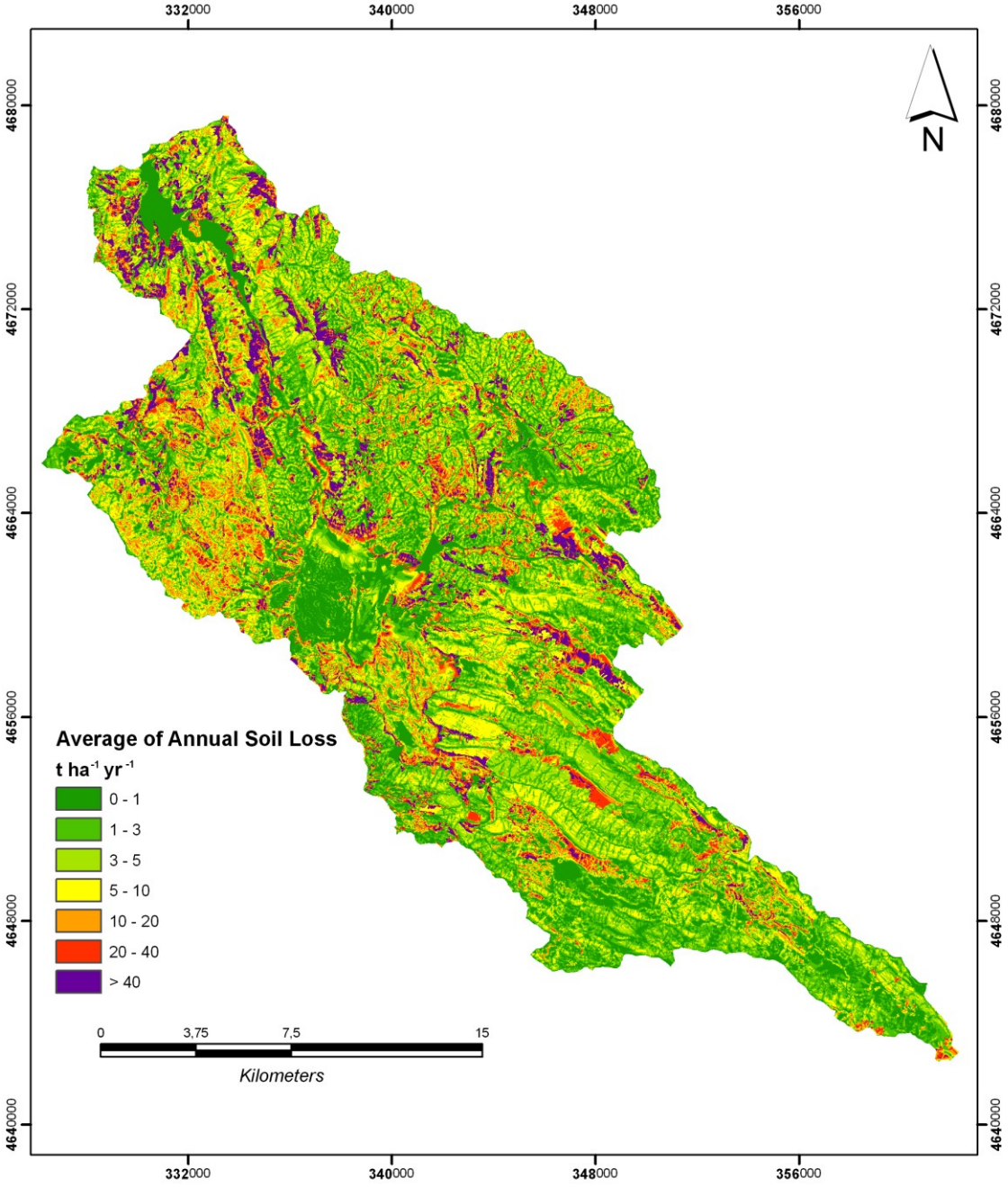

Fig. 5.7 – Predicted average annual soil erosion for the Turano watershed (1997–2005).

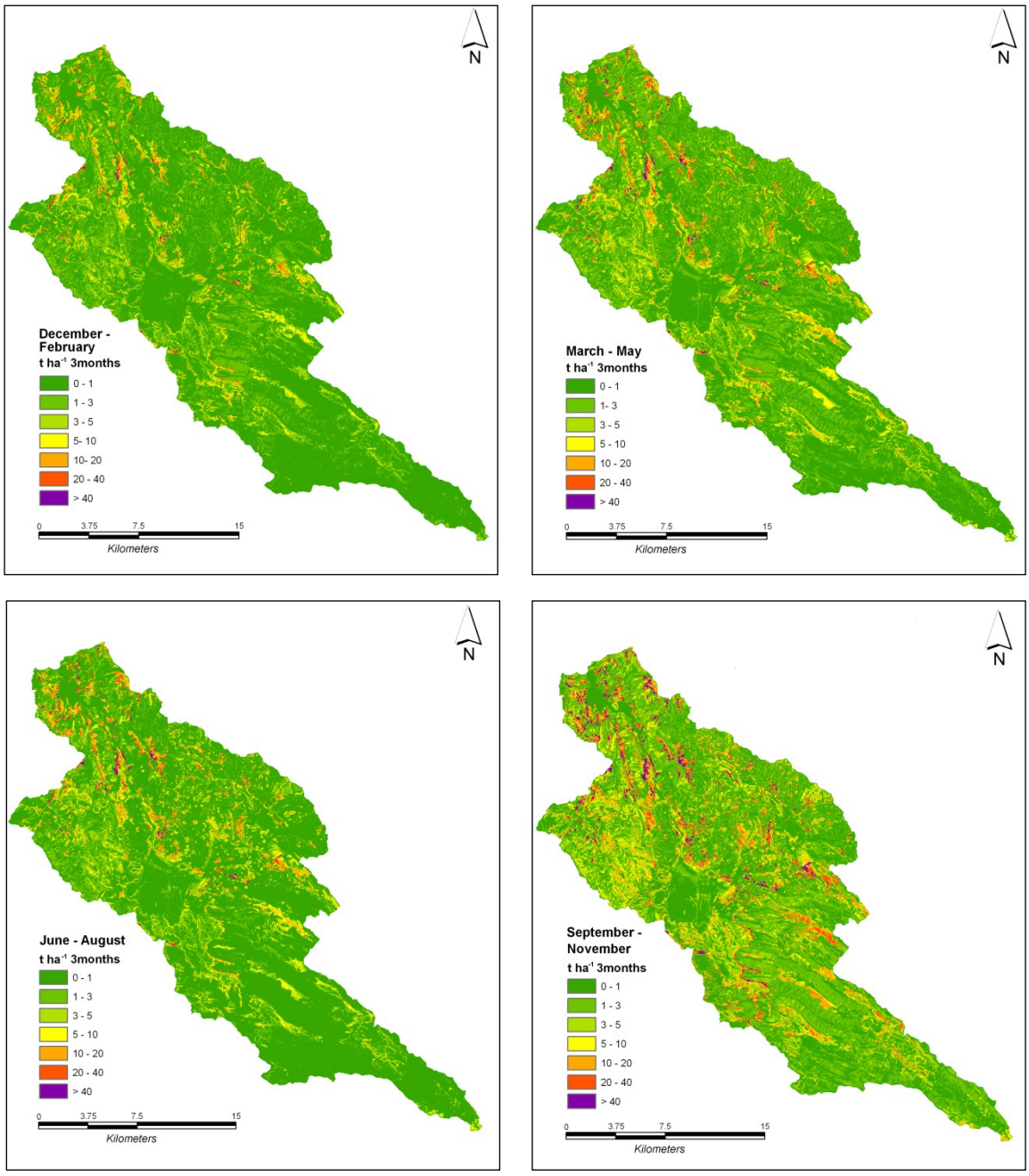

Fig. 5.8 – Predicted average seasonal soil erosion for the Turano watershed (1997–2005).

The average soil loss of pastureland is about 2.5 times that of cropland and 16.5 times higher than for forested land. Most of the forested area surface falls into the low soil erosion risk class. As mentioned above, the average soil loss in the eight years considered is equal to 3.9 t ha^{-1} yr^{-1}. The situation drastically changes if only the forested sectors involved in harvesting activities are considered in the erosion rate calculation. In these areas, erosion rates from low to extremely severe can be observed. Very severe and extremely severe erosion rates emerge in the presence of steep slopes and on more easily erodible soils. These areas, which are almost totally deprived of vegetation, according to

the RUSLE model experience an average soil loss equivalent to 18.84 t ha^{-1} yr^{-1}. The strongest erosion appeared in the first six months after the trees were cut when the soil remained almost bare. Subsequently, during the following years the erosion rates decrease and converge towards the pre-harvesting values which they hit in the fourth year after cuting. Furthermore, the outstanding peak value of 842 t ha^{-1} yr^{-1} relates to the period six months after forest cutting.

In accordance with the rainfall erosivity values the erosion rates are much higher during September and October. Apart from influencing the temporal incidence of the soil erosion process, the rainfall erosivity also highly influences the spatial distribution of erosion rates. The high erosion rates affecting the northwest sector of the watershed are strongly influenced by the fact that it is one of the watershed areas that experiences the highest erosive precipitations. Thus, concurring with RUSLE, the areas of these sectors characterized by low vegetation cover and steep slopes are the ones most significantly affected by soil erosion.

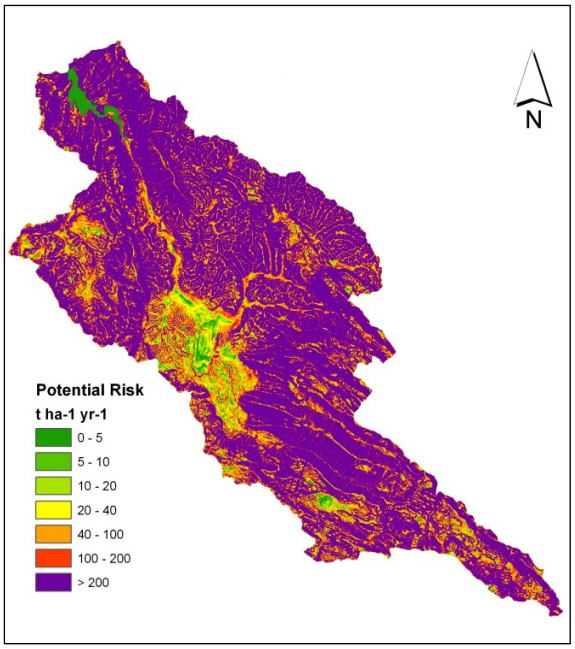

Fig. 5.9 – Potential soil erosion risk in the Turano watershed.

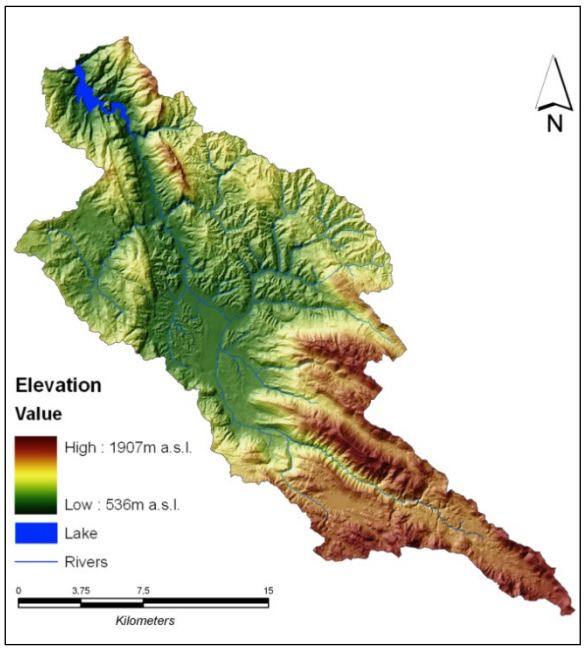

Fig. 5.10 – Digital elevation model of the Turano watershed.

Figure 5.9 illustrates the potential soil erosion risk (according to the method of van der Knijff et al., 1999) for the Turano watershed. It was assessed by running the RUSLE model considering only the basic risk factors (K-factor, LS-factor and R-factor) assuming a complete absence of vegetative cover in the study area. This allows for the isolation of the anthropogenic impacts on the land cover. Leaving the anthropogenic influence factor

unconsidered, the sectors of the watershed that are naturally more severely exposed to erosion risk can be extracted.

Furthermore, detailed maps of predicted soil erosion (1997–2005) for each sub-watershed within the Turano watershed have been subdivided and are shown in Appendix K. In addition, further details are reported in Table 5.4 and Table 5.5 illustrating the distribution of erosion classes across the study area divided by the types of land use. Figure 5.11 deals with the annual values of gross erosion from 1997 to 2005. Finally, Tables 5.6, 5.7, 5.8, 5.9 and Figures 5.12 and 5.13 provide the gross erosion values for the harvested and the undisturbed forested areas.

Table 5.4 – Soil loss according to land-use and land cover units.

Class number	Rate of erosion	Erosion risk class	Soil loss													
			Urban and built-up areas		Croplands		Pasture lands		Forest lands		Rangeland		Macchia		Olive + vineyard	
			Area	Area	Area	Area	Area	Area	Area	Area	Area	Area	Area	Area	Area	Area
			[km²]	[%]	[km²]	[%]	[km²]	[%]	[km²]	[%]	[km²]	[%]	[km²]	[%]	[km²]	[%]
1	0 – 1	very low	5.8	100	3.1	5.3	0.2	1.8	68.4	23.7	3.9	8.5	4.3	10.9	0.00	0.1
2	1 – 3	low	0	0	7	11.8	0.6	4.3	93.3	32.3	5.7	12.5	7	17.8	0.02	0.6
3	3 – 5	moderate	0	0	5.9	9.9	0.5	3.5	63.6	22	4.3	9.4	5.6	14.2	0.03	0.7
4	5 – 10	high	0	0	9.7	16.4	1	7.4	48.2	16.7	7.9	17.2	10.1	25.7	0.08	2.4
5	10 – 20	severe	0	0	10.7	18.1	1.7	12.3	8.6	3	9.5	20.9	9.7	24.7	0.19	5.6
6	20 – 40	very severe	0	0	10.3	17.5	2.5	18	5	1.7	9.7	21.1	2.6	6.7	0.36	10.6
7	>40	extreme severe	0	0	12.4	21	7.2	52.7	1.6	0.6	4.8	10.4	0	0.1	0.36	79.9
Total			5.8	100	59.2	100	13.7	100	288.7	100	45.7	100	39.5	100	3.4	100

Table 5.5 – Soil loss according to land use and land-cover units divided by slope inclination.

Class number	Slope class	Soil loss													
		Urban and built-up areas		Croplands		Pasture lands		Forest lands		Rangeland		Macchia		Olive + vineyard	
		Area	Loss rate	Area	Loss rate	Area	Loss rate	Area	Loss rate	Area	Loss rate	Area	Loss rate	Area	Loss rate
		[km²]	t ha⁻¹ yr⁻¹	[km²]	t ha⁻¹ yr⁻¹	[km²]	t ha⁻¹ yr⁻¹	[km²]	t ha⁻¹ yr⁻¹	[km²]	t ha⁻¹ yr⁻¹	[km²]	t ha⁻¹ yr⁻¹	[km²]	t ha⁻¹ yr⁻¹
1	0 – 2.5°	1.9	0.01	17.3	3.6	0.8	1.6	8.4	0.1	4.4	0.9	1.5	0.4	0.1	10
2	2.5 – 5°	1	0.02	12.6	11.3	1.1	9.6	14.4	0.4	5	3	2.7	1	0.4	29.5
3	5 – 10°	1	0.04	14.2	24.9	2.5	26	31.5	1	9.2	7.1	6.2	2.7	0.9	68.7
4	10 – 20°	1.1	0.10	12.1	55	5.1	62.1	85.6	2.8	15.3	17.1	14.9	6.8	1.5	159.1
5	>20°	0.8	0.20	3	105.9	4.2	117.7	148.7	5.7	11.8	35.7	14.2	13.7	0.6	276

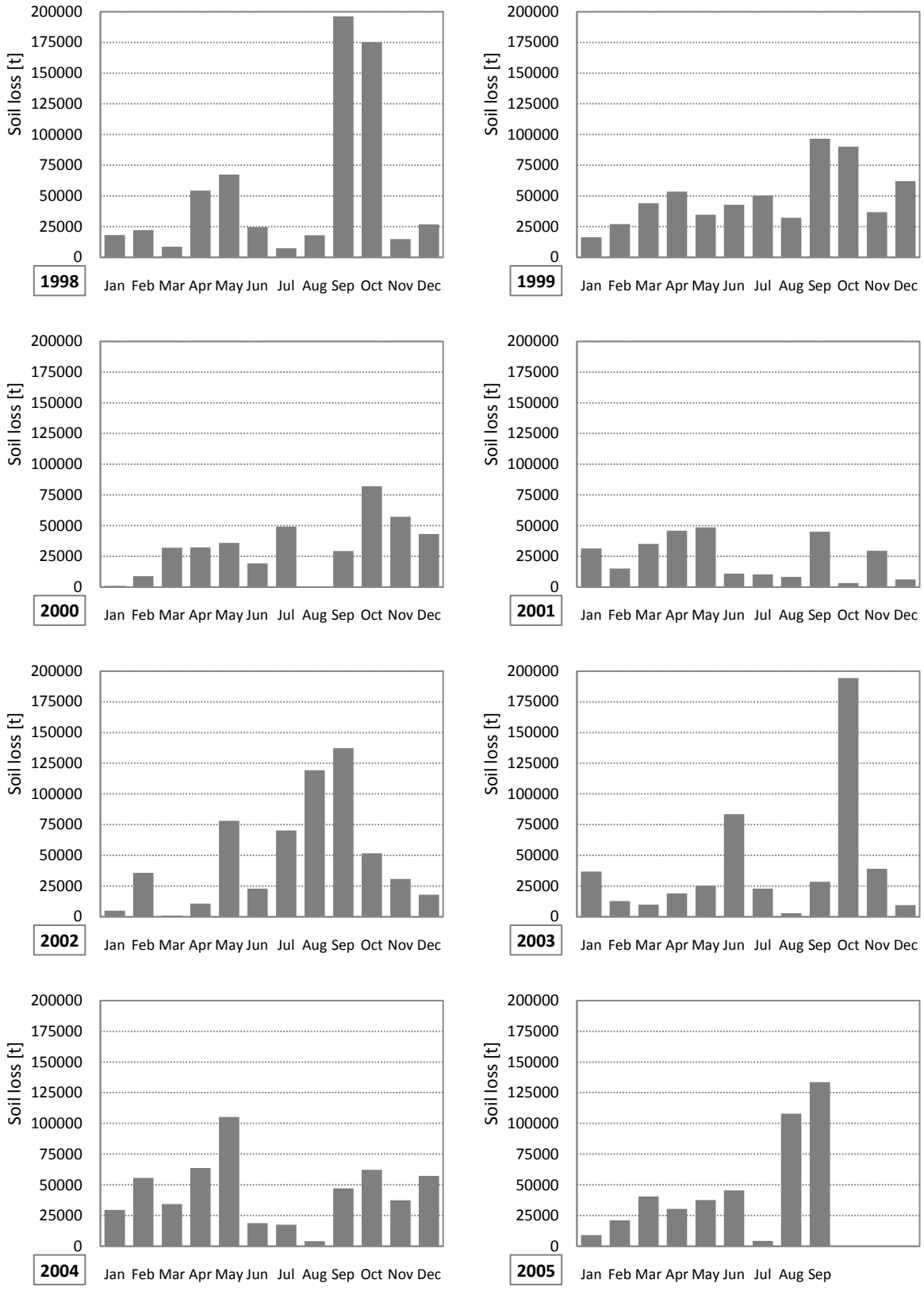

Fig. 5.11 – Monthly variation of soil loss from October 1997 to September 2005 in the Turano watershed.

Table 5.6 – Soil loss in the undisturbed forested areas (1997–2005).

Class number	Rate of erosion	Erosion risk class	Soil loss	
			Harvested forest lands	
			Area	
			[km²]	[%]
1	0 – 1	very low	67.7	25
2	1 – 3	low	91.9	34
3	3 – 5	moderate	62.2	23
4	5 – 10	high	44.9	16.6
5	10 – 20	severe	3.7	1.4
6	20 – 40	very severe	0.02	0.01
7	>40	extreme severe	0	0
Total			270.4	100

Table 5.7 – Soil loss in the areas under coppicing activities divided by slope inclination (1997-2005).

Class number	Rate of erosion	Soil loss	
		Harvested forest lands	
		Area	Soil loss rate
		[km²]	[t ha⁻¹ yr⁻¹]
1	0 – 2.5°	0.4	0.6
2	2.5 – 5°	0.7	1.8
3	5 – 10°	1.7	5.3
4	10 – 20°	5.9	14
5	>20°	10.7	27.6

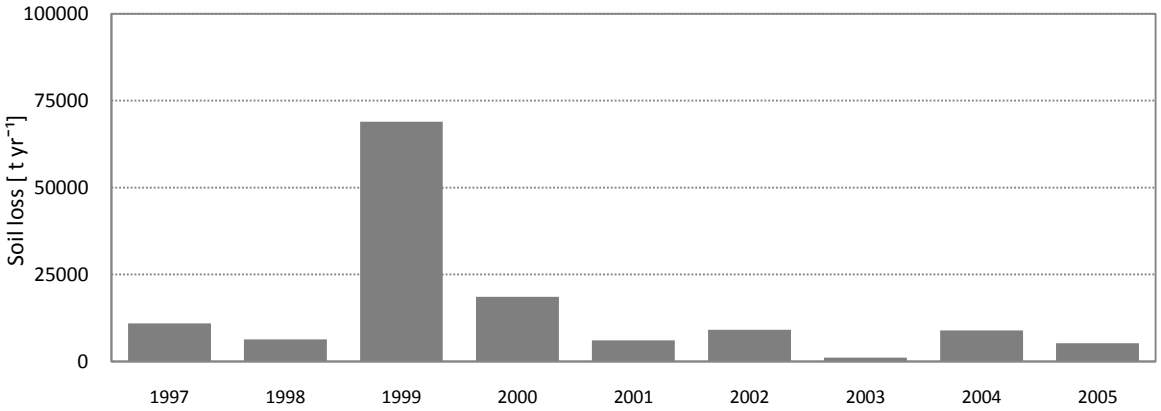

Fig. 5.12 – Soil loss in the areas under coppicing silvicultural activities divided by year.

Table 5.8 – Soil loss in the undisturbed forested areas (1997–2005).

Class number	Rate of erosion	Erosion risk class	Soil loss	
			Harvested forest lands	
			Area	
			[km²]	[%]
1	0 – 1	very low	67.7	25
2	1 – 3	low	91.9	34
3	3 – 5	moderate	62.2	23
4	5 – 10	high	44.9	16.6
5	10 – 20	severe	3.7	1.4
6	20 – 40	very severe	0.02	0.01
7	>40	extreme severe	0	0
Total soil loss			270.4	100

Table 5.9 – Soil loss in the undisturbed forested areas divided by slope inclination.

Class number	Rate of erosion	Soil loss	
		Harvested forest lands	
		Area	Soil loss rate
		[km²]	[t ha⁻¹ yr⁻¹]
1	0 – 2.5°	8	0.1
2	2.5 – 5°	13.8	0.3
3	5 – 10°	29.9	0.8
4	10 – 20°	80.1	2.1
5	>20°	138.6	4.3

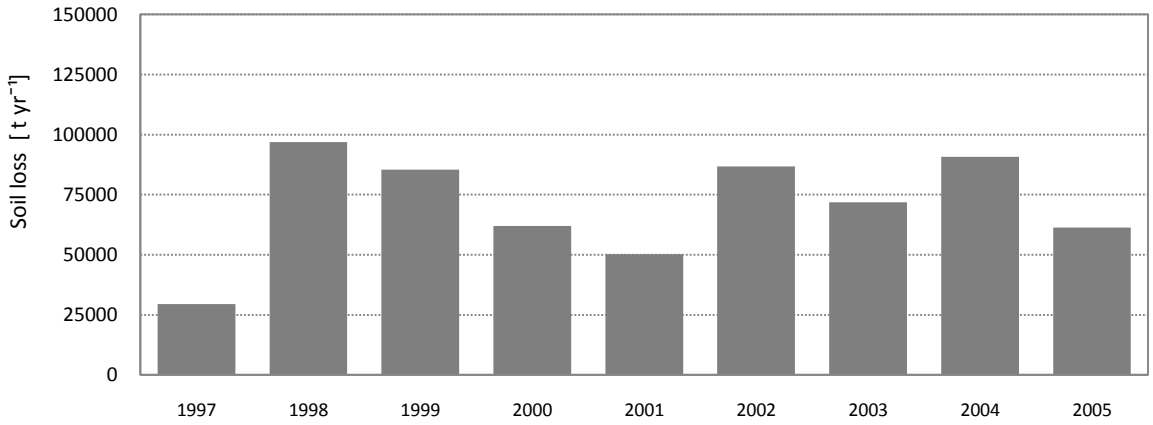

Fig. 5.13 – Soil loss in the undisturbed forested areas divided by year. For the year 1997 and 2005 only the periods from October to December and from January to September are considered, respectively.

5.2.1.3. NO-FOREST-HARVESTING SCENARIO

An additional run of the RUSLE model assuming the absence of coppice forest harvesting in these sectors results in an average soil erosion of 2.11 t ha^{-1} yr^{-1} (no cut: 4089.6 t yr^{-1}; cut: 36,515.9 t yr^{-1}). In comparison with the forest-harvesting condition the no-forest-harvesting scenario generates anine-times-lower average erosion. In this simulated context very severe erosion rates are only observable in some *impluvi* with a slope gradient greater than 35°. Under real conditions, in contrast, in the forest-harvested areas of the Turano watershed soil loss already starts to be severe (14 t ha^{-1} yr^{-1}) at slope gradients between 10° and 20°. Considering areas with slopes greater than 35° the average soil erosion rate is equal to 37.7 t ha^{-1} yr^{-1}.

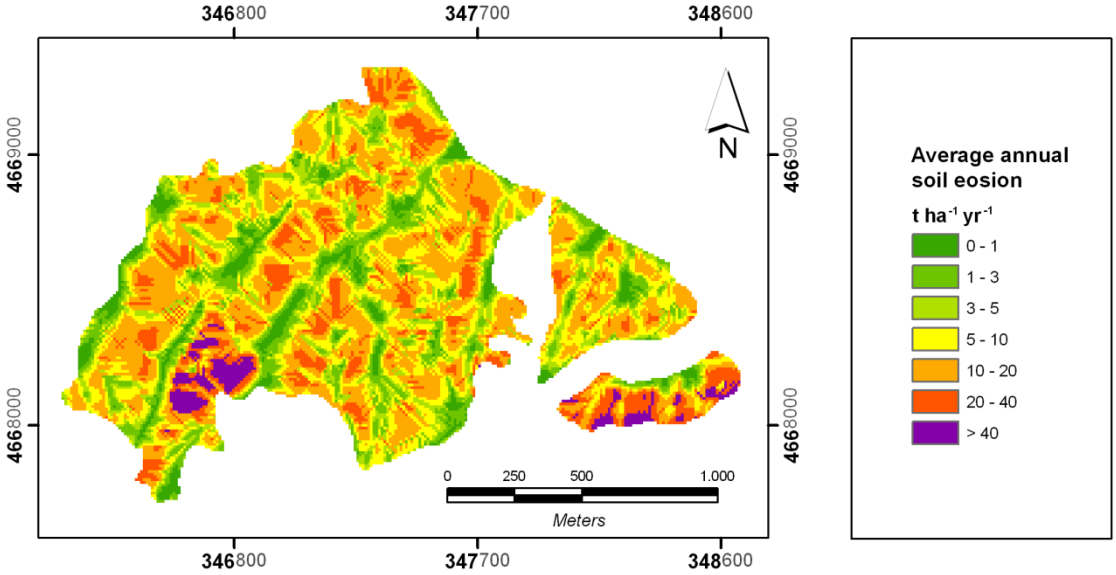

Fig. 5.14 – Predicted average annual soil erosion in harvested forested area of the Ovito sub-watershed.

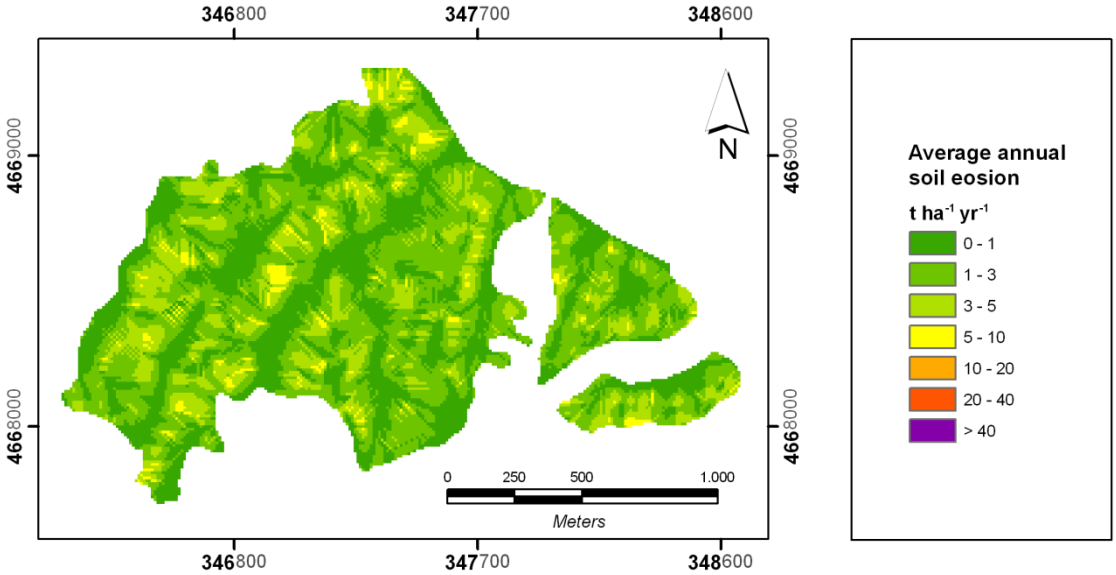

Fig. 5.15 – Predicted average annual soil erosion for the no-harvesting scenario in the Ovito sub-watershed.

5.2.2. USPED MODEL

5.2.2.1. SOIL LOSS PREDICTION

To analyze the USPED model results the same statistical approach already used for the RUSLE model was applied. The annual average net soil loss predicted by USPED in the Turano watershed is equal to 19,928.2 t ha^{-1} yr^{-1}, with an average of area-specific net soil loss of 0.43 t ha^{-1} yr^{-1}. The 4,667,412 10x10 m cells of the grid were separated into 7 classes of erosion according to the European Soil Bureau (van der Knijff et al.,1999; van der Knijff et al., 2002; Grimm et al., 2003) with the further introduction of tree deposition classes. The deposition classes are: Class 1, very low deposition (0–1 t ha^{-1} yr^{-1}); Class 2, low-moderate deposition (1–6 t ha^{-1} yr^{-1}); Class 3, high deposition (>6 t ha^{-1} yr^{-1}).

The erosion rate 0.43 t ha^{-1} yr^{-1} mentioned above correspond to net erosion value, i.e., the sediment deposition from the model is taken in account (Mitasova et al., 1999). Excluding the accumulation values, the gross erosion estimated by the USPED model at watershed scale gives rise to an annual average equal to 149,233.5 t yr^{-1} while the average area-specific gross soil loss is 3.2 t ha^{-1} yr^{-1}.

As shown in Figure 5.16 and reported in Table 5.10, a net erosion was predicted for 51.7% of the study area whereas deposition was predicted for the remaining 48.3%. Accordingly, 22.5% and 13.3% of the total watershed area (167 km^2) undergo very low and low rates of erosion, respectively. These areas are mainly located on flat plains and hills with gentle slopes, especially those that are highly vegetated. Moderate erosion appears on about 4.5% of the modeled area. High, severe and very severe erosion values of net soil loss affect each one about 4.6%, 3.2% and 2% of the watershed area, respectively. Moreover, the sectors of the basin facing extreme severe erosion account of 1.6% of the total area.

At first glance, the spatial distribution of the areas that are subject to erosion seems to be similar to the one predicted by RUSLE. However, significant differences in the erosion rates can be found as described in Chapter 5.2.3. According to Figure 5.16 the northwest slopes are more affected by erosion than the east and central ones because of the greater rainfall erosivity that interacts with the high soil erodibility. With regard to land use, recalling the RUSLE model the erosion rates of USPED model are lower. According to the USPED model the main source of sediments are the mountain pasturelands with a gross erosion rate equal to 16.02 t ha^{-1} yr^{-1}. The farmlands generate an erosion of 7.14 t ha^{-1} yr^{-1}, followed by the rangeland with 3.88 t ha^{-1} yr^{-1} and the forestland with 1.49 t ha^{-1} yr^{-1} (1.15 t ha^{-1} yr^{-1} in the undisturbed forest is observable). With regard to the macchia land-cover unit an erosion rate equal to 2.25 t ha^{-1} yr^{-1} was estimated.

Table 5.10 – Soil losses by different land use and land-cover type at Turano watershed.

Land use type	Surface in erosion		Soil loss (gross erosion)		
	Area	Soil loss percent	Total	Mean	SD
	[km²]	[%]	[t yr⁻¹]	[t ha⁻¹ yr⁻¹]	[t ha⁻¹ yr⁻¹]
Urban and built-up areas	5.8	0.02	34.7	0.06	2.4
Croplands	27.8	28.4	42213.3	7.14	15.2
Pasture lands	7.3	14.8	21915.3	16.02	30.1
Forest lands	153.2	29.0	43055.1	1.49	2.8
Rangeland	24.4	11.9	17730.1	3.88	7.3
Macchia	20.8	6.0	8888.2	2.25	4.3
Olive + vineyard	1.7	7.6	11308.7	33.09	65.9
Others	7.6	2.3	3361.1	3.96	4.4

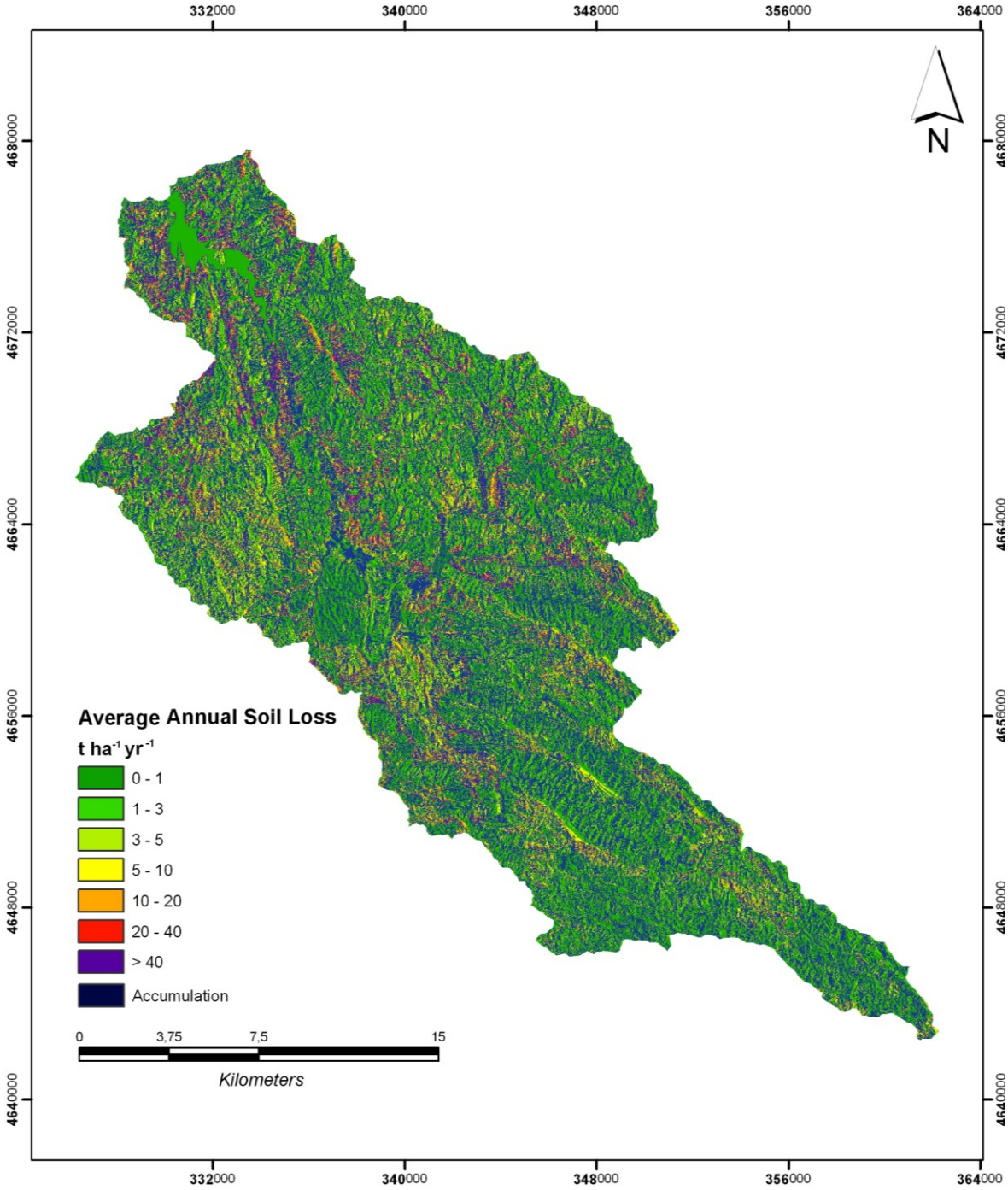

Fig. 5.16 – Predicted average annual soil erosion for the Turano watershed (1997-2005).

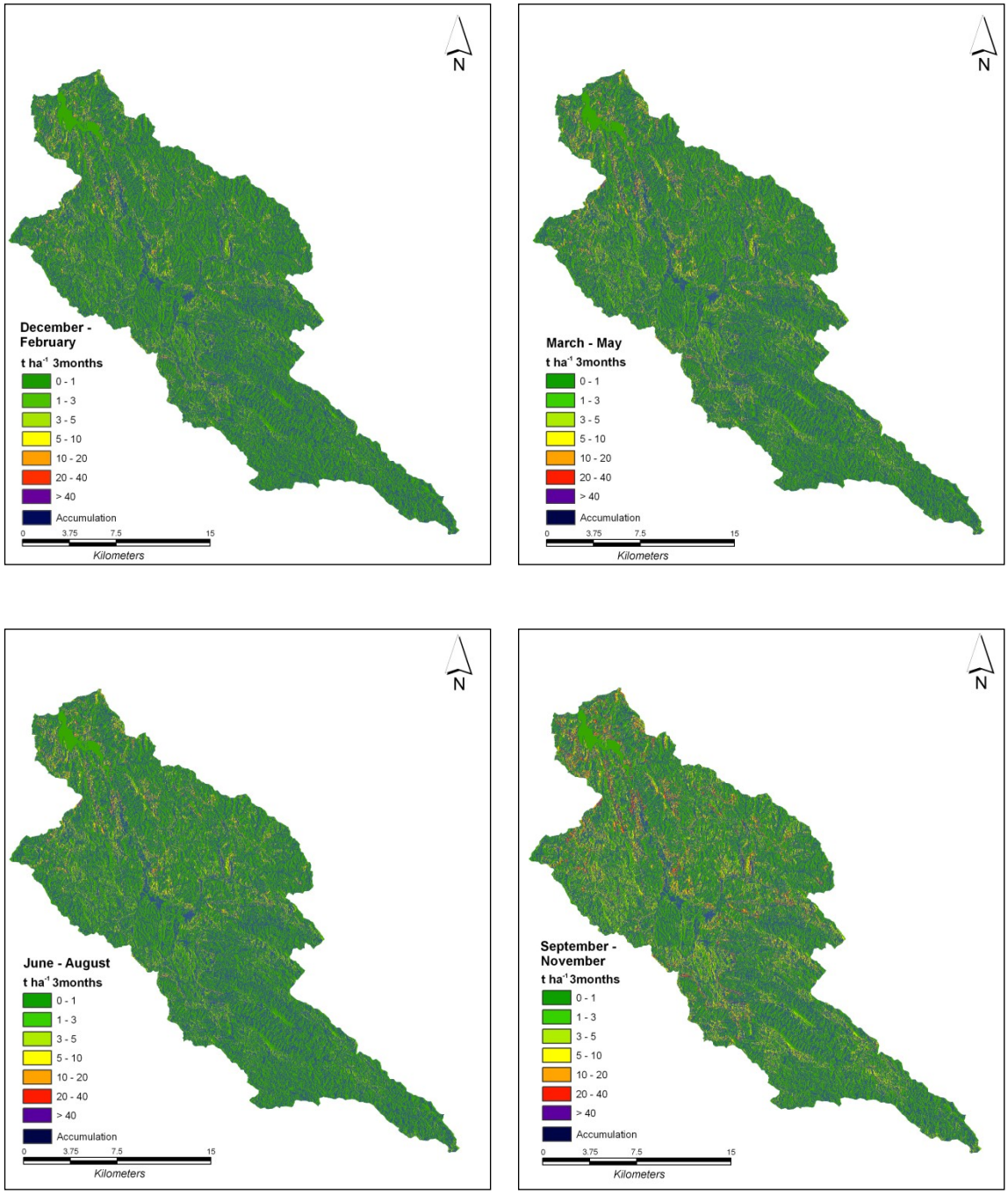

Fig. 5.17 – Predicted average seasonal soil erosion for the Turano watershed (1997–2005).

It follows that under the application of the USPED model the forestlands still remain the less soil erosion affected sectors of the watershed. For these sectors of the Turano watershed an average soil gross erosion rate equal to 1.49 t ha^{-1} yr^{-1} has been estimated for the period from September 1997 to October 2005. Yet, if only the sectors under coppicing activities are considered the erosion rate rises to 4.89 t ha^{-1} yr^{-1}.

The potential soil erosion risk (van der Knijff et al., 1999) of the USPED model was assessed using the same methodology adopted for the RUSLE model. The resulting potential erosion risk map is shown in Figure 5.18.

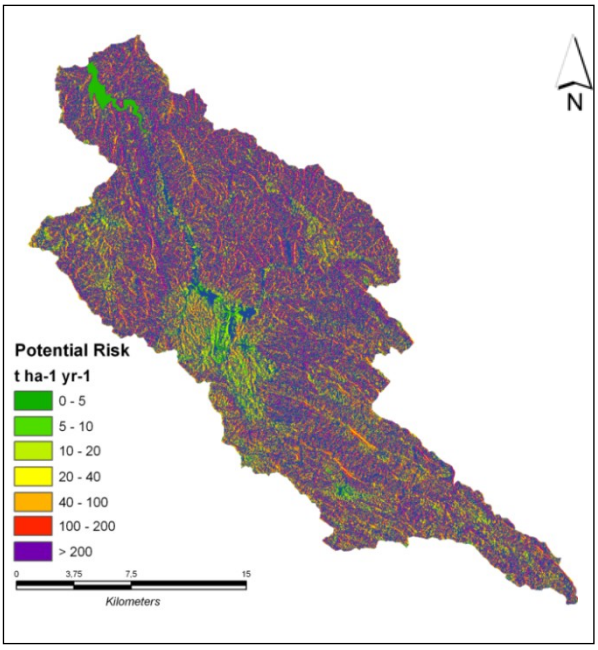

Fig. 5.18 – Potential soil erosion risk in the Turano watershed.

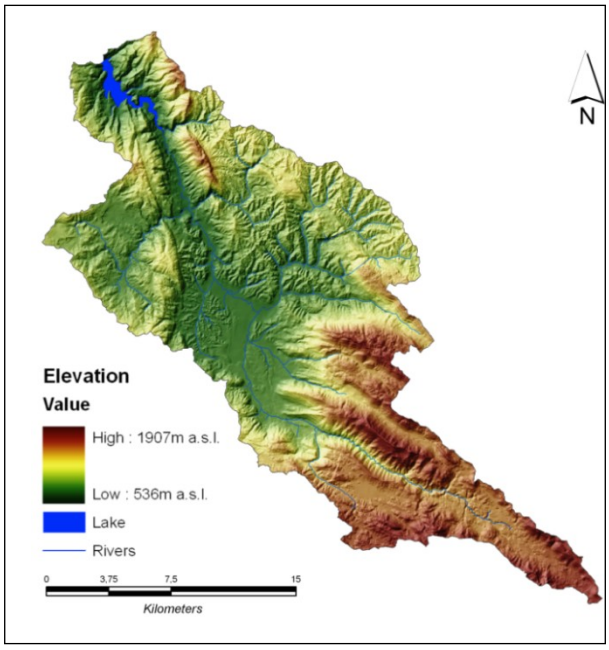

Fig. 5.19 – Digital elevation model of the Turano watershed.

In addition, further details are reported in Table 5.10 and Table 5.11 illustrating the distribution of erosion classes across the study area divided by the types of land use. Figure 5.20 deals with the annual values of gross erosion from 1997 to 2005. Finally, Tables 5.13, 5.14, 5.15, 5.16 and Figure 5.21 and 5.22 provide the gross erosion values for the harvested and the undisturbed forested areas.

Table 5.11 – Soil gross erosion according to land-cover units.

Class number	Rate of erosion	Erosion risk class	Soil loss													
			Urban and built-up areas		Croplands		Pasture lands		Forest lands		Rangeland		Macchia		Olive + vineyard	
			Area	Area	Area	Area	Area	Area	Area	Area	Area	Area	Area	Area	Area	Area
			[km²]	[%]	[km²]	[%]	[km²]	[%]	[km²]	[%]	[km²]	[%]	[km²]	[%]	[km²]	[%]
1	0 – 1	very low	3.3	100	3.7	13.3	1.6	22.2	86.9	56.7	4.3	17.6	6	29	0.03	1.6
2	1 – 3	low	0	0	5	17.9	1.4	19.7	43.2	28.2	5.7	23.6	6.8	32.4	0.06	3.5
3	3 – 5	moderate	0	0	3.3	11.7	1.5	20.2	9.6	6.3	3.8	15.6	3.4	16.5	0.06	3.6
4	5 – 10	high	0	0	5	17.9	1.1	15.6	6.8	4.4	5.2	21.2	4	14.3	0.15	8.5
5	10 – 20	severe	0	0	4.8	17.1	0.6	8	3.3	2.2	3.4	14.1	1.1	5.5	0.23	13.7
6	20 – 40	very severe	0	0	3.5	12.7	0.7	9.2	1.8	1.2	1.5	6.1	0.3	1.4	0.34	19.6
7	>40	extreme severe	0	0	2.6	9.5	0.4	5.1	1.5	1	0.4	1.8	0.2	0.9	0.85	49.5
Total			3.3	100	27.8	100	7.3	100	153.2	100	24.4	100	20.8	100	1.7	100
Deposition			Area in percent with respect to the total Turano surface area													
			[km²]	[%]	[km²]	[%]	[km²]	[%]	[km²]	[%]	[km²]	[%]	[km²]	[%]	[km²]	[%]
			0	0	31.4	14	6.4	2.9	135.5	60.6	21.4	9.6	18.6	8.3	1.7	0.8

Table 5.12 – Soil gross erosion according to land use and land-cover units divided by slope inclination.

Class number	Slope class	Soil loss													
		Urban and built-up areas		Croplands		Pasture lands		Forest lands		Rangeland		Macchia		Olive + vineyard	
		Area	Loss rate	Area	Loss rate t	Area	Loss rate	Area	Loss rate	Area	Loss rate t	Area	Loss rate	Area	Loss rate
		[km²]	t ha^{-1} yr^{-1}	[km²]	t ha^{-1} yr^{-1}	[km²]	t ha^{-1} yr^{-1}	[km²]	t ha^{-1} yr^{-1}	[km²]	t ha^{-1} yr^{-1}	[km²]	t ha^{-1} yr^{-1}	[km²]	t ha^{-1} yr^{-1}
1	0 – 2.5°	1	0.01	7.6	3.2	0.4	3.3	4	0.4	2.1	1.1	0.7	0.7	0.04	9.1
2	2.5 – 5°	0.6	0.02	5.7	8.2	0.6	8.4	7.2	0.9	2.5	2.7	1.3	1.4	0.16	20.8
3	5 – 10°	0.6	0.04	6.8	15.1	1.3	16.7	16.1	1.7	4.7	4.7	3.1	2.7	0.43	38.5
4	10 – 20°	0.6	0.09	6.1	27.9	2.7	31.2	44.4	3.1	8.4	8.2	7.8	4.3	0.76	75.5
5	>20°	0.5	0.18	1.7	46.4	2.3	46.6	81.4	3.2	6.6	11.6	7.8	5.7	0.32	109.8

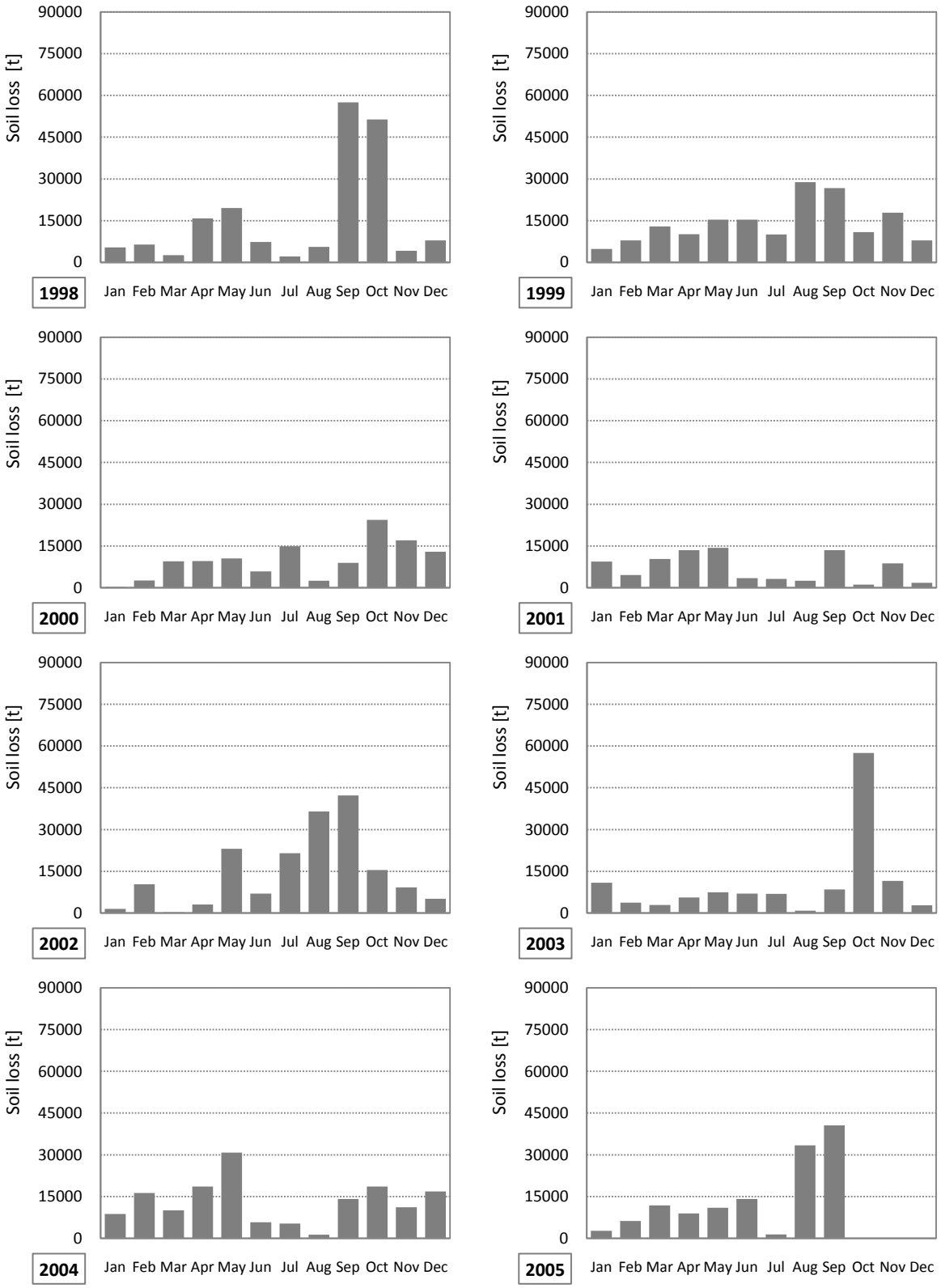

Fig. 5.20 – Monthly variation of gross soil loss from October 1997 to September 2005 in the Turano watershed.

Table 5.13 – Soil gross erosion in the areas under coppicing silvicultural activities (1997–2005).

Class number	Rate of erosion	Erosion risk class	Soil loss	
			Harvested forest lands	
			Area	
			[km²]	[%]
1	0 – 1	very low	1.5	13.9
2	1 – 3	low	2.4	22.2
3	3 – 5	moderate	1.7	16.0
4	5 – 10	high	2.5	23.4
5	10 – 20	severe	1.7	15.7
6	20 – 40	very severe	0.7	6.3
7	>40	extreme severe	0.3	2.5
Total			10.7	100

Table 5.14 – Soil gross erosion in the areas under coppicing silvicultural activities divided by slope inclination (1997–2005).

Class number	Rate of erosion	Soil loss	
		Harvested forest lands	
		Area	Soil loss rate
		[km²]	[t ha⁻¹ yr⁻¹]
1	0 – 2.5°	0.2	0.9
2	2.5 – 5°	0.4	1.7
3	5 – 10°	0.9	3.7
4	10 – 20°	3.2	7.7
5	>20°	6.1	10.9

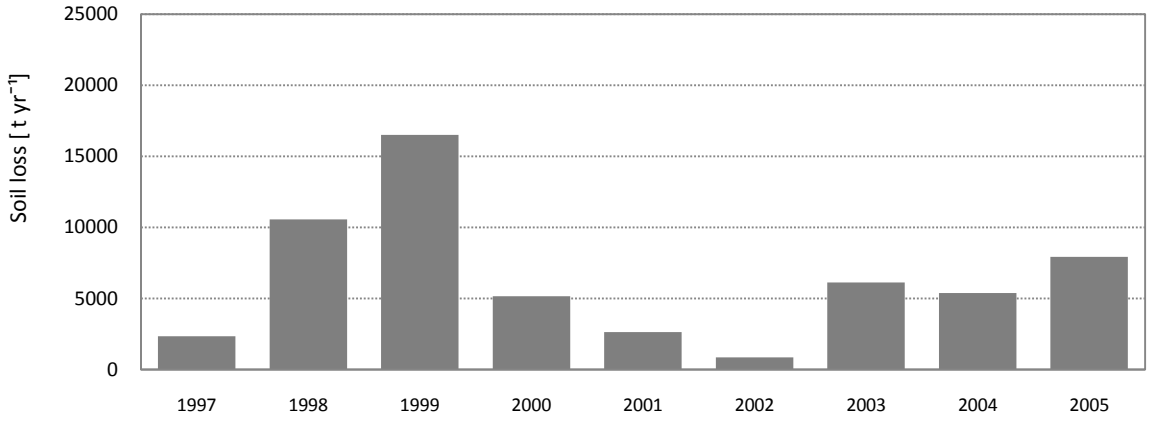

Fig. 5.21 – Soil loss in the areas under coppicing silvicultural activities divided by year.

Table 5.15 – Soil loss in the undisturbed forested areas (1997–2005).

Class number	Rate of erosion	Erosion risk class	Soil loss	
			Harvested forest lands	
			Area	
			[km²]	[%]
1	0 – 1	very low	85.5	59.8
2	1 – 3	low	41.0	28.6
3	3 – 5	moderate	8.0	5.6
4	5 – 10	high	4.4	3.0
5	10 – 20	severe	1.7	1.2
6	20 – 40	very severe	1.2	0.8
7	>40	extreme severe	1.4	0.9
Total.			143	100

Table 5.16 – Soil loss in the undisturbed forested areas divided by slope inclination (1997–2005).

Class number	Rate of erosion	Soil loss	
		Harvested forest lands	
		Area	Soil loss rate
		[km²]	[t ha^{-1} yr^{-1}]
1	0 – 2.5°	3.8	0.4
2	2.5 – 5°	6.9	0.9
3	5 – 10°	15.2	1.7
4	10 – 20°	41.5	2.8
5	>20°	75.6	2.7

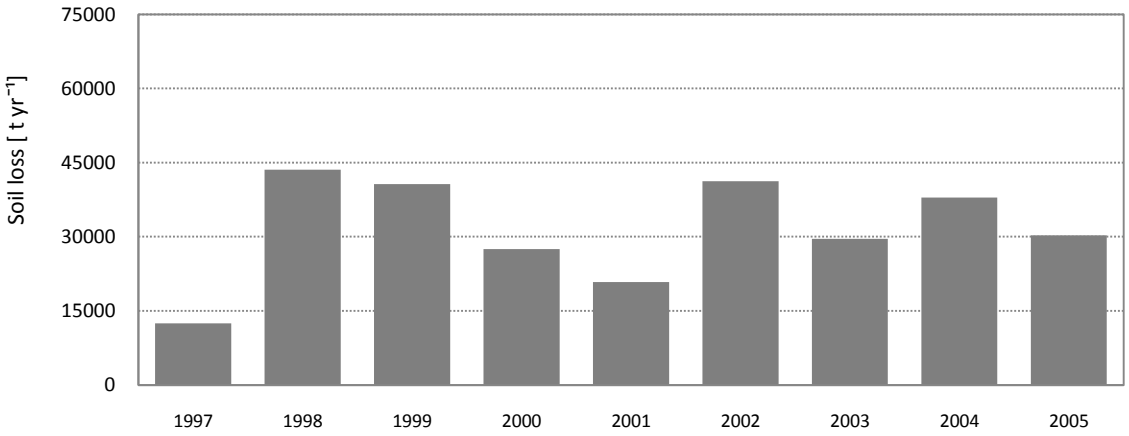

Fig. 5.22 – Soil loss in the undisturbed forested areas divided by year. For the year 1997 and 2005 only the periods from October to December and from January to September are considered, respectively.

5.2.2.2. NO-FOREST-HARVESTING SCENARIO

Appling the USPED model under the absence of coppice forest harvesting these forest sectors would be characterized by an average soil erosion of 0.43 t ha^{-1} yr^{-1} (gross erosion). In fact, this value is 11.5 times lower than the one that included forest-harvesting effects (no cut: 834.6 t yr^{-1}; cut: 9488.9 t yr^{-1}).

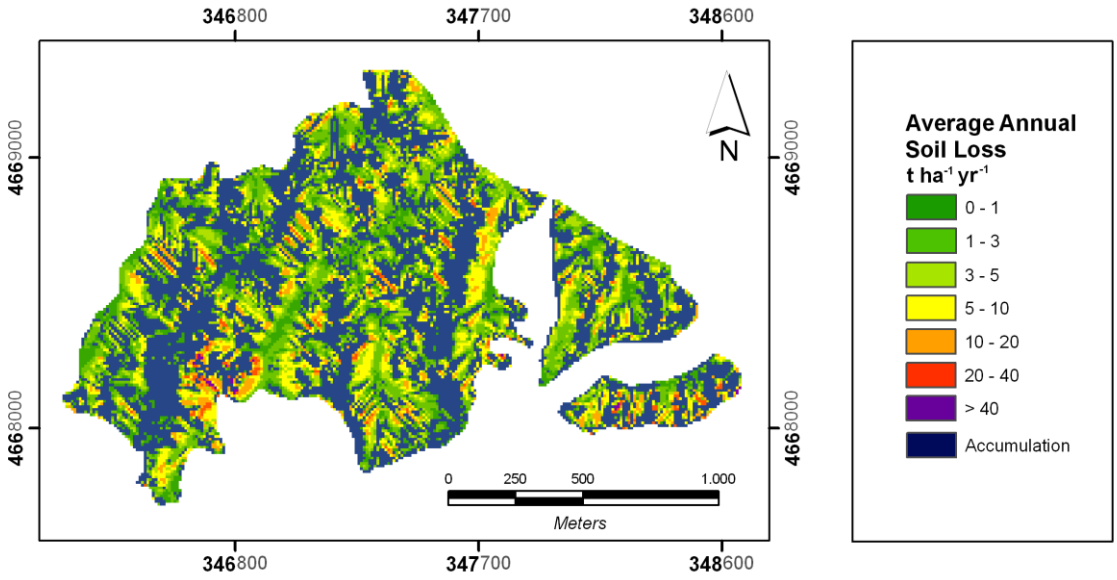

Fig. 5.23 – Predicted average annual soil erosion in harvested forested area of the Ovito sub-watershed.

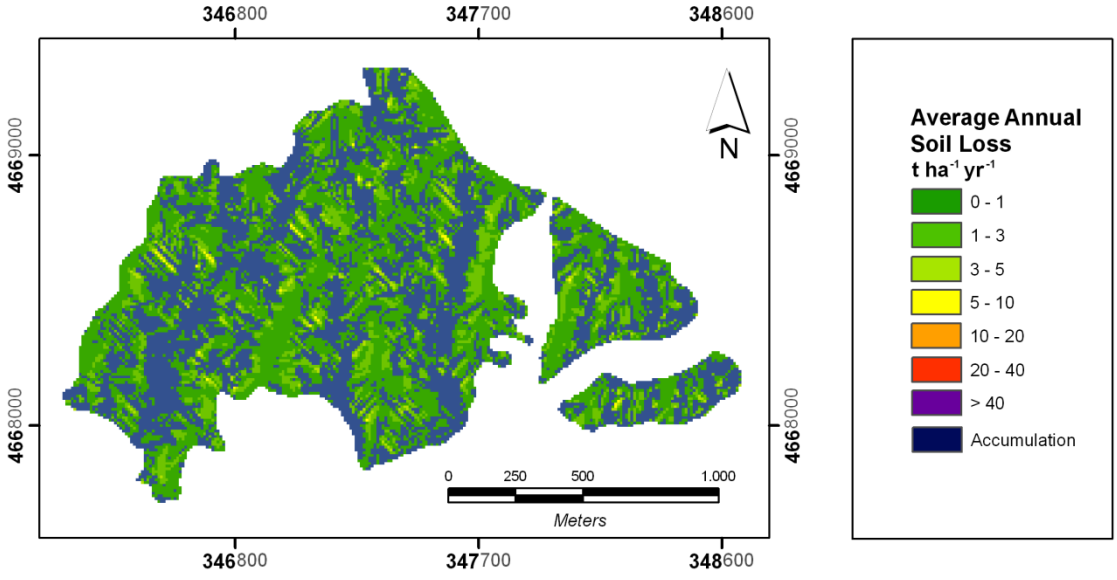

Fig. 5.24 – Predicted average annual soil erosion for the no-harvesting scenario in the Ovito sub-watershed.

5.2.3. MODEL INTERCOMPARISON

Comparing the areas in the Turano watershed affected by rill and inter-rill soil erosion processes, several differences between the two model results have been revealed. Firstly, as expected the RUSLE model provides a higher total soil loss between 1997 and 2005 compared to the USPED model since the model proposed by Renard et al. (1997) lacks the computation of sediment deposition. The RUSLE model estimates 3.5 times (364,225.2 t yr^{-1}) more eroded soil (gross erosion) than the USPED model. Accordingly, the average erosion rate predicted by the RUSLE model is higher (USPED, 3.2 t ha^{-1} yr^{-1}; RUSLE, 11 t ha^{-1} yr^{-1}). In addition, the USPED and RUSLE models predicted watershed areas prone to erosion of 51.7% and 97.8%, respectively. From the results provided in Table 5.17 it follows that the distribution for each intensity class there are rather dissimilar.

Moreover, Figure 5.25 deals with box plots representing erosion values from the model predictions and Figure 5.26 provides the spatial distribution of the differences between the RUSLE and USPED model.

Table 5.17 – Areas under erosion divided by intensity classes.

Class number	Rate of erosion	Erosion risk class	Soil loss			
			RUSLE		USPED	
			Area		Area	
			[km²]	[%]	[km²]	[%]
1	0 – 1	very low	95.2	20.4	109.5	23,5
2	1 – 3	low	114.4	24.5	62.2	13.3
3	3 – 5	moderate	80.1	17.2	21.1	4.5
4	5 – 10	high	77.1	16.5	21.6	4.6
5	10 – 20	severe	40.5	8.7	14.7	3.2
6	20 – 40	very severe	30.5	6.5	9.1	2
7	>40	extreme sev.	28.9	6.2	7.5	1.6
Total			466.7	100	245.7	51.7

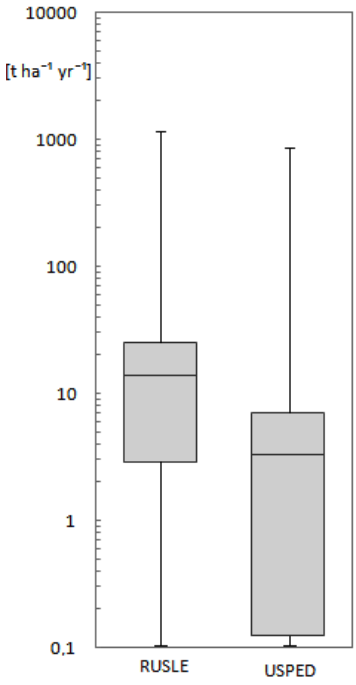

Fig. 5.25 – Box plots of the predicted soil erosion value.

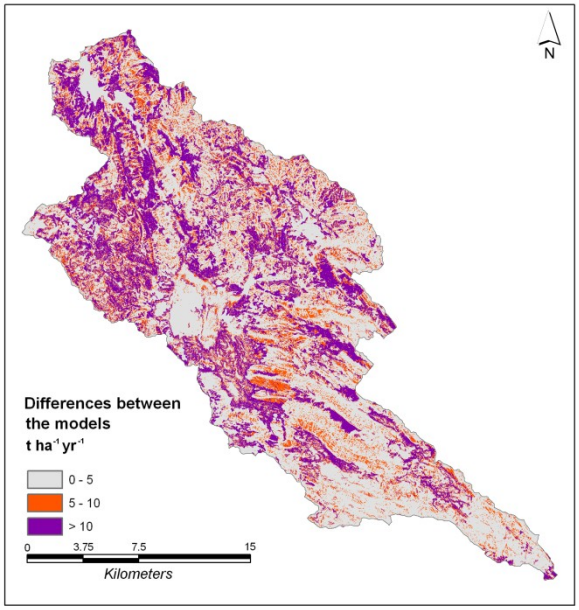

Fig. 5.26 – Difference between RUSLE and USPED models.

5.2.4. VALIDATION OF THE MODELS

Sediment yield measured by differencing bathymetric surveys for the Turano reservoir enabled to assess the extent of the erosion processes in the investigated watershed. According to ENEL/E-ON total reservoir sedimentation between September 1997 and October 2005 was about 12.296 M m³, with an annual sediment yield (SY) of about 1.537 M m³. The mass volume given a mean bulk density of 0.865 t m^{-3} (van Rompaey et al., 2005) is equal to 10,636,040 t. The annual average of the measured area-specific sediment yield derived from the lake sediments is equal to 28.48 t ha^{-1} yr^{-1} for the entire watershed surface or 32.35 t ha^{-1} yr^{-1} excluding the endorheic areas from the calculation. Several endorheic spatial units were identified in the Upper Turano Watershed (Fig. 5.27) which account for a total area of 59.15 km² (mainly located in the carbonate sector).

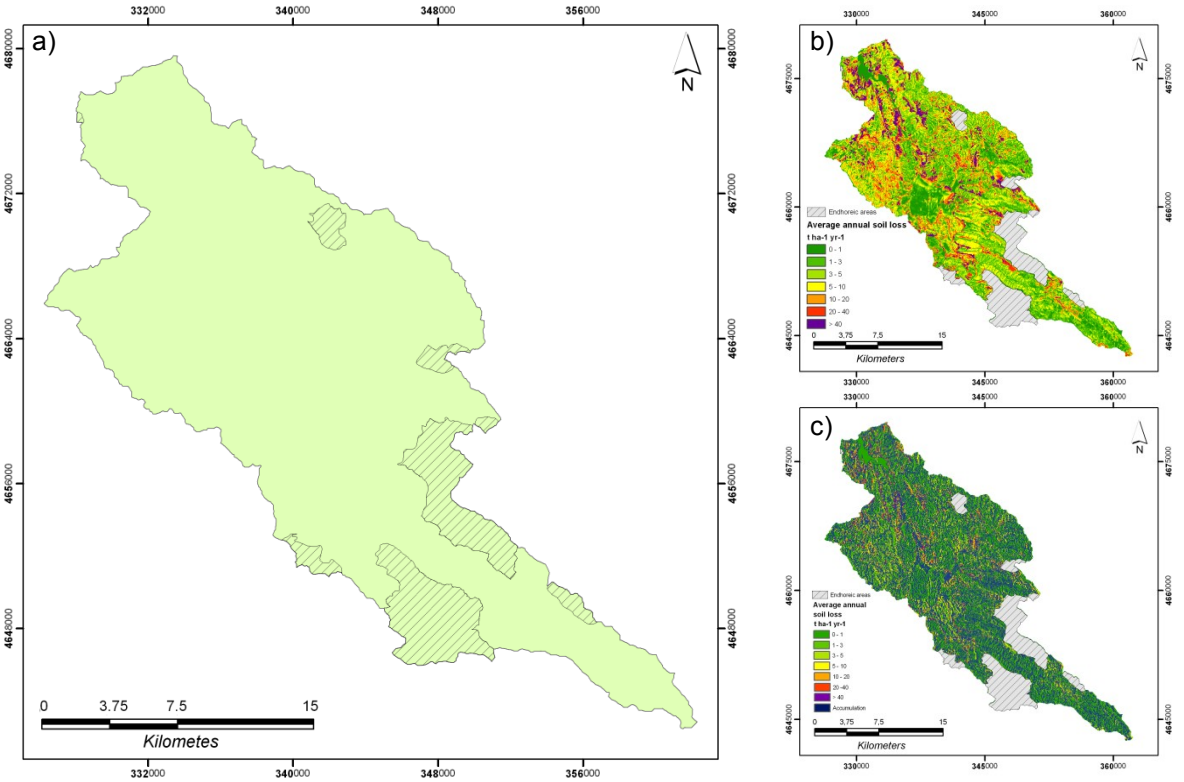

Fig. 5.27– Endorheic areas in the Turano watershed ‘a’, endorheic areas mask on the RUSLE output ‘b’ and endorheic areas mask on the USPED output ‘c’.

The grain size distribution of the lake sediments (Table 5.18) classified according to the ISSS methodology (Hynes, 1972; Marchetti, 1993) shows the prevalence of fine silt particles, subordinately clay and coarse silt.

Table 5.18 – Grain size classification of Turano Lake sediments according to ENEL/E-ON. Mass refers to sediments smaller 2 mm.

Sediment	Coarse sand		Fine sand		Coarse silt		Fine silt		Clay	
	Ø > 0.2 mm		Ø > 0.05 mm		Ø > 0.02 mm		Ø >0.002 mm		Ø <0.002 mm	
	[g/Kg]	[%]	[g/Kg]	[%]	[g/Kg]	[%]	[g/Kg]	[%]	[g/Kg]	[%]
Site 1	0	0	0	0	1	0.1	841	84.1	158	15.8
Site 2	0	0	0	0	17	1.7	881	88.1	102	10.2
Site 3	0	0	3	0.3	196	19.6	744	74.4	57	5.7

The soil loss predicted by the RUSLE model cannot be directly related to the siltation on the lake bottom. On the one hand, the sediments caused by gully erosion and river channel erosion remain unconsidered in the RUSLE model. On the other hand, the gross erosion calculated does not take into account the rate of sediment re-deposited in the river bed, on the slopes or other sediment traps. To solve, at least, the second problem and estimate the possible amount of soil re-deposited before reaching the outlet of the watershed, studies on soil erosion frequently apply a method based on sediment delivery ratio (SDR) (Ferro et al., 1998; Kinnell, 2000; Ferro et al., 2003; van Rompaey, 2005; de Vente et al., 2006). The SDR refers to the ratio between SY and gross erosion as (Maner, 1958):

$$SDR = \frac{net\ soil\ loss}{total\ soil\ erosion} \quad \text{(Eq. 6.21)}$$

So that:

$$Net\ soil\ loss = total\ soil\ erosion \cdot SDR \quad \text{(Eq. 6.22)}$$

Several studies focusing on the SDR determination have stated that there is an inverse relationship between the watershed area and this parameter (USDA, 1975; Vanoni, 1975; Tamburino et al., 1990; Bagarello et al., 1991; van Rompaey et al., 2003; van Rompaey et al., 2003b). For Italy this relationship is commonly expressed by a potential equation between the SDR and the area (Km²) of the watershed (Basso, 1995):

$$SDR = a \cdot S^{-b} \quad \text{(Eq. 6.23)}$$

The SDR has been estimated using the 'a' and 'b' coefficients derived from observations carried out in southern Italy (Eq. 5.20 – Bagarello et al., 1991) and USA (Eq. 5.19 – USDA, 1975). For the Turano watershed (excluding the 55.8 km² of endorheic sectors) the SDR value is equal to 0.08 (southern Italy approach) and 0.29 (USA approach). These SDR values fall within the range of 0.08–0.40 as predicted by the European Soil Bureau Research Center for 21 Italian watersheds (van Rompaey et al., 2003). Thus, using both SDR values as a reference (0.08 and 0.29) and considering the surface of the Turano watershed without endorheic areas, the SY (October 1997 to September 2005) would range from 33,135.9 t yr^{-1} to 120,117.6 t yr^{-1} (gross erosion without endorheic areas is

414,198.7 t yr^{-1}). These values are significantly smaller than the SY calculated by a quantification of the lake sediments.

With regard to USPED as stated in Chapter 5.4.1 the net erosion was equalized to the SY. In doing so, according to the USPED model the SY was equal to 17,545.9 t yr^{-1} in the period from October 1997 to September 2005

Through the operations of quantitative model validations both models apparently underestimate the SY and thereby presumably also the gross erosion. The predicted RUSLE SY values are about 11 (USDA SDR approach) and 40 (south Italy SDR approach) times smaller than the measured ones (1,329,505 t yr^{-1}), respectively. With regard to the USPED model, the predicted net erosion is 76 times smaller than the measured SY. The gross erosion value estimated by RUSLE, which is lower than the measured SY, is somewhat atypical and does not comply with values found in some other studies in Italy and other places in the world (see Chapter 6.3.1 for a further elaborated and in-depth comment). Note, however, that this issue does not originate from an incorrect application of the models, but rather from others factor related to the specific characteristics of the watershed. As shown in the discussion section other models such as RUSLE, PESERA and CORINE applied by the IES (Institute for Environment and Sustainability of the European Union) state erosion values even lower that the one found in this study with regard to the Turano area.

In addition, a semi-qualitative validation for the RUSLE model was performed. The method selection rests upon the level of congruence (in percent) derived from comparing the models' erosion outputs (Fig. 5.30) with the soil erosion map (Fig. 5.29) acquired from field and aerial-photo mapping (after reclassification, see Fig. 5.28). The application of this method was inspired by Gobin and Govers' model (2003) on the validation of the European Soil Erosion Risk Assessment (PESERA) also successively applied by Saavedra (2005).

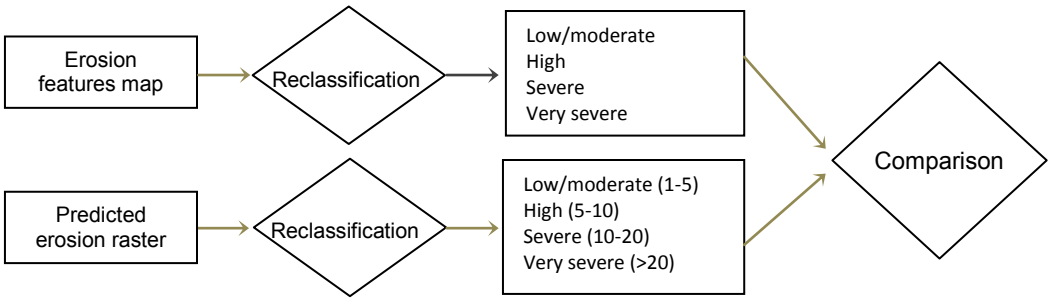

Fig. 5.28 – Scheme of the semi-qualitative validation procedure for the Ovito sub-watershed.

The results of this validation method shows a good correlation between soil erosion features, their degree of damage and the soil erosion predicted by the models (Fig. 5.31; Table 5.19). A level of congruence of 57.4% between the predicted erosion classes and

the mapped ones has been obtained. An overestimation of modeled erosion (RUSLE) occurs in 14.6% (class 1), 7.6% (class 2) and 5.1% (class 3). Underestimated erosion is observed in 15.3% of the watershed surface.

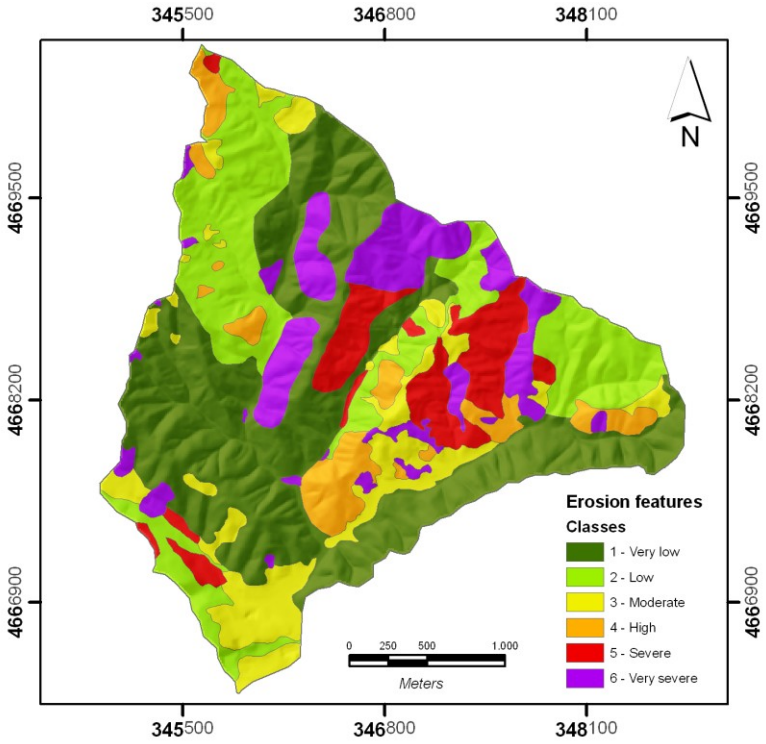

Fig. 5.29 – Ovito sub-watershed classification according to the erosion features mapped during field survey and by remote sensing.

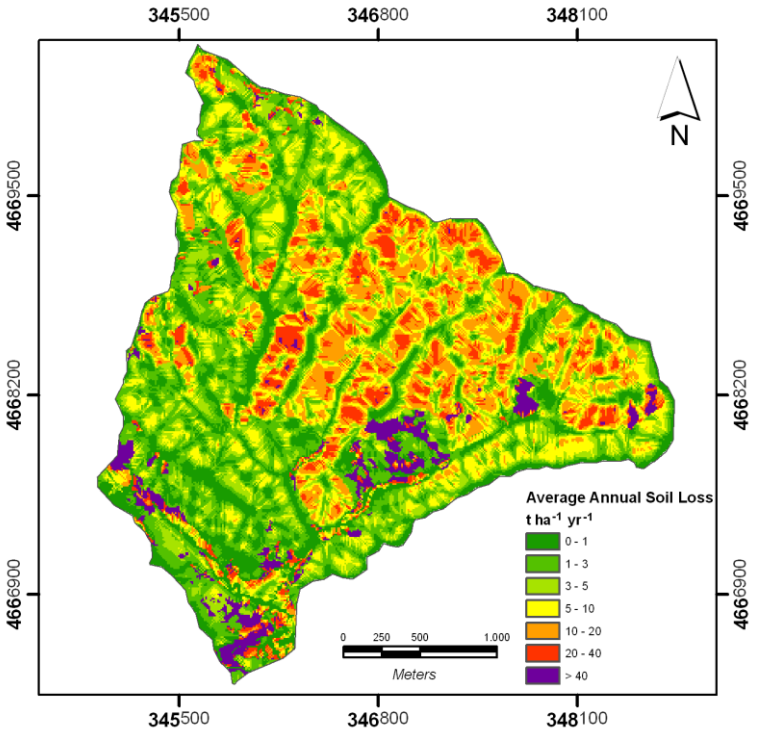

Fig. 5.30 – Predicted average annual soil erosion for the Turano watershed (1998–2009).

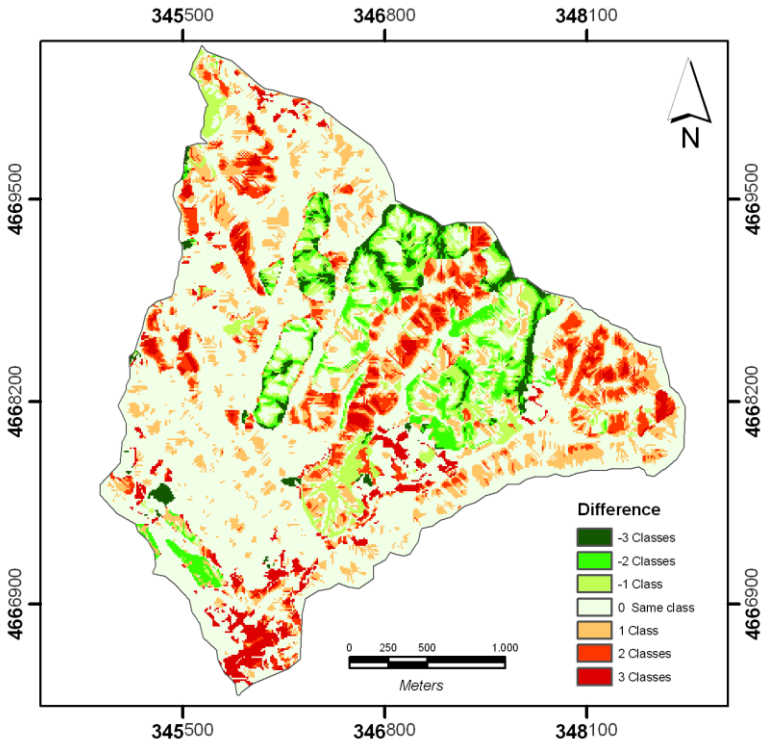

Fig. 5.31 – Result of the comparison between the erosion features map and the predicted soil erosion.

Table 5.19 – Level of agreement between the RUSLE model erosion outputs with the soil erosion features mapped.

Rate of erosion	Erosion risk reclassification	Erosion features reclassification	Area well predicted	Degree of agreement
[t ha^{-1} yr^{-1}]	[class]	[class]	[Km^2]	[%]
0-5	Low /moderate	Low /moderate	3.8	86.3
5-10	High	High	0.1	8.7
10-20	Severe	Severe	0.3	22.7
> 20	Very severe	Very severe	0.3	33.4

5.3. DISCUSSIONS

Soil is an extremely important natural resource with various ecosystems drawing directly or indirectly on soil (Boardman, 2006). The wash-out of topsoil due to hydric erosion processes is a very insidious phenomenon with impacts at a global scale (Oldeman, 1991). The fact that it unfolds its effect in various ways and at different magnitudes makes it even more of a 'hot' research topic. Farmlands have already felt the negative effects of soil erosion on their crop productivity (Morgan, 2002). In Italy, farmlands cover a surface of 155,010 km² (Eurostat, 2009) (51.4% of the Country area). The agricultural goods account for a considerable share of the domestic GDP and have a relevant share of exports (ISTAT, 2010). Thus, a multitude of research publications deal with soil erosion damage from hill cropland activities in Tuscany and Sicily. However, with regard to the processes, effects and impacts of accelerated soil erosion, research focused on Italy lacks insights into the environment's topographic heterogeneity of the Apennine region, a unit that covers a considerable area and is highly relevant for the country (water supply). Remarkably, the public and academic awareness of the soil erosion phenomenon itself and possible solutions to minimize its effects has increased simultaneously with the rising environmental impact of land use in this region.

With respect to the identified research gap, this study was carried out in a sizable watershed of the Central Apennine using and modeling approach. The two models used (RUSLE and USPED) allowed a quantification of the potential soil loss in this area. The model approach allowed for benefits from the use of high resolution input data. This, according to van der Knijff et al. (1999), Grimm et al. (2002), van Rompaey et al. (2003) and van Oost (2005) can positively influence the model results since the performance of soil erosion models significantly depends on high-resolution input data. The use of a DEM with 10x10 m cellsize for a watershed with an area greater than 400 km² is rather uncommon for soil erosion modeling. The land use and derived RUSLE C-factors are based on orthophotos (0.25x0.25 m) visual interpretation and multispectral satellite images techniques. The rainfall erosivity factor was calculated using seasonal relations exclusively created for the Turano area with sub-hourly data from the Turano stations. Moreover, this R-factor allowed the monthly soil loss estimation for the considered period covering eight years. In fact, this enabled for the consideration of spatial as well as temporal variations of soil erosion by water.

5.3.1. RESULTS OF THE TURANO WATERSHED CASE STUDY IN THE PANORAMA OF SOIL EROSION MODELING BASED ON RUSLE IN ITALY

For the study period, average gross erosion values of 3.2 t ha^{-1} yr^{-1} (USPED) and 11 t ha^{-1} yr^{-1} (RUSLE) resulted. Both RUSLE and USPED outputs are rather low compared (Table 5.20) to most soil erosion rates of these two models executed in Italy.

Taking RUSLE into consideration, the National Research Council (CNR) estimated an annual erosion rate equal to 30.6 t ha^{-1} yr^{-1} for the entire region of Calabria (15,075 km²) (Terranova et al., 2009). Within two Sicilian watersheds, Candela et al. (2006) estimated high erosion rates of about 56.2 to 128.9 t ha^{-1} yr^{-1} for the Comunelli watershed (82 km²) and about 59.8 to 100.3 t ha^{-1} yr^{-1} for the Disueri watershed (238 km²). With regard to the Pozzillo watershed in Sicily, Amore et al. (2004) estimated an average soil loss of 13.4 t ha^{-1} yr^{-1} for a period of 25 years. Note, however, that they applied the USLE (Wischmeier and Smith,1978). Using RUSLE for the Pozzillo watershed, van Rompaey et al. (2003) predicted soil erosion of 144.5 t ha yr. In Campania, Zamboni, (2007) using the RUSLE model estimate 57 t ha^{-1} yr^{-1} in a watershed covered to 25.8% by forest vegetation. Märker (2004), found a rather low erosion rate in a watershed in Sicily (2.39 t ha^{-1} yr^{-1}; Agnesi et al., 2004) while in Tuscany the RUSLE model predicted a rise in soil loss of up to approximately 19 t ha^{-1} yr^{-1} (Märker et al., 2008). In contrast, research studies at an Italian national scale based on the USLE and RUSLE model proposed by the European Commission (European Soil Bureau) showed lower erosion rates compared to studies developed at a watershed scale (van der Knijff et al., 1999; Grimm et al., 2003; Bosco, personal communication - 2011). For the Turano watershed, van der Knijff et al. (1999) estimated an average annual soil loss of 9.28 t ha^{-1} yr^{-1}. Bosco (personal communication - 2011) estimated, based on the latest version of RUSLE applied by the European Commission, an erosion rate equal to 6.5 t ha^{-1} yr^{-1} (provisional data) for the Turano watershed. For the Turano watershed the PESERA model (Pan-European Soil Erosion Risk Assessment) (Gobin et al., 1999), a physical based and spatial-distributed model developed to quantify soil erosion for the member states of the EU with 1 km spatial resolution, has been applied. Results also indicate a rather low erosion risk (1.18 t ha^{-1} yr^{-1}).

With regard to USPED, according to the best knowledge of the author four publications exist that focus on Italy. In Tuscany, Pelacani et al. (2008) estimated a net erosion rate equal to 5.3 t ha^{-1} yr^{-1} in a small watershed of 15 km² (upper Orme watershed). In bigger watersheds of Sicily, Candela et al. (2006) estimated soil losses (gross erosion) of 213.9 to 432.9 t ha^{-1} yr^{-1} for the Comunelli watershed (82 km²) and 219.5 to 351.4 t ha^{-1} yr^{-1} for the Disueri watershed (238 km²). The latest study proposed by Capolongo et al. (2008)

focusing on the Salandrella-Cavone watershed (74.7 km², Basilicata), computed a soil loss value equal to x t ha⁻¹ yr⁻¹ (gross erosion).

Applying a modified version of RUSLE proposed by researchers of the European Commission (WaTEM/SEDEM – van Rompaey et al., 2003) in 21 Italian watersheds, results reveal gross erosion rates ranging from 12.1 to 144.5 t ha⁻¹ yr⁻¹ with an average value of 47.1 t ha⁻¹ yr⁻¹.

Table 5.20 – RUSLE and USPED models applications in Italy (m.d., missing data; * estimated value).

Site	Size	Model	Soil loss	Fores	Cropland	Cellsize	Author
	[km²]	[-]	[t ha⁻¹ yr⁻¹]	[%]	[%]	[m]	
Turano, Lazio/Abruzzo	466.7	RUSLE	11	61.7	12.6	10	Present study
Turano, Lazio/Abruzzo	466.7	USPED	3.2	61.7	12.6	10	Present study
Turano, Lazio/Abruzzo	466.7	USLE	9.28	61.7	12.6	250	Van der Knijff (1999)
Turano, Lazio/Abruzzo	466.7	PESERA	1.18	61.7	12.6	1000	Gobin et al. (1999)
Turano, Lazio/Abruzzo	466.7	RUSLE	6.5	61.7	12.6	100	Bosco (2011)
Albegna, Tuscany	75	RUSLE	19*	17	m.d.	m.d.	Marker et al. (2008)
Tusciano, Campania	260	RUSLE	57	25.8	56.9	20	Zamboni (2007)
Calabria, Calabria region	15,075	RUSLE	30.6	31.9	37	40	Terranova et al. (2009)
Pozillo, Sicily	570	USLE	13.4	9	52.6	25	Amore et al. (2004)
Pozzillo, Sicily	570	RUSLE	144.5	9	52.6	75	Van Rompaey et al. (2003)
San Leonardo, Sicily	245	RUSLE	2.39	m.d.	m.d.	40	Agresi et al. (2004)
Salandrella-Cavone	74.7	USPED	40.3	4.5	67.6	25	Capolongo et al. (2008)
Comunelli, sicily	82	RUSLE	56.2 – 128.9	m.d.	m.d.	20	Candela et al. (2006)
Comunelli, Sicily	82	USPED	213.9 – 432.9	m.d.	m.d.	20	Candela et al. (2006)
Disueri	238	RUSLE	59.8 – 100.3	12	67.3	20	Candela et al. (2006)
Disueri	238	USPED	219.5 – 351.4	12	67.3	20	Candela et al. (2006)

In most of the cases the above-mentioned studies used different methods to compute the (R)USLE parameter and the more important different resolution of the data. The major difference between the discussed RUSLE-based models is rooted in the estimation of the rainfall erosivity. All studies apply different approaches. The R-factor is even calculated by using equations developed for different geographic areas in some cases (Candela et al., 2006; Märker et al., 2008). Focusing on Sicily, Candela et al. (2006) quantified a divergence in the estimated erosion rates of RUSLE compared to USPED of about 100%

which they related to the methods used to estimate the R-factor. In the two latest studies published in international journals (Märker et al., 2008; Terranova et al., 2009) the calculated RUSLE R-factor is almost twice as big as the one calculated for the Turano watershed. Terranova et al. (2009), in the Apennine region of Calabria, calculated R-factors of up to 6000 MJ mm h^{-1} ha^{-1} yr^{-1} in mountainous areas with rainfall of 1500 mm per year. Märker et al. (2008) presented R-factor values from 3200 to 5000 MJ mm h^{-1} ha^{-1} yr in Tuscany (period 1960–1990) based on rainfall values ranging from 712 to 1460 mm per year. Terranova et al. (2009) used a relationship based on a correlation coefficient (R^2=0.938) proposed in a diploma thesis (Sorrentino, 2001) for the Calabria region. For the RUSLE application in Tuscany Märker et al. (2008) adopted an equation developed by Rufino et al. (1993) for the Parana location in Brazil. The comparison of the R-factor estimated according to the RUSLE handbook (Renard et al., 1997) using the 30 min rainfall data of the Posticciola stations (northern sector of the Turano watershed) and the R-factor values calculated following the methods adopted in the two studies discussed above show that the latter tend to overestimate the R-factor in the Turano area (Table 5.20).

For instance, if the present study applied the equation proposed by Rufino et al. (1993) for the R-factor estimation, the resulting soil loss would be 114.5% higher than the one estimated by RUSLE handbook (Renard et al., 1997). Thus, the average soil loss predicted would be 23.6 t ha^{-1} yr^{-1}. A similar situation results using the USPED model.

Table 5.21 – Comparison between different techniques for R-factor estimation.

Method	Rainfall erosivity	Variation with Renard et al. method
	[MJ mm h^{-1} ha^{-1} yr^{-1}]	[%]
Renard et al. (1997)	2130.5	-
Rufino et al. (1993)	4569.8	+ 114.5
Sorrentino (2001)	2522.3	+ 18.4

Moreover, all of the studies so far proposed in Italy consider the effect of a possible snow cover of the ground surface during the winter season. As observed in this study (see Chapter 5.2.3) on the Apennine mountain areas above 900 m a.s.l. snowfalls are frequent and the snow cover may persist on the soil for weeks or months based on the altitudinal point. The snow as well as the deriving gelifluction of soil might reduce the erosive power (rainsplash) of the rainstorms during this time. Allowance has been made for this in the Turano watershed study area by adjusting (reduction) the erosive R-factor in the presence of ground snow cover for areas with elevation exceeding 1000 m a.s.l.

This thesis repeatedly highlighted the importance of the DEM resolution. Comparing three different DEM for the Turano watershed (SRTM – 90m; ASTER DEM – 30m; topographic

map 1:25,000 scale – 10 m) a significant decrease in the mean slope can be observed as the grid resolution becomes coarser. Consistently, the mean LS-factor and the mean erosion rate both vary with the change of the DEM resolution. Van Rompaey et al. (2003) stated that the DEM resolution plays a primary role for the accuracy of the RUSLE soil loss prediction.

The use of different procedures and diverse input data resolution for the application of the RUSLE-based models in Italy complicates the comparison of the results. Furthermore, one must also assume an increase of the uncertainty inherent in the model outcomes due to the weak input data frequently used. This uncertainty adds to the structural model deficiencies (Kinnell, 2008) compromising even more the model outcomes. It clearly follows that the general experiences gained across a country cannot simply be merged in order to present a reliable overview of the impacts of soil erosion in a specific area.

5.3.2. FACTORS CONDITIONING SOIL EROSION MODELING IN THE TURANO WATERSHED

In the case of the Turano watershed, among the factors affecting soil erosion in the Apennine intra-mountainous watershed the C- and the LS-factor were identified as the most important. Their effects affect the soil erosion risk even more severely than the rainfall erosivity. The rather low soil erosion rates of the densely vegetated forest rarely rise to alarming erosion risk rates. This is true also in the wooded sectors of the watershed undergoing higher erosivity of the precipitation. Rather high values of soil loss appear only infrequently in areas where the relief creates the conditions for very high LS-factor. According to this, the forest covering about 61.7% of the Turano watershed surface justifies the low values of soil loss estimated by the models. This may at least partly explain the difference between the Turano and the other Italian watersheds in terms of the predicted soil erosion rates. In fact, the other watersheds have a considerably lower forest cover and a higher percentage of croplands (Table 5.20). However, in the forest sector, areas that are potentially prone to high and severe erosion processes have also been spotted. These are the forested areas involved in tree-harvesting activities which represent high-predicted soil erosion rates and have been classified among areas of primary soil erosion risk according to both models. The scenarios proposed as well as the potential soil erosion risk map (van der Knijff et al., 1999) illustrate how the lack of vegetation amplifies the magnitude of the erosion processes. Moreover, the fact that 68.4% of the forest coppice harvested in the study period falls into the pelitic-arenaceous geological sector greatly increases the soil erosion risk. As a matter of fact, this impermeable substratum (Agostini, 1994) is responsible for a high river discharge

coefficient which according to studies in the area by Callori di Vignale (1981) results in 39.3% per year, reaching its peak during winter (73%).

The rainfall erosivity value, more than the total rainfall amount, affects the occurrence of the highest soil erosion rates. Hence, the highest values of predicted soil erosion occur in this area between September and January. In addition, during the period from November to January the high erosivity of the rainstorms in combination with the significantly lower vegetation cover (NDVI data) increases the soil erosion rates.

Concerning the soil parameters, for a watershed with the spatial and topographical conformation of the Turano they constitute an important source of uncertainty. This is due to both, the lack of adequate information on soil taxonomy (i.e. grain size) and the 'structural deficiencies' of the RUSLE model. Firstly, the spatial resolution of soil maps in Italy is too low and their taxonomy information has to be integrated by using results of different studies developed in the area. Secondly, following Renard et al.'s (1997) procedure, the K-factor is defined exclusively by the grain size pattern of the soil. The application of this method in the Turano watershed reveals Dystri Leptic Cambisols of the carbonatic lithological units as the most erodible soils. These soils account for two times as much erodible soil than the Endolepti Calcaric Cambisols covering the pelitic-arenaceous lithological sector. Since in both cases they are in their largest part shallow soils a more determinant rule of the lithological substratum in the erosional process can be assumed. In the experimental fieldwork used for the (R)USLE model elaboration the effect of the lithological basement on soil erosion processes was not considered because in well-developed agricultural soils, with gentle slope gradients, it is irrelevant. Thus, neglecting the lithological characteristic in this kind of mountainous area would most likely result in a limited soil erodibility factor estimation. Moreover, as stated by van der Knijff et al. (1999), the (R)USLE-based models have high uncertainties, especially in their procedure of K-factor estimation. Some important factors considerably influencing soil erosion are not taken into consideration, for instance the exclusion of the effects of stones and rock fragments in the soil from the K-factor computation.

5.3.3. SOIL EROSION RATES IN CROPLANDS AND ENVIRONMENTAL RISK

For the croplands, annual erosion rates of 25.94 and 7.14 t ha^{-1} yr^{-1} (modeled gross erosion) by the RUSLE and the USPED model, respectively, were obtained. The average predicted change in soil loss varies with regard to the type of agricultural area. If the rate of 10 t ha^{-1} yr^{-1} is considered as the critical threshold for these kinds of environments, as currently indicated in the literature (Wischmeier and Smith, 1978; Morgan, 2005), 56.5% (RUSLE) and 30% (USPED) of the croplands of the Turano watershed lie above this

threshold. Morgan (2005) considered this 'erosion rate value as maximum possible rate of erosion at which soil fertility can be maintained over 20–25 years.' Hence, some sectors of the Turano watershed could potentially already suffer from decreasing fertility. Furthermore, recent studies in Europe converge on identifying soil loss greater than 1 t ha^{-1} yr^{-1} already unsustainable for the long term (Jones et al., 2004; Verheijen et al., 2009). Verheijen et al. (2009) emphasized that according to the UE Water Framework Directive the surface water of the UE countries should be kept in a good ecological status. However, the US Department of Agriculture accepts just 1 t ha^{-1} yr^{-1} to maintain water quality (Montgomery, 2007). Obviously, if the erosion rates modeled in this study correspond to the actual levels of soil erosion in the Turano watershed, several locations can be expected to be subject to accelerated soil erosion processes causing both landscape and surface water degradation.

5.3.4. VALIDATION OF MODEL RESULTS

Regarding the validation operations of the model outcomes, a clear distinction between the qualitative and quantitative aspect needs to be made.

According to the semi-qualitatively validation presented in Chapter 5.2.4 the result achieved by the presented modeling approach (RUSLE) can be considered valid. The model represents well the different magnitudes of soil erosion mapped during the field survey in the selected sub-watershed. Moreover, both field and remote-sensing observations in selected locations across the Turano watershed where both models suggested high erosion rates confirm the good quality of soil loss prediction of the models. With regard to the soil deposition areas predicted by the USPED, the model seems to be less precise. Often, evident signs of erosion have been found in the Ovito sub-watershed while the model predicts high deposition values.

In addition, correlating the soil gross erosion rates derived by the RUSLE model for the main land-use units of the Turano watershed (i.e., cropland, forest, grassland, macchia, olive and vineyard) with the average values measured by plot experiments in Europe (Cerdan et al., 2010) highly insightful information was acquired. A high correlation coefficient (R^2=0.971; α<0.01) indicates a strong relationship. One can thus assume that the model represents well the differences in the hillslope erosion rates in the different land-use classes. With a correlation of R^2=0.981 (α<0.01) the situation of the USPED model is similar. In this way, the outcomes of the models are considered reliable, at least as soil erosion risk indicators.

Contrariwise, the assumption made for the semi-qualitative validation cannot be transferred to the quantitative approach. The measured SY values are considerably

different compared to the modeled ones. Both, the modeled SY values as well as the modeled gross erosion values obtained from the RUSLE and USPED models are much lower than the sediments' mass volume measured in the lake bottom. Even the gross erosion values of the RUSLE and USPED model are about 3 and 11 times, respectively, lower than the lake siltation. Moreover, the measured SY values could be even higher if the value of 1.113 t m^{-3} recently estimated by de Vente (2006) was used instead of the average bulk density of 0.865 t m^{-3} proposed by van Rompeay (2005) to convert the sediment volume to mass in watersheds. De Vente (2006) stated that the bulk density of 0.865 t m^{-3} must be considered as rather low compared to other values reported in the literature. Accordingly, the estimation of bulk density in other Italian reservoirs (Amore et al. (2004) is much higher than the one proposed by van Rompeay (2005).

Most importantly, the results of the quantitative estimation show that the RUSLE-based model, also when applied with high-resolution data, cannot provide useful quantitative SY predictions in complex watersheds such as Turano. Consequently, the modeled soil erosion rates also cannot be quantitatively validated. The first and most obvious reason for this situation is due to the fact that both models are based on the (R)USLE plot experiments and consider only the sediment produced by inter-rill and rill erosion processes. This means that several morphological processes able to contribute to the watershed SY are not accounted for by using RUSLE-based models. Osterkamp and Toy (1997) stated that where splash and sheet erosion are the dominant processes of soil erosion at small scale the SY generally can be relatively low. If the investigated area increases, allowance in the model must be made for more erosion processes (e.g., rill, megarill, gully, bank and channel erosion, landslide) resulting in a SY rise (Osterkamp and Toy, 1997). Thus, the soil loss predicted by RUSLE-based models in complex watersheds might often represent only a minority share of the total eroded sediments in the watershed. In fact, this is the case for the Turano watershed.

In general, in the Mediterranean region due to the high erosivity power of the rainstorms (Morgan, 1996) an increase of rivers' SY is attributed to gully erosion. Poesen et al. (2006) in a review paper showed that this kind of landform may produce erosion rates ranging from 1.1 to 455 t ha^{-1} yr^{-1} in the Mediterranean region. Considering gully erosion by means of RUSLE application, some authors stated that the application of RUSLE-based models using high-resolution DEM and the Moore and G. Burch (1986) method based on flow accumulation for the LS-factor computation, permits to consider the effect of the concentrated flow, namely the gully erosion (Van der Knijff et al., 1999; Saavedra, 2005). For the case of the Turano watershed in this study it is impossible to state whether the gully erosion effect is considered or not. However, the large discrepancy between the

predicted soil loss and the lake siltation leads to the suggestion that gully erosion is not well estimated and further prolific sediment sources play a very important role for the Turano watershed SY.

Kinnell (2008) stated that the watershed sediment discharge may contain quantities of sediment eroded directly in the river network. Furthermore, several other studies note factors that may greatly increase the watershed SY, such as the occurrence of landslides (de Vente et al., 2006; Lazzari, 2010), hydrological characteristics of the slopes (Kinnell, 2008), the watershed storage capacity (Parsons et al., 2006) and the drainage network pattern (Ciccacci et al., 1983; Grauso et al., 2008) among others.

Parsons et al., (2006) concluded their work by stating that the concept of sediment delivery is a fallacy. In modeling the sediment flux and creating valid practical tools for watershed management geomorphologists are advised to elucidate the links between the various components of the sediment cascade that create landscape change (Parsons et al., 2006). Given the various uncertainties, at present, the correct estimation and validation of upland soil erosion seems rather unrealistic (Boardman, 2006).

In conclusion, this study shows that due to the complexity of the Apennine intermountain watershed, with the presented models researchers cannot provide reliable quantitative predictions of SY and therefore most likely also not of the erosion rates. According to the state of the art, reliable SY and quantitative soil erosion prediction must be considered as an idea. With respect to soil erosion rates, however, a valuable element of modeling rests upon the strong correlation between the values predicted by models and the measured plot experiments in Europe (Cerdan et al., 2010). Using appropriate R-factor and C-factor input data, at best locally estimated, it is possible to represent well the erosion rates of different land uses, and consequently, estimate well the soil erosion risk. Thus, the RUSLE-based models are probably the best tools currently available to derive soil erosion risk predictions as their results are at least qualitatively valid in medium-, large-scale watersheds. In fact, the RUSLE model enables to identify areas potentially prone to higher soil erosion risks. Indeed, from the 1990s on, the European Commission has adopted the USLE (Van der Knijff et al., 1999), RUSLE (Grimm et al., 2003) and its derivatives (Van Rompaey et al., 2003) for soil erosion risk assessment in Italy. In 2011 a new application of the RUSLE model will be released by the European Soil Bureau (Bosco, personal communication) for Europe in general. This indicates that the RUSLE model, despite its limitations, still represents the main tool for performimg soil erosion risk analysis not only in the U.S. (NRCS, 2009) but also in Europe (European Commission, 2011).

This study observed the importance of forest management with regard to the risk of accelerated soil erosion processes for both, forestlands and the drainage network quality.

The occurrence of accelerated soil erosion processes induced by human activities in forestlands is still subject to little attention from both, researchers as well as decision makers in forest management positions. Given the severe long-term implications, a deeper understanding of the soil erosion risk linked to forest-harvesting activities in Italy is an important goal for future research. To expand the understanding of accelerated soil erosion risk in Italy, the forestlands under coppicing silvicultural activities require further in-depth study. To advance scholars' understanding of the accelerated soil erosion magnitude in forestlands, the following part of the thesis (Chapter 7) is dedicated to estimating the short-term impact of forest harvesting in the Turano watershed. First, the issue of the huge SY measured in Turano Lake will be analyzed and discussed (Chapter 6).

CHAPTER 6

Sediment Yield Prediction for the Turano Watershed

6. SEDIMENT YIELD PREDICTION FOR THE TURANO WATERSHED

As stated in the previous chapter, the very high SY measured for the Turano watersheds cannot quantitatively be predicted using the RUSLE-based model. This is because the inter-rill and rill erosion processes considered in the RUSLE equation do not seem to play a dominant role for the SY in the context of the Turano watershed. In an attempt to quantitatively assess the impact of the geomorphological structure of the Turano watershed on its SY, an empirical equation proposed by Ciccacci et al. (1986) was applied. This equation is able to sufficiently well predict the suspended sediment yield (SSY) for Italian watersheds on the base of some geomorphic parameters. According to Ciccacci et al. (1977, 1980, 1981, 1986) these geomorphic parameters express the main erosion-influencing features of the Italian drainage basins and networks.

6.1. METHODOLOGY

6.1.1. MODEL DESCRIPTION

The Tu index is a set of equations with high determination coefficients derived by Ciccacci et al. (1981, 1986) through statistically correlating the measured values of suspended sediment yield (SSY) at the outlets of 20 gauged Italian watersheds with selected geomorphic and climatic parameters. The idea of the Tu index is that river sediment yields can be considered to be measures of the erosion processes at watershed scale (Della Seta et al., 2009). Because of this, the SSY (t km^{-2} yr^{-1}) can be considered to be the most representative expression of erosion rate inasmuch as it consists of data frequently available and as it represents about 90% of the total sediment yield (SY) in rivers in humid climates (Cooke and Doornkamp, 1974). Several studies based on the Tu index method were published in national (Del Monte, 1996; Massaro et al., 1996; Del Monte et al., 2002; Del Monte 2003; Sbarra, 2004; Zamponi, 2007; Agnesi et al., 2006; Di Lisio et al., 2010; Lazzari and Schiattarella 2010; Gioia et al., 2011) as well as international journals (Farabegoli and Agostini, 2000; Grauso et al., 2008; Della Seta et al., 2007; Della Seta et al., 2009). Moreover, these equations are used by government research institutes (CNR – Brunori et al., 1998; ENEA – Grasso et al., 2007; Grauso et al., 2008b) to estimate the soil erosion rate to obviate the lack of measured data across the country.

Following the aim of this part of the thesis, from the equations proposed by Ciccacci et al., (1981; 1983; 1986; 1988; 1992) and Lupia Palmieri et al., (1995) the equations based on the SSY estimation through geomorphic parameters were considered. More precisely, the parameters in matter are the drainage density (Dd, Horton, 1945) and the hierarchical anomaly index (Δa, Avena et al., 1967). Several studies have provided evidence that parameters like Dd and Δa are representative for those drainage network features that strongly affect denudation intensity (Dramis and Gentili, 1977; Tokunaga, 1984; Marini,

1995; Tokunaga, 2000; Del Monte et al., 2002; Della seta et al., 2007, Della seta et al., 2009). The applied equations are:

$$Log\ Tu = 1.44780 + 0.32619 \cdot Dd + 0.10247 \cdot \Delta a \qquad if\ Dd < 6 \quad \text{(Eq. 6.1)}$$

$$Log\ Tu = 1.05954 + 2.79687 \cdot LogDd + 0.13985 \cdot \Delta a \qquad if\ Dd \geq 6 \quad \text{(Eq. 6.2)}$$

Moreover, Ciccacci (2010, personal communication) recommended the division into sub-watersheds when applying Tu index methods for medium/large scale watersheds. Subsequently, Equation 6.1 or 6.2 should be applied for each sub-watershed unit.

6.1.2. EXTRAPOLATION OF TURANO DRAINAGE NETWORK AND SUB-WATERSHED

The Turano sub-watershed delineation was carried out using GIS techniques. More specifically, the ArcHydro tool developed by the Center for Research in Water Resources at the University of Texas, Austin was used (2010). The input data consisted of a DEM 10x10 m cell-size resolution derived by topographic maps scaled 1:25,000 (see Chapter 5.2.2.3). The streams derived from the digitalization of the topographic map 1:25,000 were 'borned' according to their order (Strahler, 1952) on the filled DEM with the AgreeDem technique (ArcHydro's tool). Subsequently, following O'Callaghan and Mark's (1984) method of flow accumulation the sub-watersheds were extracted from the filled DEM. The drainage network was improved with other streams obtained by visual interpretation of the aerial photographs, FlowAccumulation and DEM analysis as well as information acquired from 1:10,000 scale topographic maps.

After their acquisition the streams of the complete drainage network were classified according to the procedure of Strahler (1952). As suggested by Ciccacci et al. (1986), the endorheic area and the anthropogenically formed streams (canals) were not taken into account. Δa was calculated for each sub-watershed according to the method proposed by (Avena et al., 1967) following the computation of the hierarchical anomaly number G_a (for more information see Avena et al., 1967)

6.1.3. STATISTICAL ANALYSIS

The statistical correlations between the predicted SY (Tu) values and the morphological characteristics (i.e., area, average slope gradient, average gradient of the streams) for each sub-watershed of the Turano watershed were analyzed.

In addition, the statistical relationships between the measured SY values of 41 Italian watersheds (database of ISSDS [Research Institute for the Study and Defend of Soil], in de Vente et al., 2006, plus the Turano watershed) and their properties, such as arable land, area, annual precipitation and average slope gradient were calculated.

6.2. RESULTS

6.2.1. TURANO DRAINAGE NETWORK CLASSIFICATION AND SUB-WATERSHED DIVISION

The number of streams identified equals 6944 for a cumulative length of 1946.7 km. The entire watershed is a seventh-order watershed. Table 6.1 and Figure 6.1 show the characteristics of the Turano drainage network reclassified following Strahler (1952). In addition, Table 6.2 and Figure 6.2 also provide the drainage network characteristics after excluding of the endorheic areas identified within the Turano watershed. The result of the geomorphological analysis for each sub-watershed is presented in Appendix K.

Table 6.1 – Characteristics of the drainage network of the Turano watershed.

Stream order	Streams	Total length	Average length	L. SD	L. Max	L. Min
	[nr.]	[km]	[Km]	[Km]	[Km]	[Km]
1	5332	1092.8	0.20	0.18	2.18	0.0007
2	1248	406.3	0.34	0.32	3.32	0.002
3	282	234.15	0.83	0.85	6.42	0.0016
4	63	88.64	1.4	1.29	6.49	0.009
5	15	71.6	4.77	3.68	14.74	1.48
6	3	28.15	9.38	4.58	12.39	4.1
7	1	25.07	-	-	-	-
Totale	6944	1946.7				

Table 6.2 – Characteristics of the Turano drainage network without the endorheic areas.

Stream order	Streams	Total length	Average length	L. SD	L. Max	L. Min
	[nr.]	[km]	[Km]	[Km]	[Km]	[Km]
1	4821	986.37	0.20	0.18	2.18	0.009
2	1132	367.66	0.32	0.35	3.32	0.002
3	259	218.57	0.84	0.86	6.42	0.0016
4	58	86.02	1.48	1.31	6.49	0.009
5	15	70.07	4.67	3.63	14.74	1.48
6	3	28.15	9.38	4.58	12.39	4.1
7	1	25.07	-	-		-
Totale	6289	1781.91				

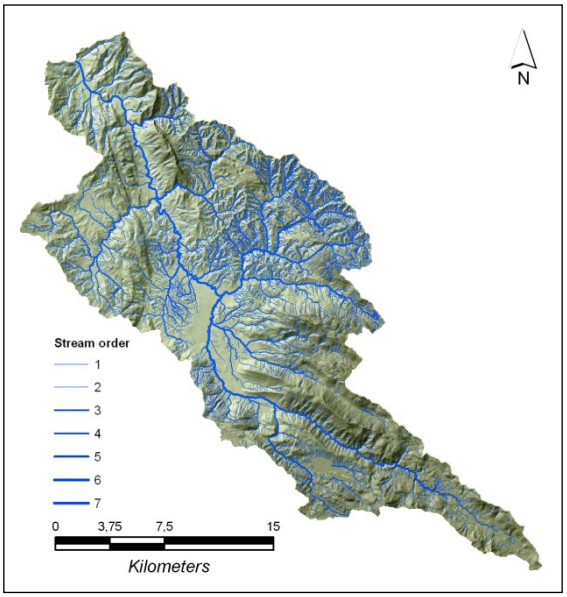

Fig. 6.1 – Turano drainage network.

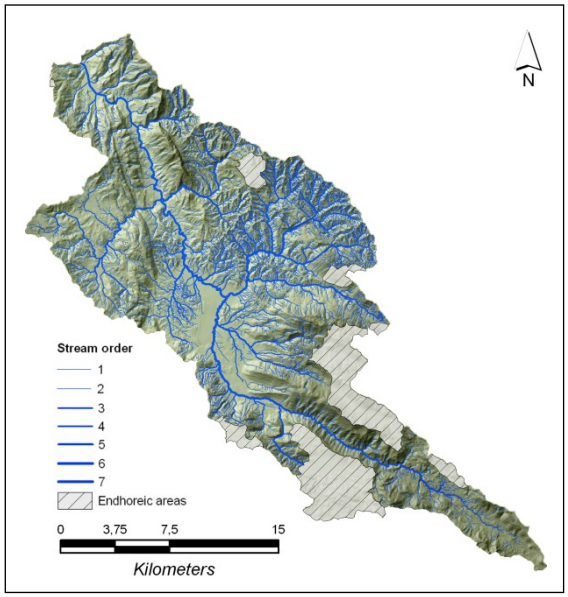

Fig. 6.2 – Turano without endorheic areas.

6.2.2. TU INDEX

The values of the Dd and Δa parameters have been calculated for each Turano sub-watershed (Table 6.3). The lowest values of the hierarchical anomaly density number (Ga) have been found in the sub-watershed I7, I5, F2 and A9. The first three sub-watersheds are located in the northwestern sector of the Turano watershed on lithological substrata mainly composed of marl, while the A9 watershed is located in the Cretaceous carbonatic sector. Maximum values of Ga can be found in the central-eastern sector of the watershed where the pelitic-arenaceous lithotype dominate (sub-watershed B2, B5, B9 and G1).

The calculated annual SY values in the Turano sub-watersheds range from 2.2 to 105 t ha^{-1} yr^{-1} (Table 6.3; Fig. 6.3). An average area-specific SY of 21.8 t ha^{-1} yr^{-1} was predicted for the entire watershed area. Accordingly, the predicted value of annual sediment accumulated in the Turano watershed amounts to 873,296.5 t yr^{-1}. The difference between the SY measured and predicted by the Tu index method is 296,979.5 t yr^{-1}.

Table 6.3 – Geomorphic parameters of the drainage network within the Turano sub-watershed.

Sub-watershed	Hierarchic order	Area	Dd	ga	Δa	Average slope	TU
		[ha^{-1}]	[Km/Km^2]	[-]	[-]	[degree]	[t ha^{-1} yr^{-1}]
A1-A10	6	58.9	2.5	644	254.2	19.8	3.3
A4	5	6.5	4.5	72	16.2	20.9	10.0
A5	5	9.0	3.4	47	13.7	21.7	4.3
A6	4	9.6	4.2	36	8.6	18.5	7.1
A7	5	4.9	3.8	25	6.6	14.0	5.8
A8	4	4.8	4.9	18	3.7	12.9	12.2
A9	4	5.1	3.2	27	8.6	19.1	3.8
A11-A12	6	4.3	5.3	27	5.1	17.4	17.5
A13	4	8.0	2.5	26	10.4	15.2	2.2
A14-A15	6	13.0	3.4	99	29.5	12.7	4.5
B1	5	8.4	8.5	198	23.3	16.7	59.1
B2	6	13.4	9.3	521	56.3	19.3	80.5
B3	4	4.8	8.5	129	15.2	19.7	57.3
B4	4	3.7	8.2	80	9.8	20.8	50.9
B5	5	5.9	6.6	236	35.7	19.9	62.8
B6	6	4.7	5.0	232	46.6	15.2	28.4
B7	5	7.4	5.9	140	23.7	18.5	31.7
B8	6	0.4	7.6	13	1.7	15.8	51.1
B9	6	8.7	9.1	506	55.6	18.5	91.1
B10	5	23.9	5.4	606	111.7	19.0	23.6
B11-A16	6	4.8	3.5	174	49.4	7.3	15.5
C1	5	22.6	4.2	206	49.1	12.9	7.8
D1	7	8.1	4.7	317	68.1	6.8	17.7
D2	5	4.7	8.0	128	16.1	14.8	50.2
D3	7	15.0	4.8	792	164.6	15.6	29.4
E1	4	5.1	5.2	45	8.6	20.7	16.4
E2	5	5.7	5.4	64	11.8	21.6	19.5
E3	5	7.3	4.1	106	25.8	18.5	8.6
E4	5	7.2	5.8	104	18.1	18.6	25.3
E5	6	4.7	2.3	105	45.3	23.1	6.9
F1	4	12.9	3.2	51	16.1	12.0	3.5
F2	5	5.2	4.0	5	1.3	13.2	5.6
F3	4	7.5	3.9	45	11.4	15.1	6.4
F4	5	7.3	3.2	81	25.2	15.6	4.9
F5	3	7.5	2.7	18	6.7	11.9	2.4
F6	5	12.3	2.7	119	43.5	15.3	3.7
G1	7	17.2	2.4	733	304.6	20.7	105.0
H1	5	10.2	4.5	155	34.5	25.9	10.8
I1	3	11.9	2.7	316	118.0	22.1	8.6
I2	4	6.1	3.4	32	9.4	22.6	4.5
I3	4	8.1	3.8	78	20.5	17.6	6.3
I4	3	3.0	3.2	37	11.5	22.1	4.7
I5	3	3.8	2.5	33	13.0	16.8	3.2
I6	3	3.6	2.7	67	24.4	20.4	5.9
I7	7	3,5	2.4	89	37,7	16,7	9.5
Turano		466.7	4.17	7,582	41.6	17.1	21.8

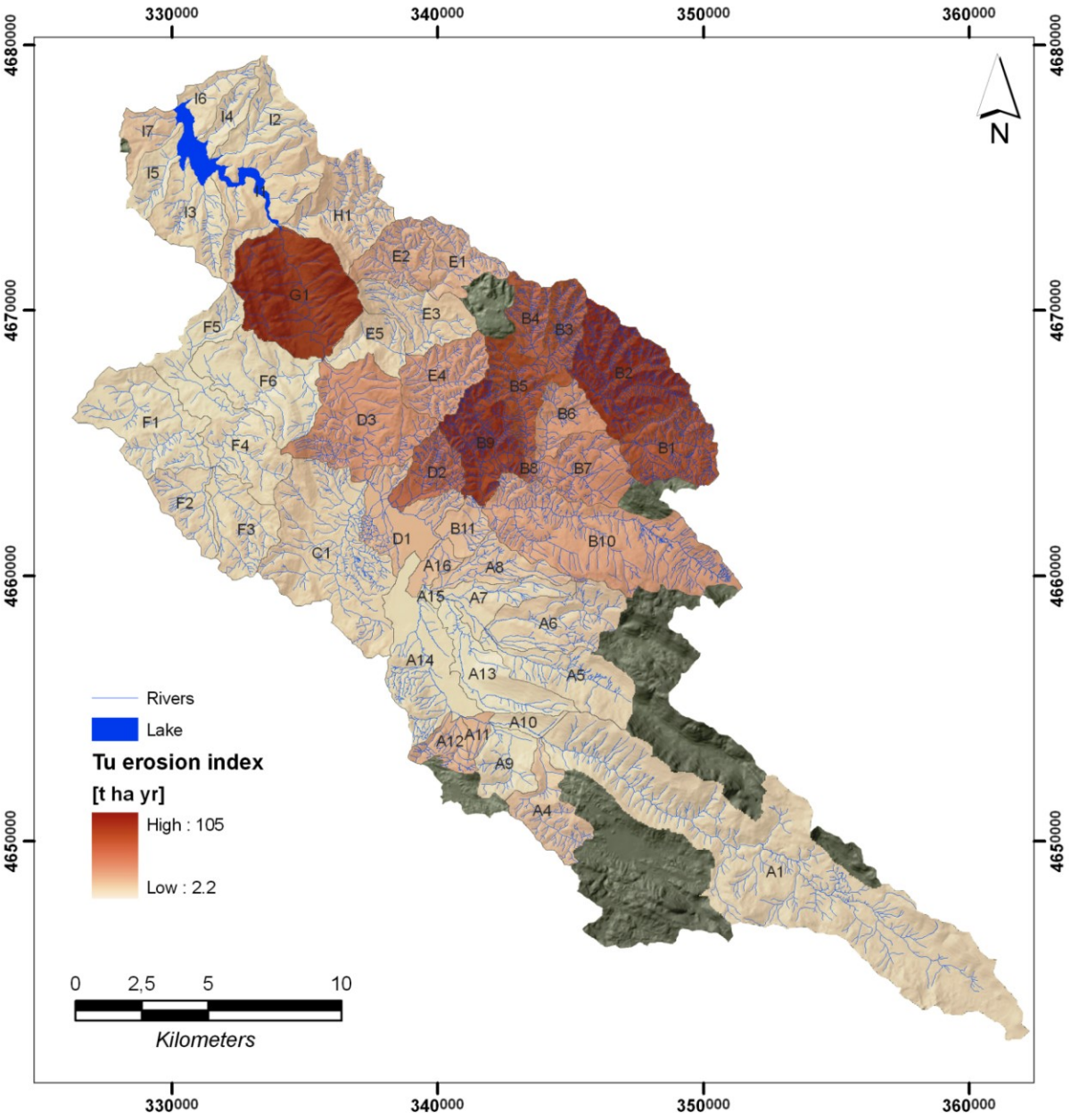

Fig. 6.3 – Map of the erosion index for the Turano sub-watershed.

6.2.3. STATISTICAL ANALYSIS

The statistical relationship between the Tu values and sub-watershed area shows an extremely weak correlation (R^2=-0.031; n= 45; insignificant). The same it is true for the relationship between the Tu values and both, the average slope gradient (R^2=0.148; n=45; insignificant) and the average stream gradient (R^2=0.123; n=45; insignificant).

With regard to the statistical relationship between the measured SY of 41 Italian watersheds and their characteristics, the highest correlation coefficient calculated is R^2= -0.488 (n= 41; $\alpha<0.01$) (SY versus mean slope gradient). The other determination coefficients between SY and watershed characteristics are: size R^2=0.308 (n= 41; insignificant), rainfall R^2=-0.244 (n=41; insignificant) and arable land R^2=273 (n=41; insig.).

6.3. DISCUSSIONS

The application of the Tu index for the quantification for the Turano watershed best performed for the SY estimation. The Turano watershed size and the nature of the geological basement fit with the watershed characteristics for which the Tu index equation was originally developed. In fact, the equation applied was derived by regression analysis from watersheds mainly emplaced on terrigenous lithotypes. According to Ciccacci et al. (1986) and other authors (Ciccacci et al., 2006; Della Seta et al., 2007; Della Seta et al., 2007), it can offer a realistic measure of the erosional processes which supply sediments to rivers.

The existence of very fine material in Turano Lake sediments indicates a prevalence of suspended sediments on river transport near its outlet (Table 5.18, Chapter 5.2.4). This conforms to Cooke and Doornkamp (1974) who posited that the suspended sediment yield may represent up to 90% of total sediment yield by river in humid climate conditions. This is even truer in areas where terrigenous rocks prevail (Grasso et al., 2008). Unfortunately, due to the unavailability of Turano Lake bathymetric survey data further reasoning on the sedimentation dynamics is precluded.

As stated by Ciccacci et al. (1986), the attempt to estimate the sedimentation in reservoirs of central Italy offered predicted SSY values consistent with the data obtained from bathymetric surveys (Ciccacci et al., 1983). Using the parameters Dd and Δa as independent variables for the SY prediction, Ciccacci et al. (1986) obtained a very high coefficient of determination (r^2=0.96) and an average error percentage between the observed and predicted data of 13–14%. The application of the Tu index method for the Turano watershed confirmed the rather good ability of the Ciccacci et al. (1986) approach to predict the SSY for the central Italy area. Here, the error percentage between the observed and predicted data is 25.4%.

Due to its simple structure, the applied equations do not directly consider any factor influencing the soil erosion processes on the uplands (for instance land use, soil erodibility, rainfall erosivity, slope steepness and length). Consequently, the outcomes of the equations cannot be linked to accelerated soil erosion due to the short-term anthropogenic impact. Being based on geomorphic parameters, this indirect method reasonably expresses the medium-time-scale response of the drainage network to disequilibrium conditions induced by Quaternary climate oscillation and uplift (Della Seta et al., 2009). Gioia et al. (2011) suggested that the Tu index can be considered a suitable tool for the estimation of the medium- to long-term denudation rate in watersheds characterized by fluvial processes largely acting on terrigenous deposits.

From the observations made above a close relationship can be inferred between drainage network and SY in the watershed observed by Ciccacci et al. (1986). More precisely, Italian watersheds with a strong link between heavy river SY values and the morphological properties of the drainage system (Dramis and Gentili, 1977; Del Monte et al., 2002; Della seta et al., 2007) seem to highly dependent on the presence of terrigenous lithotypes (marl and sandstone, Bizzini et al., 2009). Contrarily, as already noted by Ciccacci et al. (1981) Tu index values have only weak correlations with climatic parameters such as total rainfall, Fournier's Climatic Index p^2/P (where p is the highest monthly rainfall and P is the mean annual rainfall) (Fournier, 1960) and P σm (where σ is the standard deviation of the rainfall of the twelve months of a given year from their respective average) (Ciccacci et al., 1977). There is also only a weak correlation between SY and the river water discharge Q (m^3/s) (Ciccacci, 1980).

Directly or indirectly, the parameters Δa and Dd influence the river sediment discharge in the Italian rivers. Findings of recent studies have reinforced the idea that the topological behaviors of the river network can be meaningfully related to the SSY for Italian watersheds (Grauso et al., 2008a, Grauso et al., 2008b).

The results derived from the Turano watershed study at hand as well as the implications of the numerous studies listed here, indicate the important role of the geological and structural characteristics of Italian watersheds and their drainage network patterns for the river sediment discharge values. The complex Italian tectonic history and its relatively young bedrock dominated by arenaceous-sandy and clayey lithological units may highly complicate the SY prediction using the modified version of the USLE model (Williams, 1975, van Rompaey et al., 2003) or physical based models like SHESED (Wicks and Bathurst, 1996). In fact, it also became apparent that the poor SY prediction results obtained from the application of these models in Italy are not representative of the better results that these models provided for other European countries (de Vente et al., 2006; van Rompaey et al., 2003; van Rompaey et al., 2003b). The reason for this appears to be because these models represent the human-induced erosion processes on the slopes (mostly inter-rill and rill). As pointed out by Kirkby and Cox (1995) and other studies (Osterkamp and Toy, 1997; Bryan, 2000) hydrological processes responsible for these kinds of erosion process formation seem to be prominent at the hillslope scale.

The poor results of a multiple regression analysis of the SY as the dependent variable and three parameters considered mainly responsible for hillslope-scale soil erosion processes (i.e., average slope, arable land and annual precipitation) for 41 Italian watersheds suggest a reconsideration of the role of human-induced erosion on the uplands as the main source of sediment load in Italian rivers. As shown in the output table of the multiple regression

analysis the model based on the relationship between arable lands, upland slope gradient, annual precipitation and the SY values reveals an R^2 of only 0.30 ($\alpha<0.01$) leaving 70% of the overall SY variance unexplained. Thus, it would have been interesting to have introduced additional factors such as forest coverage, other land-use units, surface of the alluvial plain, or soils in the multiple regression analysis, but these data were not released for public use (ISSDS, Bazzoffi, 2010 personal communication).

Table 6.4 – Main characteristics of 41 Italia watersheds.

Watershed	Size	Average slope gradient	Rainfall	Drainage density	Arable land	Observed SSY
	[km²]	[%]	[mm]	[km/km²]	[%]	[t ha⁻¹ yr⁻¹]
Ancipa	50	17.8	837	2	0	5.6
Barcis	390	59.9	1644	4.3	1.2	5.2
Bau Mela	95	26.2	967	3.8	33.9	0.7
Boreca	42	44.7	883	2.9	1.3	0.9
Campo Tartano	48	55	1617	1.9	0	0.9
Carona	45	49.2	2012	3	0.7	0.2
Castello	68	48.4	1123	6.9	0	3.7
Cignana	12	51	936	1	0	0
Disueri	249	11.3	607	2.2	67.3	16.8
Flumendosa	602	26.3	765	3.1	20	0.9
Fortezza	661	49.2	907	4	0.5	0.6
Gammauta	91	24.3	796	3.7	71.7	1.6
Lavagnina	43	30.4	1115	6.1	0.9	4.1
Letino	13	24.3	1406	0.6	7.7	0.5
Locone	245	6.9	707	2.4	87.8	1.7
Maira	54	50.3	990	2.1	1.7	0.2
Mignano	87	20.5	877	4	39.2	12.8
Molato	81	19.6	792	4.1	47.8	10.1
Mulargia	171	11.9	741	3.3	35.8	10.3
Muro Lucano	36	19.6	871	2.9	33.8	12.2
Ortiglietto	142	22.1	1027	6.2	3.8	6.9
Ozola	11	37.1	1414	2	0	2.5
Pagnona	55	58.4	1490	4.1	0	0.5
Pavana	40	36.5	1304	5.9	0.7	2.7
Place Moulin	68	60.2	857	0.7	0	2.3
Ponte Fontanelle	352	19.6	750	3	15.5	6.7
Pontecosi	234	31.9	1353	3.7	14.7	1.6
Pozzillo	578	16.9	765	2.3	52.7	19.6
Prizzi	21	14.5	780	2.8	76.8	5.7
Quarto	219	26	1049	2.6	25.6	12
Riolunato	155	30.3	1257	3.8	21.1	4.7
Rochemolles	24	49.8	736	1.8	0	0.1
Santa Luce	40	9.9	966	3.8	69.6	9.2
Scalere	14	25.1	1180	4	47	0.9
Scandarella	39	15.2	913	2.7	24.9	4.9
Serra Di Corvo	298	5.7	737	2.4	87.9	1.9
Suviana	75	33.4	1316	5.2	3.7	3.9
Torre Crosis	86	41.2	2377	4.5	4.4	1.2
Turano	466	401.7	1204	4.2	17.3	32.3
Vodo	333	44.6	1232	1.9	0.6	1.2

The findings above call for a reflection on the possible overestimation of the erosion rates obtained by RUSLE-based model applications in Italy. According to the author's best

knowledge the comparison of gross erosion values predicted by RUSLE for Italian watersheds with the SY resulted in gross erosion values smaller than the SY in only two other cases (Agnesi, 2006; Amore et al., 2004). An increased average soil loss value occurred from merging the results of the RUSLE-based model application in 30 Italian watersheds (about 48.1 t ha^{-1} yr^{-1}). In almost all studies presented for Italy so far, the erosion values resulting from inter-rill and rill processes calculated by the models have been sufficient to justify the river sediment discharge.

Van Rompaey et al., (2003) applying a revised RUSLE (the WaTEM/SEDEM model) for 22 Italian watersheds observed SY values lower than the predicted erosion, with SDR ranging from 0.06 to 0.68 in all watersheds. In doing so, none of these 21 Italian watersheds (Appendix H) experienced a situation of gross erosion smaller than the SY as in the case of the Turano watershed. This fact calls for some further consideration. Firstly, it is statistically surprising that a RUSLE based model such as the WaTEM/SEDEM model delivers gross erosion values lower than the SY for any of the 21 observed watersheds. Secondly, de Vente et al. (2006) applied semi-qualitatively models using part of the watershed of the same database of van Rompaey et al. (2003). They noted a relevant improvement of the soil erosion prediction when the aspect of landslide is considered. De Vente et al. (2006) concluded that the SY for most of the examined Italian watersheds is dominated by other erosion forms (e.g., landslide, gully and bank erosion) rather than upland processes. Thirdly, the average soil erosion of 46.2 t ha^{-1} yr^{-1}predicted for the 21 watersheds is presumably too high to be solely attributed to inter-rill and rill processes. In addition, such an erosion rate is in discordance with other studies performed at a national scale (R)USLE (Van der Knijff et al.,1999; Grimm et al., 2003; Bosco, personal communication) and PESERA (Gobin et al., 1999).

For instance, the study of the Pozzillo watershed in Sicily presented by van Rompaey et al. (2003) seems to be an evident case of upland erosion overestimation. Together with the Turano watershed, the Pozzillo watershed with a substratum largely covered by marly clay and sandy limestone is among the Italian watersheds with the highest SY (19.6 t ha^{-1} yr^{-1}) (Bazzoffi, 1996). By using the USLE model, Amore et al. (2004) could predict 13.4 t ha^{-1} yr^{-1} of gross erosion. As a consequence, in the Pozzillo watershed similar to the Turano the inter-rill and rill processes represent only a small share of the SY. However, using the WaTEM/SEDEM model van Rompaey et al. (2003) predicted a gross erosion rate of 144.5 t ha^{-1} yr^{-1} with a SDR of 0.13 (modeled SY equals 19.2 t ha^{-1} yr^{-1}).

To conclude, the RUSLE model predicted 414,198.7 t yr^{-1} of gross erosion with respect to the Turano watershed. This value amounts to approximately one-third of the annual average sediment accumulated in the Turano watershed which equals 1,329,505 t yr^{-1}.

Moreover, it is worth mentioning that the gross erosion values on an annual time-scale estimated by (R)USLE tend to overestimate soil loss (Kinnell, 2008) and that only a rather small share of it may reach the watershed outlet (van Rompaey et al., 2003). Thus, according to a rough estimation the share of SY amenable to soil erosion processes due to land use may cover only 15–20% of the total SY. Following three years of observation by remote sensing, field surveys and experiments in the area the following factors have been identified as responsible for the high solid river transportation:

- Drainage density. The Dd affects the river solid discharge in two major ways. First of all, high Dd values increase the eroded upland particles' probability of reaching the drainage network instead of being re-deposited on the footslope. Secondarily, the presence of lithotypes, which are easily erodible such as marl and pelitic-arenaceous units, favors riverbed erosion and river bank denudation processes.

- Geographical distribution of the lithological substratum. In the Turano watershed the high denudation rates associated with the lithological terrigenous sector are abundantly represented by alluvial and colluvial deposits in its valleys. In contrast, these kinds of Quaternary deposits are rather low in the carbonatic sectors. It is a fact that the terrigenous rocks occupy the area near the watershed outlet. Thus, it is reasonable to assume a rise in the SDR because of the short distance between a high sediment source and the basin outlet (Walling, 1983; Morris and Fan, 1998).

- Geographical distribution of the farmlands. The high impact of gully erosion on the river SY values is well recognized (Poesen et al., 2006). Nevertheless, gullies have not been noticed during fieldwork in the agricultural areas of the Turano watershed. The low slope gradients do not particularly lend themselves to gully formation. However, on the one hand a marked localization of farmlands on the flat alluvial plains can reduce the occurrence of high erosion rates. On the other hand, farmlands in the proximity of the main stream channels facilitate the movement of eroded soil particles in order to reach the drainage network, i.e., the watershed outlet. The formation of ephemeral gullies during winter and the existence of mega-rills likely transfers sizeable amounts of sediments into the drainage network.

- Landslides. According to de Vente et al. (2006), model coefficients significantly increase when landslides are taken into account in semi-quantitatively models for Italian watersheds. According to the ISPRA database (2010,) during the period between the two bathymetric surveys landslide events have been very low. However, the occurrence of some landslides in the final segment of the main stream, just in the proximity of Turano Lake, becomes highly relevant in this context. Some landslide scarp edges are even

visible around the reservoirs. As suggested by de Vente et al. (2006), the presence of earth flows in that watershed location and solifluction near the stream channels of the terrigenous sector may play a primary role due to the fact that the lake siltation value is very high. In addition, Lazzari and Schiattarella (2010) observed that, if not deposited in the stream channels, the material from landslides and related slope movement processes can be a source of sediments for a period of time stretching from only a few months to thousand years.

- Forest harvesting. According to the model results as well as the experimental activities presented in Chapter 3.4, the silvicultural coppicing activities have a huge impact in the soil erosion processes in the area. Since the area of tree-harvesting activities is profusely located in the pelitic-arenaceous geological sector close to the watershed outlet with a dense drainage network (Dd 6.4), the probability that the sediment eroded on the hillslopes reaches the streams significantly increases. According to the rather high slope gradient of the streams and their torrential nature the eroded sediments can be easily transported downstream. Finally, a relevant gully formation has been found in the harvested area as explained in Chapter 8.3.1.

Table 6.5 – Characteristics of the watershed used by van Rompaey (2005).

Watershed	Type	Size	Slope grad.	Rainfall	SY
		[Km²]	[%]	[mm]	[t ha^{-1} yr^{-1}]
Ancipa	South	50	17.76	649	5.6
Barcis	Alps	390	59.92	1945	5.2
Castello	Alps	68	48.37	907	3.7
Cignana	Alps	12	51.03	913	0.0
Desueri	South	249	11.27	650	16.8
Flumendosa	South	697	26.28	950	0.9
Gammauta	South	91	24.33	792	1.6
Lavagnina	Alps	43	30.43	1592	4.1
Letino	South	13	24.3	1500	0.5
Mignano	Alps	87	20.48	993	12.8
Mulargia	South	171	11.86	711	10.3
Placemoulin	Alps	68	60.17	913	2.3
P. Fontanelle	South	352	19.55	823	6.7
Pozzillo	South	578	16.86	658	19.6
Prizzi	South	21	14.5	792	5.7
Rochemolles	Alps	24	49.81	901	0.1
Santa Luce	Central	40	9.91	684	9.2
Scalere	Central	14	25.05	1600	0.9
Scandarella	Central	39	15.24	881	4.9
Serra di Corvo	South	298	5.73	473	1.9
Suviana	Central	75	33.44	1631	3.8

Chapter 7

Measurement of Soil Erosion at Hillslope-scale: Field Monitoring

7. MEASUREMENT OF SOIL EROSION AT HILLSLOPE-SCALE: FIELD MONITORING

As revealed during the modeling of soil erosion on a watershed scale the forest regions subject to harvesting activities and agricultural and grazing sectors are the areas primarily affected by accelerated soil loss. In accordance with the results of the soil erosion prediction models the harvested forest sectors generated up to 292,127 t (RUSLE) of eroded sediments during the entire considered period. This value is about nine times larger than the amount of erosion produced in the same area within a scenario of undisturbed conditions which is equal to 32,717 t. This situation emphasizes the critical role that forest harvesting plays in soil erosion processes. Moreover, it also stresses the need to observe how these processes evolve in reality because of the importance to remember, as the reliability of the RUSLE model outcomes and those of the other models based on its parameter decries in non-agricultural areas. Thus, to gain an understanding of this phenomenon the investigation of the relationship between this forest management technique and the acceleration of soil erosion processes is essential.

This part of the study has been carried out with the purpose of verifying the effects of the forest harvesting related to coppicing forest management technique on hydrology and soil erosion in a sensitive sector of the Central Apennine.

The experimental activities conducted rest on the hypothesis that forest harvesting in arenaceous torbiditic-dominated substratum watersheds may be a hotspot for soil erosion in the Apennine areas. This is due to the impermeability propensity of these lithologies that especially characterizes the more pelitic layers (Agostini, 1994). In addition, the combined effect of the low infiltration capacity of the Cambisols with the geological substratum composition is responsible for a high generation of overland flow.

7.1. STUDY SITES DESCRIPTION

Two first-order watersheds, named EX-01 and EX-02, have been selected to carry out direct observations and quantifications of the topsoil morphological evolution under two different forest management approaches. The experimental watersheds are located inside the Regional Nature Reserve of Monti Cervia and Navegna (UTM coordinates 4674045N and 338150E). These are typical first-order mountainous watersheds of the terrigenous units of the Turano watershed. The EX-01 watershed is 1002 m a.s.l. and stretches from 939m to 1034 m a.s.l. with an area about 1.97 ha. The length of the main stream is 196 m and the mean catchment width is 80 m. The mean stream gradient is 11 degrees and the mean slope gradient is 24 degrees. EX-02 presents similar topographical characteristics within an investigated area of 2.24 ha area (Table 7.1).

Both watersheds are incised into the middle Miocene torbidite in pelitic-arenaceous facies (CARG map 358). According to Bertolani et al. (1994), the particle size composition of this rock is 53.1% sand (0.5–0.063 mm), 46.7% silt (0.063–0.0039 mm) and 0.2% clay (< 0.0039 mm). The predominant soil is a not very well-developed yellow-brown (7.5YR 3/2-10YR 4/4) Endoleptic Cambisol formed by alteration of the parent material.

The average annual rainfall according to the data measured by the meteorological station of Collalto Sabino (1000 m a.s.l.) for the period from 1921 to 1984 is 1270 mm, while the average annual temperature is around 11.3 °C.

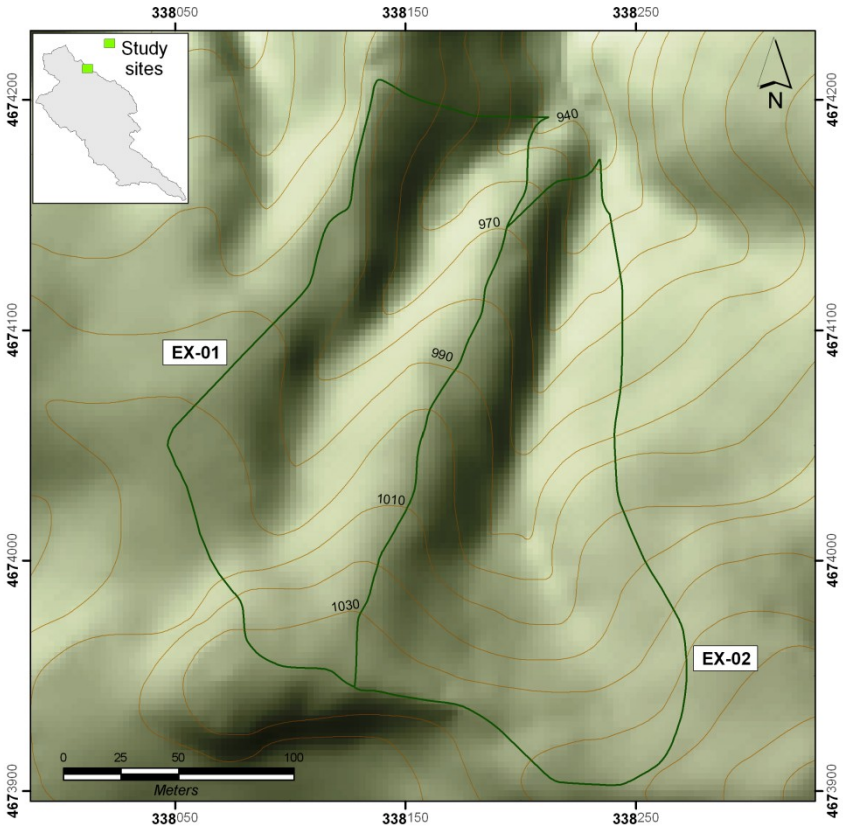

Fig. 7.1 – Study sites.

Table 7.1 – Characteristics of the study sites

Name	Area	Altitude			Slope gradient			Stream length	Stream slope
		Mean	Max	Min	Mean	Min	Max		
	[Ha]	[m a.s.l.]	[m a.s.l.]	[m a.s.l.]	[degree]	[degree]	[degree]	[m]	[degree]
EX-01	1.97	989	1034	939	23.8	0.15	47.1	196	11°
Ex-02	2.24	1002	1048	938	27.5	0.35	51.71	211	24°

.

The EX-01 area belongs to the forested sectors of the Turano watershed that is under coppicing silvicultural practices. The coppice trees (*Acerus*, *Quercus pubescens* and oak) have grown naturally without any pruning since the last timber harvesting in 1990.

Between May 2008 and December 2009 the vegetation was harvested entirely using the shelterwood technique (about 150 trees ha^{-1} standing after clear-cut). The harvested timber was manually extracted from the watersheds and the harvesting operations were performed in two steps: The first cut involved the central southern sector which amounted to 78% of the total watershed surface between May 2008 and June 2008. Then, the remaining 22% of tree vegetation was cleared in November 2009. In contrast, the EX-02 area, despite it bordering the EX-01 watershed, has not been involved in timber-harvesting activities. The vegetation in EX-02 is a mixed forest of coppice trees similar to those in EX-01 before cutting but there are also some *Castanea Sativa* trees. Here, the tree density is approximately 2400 trees ha^{-1} and the tree heights range from 7 to 15 m (average: 13.5m).

7.2. METHODOLOGY

7.2.1. FIELDWORK ACTIVITIES

7.2.1.1. GEOMORPHOLOGICAL MAPPING

Geomorphological field surveys were carried out in the area during the entire period of the Ph.D. In August 2008 during the first field survey the natural geomorphological forms as well as the anthropogenically-induced forms in the two watersheds were mapped. The topography of EX-01 was delineated using D-GPS and a tachymeter while a DEM based on contour lines of a 1:10,000 scale topographic maps (CTR LAZIO) was created for both watersheds. The following field surveys focused on mapping the soil erosion features.

7.2.1.2. MEASURING CHANGE OF SURFACE LEVEL

To ensure a continuous observation of the soil surface changes caused by water erosion a widely-used method was applied. More precisely, metallic stakes (also called pins, spikes or pegs) were driven into the soil so that the top of the stake (in other techniques the middle point) gives a datum from which changes in the soil surface level can be measured. The stake technique was considered as the best method to enable the estimation of soil erosion rates in areas where electronic instrumentation could not be installed (Hudson et al., 1993). Moreover, the stake has a low impact on the environment, and when used in an appropriate number these stakes give a plausible measurement of the soil erosion volume (Takei et al., 1981; Sirvent et al., 1997; Smith and Dragovich, 2008).

In the EX-01 watershed 70 metallic stakes with a diameter of 10 mm and a length of around 500 mm were placed across the watershed surface in July 2008. The stakes, coated with an antioxidant varnish, were equipped with a safety plastic hat. The original soil surface level is indicated by an iron ring (inexorable) fixed onto the stake. Due to the rather high slopes of the watershed the rings were fixed inclined, approximately between

25° and 35°, onto the metallic stakes. Along the watershed surface the stakes were distributed in different patterns. In doing so, a few different forms for monitoring were created as given in Table 7.2. Further, using a Leica tachymeter and two DGPS devices the location of each stake as well as the hillslope characteristics were acquired and imported into a GIS environment.

15 iron stakes were placed into the EX-02 watershed. The lower amount of stakes is due to the poorer soil erosion signs found in the areas during the preliminary geomorphological mapping phase. Accordingly, the placement of a higher number of stakes in the EX-01 watershed was considered more beneficial.

The changes of soil surface measured by the iron stakes were checked every four months according to the annual variations of rainfall patterns in January, May and September. In doing so, between January 2009 and September 2010 six metallic stake readings were taken.

Table 7.2 – Monitoring stations.

Monitoring form code	Monitoring form type	Number of metallic stakes	Watershed	Description	Monitored period
P-1	Slope cross-profile	15	EX-01	Slope aspect: northwest Length: 50 m Slope gradient: 25/30° Distance between Stakes: 3 m	From:8/2008 To: 4/2010
P-2	Slope cross - profile	11	EX-01	Slope aspect: northwest Length: 35 m Slope gradient: 30/33° Distance between Stakes: 3 m	From:8/2008 To: 4/2010
Plot-1	Plot	26	EX-01	Slope aspect: northwest Area: 60m² Slope gradient: 15-35° Distance between stakes:1.5/2m	From:8/2008 To: 01/2010
Plot-2	Plot	15	EX-02	Slope aspect: southeast Area: 24 m² Slope gradient: 18° Distance between Stakes: 2 m	From:8/2008 To: 4/2010
Plot-3	Plot	8	EX-01	Slope aspect: northwest Area: 18m² Slope gradient: 30° Distance between Stakes: 1.5/3 m	From:1/2010 To: 7/2010
Plot-4	Plot	8	EX-01	Slope aspect: northwest Area: 18m² Slope gradient: 12° Distance between Stakes: 1.5/3 m	From:1/2010 To: 7/2010
V-shaped	Profile	8	EX-01	Slope aspect: NW-SE Length: 5 m Slope gradient: 8° Distance between Stakes: 0.5 m	From:8/2008 To: 4/2010
Free-stakes	Random points	10	EX-01	Slope aspect: southeast Area: over the southeast slope Slope gradient: 10-30° Distance between Stakes: -	From:8/2008 To: 4/2010

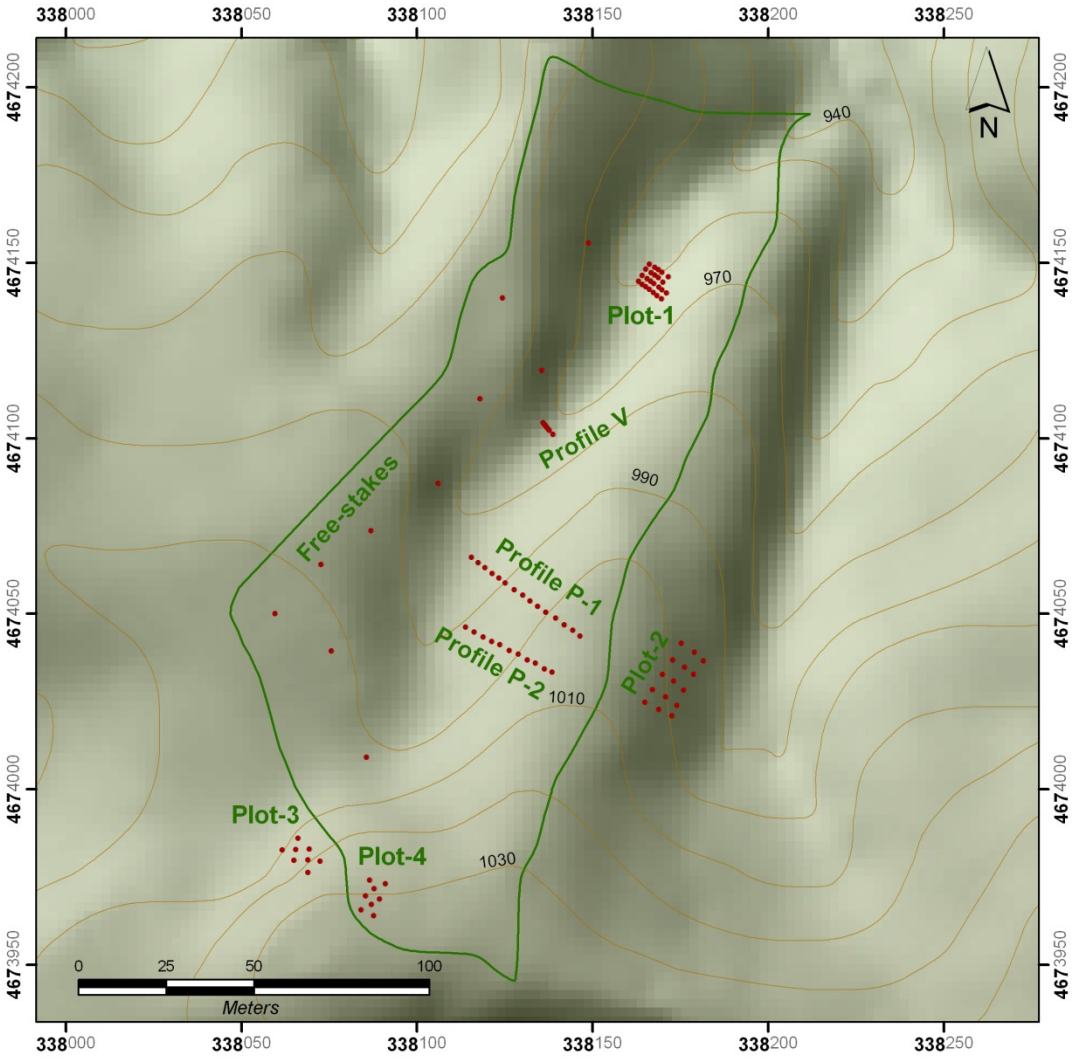

Fig. 7.2 – Destribution of the metallic stakes across the experimental watersheds.

Fig. 7.3 – Some stakes before to be placed.

Fig. 7.4 – Some stakes of Plot-01.

7.2.1.3. SOIL SAMPLING PROCEDURE

The soil sample activity was carried out during the first fieldwork in September 2008. This part of the work followed a geometrical and morphometrical analysis of the area in a GIS environment where the locations and distance intervals of soil sampling were established. Thus, GPS-guided systematic sampling of 35 samples was collected at intervals of about 30 m along straight lines (11° downstream inclined) starting from the contours of 1000, 990 and 985 m a.s.l.. About 100 g of soil was collected on a 0–10 cm soil depth. Furthermore, along two transverse cross-sections 20 soil profiles with PVC pipes at 0–30 cm soil depth were collected. Finally, a soil cross-section from 0–72 cm was carried out.

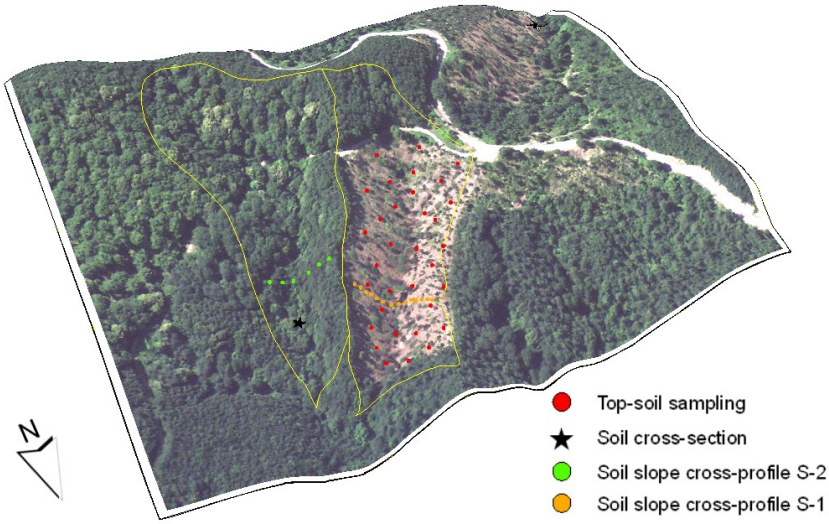

Fig. 7.5 – Soil sampling locations. Orthophoto source: Lazio Region2008.

7.2.1.4. INFILTRATION AND LIQUID/SOLID DISCHARGE MEASUREMENTS

Climate information for the period of experimental activities were acquired by the meteorological station of Collalto Sabino located 6.7 km S-E of the EX-01 and EX-02 watersheds. During the period from July until October 2009 rainfall measurements were performed directly in situ using a pluviometer located on the highest point of the EX-01 watershed. The purpose of these field measurements was to obtain rainfall data measured in the experimental watersheds to correlate it with the run-off and soil loss data measured by plot experiments.

In EX-01 two small plots to carry out the measurement of run-off and soil loss rate for each rainstorm event between July and October 2009 were created (HPt-01 and HPt-02). The plots whose locations are reported in Figure 7.6 (detailed in Table 7.4), were located on hillslopes with almost homogeneous slope gradient (slope difference about 2°) and similar slope aspect exposure. No significant differences of the two plots in terms of their surface characteristics, parent material and soil type were found. The only elements of their

differentiation were the vegetation cover and the forest ground litter. HPt-01 was located in the section of the watershed with bare soil owing to the forest harvesting in May and June 2008. During the first year after vegetation cut the forest ground litter was completely washed out by overland flow leaving a bare soil. Contrarily, HPt-02 was located in the upper part of the watershed under undisturbed tree vegetation showing a thick litter (about 2–3 cm) on the soil.

The plots were bounded with wood boards sealed with weatherproof plastic foil fixed at a soil depth of 0.1 m. Both, overland flow and soil loss were drained into plastic containers with 50 l capacities which collected water and sediments after each rainfall event. The rainfall events were monitored using the instantaneous rainfall data measured by the meteorological station of Collalto Sabino (Hydrographic and Oceanographic Institute of Rome, real-time online source, 2009). In this way, every time a rainfall event was recorded by the Collalto Sabino meteorological station, pluviometer and the plot containers in the EX-01 watershed were checked. In cases of water and sediments inside the containers they were measured and sampled.

During the period from 15th July to 4th November 2009, 19 rainfall events were observed (Table 7.3). The plot experiments had to be interrupted on 6th November 2009 because the area of watershed where HPt-02 was located was also harvested. In addition, HPt-02 was dissembled and rendered completely unusable. As a consequence, it was impossible to carry out the plot measurement campaign until January as originally planned. For this reason, during the fieldwork in January 2010 additional metallic stakes were inserted into the sector recently harvested so to form two other monitoring stations with a total of 16 stakes (Plot-3 and Plot-4).

Table 7.3 – Rainfall events.

Rainfall events	Code	Rainfall
	[-]	[mm]
14.07.09	EV-1	1.8
18.07.09	EV-2	2.3
12.08.09	EV-3	15.0
13.08.09	EV-4	3.2
14.08.09	EV-5	1.8
23.08.09	EV-6	2.9
27.08.09	EV-7	3.0
31.08.09	EV-8	2.8
12.09.09	EV-9	2.1
15.09.09	EV-10	55.3
15.09.09	EV-11	13.4
19.09.09	EV-12	2.5
21.09.09	EV-13	2.7
30.09.09	EV-14	1.6
2.10.09	EV-15	5.5
10-12.10.09	EV-16	24.4
22-24.10.09	EV-17	133.7
2.11.09	EV-18	21.9
4.11.09	EV-19	12.2

Furthermore, during the same fieldwork campaign several measures of the hydraulic conductivity performed with a mini-disk infiltrometer (ENVCO, 2010) were carried out. The hydraulic conductivity was calculated using the measured cumulative infiltration versus time according to the method proposed by Zhang (1997). The sites where the data were collected were selected across the watershed considering the Topographic Index (Beven and Kirkby, 1979) extracted by the DEM 5 m cellsize by raster calculator in ArcGis 9.3. At the end of the operation 21 punctual hydraulic conductivity measures had been collected. In addition, an observation of the soil moisture content and the soil temperatures in the sunny and shady hillslopes was carried out.

Table 7.4 – The characteristics of the sampled area.

Plot characteristics								
	Drainage area	Altitude	Slope	Aspect	Soil content			
					Sand	Silt	Clay	O.M.
	[m²]	[m a.s.l]	[%]	[-]	[%]			
Plot 1	1.55	1000	18.7	Northeast	39.7	52.9	7.4	4.9
Plot 2	1.55	1015	21.6	Northwest	34.1	56.7	9.2	5

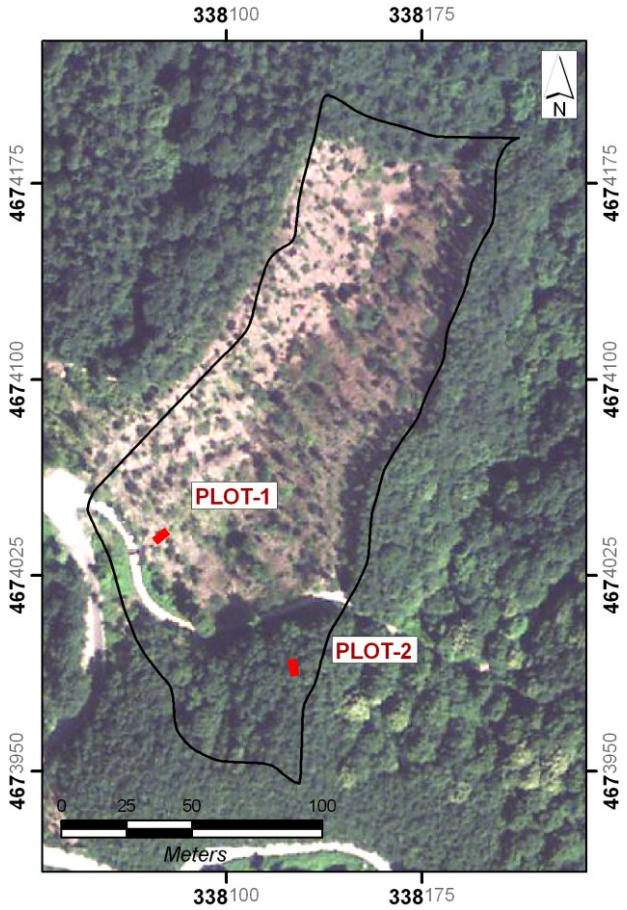

Fig. 7.6 – Hydro-plot locations. Orthophoto source: Lazio Region2008.

7.2.2. LABORATORY SOIL SAMPLES ANALYSIS

The laboratory analyses of the soil samples collected during the fieldwork in 2008 and 2009 were performed at the Physical Geography Laboratory, FU Berlin. The samples were dried in an oven at 50°C and the soil skeleton (the >2 mm fraction) was subsequently separated. Afterwards, for each sample the soil fraction less than 2 mm in diameter was sub-sampled and a portion of it was homogenized by milling. Next, some analyses were performed on the soil samples to determine the erodibility (K-factor) values. Additionally these results were utilized with soil profiles sampled in other sectors of the Turano watershed to estimate the soil erosivity input parameter for the applied soil erosion prediction models (Chapter 5.2.2.2).

The organic and inorganic carbon content was determined using the Woesthoff Carmhograph. Total carbon (TU) content was measured by heating the samples to 1000°C in oxygen atmosphere followed by conductivity quantification of the evolved CO_2 in a 20 ml 0.05 N NaOH solution. The total inorganic carbon (TIC) content was measured by a similar conductometric method as the one applied for the TU content where the CO_2 was evolved through H_3PO_4 acid treatment. Subsequently, the total organic carbon (TOC) content for each sample was given by subtraction of TIC to TC.

The analysis of the grain size distribution was the only analysis not performed in the FU laboratories. Grain size was measured using a Laser Diffraction Spectrophotometer (LDS) from the Helmholtz-Zentrum Potsdam and ARSAA Abruzzo. To do that, previous soil samples were pretreated with hydrogen peroxide (H_2O_2) at 20% and hydrochloric acid (HCl) in order to remove the vegetation and carbonates, respectively. With the LDS method the soil samples were divided into 16 grain size classes and the granulometric curves were extracted.

Bulk density measurements were performed on seven soil samples taken by a 6 cm diameter ring (10 cm depth) in proximity to the sites of the infiltration tests. The ring was driven into the soil to a depth of 6 cm and the soil samples collected were carefully placed in plastic bags. Once in laboratory, the samples were weighed while still wrapped in the bag to have the total weight. Afterwards the samples were dried in an oven at 105°C for 24 h and reweighted so that bulk density values for each sample were given by the ratio between volume and weight.

The pH values were measured on a 10 g soil sample within a solution of 25 ml 0.01 M $CaCl_2$ with a pH meter (model ‘pH 320’, company WTW) with 0.01 pH resolution. The operation was repeated twice for each sample and the average was considered as the final pH value.

The electrical conductivity (EH) values were measured on a 10 g soil sample mixed with distilled aqua by eH-meter (model LF 91, company WTW). As already performed for the pH, the EH measurement operation was also repeated twice and the average was considered as the final value.

Finally, soil colors of the soil samples were given from visual observation using the Munsell color chart.

7.2.3. GIS OPERATIONS

As mentioned above, the stakes and soil sample locations were georeferenced in the field using two DGPS devices and a tachymeter. In doing so, they could be acquired in ArcGis as punctual information (point shapefile) already with X, Y and Z coordinates. The parameters derived from fieldwork and from laboratory activities were inserted into the shapefile's attribute table. Finally, from the soil samples data were derived through Distance Weighting interpolation method (n=35; set 5 neighbors) maps contending soil information, e.g., skeleton, grain size distribution, TIC and TOC content and RUSLE K-factor. From the locations of the iron stakes the erosion rates and net erosion were derived.

Furthermore, for the fieldwork watershed observation period of EX-01 and EX02 RUSLE and USPED prediction soil erosion models were applied as well. The methods used are basically the ones proposed in equation 5.17 and 5.20 (Chapter 5). The R-factor was computed according to the RUSLE handbook instructions (Renard et al., 1997) using the sub-hourly pluviograph data (15-minute intervals) of the new Collalto Sabino climatic station (data available since 2005). The LS- and C-factor were estimated using the same techniques already applied for the Turano watershed, i.e., Eq. 5.11 and the method shown in Figure 5.5 respectively. The P-factor was considered constant (equal to 1). For the K-factor (Eq. 5.9), the spatial variations according to the maps of soil grain size distribution (Fig. 7.16, 7.17 and 7.18) were considered.

7.3. RESULTS

7.3.1. GEOMORPHOLOGICAL SURVEY

The Ex-01 and Ex-02 watersheds are located in a low mountain area sector almost completely composed of middle Miocene torbidite substratum. In the proximity of the investigated sites the landscape presents the conformation of a geologically young environment strongly shaped by weathering and fluvial erosion processes. Here, landforms resulting from extremely active hydric erosion are widely visible. The observation of the surface hydrography in this geological sector of the Turano watershed (Fig. 3.19) reveals a drainage network with high hierarchical organization, highlighting the dominant role of the fluvial erosion among the exogenous processes.

The erosion forms resulting from the concentrated surface overland flow are primarily represented by V-shaped valleys. Generally, these valleys show low to moderate structural asymmetry that seems to be mainly controlled by the strike and dip of the rock layers. Noteworthy, among the active forms of deposits in the valleys there are more or less extended colluvial deposits while fan-shaped and alluvial deposits can only be found in the main valleys. Here, because of the sediment deposition some valleys assume a flat-bottomed structure.

Some of the morphometric parameters, such as average slope gradient, slope aspect, watershed dimension, stream length etc., of the two selected watersheds have statistically been compared with the parameters of the other first-order watershed of the considered geological sector. As a result the watersheds selected can be considered sufficiently representative for the common geomorphological characteristics. The surface and average slope gradient of the EX-01 and EX-02 watersheds correspond to the average of the remaining first-order watersheds observed.

The geomorphological information acquired in the EX-01 and EX-02 watersheds during the first two field surveys confirmed the general observations made by remote-sensing and GIS operation. The current state of the watersheds is the result of denudation processes that shaped them in a very effective way. However, at present the signs attributable to slope denudation processes represent marked differences between the EX-01 and EX-02 watersheds. The EX-01 watershed is the only one which displays noticeable erosional damages. The observed erosion forms are essentially associated with the set of morphogenetic processes of the splash erosion and wash-out (i.e., sheet erosion and rills erosion) which occur at different spatial intensity all over the slopes. The effects of these processes are also detectable in the wooded EX-02 watershed. Hire, notwithstanding the abundant ground litter the signs of water erosion are still identifiable in the sectors poorly covered by ground litter. This also becomes apparent as the effects of water erosion have

a much lower intensity compared to the forms of erosion identified in the EX-01 watershed and can be considered negligible. Also note that in the EX-01 watershed the ground litter had already diffusely been washed away by August 2008 (a few months after the forest harvesting). Consistently, in January 2009 the almost total absence of ground litter was observed.

The noticeable signs of soil erosion on the slopes of the EX-01 watershed observed during the first survey shortly after forest harvesting turned into severe erosional damages as detected in the following surveys. This provides tangible evidence of the influence of the lacking forest vegetation. The almost total absence of low vegetation and grass in fact resulted in the exposure of bare soil after tree harvesting. Once the ground litter had been removed the combined effect of rainfall and overland flow could effectively work on the soil starting to severely erode it.

The emergence and evolution of soil erosional features in the EX-01 watershed have been quick and evident. Photos taken in different periods during the two years after the removal of the trees clearly show the effects of soil washing (Fig. 7.7).

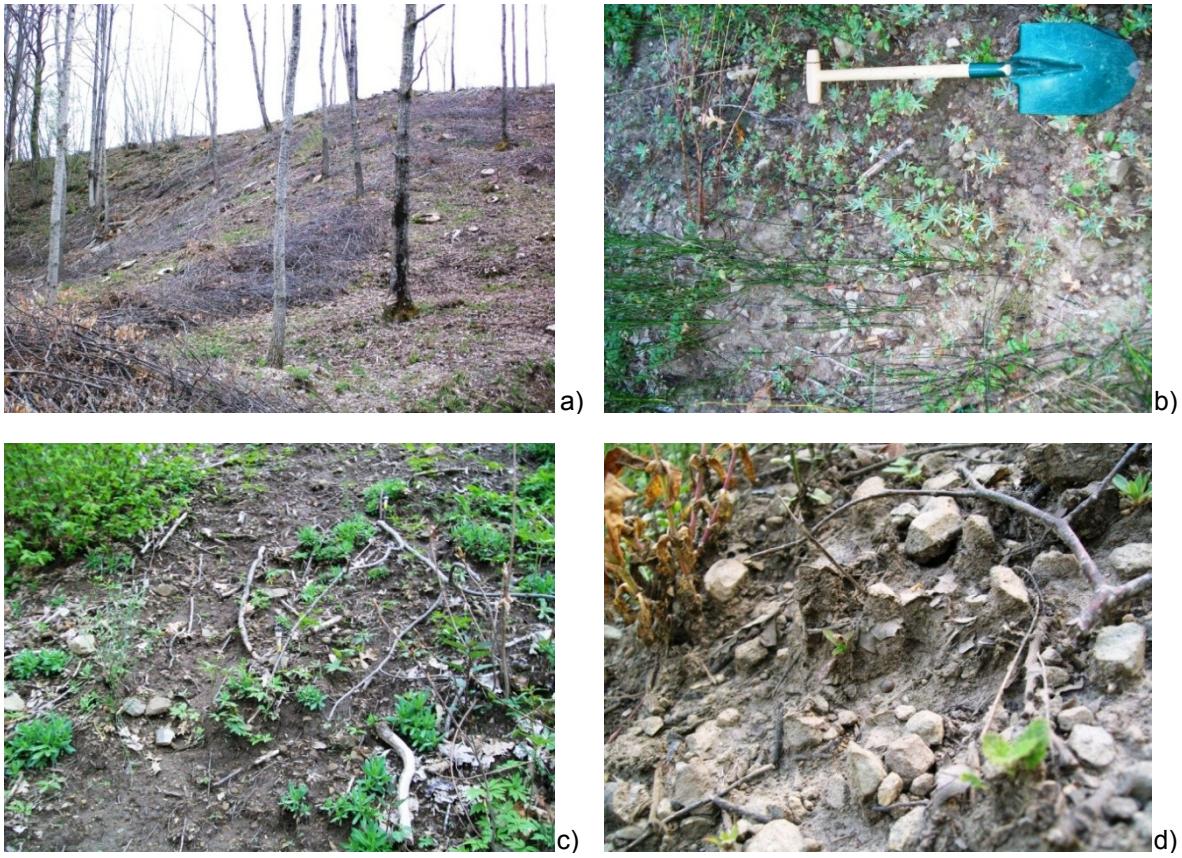

Fig. 7.7 – Erosion features. a) Area shortly after the trees-harvesting still presenting a good ground litter cover. b) Area under combined effect of inter-rill and rill erosion processes. c) Area washed by concentrated run-off. d) Minute morphological detail of an area where an erosion of the soil higher than 1 cm occurred.

Apart from the main drainageways, further forms of erosion due to concentrated overland flow are absent in the two drainage units. Both watersheds tend to bifurcate in the headwater areas but the concentrated surface run-off has not yet established as a dominant process. Here, the land surface evolves predominantly under the effects of inter-rill erosion and with a minor extent of rills erosion assuming a concave-concave complex curvature.

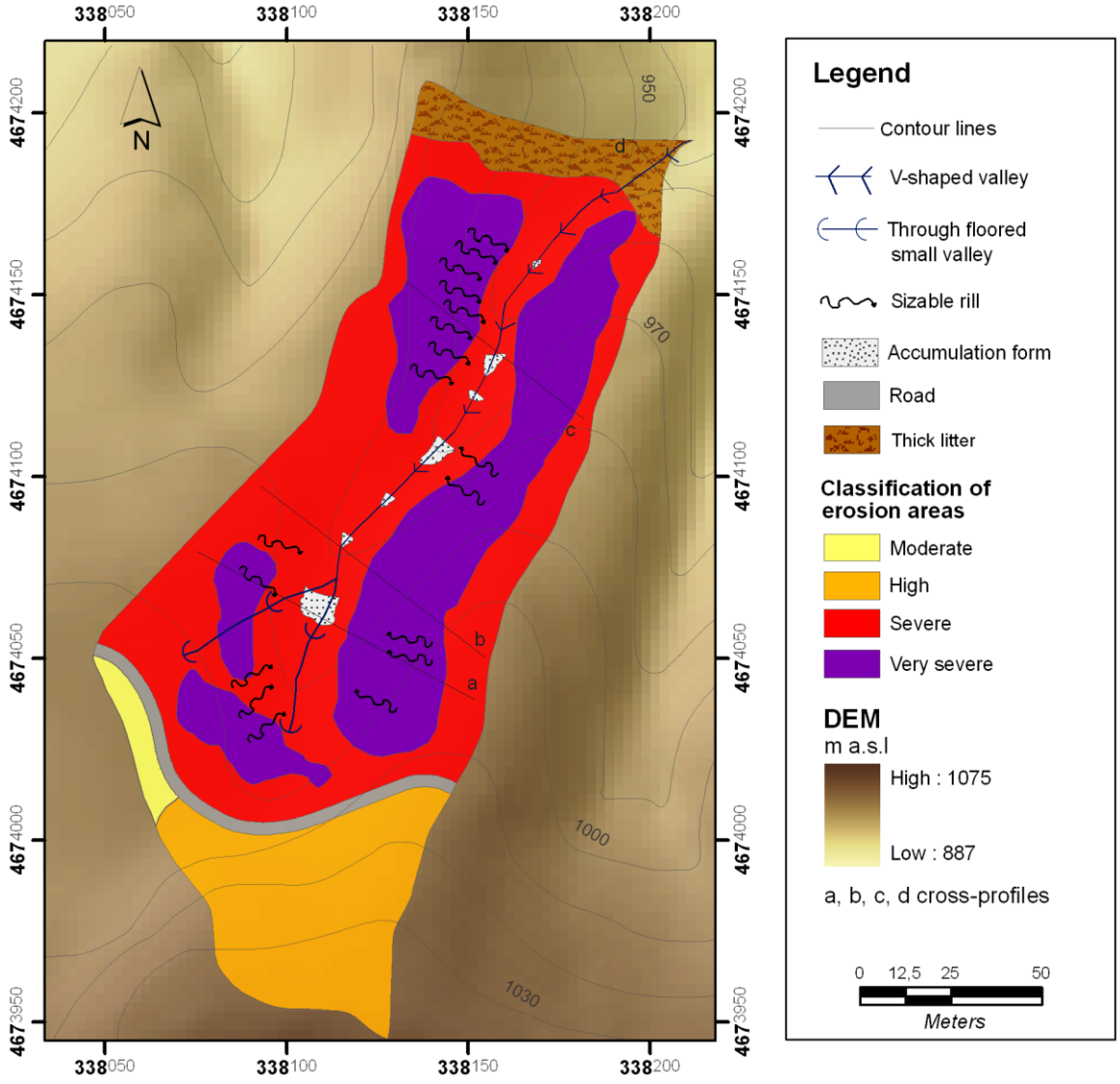

Fig. 7.8 – Geomorphological map EX-01 watershed.

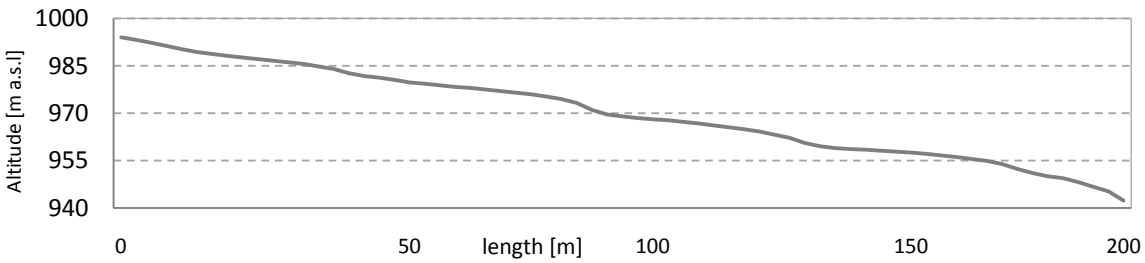

Fig. 7.9 – Longitudinal profile of the EX-01 watershed drainageway.

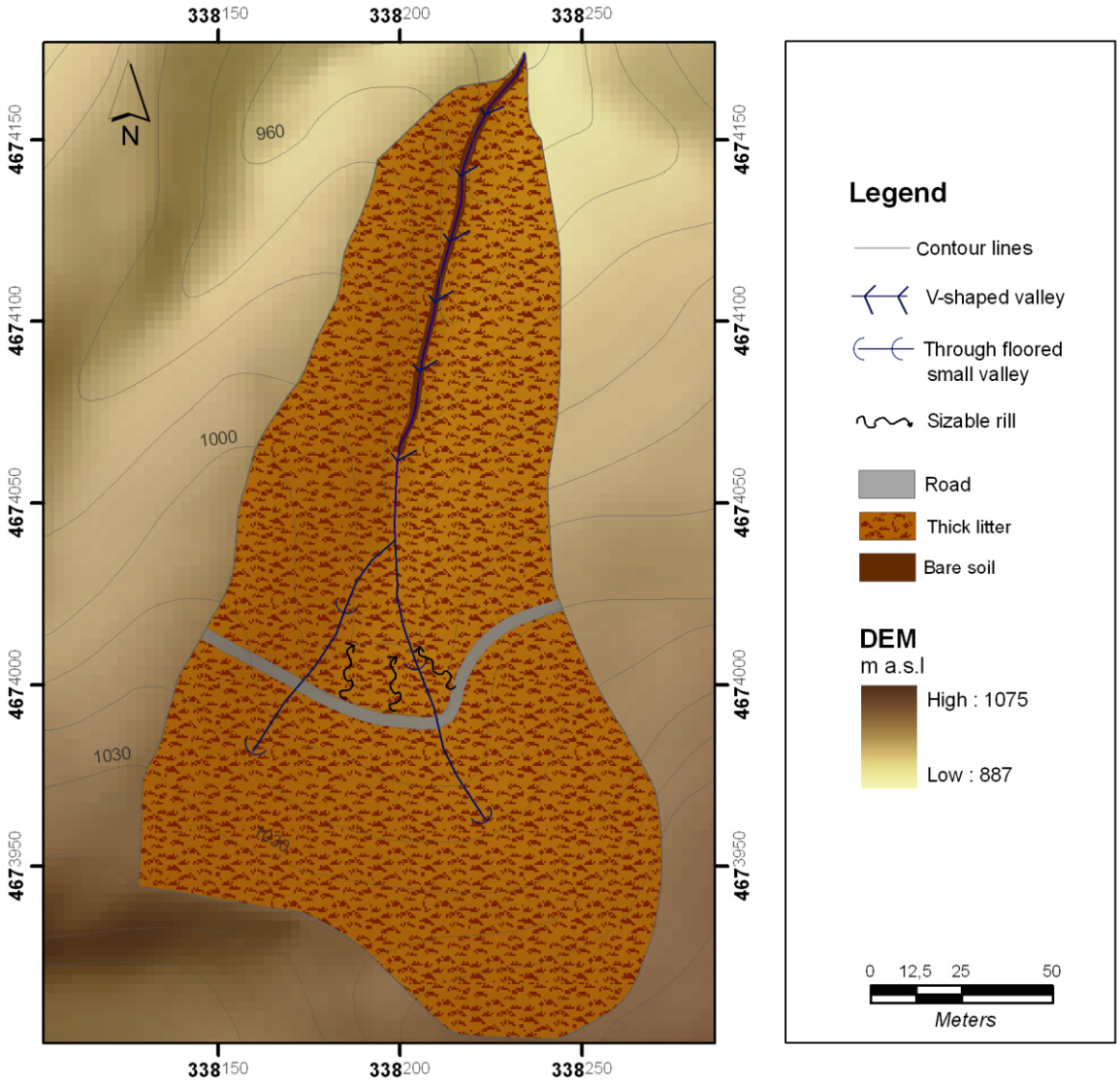

Fig. 7.10 – Geomorphological map EX-02 watershed.

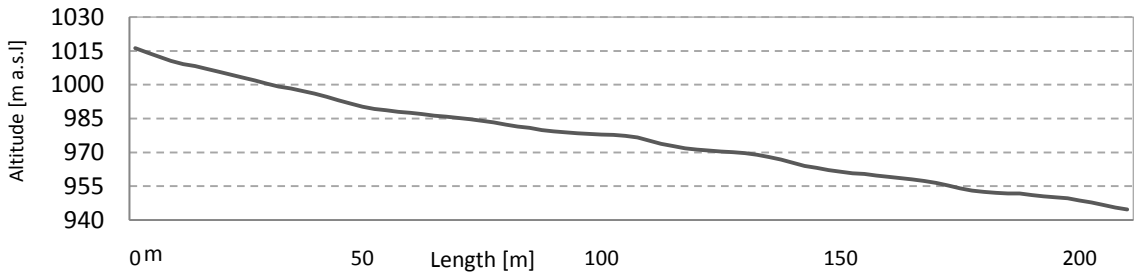

Fig. 7.11 – Longitudinal profile of the EX-01 watershed drainageway.

The harvested watershed still shows evidence of the previous clear-cut during 1994. Following the stream profiles of the two watersheds important differences in their stream channels can be observed. Although the stream profile of the watersheds display in both cases a rather straight trend in the EX-01, the presence of some atypical landforms was observed. These sub-plane forms, mostly looking like small terraces, are located along the

drainageway in the valley bottom (Fig. 7.8). These forms in such an environment are reminiscent of knickpoint landforms. However, following an in-depth examination the link between the formation of these landforms and sediment deposition became obvious. Similar structures cannot be observed in the undisturbed watershed EX-02. They are evidently the result of human interference in the area. It is likely that the leftover and process waste of the trees cut down in spring 1994 were left on the slopes. Consequently, during autumn the running flow of the heavy precipitation transported the discarded wood (mainly tree branches of various sizes) towards the valley bottom. Here, the accumulation of branches combined with the sediments and leaves gave rise to an effect similar to a 'beaver dam'. Over the years this material accumulation trapped parts of the sediments eroded and transported from the valley side slopes. Along the EX-01 watershed stream seven of these atypical accumulation forms with different sizes were mapped (Fig. 7.12).

During the period under observation the above-described accumulation forms in the watershed EX-01 were subject to increased linear erosion on the V-shaped drainageway that crosses them. At the same time, by placing metallic stakes a deposition of new sediments with thickness ranging from 10 to 35 cm on the rest of these accumulation forms was measured.

Three valley cross-profiles in the watershed, out of which one included a deposition form (Fig. 7.8 and Fig. 7.13), were measured using a Leica tachymeter for the headwater area (a), the middle watershed (b) and the area near the outlet (c). An additional valley cross-profile of the watershed outlet was acquired manually (d). While the upper part of the watershed is exposed to the northwest-facing slopes longer and with higher inclination compared to the southeast ones, the sector alongside its outlet is characterized by contrasting conditions. The slopes are fairly straight with a low propensity of concavity in the upper part of the watershed and convexity near its mouth area. According to the profiles, the valley is asymmetric V-shaped with the slope angle becoming more acute moving downstream. Near the watershed outlet the drainageway deeply incises the rock basement cultivating a form like a small gorge. Furthermore, observing the slopes under the ongoing denudation processes the tendency of the slopes to gain a 'regularized slope shape' with low sediment accumulation downslope (Castiglioni, 1986) evidently follows. With this morphodynamic evolution the slopes valley tend to assume a more stable conformation (Fig. 7.13). In the specific case of the EX-01-studied watershed the process is at a rather advanced stage. The sediment eroded upslope is only partially accumulated downslope because it is limited by active overland flow transport processes. In doing so, the gradient of the slopes decreases with time but the slopes simultaneously tend to exhibit a parallel retreat.

Finally, the last landform to be mentioned has an anthropogenic origin. It consists of an unpaved road crossing the watersheds in their headwater sector in N-W to S-E direction. A gutter on the side of the road collects the overland flow coming from the upper part of the watersheds and takes it down the road instead of letting it flow further downslope. Apart from this, no further relevant influences of the road on the morphological evolution of the investigated sites have been assumed.

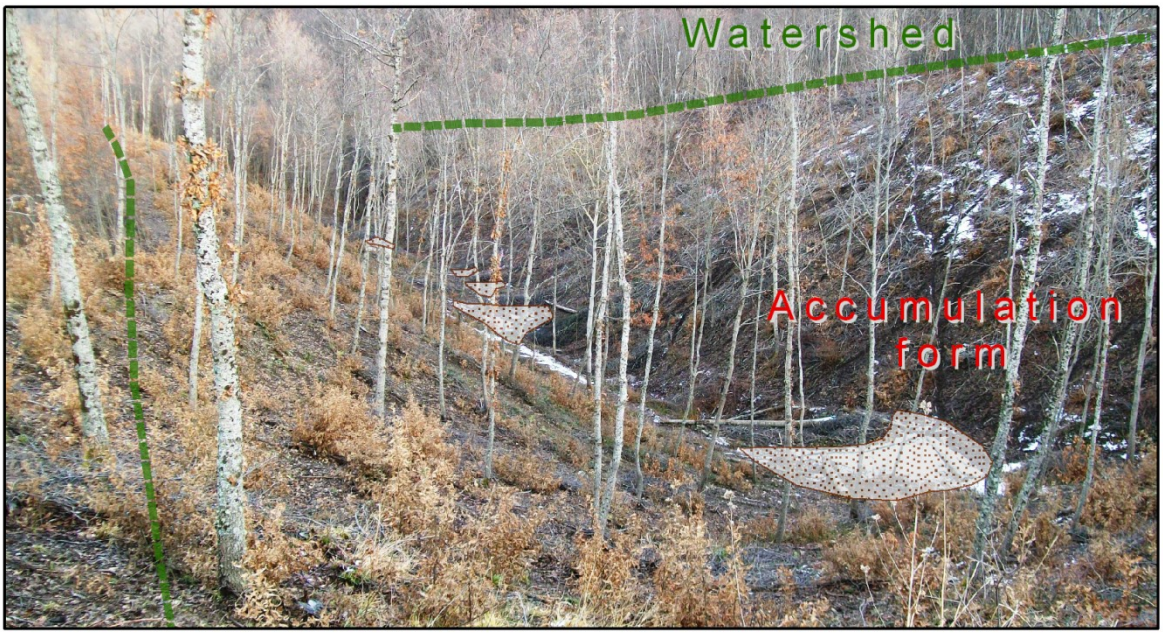

Fig. 7.12 – Photo of the EX-01 watershed (January 2009).

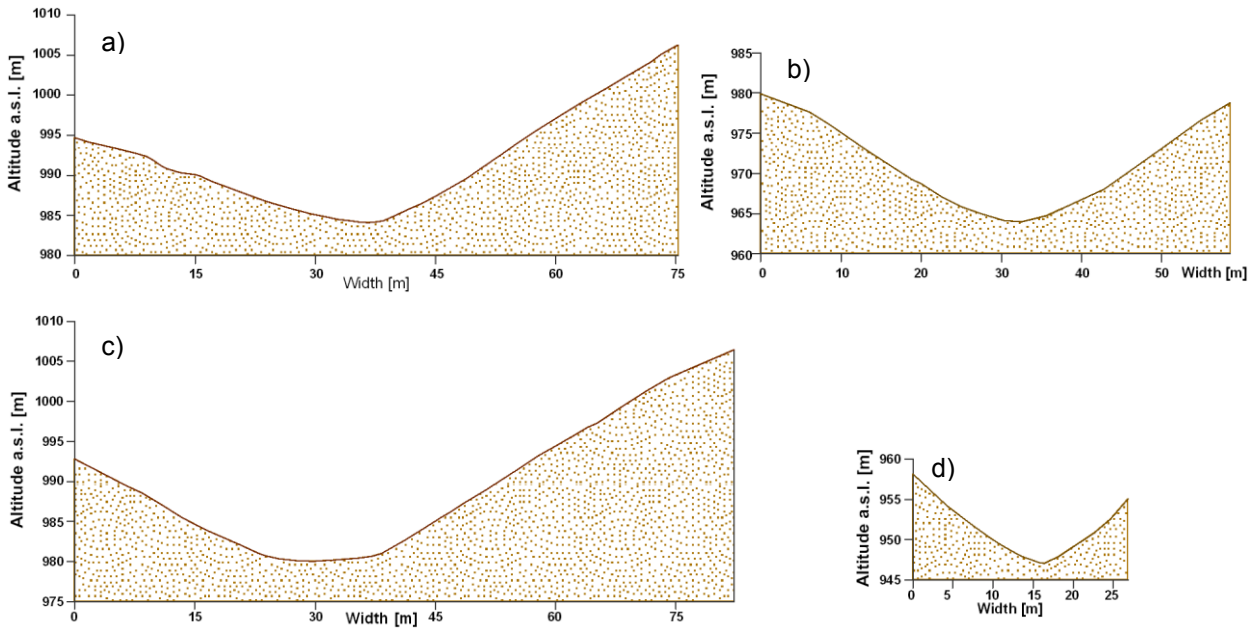

Fig. 7.13 – Valley EX-01 cross-profiles A-D.

7.3.2. PHYSICAL-CHEMICAL CHARACTERISTICS OF THE SOIL

The field observation revealed that the entire watershed's surface is pedogenized in nature. The soil thickness ranges from a few centimeters in the upslopes to about one meter near the valley bottom.

Valuable knowledge of the soil profile characteristics was gained in the field through carrying out a soil profile analysis of the hydrographic left slope of the EX-02 watershed near the valley bottom. The soil can be classified as a Typic Eutrudepts fine-loamy mixed mesic according to the Soil Taxonomy (1998) classification. The soil is moderately deep (72 cm) (Fig. 7.14). The horizons show an O-A-Bw-C-R sequence, with darker A horizons richer in organic matter with moderate rooting. Across the profile the color of the matrix ranges from dark brown to yellowish brown (7.5 YR 3/2 – 10YR 4/4). The grain size composition in the profile is characterized by fine material, a fact that is consistent with the fine particle size composition of the rock in the area (Bertolani et al., 1994). The moderate amount of skeleton (Ø>2mm) on the surface greatly increases with the profile depth resulting in very high amounts near the rock basement (horizon C). Stones sizes of up to 2–3 cm can widely be observed along the soil profile. No carbonate content was found in the upper part of the profile according to the Hcl test. In contrast, the deep horizons showed moderate reaction to the acid. This could be a consequence of residual $CaCO_3$ in the deeper part of the soil profile. Yet, it could also be due to a slight internal reorganization of the carbonates. Nevertheless, no signs of calcareous layers or nodular concretions were present. The parent material showed a high reaction to the Hcl contact. Observing the lithological fragments in the soil with a magnifying glass, traces of carbonates were found in the form of intergranular cement. Some brownish and red concretions (Fe Mn nodules) are present in the lower part of the profile, which could indicate the probable presence of temporary waterlogged.

Table 7.5 – Characteristics of the soil profile in EX-02.

Location characteristics	
Elevation [m a.s.l.]	970
Land use	Forestland
Slope gradient	About 25°
Landscape form	V-shaped valley
Landform	Footslope
Permeability	Mesic
Erosion/deposit	Deposition
Soil fraction [Ø] > 2 mm	25-30 %
Surface stoniness	Low

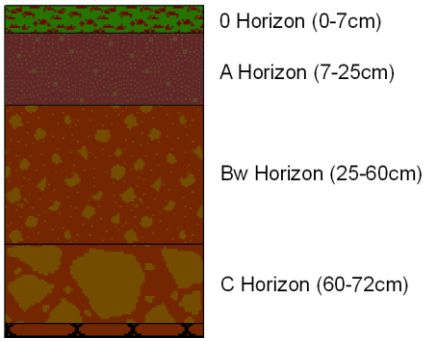

Fig. 7.14 – Soil horizons.

According to the purpose to measure the changes of the soil surface level in forest-harvested areas, additional information on the topsoil characteristics and their spatial distribution in the watershed EX-01 was acquired. 20 soil profiles (14 in EX-01, 6 in EX-02) at a 0-to-30cm soil depth and 35 samples (EX-01) at a 0-to-10 cm soil depth were collected in August 2008. During January 2009 seven additional soil samples (EX-01) at a 6 cm depth were collected for bulk density estimations. Information about the chemical-physic properties (i.e., grain size, organic and inorganic carbon, pH, electrical conductivity) and physic properties (bulk density) were obtained through laboratory work.

The 20 soil profiles at 0 to 30 cm represent longitudinal sections of the two watersheds, while the other 35 samples at 0–10 cm can be considered as surface hotspots. These surface hotspots were sampled following altitudinal levels worked out by GIS geometrical analysis. In the following the three watershed elevation levels will be termed low (from 955 to 985 m a.s.l.), medium (from 965 to 990 m a.s.l.) and high (from 970 to 1000 m a.s.l.).

The grain size analysis (LDS method) showed similar distribution patterns of the soil particles in the area (SD: clay: 1.6, silt: 4.8, sand: 6.1). The silt content is the dominant soil fraction (average 51%) while the clay content is low and ranges from 4.9% (A-6) to 10.4% (B-6). Figure 7.15 provides some grain size curves obtained from the laboratory data analysis. Table 7.6 presents the main statistics about the grain size data.

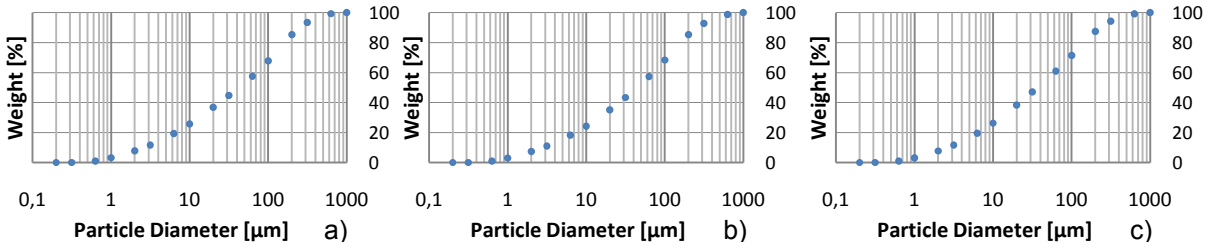

Fig. 7.15 – Grain size distribution curves derived by the average of the soil samples for three watershed elevation levels (a.low; b. medium; c.high).

Table 7.6 – Main statistics of the soil samples.

Main statistics	Grain size fractiones			O.M.
	Sand	Silt	Clay	
	2mm>Ø>0.063	0.063>Ø<0.002	Ø>0.002	
	[%]	[%]	[%]	[%]
Mean	41.3	51	7.7	4.7
Median	40.5	52	7.6	3.9
SD	37.2	23.1	2.5	2.7
Variance	6.1	4.8	1.6	7.5
Skewness	1	-0.9	-0.2	1.8
Coefficient of variation	0.15	0.09	0.2	0.58

The soil texture triangle (Fig. 7.16) shows 12 major textural classes and the particle size scale as defined by USDA (2010). More importantly, it presents the results obtained from

the soil samples' particle sizes. The prevalent textural class are silt loam (60.6%), sandy loam (30.3%) and loam (9.1%). With regard to the spatial variability no significant differences of soil grain size in the watershed were found. Clay, silt and sand as well as their sub-classifications did not show differences in their patterns between the low, medium and upper part of the slopes. In contrast, there is a significant difference in the distribution of soil fraction greater than 2 mm. For the slope positions of the samples a positive trend was observed. More precisely, the average percentage of skeleton in the soil increases from 21.5% in the valley bottom to 27% in the soil sampled in the medium level up to 46.4% in the top level of the slopes.

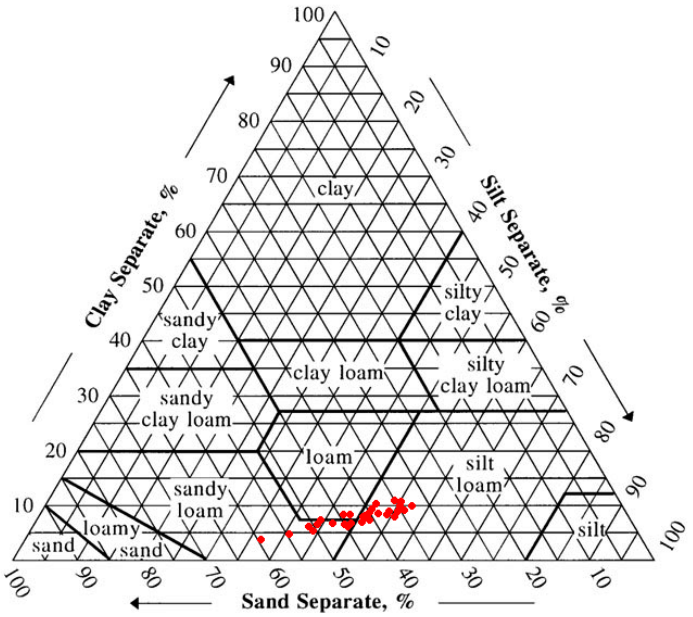

Fig. 7.16 – Soil texture classes of the EX-01 samples according to the USDA (2010) soil texture triangle.

The surface soil layer shows an average total carbon content (TC [mass %]) equal to 4.13 (low), 5.61 (medium) and 4.92 (high). According to 0–30cm depth soil profiles, the organic carbon content (TOC [mass %]) of the samples shows a vertical pattern with a high content at the top that decreases with depth. The TOC values in the watershed range from 0.74 to 14.84%, while the averages values are 4.1, 5.57, and 4.46, for low, medium and high watershed positions, respectively. No significant difference was found observing TOC spatial distribution along the slopes. With regard to the total inorganic carbon (TIC [mass %]) none of the samples with origins from medium to low valley slope positions showed any reaction to the Hcl. Contrarily, the 33% of the samples from the high slope positions had low to moderate reactions to the acid. Through LoI and Woesthoff Carmhograph analysis a higher content in inorganic carbon in the upper slopes was confirmed. Nonetheless, the sediments show a rather low content in inorganic carbon (Table 7.7).

Table 7.7 – Averages of organic and inorganic carbon for 35 samples at 0–10cm depth.

Elevation levels	TOC Woesthoff	TIC Woesthoff	Lol 550°	Lol 880°
	Average [%]	Average [%]	Average [%]	Average [%]
Low	4.1	0.03	4.9	0.27
Medium	5.57	0.04	7	0.26
High	4.46	0.46	5.6	0.61

The electric conductivity (EC; Table. 7.8) values of the soil samples range from 110.2 [µS/cm] to 336.6 [µS/cm] (mean=172.3, SD=65.4). The analysis did not reveal a regular pattern of susceptibility for the samples within the watershed. No relationship between the slope position and the EC values was observed. Moreover, the EC shows a positive relationship with the TOC (n=12; R^2=0.816; α<0.01) while it does not show any statistically significant relationship to the other physical and chemical components.

Table 7.8 – Averages of electric conductivity for 12 samples at 0–10 cm depth.

Elevation levels	Electric conductivity			
	[µS/cm]			
	Average	SD	Min	Max
Low	160.5	55.1	112.9	216.8
Medium	208.4	88	138.9	336.6
High	139.7	26.7	110.2	162.2

Likewise, with regard to pH-values (Table 7.9) no clear pattern could be determined. In almost all sampling points the EX-01 watershed has acid soils with pH-values from 4.12 to 5.49 (mean=5.2, SD=0.97). According to the USDA classification (1993), 17% of the samples are extremely acid, 43% are very strongly acid, 17% are strongly acid and 8% are moderately acid. Only two samples resulted in slightly alkaline values (pH=7.05). These are the samples that showed the highest reaction to Hcl which is also consistent with the high values of 2.1% (sample A-5) and 0.95% (sample A9) obtained from the TIC analysis. Thus, this sub-alkaline reaction can logically be related to the carbonate fraction in the soils showing their significant influence on the pH value. In fact, the TIC correlates well with the pH values (n=12; R^2=0.794; α<0.01).

Table 7.9 – Average pH values for 12 samples at 0– 10 cm depth.

Elevation levels	pH			
	Average	SD	Min	Max
Low	5.05	1.6	4.5	5.5
Medium	4.91	0.5	4.5	5.6
High	5.66	0.5	4.1	7.1

The bulk density analysis shows values ranging from 1.05 g cm^{-3} to 1.55 g cm^{-3} (Table 7.10). The differences indicate the variability in the physic characteristics of the soil due to factors such as organic matter, porosity, macro pores, soil compaction, surface crusts,

skeleton fraction etc. The resulting mean bulk density value of 1.23 g/cm^{-3} was considered representative for the watershed to estimate the mass volume.

Table 7.10 – Bulk density of 8 samples at 6 cm depth.

Lab-Id	Bulk density
	[g/cm^3]
Bd-EX01-01	1.15
Bd-EX01-02	1.2
Bd-EX01-03	1.55
Bd-EX01-04	1.24
Bd-EX01-05	1.35
Bd-EX01-06	1.1
Bd-EX01-07	1.05
Average	1.23

7.3.3. GIS PROCESSING OF THE ANALYTIC DATA

For the mapping of soil properties some geostatistical techniques in a GIS environment were applied. Through the inverse distance weighting interpolation method (ArcGis 9.3; set 5 neighbors) the soil properties data acquired from punctual observations were converted to continuous field data so that the spatial patterns sampled could include watershed points not sampled. In doing so, maps of the spatial distribution of soil skeleton, grain size, TOC, TIC and RUSLE K-factor were created. For the bulk density, the average value was assumed to be representative for the entire watershed. The related maps are shown from Figure 7.17 to Figure 7.22.

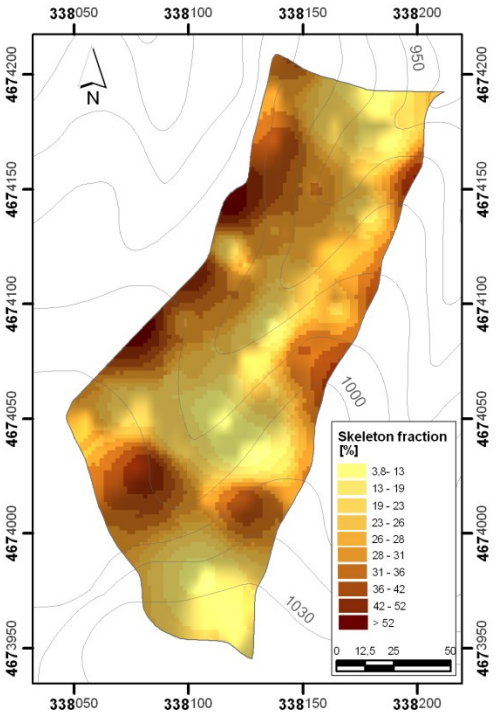

Fig. 7.17 – Spatial variation of skeleton fraction.

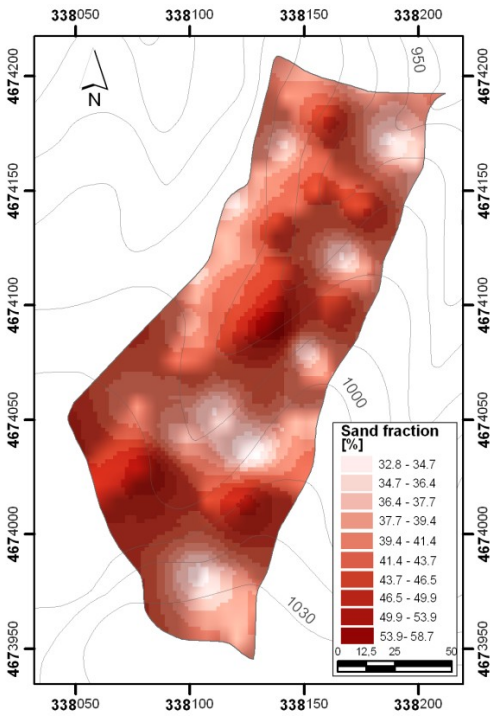

Fig. 7.18 – Spatial variation of sand fraction.

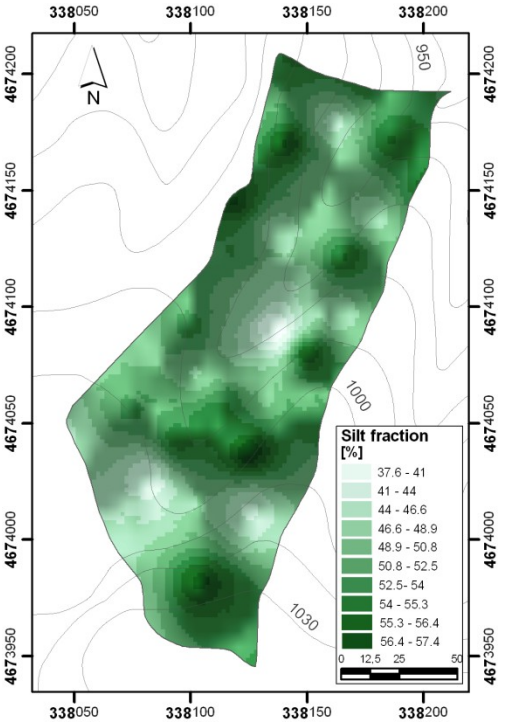

Fig. 7.19 – Spatial variation of silt fraction.

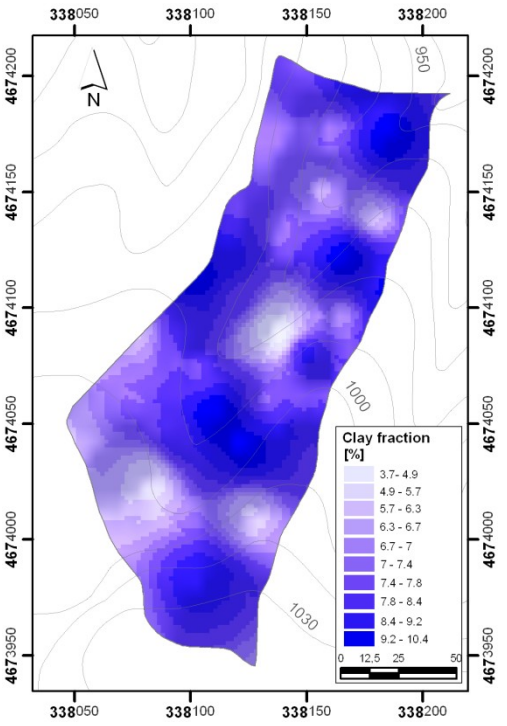

Fig. 7.20 – Spatial variation of clay fraction.

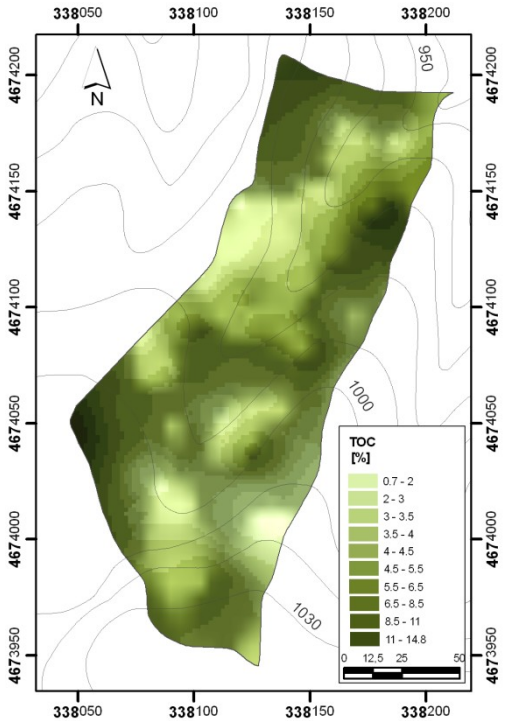

Fig. 7.21 – Spatial variation of TOC.

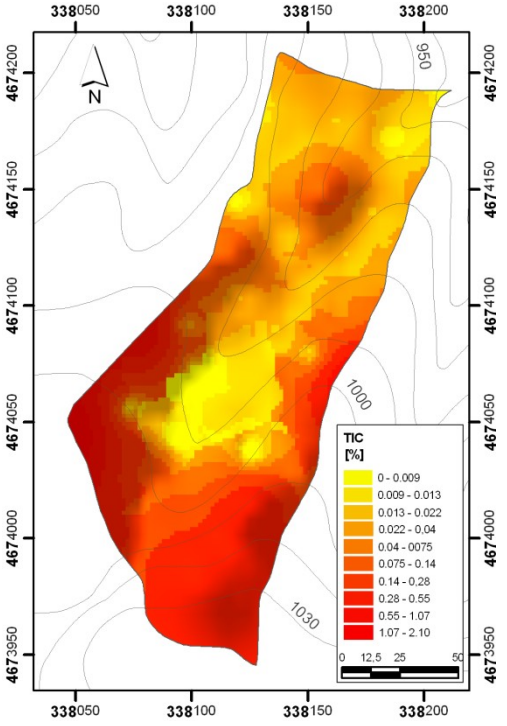

Fig. 7.22 – Spatial variation of TIC.

7.3.4. MEASUREMENTS IN PLOT OF WATER AND SEDIMENT YIELDS

The monitoring of the meteorological inputs and liquid/solid outputs in plots installed in the experimental watershed EX-01 was carried out in order to obtain information about the hydrological behavior of areas with similar geomorphological and soil characteristics but different land-use management. The rainfall/run-off observations were carried out from 9th July 2009 to 4th November 2009. Although this period does not perfectly fulfill the requirements of a valid rainfall/run-off analysis, the data acquired allowed for a good understanding of the hydrological response of undisturbed and disturbed forested in the investigated area.

During these four months about 308.3 mm of rainfall divided into 19 rainstorm events were measured, of which only 9 resulted in overland flow (Fig 7.23). This in turn means that about 284.6 mm corresponding to 92.3% produced overland flow. The minimum amount of rainfall with the ability to generate run-off was 3.2 mm (August 13th 2009).

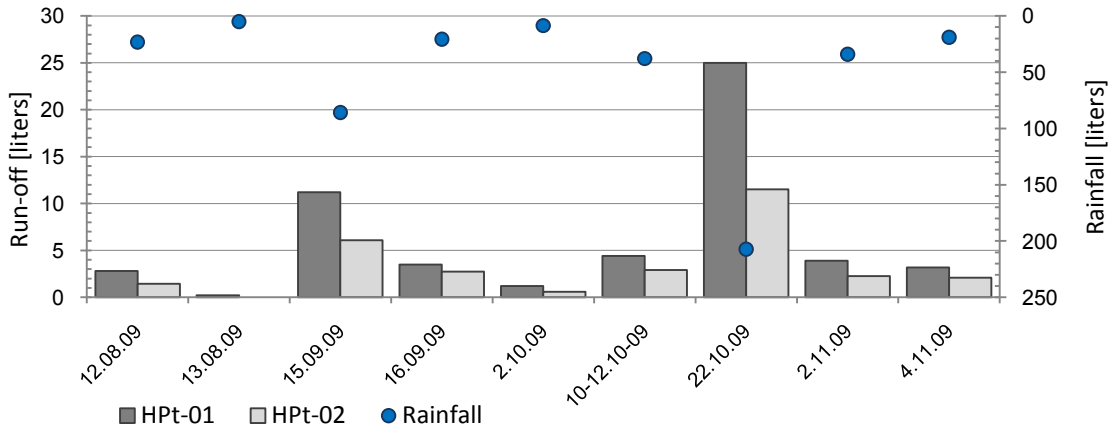

Fig. 7.23 – Plot rainfall-run-off measurements.

Table 7.11 shows the rainstorm events that produced overland flow in the two plots and provides information regarding the liquid input/output in the plots for each event. The sediment outputs for both plots are available for three rainfall events with greater magnitude (Table 7.12).

From the analysis of the data shown in Table 7.12 it follows that both plots had the same frequency of rainfall events resulting in overland flow. Nevertheless, the difference in both water and sediment yields of the two plots is also highly evident. The plot in the harvested area was much more sensitive to run-off generation as indicated by the run-off values ranging from 0.13 to 16.1 l m² during the study period (run-off coefficients from 4% to 16.8%). In contrast, in the area covered by forest vegetation the run-off yield amounts to about 53.4% of the run-off in the disturbed forest area with values for single events between 0 to 7.4 l m² (run-off coefficients from 0% to 13.2%).

The sediment yields of the three considered events also supported the significant difference of the plots. The cumulative sediment yield for the three events is 733.9 g m^{-2} for HPlot-01 and 31.1 g m^{-2} for HPlot-02. The amount of sediments washed in HPlot-01 is 24 times higher than in HPlot-02.

Table 7.11 – Liquid yield values for individual storm event in the two plots [* all the 19 storms].

Date	Rainfall		Run-off		Run-off coefficient	
	HPlot-01 and HPlot-02		HPlot-01	HPlot-02	HPlot-01	HPlot-02
	[mm]	[liters]	[liters]	[liters]	[%]	[%]
12.08.09	15	23.3	2.8	1.5	11.8	6.2
13.08.09	3.2	5	0.2	0	4	0
15.09.09	55.3	85.7	11.2	6.1	13.1	7.1
16.09.09	13.4	20.8	3.5	2.7	16.8	13.2
02.10.09	5.5	8.5	1.2	0.6	14.3	8.1
10-12.10-09	24.4	37.8	4.4	2.9	11.7	6.9
22-24.10.09	133.7	207.2	25	11.5	11.7	5.4
2.11.09	21.9	33.9	3.9	2.3	11.4	6.7
4.11.09	12.2	18.9	3.2	2.1	17	11
Total	308.3*	441.1	55.4	29.6	11.4	6.1

Table 7.12 – Plot sediment yield values of the three storm events observed.

Date	Rainfall	Sediment output	
		HPlot-01	HPlot-02
	[mm]	[g m^{-2}]	[g m^{-2}]
15.09.09	55.3	122.8	7.9
10-12.10.09	24.4	30.5	0.9
22-24.10.09	133.7	580.6	22.3
Total	213.4	733.9	31.1

Rainfall intensity of considered events could not be recorded due to research restrictions. The comparison between the data acquired insitu using a pluviometer with the data recorded by the pluviographs of the Hydrographic and Oceanographic Institute of Rome (2009) did not provide satisfactory results. Therefore, the sub-hourly data recorded by the Hydrographic and Oceanographic Institute of Rome (2009) stations were considered incompatibly to estimate the rainfall intensity in the study area. Both, liquid and solid outputs of the plots could only be correlated with total rainfall amount (Fig. 7.24 Fig. 7.25).

The water yields measured for each event in the plots highly positively correlated with the rainfall amount as shown in Fig. 7.24 ($\alpha<0.01$). Despite the low number of measured events, the sediment yield data show a positive linear trend (Fig. 7.25).

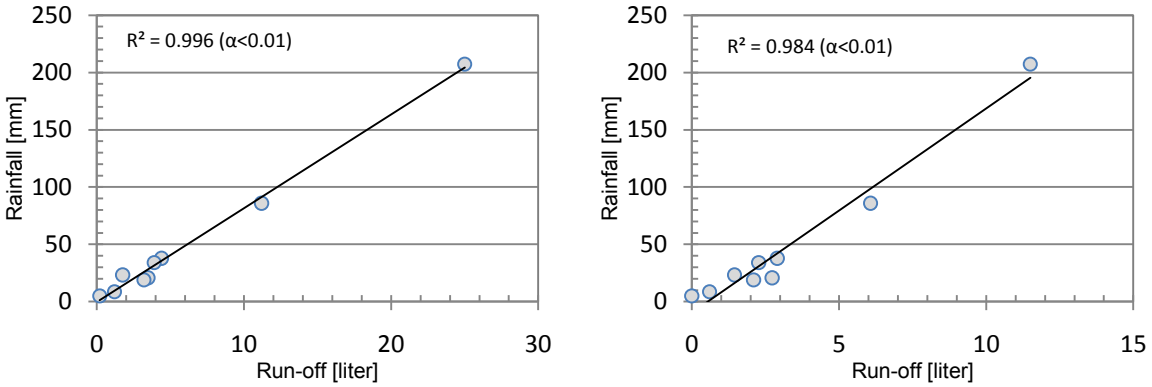

Fig. 7.24 – Relationship between rainfall and run-off: a) HPlot-01; b) HPlot-02.

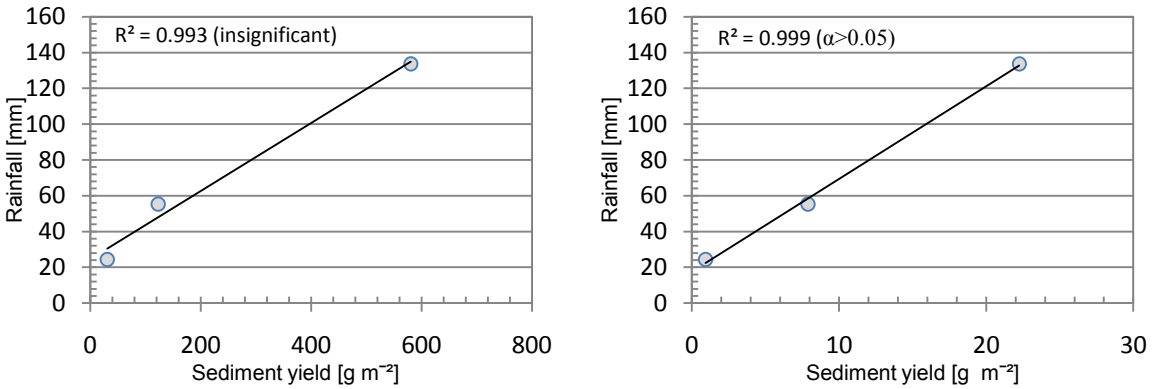

Fig. 7.25 – Relationship between rainfall and sediment yield: a) HPlot-01; b) HPlot-02.

In an additional analysis the hypothetical case that the EX-01 and EX-02 watersheds would hydrologically respond in the same way as HPlot-01 and HPlot-02 was assumed. Hypothetically, uniform erosion was assumed. In addition, the absence of any further entrained particle deposition by flow due to an increase of slope length was assumed for the two physiographic units (hypothetical assumption not possible in nature, Parson et al., 2006). As a result of this speculative scenario, during the three considered storms the EX-01 watershed (1.97 ha) would produce 516,013 l of overland flow that together with the rain splash effect would wash away 14.46 t of sediments. On the other hand, the investigated area of the EX-02 watershed (2.24 ha) would produce 296,258 l of overland flow and 0.70 t of sediments. Consequently, in this scenario the EX-01 watershed would produce approximately twice as much run-off per m^{-2} compared to EX-02. Remarkably, the magnitude of soil erosion in harvested watershed areas would be 21 times higher.

7.3.5. HYDRAULIC CONDUCTIVITY AND THE FACTORS INFLUENCING ITS VARIABILITY IN THE EX-01 WATERSHED

The results of the hydraulic conductivity (Kh) analysis in the area showed a marked variability of the parameter within the watershed. The measurements were carried out

using a mini disk infiltrometer (Zhang method, 1997) in July 2009 during a dry and warm period. These measurements revealed that the infiltration capacity (IC) varies under the influence of the soil moisture content in two ways: Firstly, the IC decreases with the downslope movement in the watersheds due to the influence of the corresponding increase of the moisture content (Beven and Kirkby, 1979). Secondly, the sunny slopes (southeast exposed) of the watershed have lower moisture content than the shady ones (northwest exposed) so that the IC tends to decrease on the slopes facing northwest. The measured Kh-values range from 0 to 3.89 cm h^{-1} (Fig. 7.27). The Kh average on the slopes (excluding the values equal to 0 measured on the sutured soil of the ephemeral stream) is equal to 1.69 cm h^{-1}.

Furthermore, on 25th July (at around 10 o'clock) during stable weather conditions some soil temperature measurements were performed. On the soil surface a temperature differences between the sunny and shady slopes of more than 22°C was recorded. Beyond this the temperature was also observed at different soil depths, resulting in a lower amplitude of the temperature differences equal to 5.1°C (20 cm depth) and 4.2°C (35 cm depth).

The ArcGis 'areal solar radiation' tool provided a calculation of the potential annual insolation of the hydrographical left and right slopes for the EX-01 watershed (Rich et al., 1994; Fu and Rich, 2002). The resulting raster format (Fig. 7.26) illustrates that the sunny slopes facing southeast have higher annual insolation values than the slopes facing northwest (Wh m^{-2}).

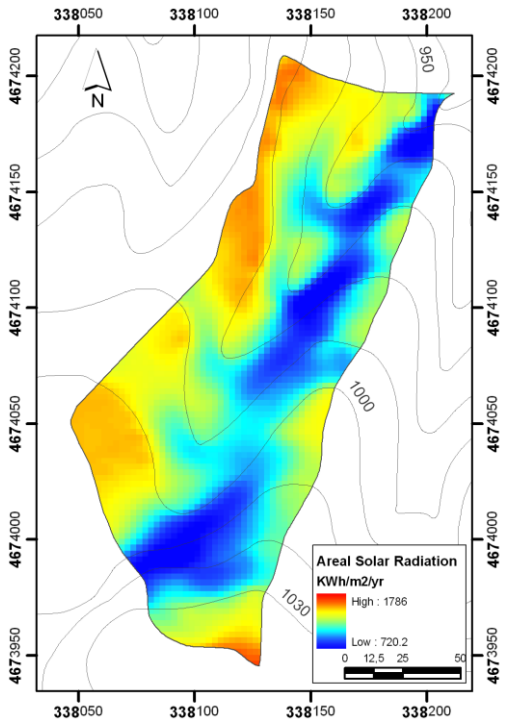

Fig. 7.26 – Areal solar radiation' for the years 2009.

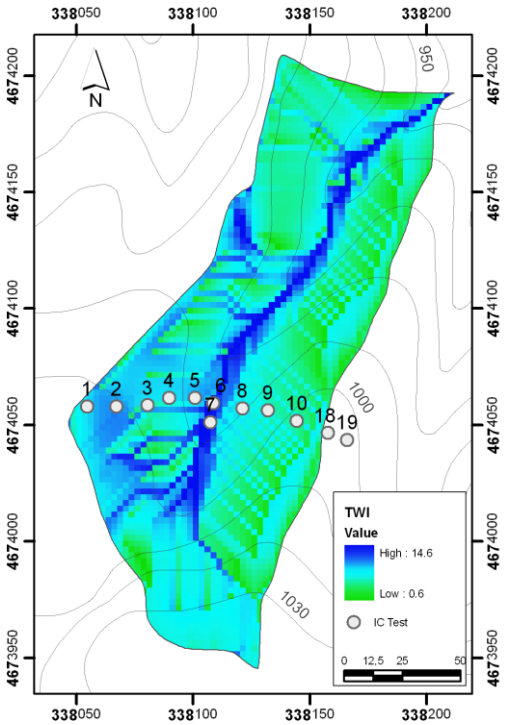

Fig. 7.27 – TWI index with the infiltration test sites.

Soil temperatures	
	[°C]
Depth	Sunny slope
0	44
5	31.2
10	26.8
15	25.8
20	24.9
20	24.7
30	24.2
35	23.8

Table 7.13 – Temperature measurements25th July 2009

Test-ID	Hydraulic cond.
	[cm h^{-1}]
IC-1	1.4
IC-2	1.73
IC-3	2.88
IC-4	1.30
IC-5	0.47
IC-6	0
IC-7	0
IC-8	0.36
IC-9	0.9
IC-10	0.86
IC-18*	3.89
IC-19*	2.99

Table 7.14 – Hydraulic conductivityEx-01 [*measuring made in the vegetated area]

7.3.6. SOIL EROSION RESPONSE

To carry out an on-site quantification of the erosional processes, metallic stakes were placed and periodically checked in the EX-01 (n=70) and EX-02 (n=15) watersheds. In doing so, eight control stations to provide information about the effective magnitude of surface level changes in the two examined watersheds were set up.

The first field mapping activities in August 2008 have already revealed a tendency of the EX-01 watershed to be more prone to soil erosion than EX-02. This propensity of the EX-01 watershed slopes to be subject to accelerated water erosion was confirmed by subsequent field mapping and also by measurement of soil surface changes. In 18.8%, 26.1% and 55.1% of the stakes placed in the EX-01 watershed variations (erosion or accumulation of sediment) equal or bigger than 0–5 mm, 5–10 mm and >10 mm respectively, were recorded. In contrast, in EX-02 none of the stakes measured values of soil surface change higher than 0.5 mm. Here, over the entire study period the changes measured equal a maximum erosion of -0.5 mm and a maximum deposition of 0.3 mm.

The measured amount of soil surface change due to the combined effects of rain-splash, inter-rill and rills erosion processes shows significant differences between the two areas with distinct forest land-use management. An analysis of the average punctual surface level changes (Aug. 2008 to Jan. 2010) reveals a lower net loss of -0.027mm (SD ± 0.24 mm) for the undisturbed slope areas compared to a loss of -0.57mm (SD ± 2.31 mm) in the harvested areas (Table 7.15). The cumulative surface level variation of the observation points in the EX-01 watershed is 98 times bigger than the one of EX-02 during the considered study period. A graphical explication of the observed soil surface changes for each stake is provided in Appendix I.

Table 7.15 – Statistics of soil surface changes for the undisturbed and harvested slopes of the experimental watersheds. The period from 8th September 2008 to 5th January 2010 is reported because more stakes were in place.

Checking day	Days	Rainfall	No. of storms > 10 mm	Rainfall erosivity	Average surface change	
					Ex-02	Ex-01
	[-]	[mm]	[-]	[MJ mm h^{-1} ha^{-1}]	[cm]	[cm]
4-Jan-09	116	717.4	19	1571	0.025	-0.52
6-may-09	238	430	14	157.5	0.02	-0.47
8-Sep-09	361	144.2	5	138.3	0.007	-0.42
8-Jan-10	480	687.8	21	962.7	-0.025	-0.57

Table 7.16 – Min. and max. surface level variation measured during the experimental period from 8th September 2008 to 5th January 2010.

Checking day	Ex-01				Ex-02			
	Net erosion		Net deposition		Net erosion		Net deposition	
	Max	Min	Max	Min	Max	Min	Max	Min
	[cm]	[cm]	[cm]	[cm]	[cm]	[cm]	[cm]	[cm]
4-Jan-09	-6	-0.2	8	0.1	-0.2	-0.1	0.5	0.1
6-may-09	-6.2	-0.1	7.3	0.2	-0.3	-0.1	0.4	0.1
8-Sep-09	-6	-0.2	7.1	0.2	-0.3	-0.1	0.4	0.1
8-Jan-10	-7.1	-0.2	7	0.1	-0.5	-0.2	0.3	0.1

With respect to the data acquired in six different control stations (for more details see Chapter 7.2.1.1) in the EX-01 and EX-02 watersheds the first control station (Plot-1, EX-01 watershed) consists of a plot with rectangular shape including 26 stakes. The stakes were placed with a 1.5x2 m distance separating them. The soil surface acquired by using the tachymeter during August 2008 was interpolated through the inverse distance weighting interpolation method (5 neighbors included) and 24 points (Fig. 7.28a). The slope has a mean inclination of about 25° and was covered by low ground litter and very sparse grass. The slope aspect is 318°. The soil is sandy loam with 0.02% TIC and 9.8% TOC. The surface skeleton was about 21.4% and the pH and EC values were equal to 4.7 pH and

168 µS/cm, respectively. The interpolation of the soil surface level changes observed on the 24 stakes of Plot-1 in January 2010 (Fig. 7.28b) resulted in a net soil loss for 73.9% of the plot area equivalent to 0.34 m³ of sediment (Fig. 7.28c). During this period 76% of the referenced points were subject to a surface change ranging from -0.3 cm to -4.3 cm.

The second and third control stations form two profiles and are located on the valley slopes facing southwards (slope aspect about 315°). In these straight slopes profiles (Profile P-1 and Profile P2) a total of 26 stakes were driven into the soil. According to the samples analyzed, here the soil has a prevalent silt loam texture with organic matter ranging from 2.9% to 5.6%. The inorganic carbon content is rather low decreasing down slope from 0.012% to 0.2%. The average slope gradient amounted to approximately 28° (min. 25°; max. 33°). Figure 7.29 presents the longitudinal profile of the slopes and the stakes' positions. According to the observation during January 2010, 66.7% of the profile P-1 control points and 90.9% of the P-2 control points were subject to erosion. This results in a P-1 profile average of soil surface change of about -0.31 cm (SD=3.17) and -1.24 cm (SD=1.31) for profile P-2 profile.

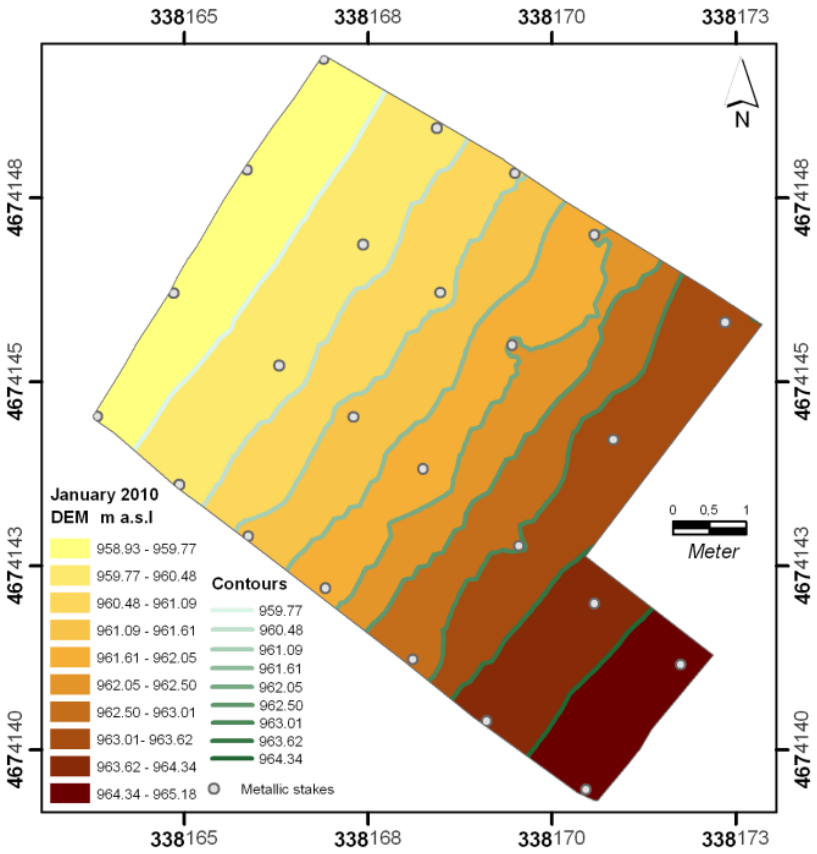

Fig. 7.28 – Soil surface in the Plot-01 during August 2008.

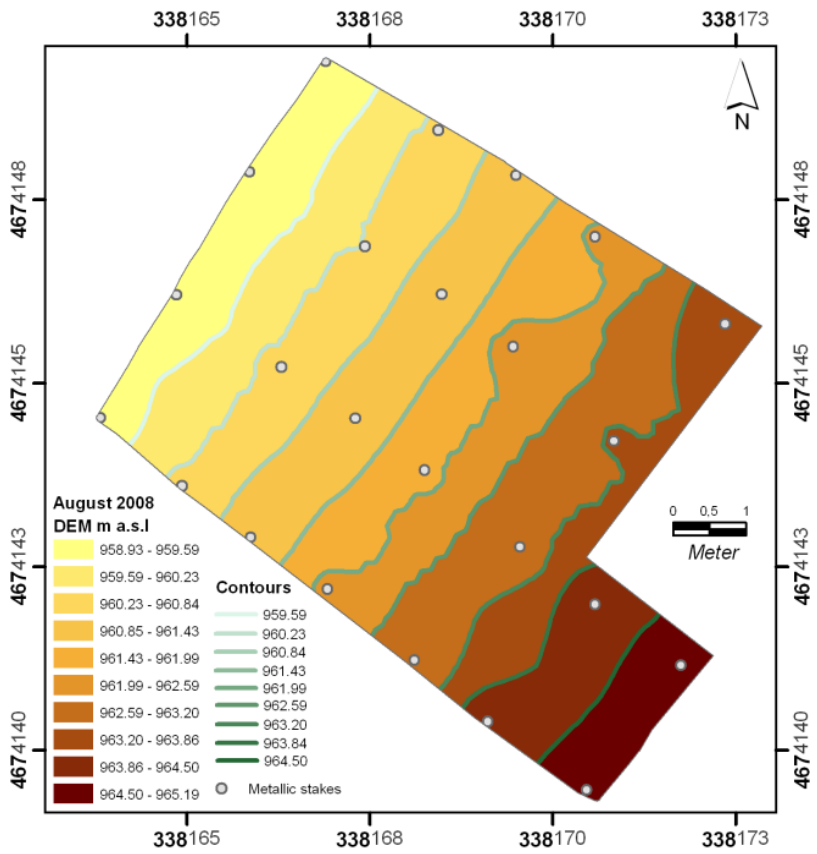

Fig. 7.29 – Soil surface in the Plot-01 during January 2010.

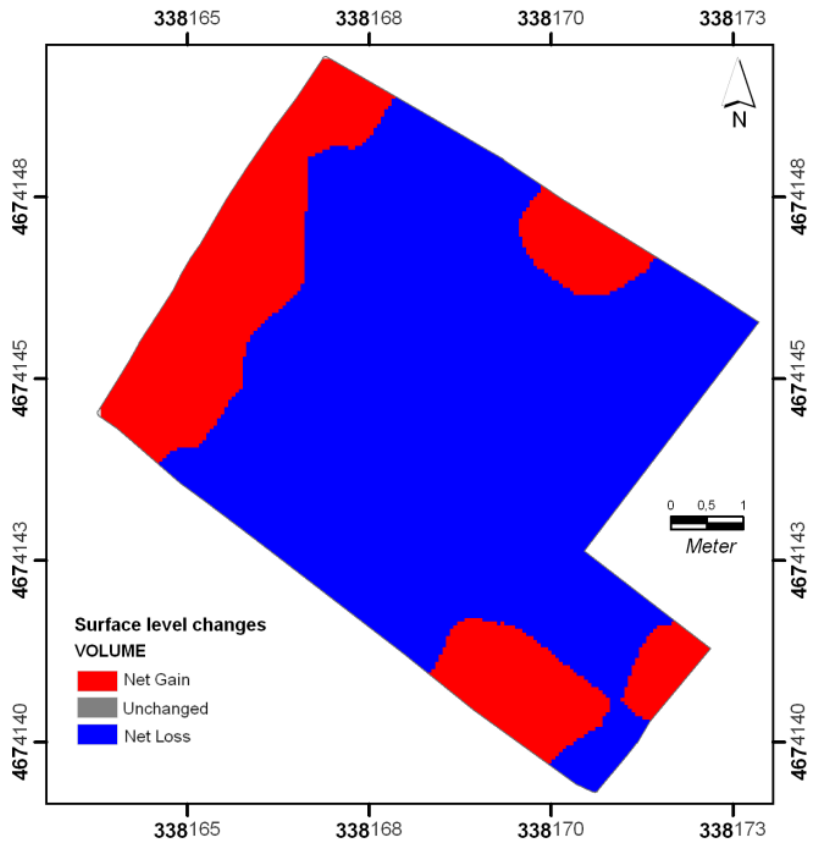

Fig. 7.30 – Soil surface difference in the Plot-01.

Fig. 7.31 – Some stakes of the Plot-01.

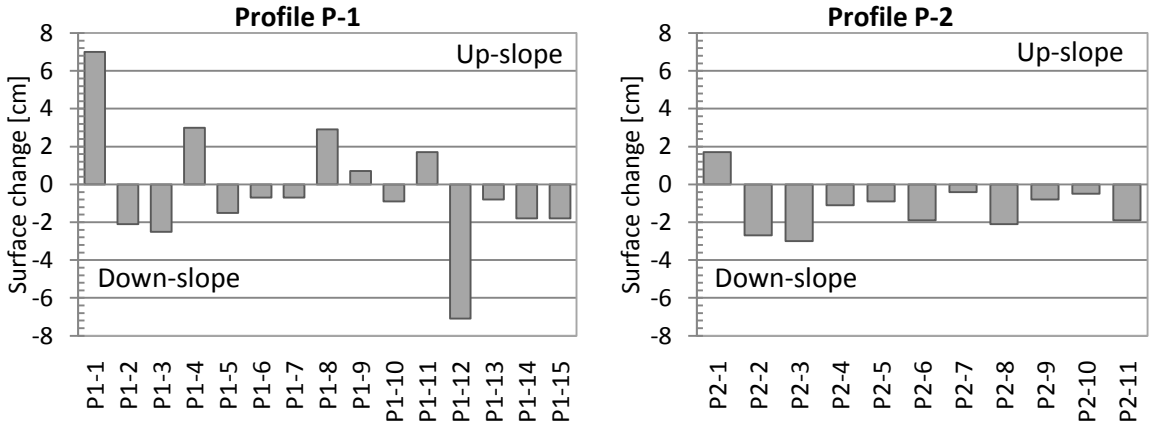

Fig. 7.32 – Surface changes in the station profile P-1 and profile P-2.

The V-shaped profile, composed of eight stakes in the proximity of the foot of the slopes, recorded a net deposition of 0.72 cm. The tendency of net gain of surface in the lower parts of the slopes is consistent with the stakes at the further stations. Almost all stakes positioned at the foot of the slopes provided evidence of sediment accumulation, ranging from 0.3 to 7 cm.

An additional control station in the EX-01 watershed refers to 10 stakes randomly located on the slopes exposed northwards. Here, about 70% of the measured points show erosion with an average of -0.63 cm (SD=1.31).

With regard to the EX-02 watershed the 15 stakes were placed forming a plot with rectangular shape. Due to the vegetation conditions a DEM based on tachymeter could not be created so that the slope gradient was measured manually (25-30°). The silt loam soil is richer in organic matter (10.3%) than the EX-01 control stations and covered by a

discontinuous thin ground litter (to drive stakes into the soil, points with low ground liter were selected). Here, 5 out of 15 observation points indicated erosion during the observation in January 2010. However, the observed soil surface changes are low, ranging from a minimum value of -0.2 cm to a maximum value of -0.5 cm. The biggest accumulation value recorded was 0.3 cm (from August 2008 to April 2010). Consequently, the mean derived from all stakes forming Plot-2 shows a net loss equal to -0.027 cm.

Next, the changes of surface level due to water erosion measured along the slopes of the two experimental first-order watersheds were converted into estimated net soil loss. To do this, it became necessary to consider the high content of organic matter in the soil of the study area in order to prepare for the soil bulk density calculation. For this purpose, the organic carbon values reported in the map of Figure 7.21 were used (values derived by the Woesthoff Carmhograph method). The resulting organic carbon percentages in the soil of the area where the stakes are located range from 2.9% to 9.8%. Accordingly, the mean bulk density of the organic fraction in the soil is equal to 0.08 g cm^{-3} while it amounts to 1.15 g cm^{-3} for the mineral soil components.

Finally, during the period from August 2008 to January 2010 rates of net soil loss of 49 t ha^{-1} yr^{-1} for the harvested and 2.3 t ha^{-1} yr^{-1} for the undisturbed forested areas were estimated (Table 7.17). However, these net loss values are averages including both, high net erosion values (upper-sector watershed) and high net deposition values (foot of the slopes). In fact, according to the stakes the ongoing hydric erosion processes unfold their effects on the slopes in different ways. 25 out of 70 (36.2%) stakes placed in the harvested watershed indicated a negative surface level change greater than 1 cm. It follows that a sizable part of the observed area is subject to a net soil loss ranging from 86 t ha^{-1} yr^{-1} (-1 cm) to 612 t ha^{-1} yr^{-1} (P1-12 location, -7.1 cm of soil surface change due to rill erosion) while other locations experienced ample sediment accumulation.

Table 7.17 – Bulk density of the soil mineral fraction.

Experimental watershed	Estimated mean mineral soil components	Estimated mean mineral
	[g cm^{-3}]	[t ha^{-1} yr^{-1}]
EX-01	1.15	49
EX-02	1.10	2.3

7.3.7. SOIL EROSION MODELING

Soil erosion models were applied for the EX-01 experimental site as a final operation. The RUSLE and USPED models were applied for the experimental watersheds using the same procedure as described in Chapter 6.1.2.1. During the considered period (September 2008 to January 2010) gross soil erosion rates for the EX-01 watershed equal to 46.2 t ha^{-1}

(RUSLE model, Fig. 7.30a) and 55.8 t ha^{-1} (USPED model, Fig. 7.30b) were predicted. Therefore, the erosion and sedimentation (USPED) rates for the analyzed period were converted into cm yr^{-1} using the total soil bulk density value of 1.23 g cm^{-3} (Fig. 7.31c and 8.31d). Finally, the erosion rates of the two models were compared with the results obtained from the metallic stakes (Table 7.18 and Fig. 7.30).

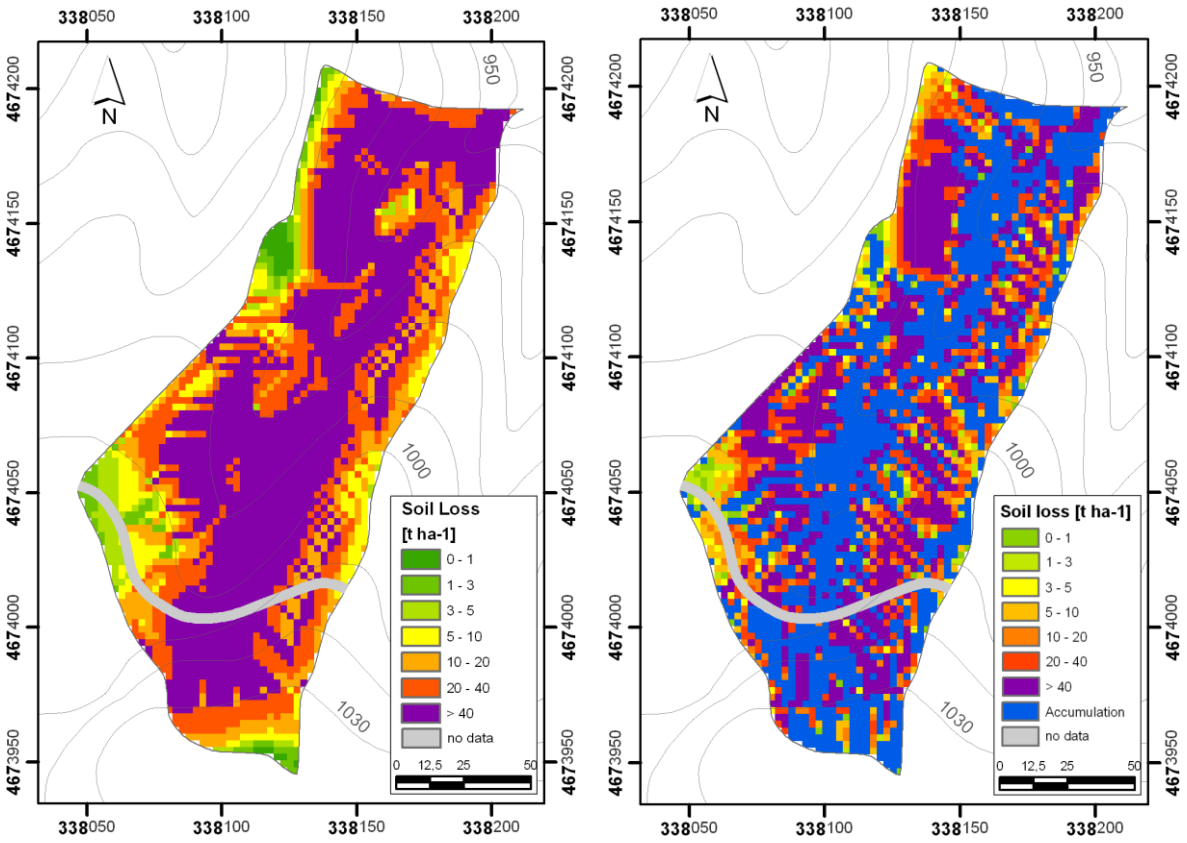

Fig. 7.33 – Modeled soil loss from 1st September 2008 to 8th January 2010: a) RUSLE soil erosion map; b) USPED soil erosion/deposition map.

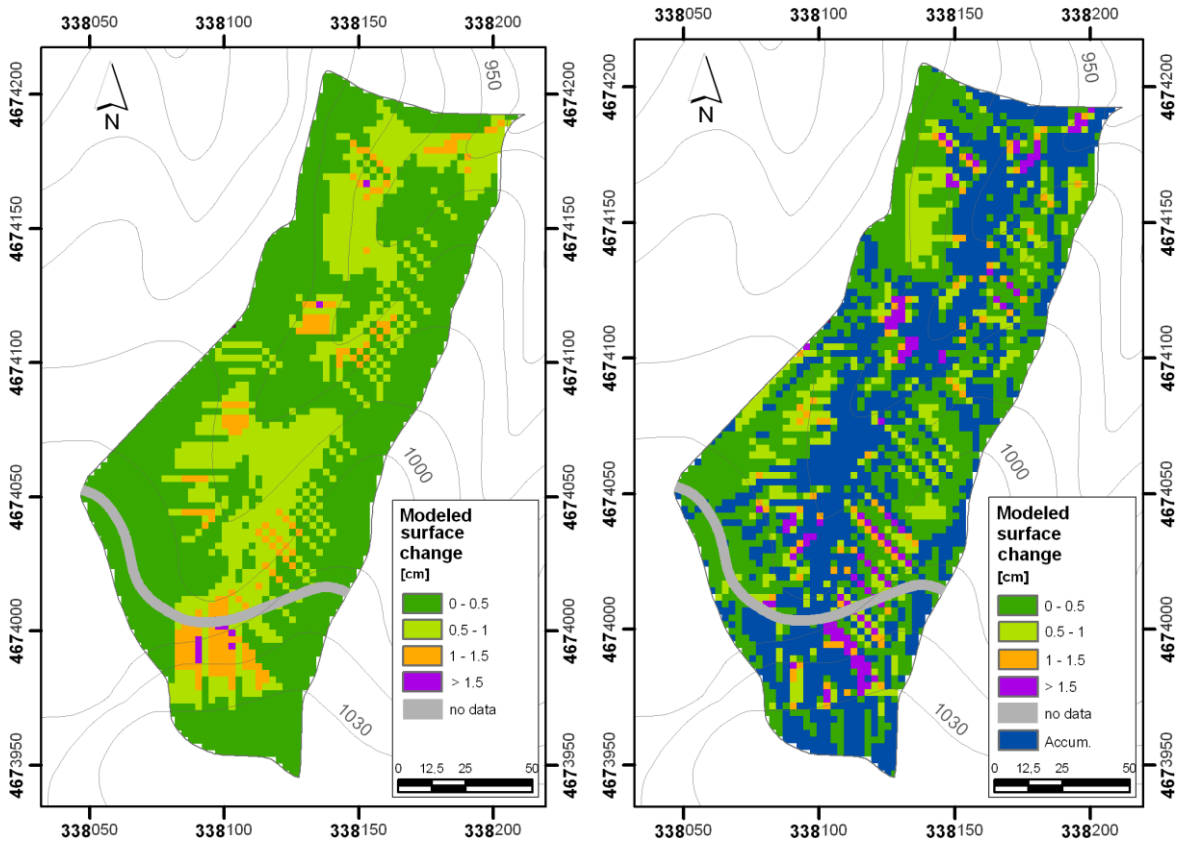

Fig. 7.34 – Modeled surface change in centimeters from 1st September 2008 to 8th January 2010: a) RUSLE soil erosion map; b) USPED soil erosion/deposition map.

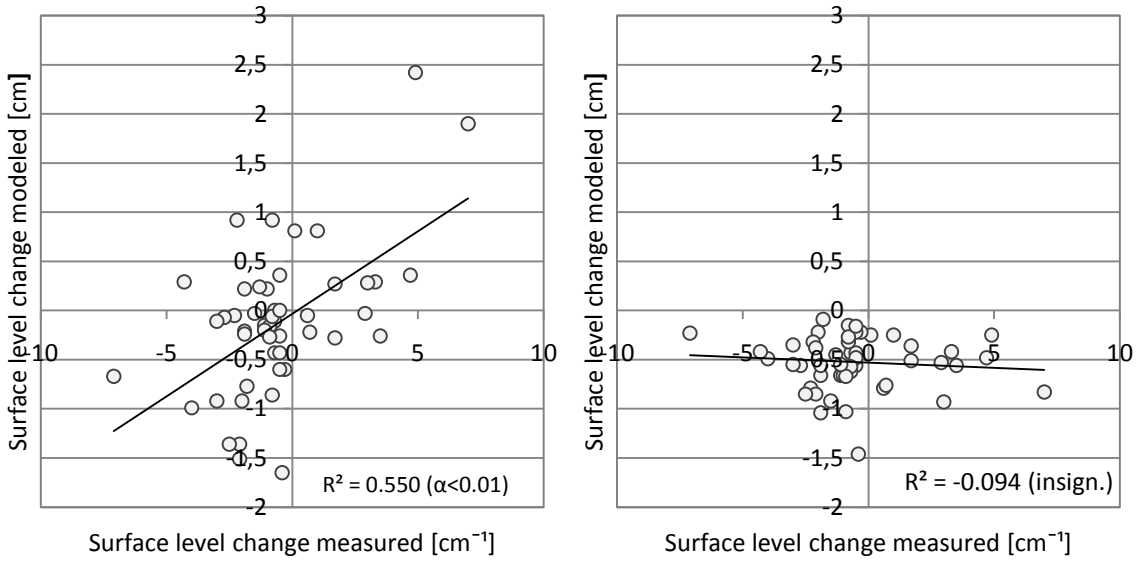

Fig. 7.35 – Relationship between soil loss measured by stakes and the soil loss modeled by the USPED (a) and RUSLE (b) models in the EX-01 watershed.

Table 7.18 – Comparison between soil loss measured by stakes and the soil loss modeled by the RUSLE and USPED models in the EX-01 watershed.

Plot 1	Stakes	USPED	RUSLE
	cm	cm	cm
Plot-01	1.00	0.81	-0.25
Plot-02	0.10	0.81	-0.25
Plot-03	4.90	2.42	-0.25
Plot-04	3.50	-0.26	-0.56
Plot-05	-0.50	-0.26	-0.56
Plot-06	-0.70	-0.43	-0.43
Plot-07	-0.50	-0.43	-0.43
Plot-08	-0.30	-0.60	-0.22
Plot-09	-0.50	-0.60	-0.22
Plot-10	-2.00	-0.92	-0.22
Plot-11	-2.20	0.92	-0.32
Plot-12	-0.80	0.92	-0.32
Plot-13	-1.10	-0.15	-0.66
Plot-14	-1.00	0.22	-0.66
Plot-15	-3.00	-0.92	-0.35
Plot-16	3.30	0.29	-0.42
Plot-17	-0.50	0.36	-0.48
Plot-18	-1.90	0.22	-0.66
Plot-19	-4.00	-0.99	-0.49
Plot-20	-4.30	0.29	-0.42
Plot-21	4.70	0.36	-0.48
Plot-22	-2.30	-0.05	-0.79
Plot-23	0.60	-0.05	-0.79
Plot-24	-1.30	0.24	-0.45

Profile 1	Stakes	USPED	RUSLE
	cm	cm	cm
P-01	7.00	1.90	-0.83
P-02	-2.10	-1.36	-0.85
P-03	-2.50	-1.36	-0.85
P-04	3.00	0.28	-0.93
P-05	-1.50	-0.03	-0.92
P-06	-0.70	-0.11	-0.62
P-07	-0.70	0.00	-0.57
P-08	2.90	-0.03	-0.53
P-09	0.70	-0.22	-0.76
P-10	-0.90	-0.16	-0.67
P-11	1.70	-0.28	-0.36
P-12	-7.10	-0.67	-0.23
P-13	-0.80	-0.86	-0.15
P-14	-1.80	-0.77	-0.09
P-15	-1.80	-0.77	-0.09
Profile 2	Pins	USPED	RUSLE
P2-1	1.7	0.27	-0.51
P2-2	-2.7	-0.07	-0.56
P2-3	-3	-0.11	-0.55
P2-4	-1.1	-0.2	-0.55
P2-5	-0.9	-0.27	-1.03
P2-6	-1.9	-0.21	-1.04
P2-7	-0.4	-1.65	-1.46
P2-8	-2.1	-1.51	-0.38
P2-9	-0.8	-0.06	-0.27
P2-10	-0.5	0	-0.16
P2-11	-1.9	-0.24	-0.56

7.4. DISCUSSIONS

To assess the nature of the post-harvesting hillslope erosion response the soil surface level change in a small first-order watershed was investigated by using metallic stakes. The resulting change in the soil surface level recorded by the stakes was compared with a further set of stakes driven into the soil of a neighboring wooded watershed. For this operation some control stations were set up with a total of 85 metallic stakes. In addition, the changes in the surface level values documented were further compared with the soil loss values predicted by the RUSLE and USPED models.

7.4.1. EROSION SUSCEPTIBILITY OF THE EXPERIMENTAL SITE

According to the DEM, the harvested EX-01 watershed generated by topographical maps at a 1:10,000 scale (CTR Lazio) show quite steep slopes. The DEM shows a slope average of 23.8° with hillslopes ranging from 0.2° to 47°. The comparison between the cross-profile measured by using the Leica tachymeter and the adopted DEM suggests that the DEM tends to underestimate the hillslope gradients. The length-slope factor (LS-factor RUSLE) shows a moderately high average value of 5.9 (SD= 4.6) with local high values (from 20 to 25) on the hillslopes. Several studies emphasized that the erosion of soil from a slope increases as the slope gradient and length increase (Bryan, 2000). While both inter-rill and rill erosion processes increase with increasing slope gradients (Lattanzi et al.,1974; Moss, 1988; Fox and Bryan, 1982; Kinnell, 1990; Bryan, 2000) the increase of slope length seems to affect mainly the rill erosion processes (Bradford and Huang, 1993; Haan et al., 1994). Analyzing the database of plot soil erosion measurements of European countries, Cerdan et al. (2010) found a positive relationship between erosion rates and slope length. As expected, this relationship becomes more evident in bare and arable lands (Cerdan et al., 2010). Under bare soil conditions, run-off rates are relatively high and the amount of total run-off increases and converges in the downslope direction. This means that both the detachment capacity and the transporting capacity grow in the downslope direction and the erosion rate increases with slope length (Govers, 1991). Furthermore, Torri and Poesen (1992) posited the essential role the slope gradient plays for soil erosion processes since it greatly influences the rainsplash processes. When a raindrop hits the soil surface, it creates a crater on the soil surface. This can be attributed to the energy exercised by the raindrops on the soil surface causing something similar to a small explosion (Dunne and Leopold, 1978). In doing so, both soil particles and water are displaced from the contact point through the so-called crown of lateral jets of water (Torri and Poesen, 1992). Torri and Poesen (1992) noted that in areas of steep slopes the particles of soil ‘ejected’ by the lateral jets of the water obviously cover greater distances

on their move in a downslope direction compared to the particles ejected in other directions. Thus, following the above-mentioned studies, the topographical conformation of the study site may encourage both inter-rill and rill denudational processes.

As evidenced by the field observations and use of the ArcGis 'Areal Solar Radiation' tool (Dubayah and Rich, 1995; Fu and Rich; 2002), the topography of the area also has an impact on solar radiation. The diverse insolation values found across the EX-01 watershed suggest different dynamics of the soil moisture regime on the south- and north-facing slopes. This fact, consistent with the infiltration capacity test, affects the hydraulic process of water infiltration into the soils. The variation of soil moisture linked to the slope aspect values also seems to influence the types and density of the herbaceous cover. Observing an area of the Turano watershed, Abbate et al. (1994) noted a pattern in the slope vegetation which is driven by the slope aspect exposure. In fact, during spring and summer after tree harvesting a faster coppice re-growth as well as a slight increase in the grass cover was observed on the shady and humid north-facing slopes of the EX-01 watershed compared to the sunny south-facing slopes. These factors represent aspect-controlled microclimatic conditions that can influence soil erosion processes on the different slopes. Moreover, the contrasting soil temperatures recorded in the south- and the north-facing slopes may also have an impact on the physical processes of soil erosion. According to Ariathurai and Arulanandan (1978), soil erosion rates increase with a rise in temperature because an increase of soil temperature reduces the cohesion of the clay particles (Rapetti et al., 2006).

The soil erosion dynamics in the EX-01 watershed may also be influenced by the general temperature dynamics in the area. According to field observations, the soils of the area (about 1000 m a.s.l.) may be temporarily frozen during the period with likely snow cover from December to January. Studies have recognized that the freeze-thaw usually increases soil erodibility (Bryan, 2000). Its impact varies with soil moisture, daily temperature range and soil texture.

Regarding the canopy cover, the absence of a vegetation cover due to logging practices highly influences the process of soil erosion in the observed watershed. The negative relationship between the canopy cover density and the soil erosion rates has been well recognized in research (Dissmeyer and Foster 1984). The forest vegetation, as demonstrated by numerous studies, is a very effective means of soil protection, especially when the tree vegetation is accompanied by an herbaceous cover (Teklehaimanot, 1991; El-Hassanin et al., 1993). Two main factors determine the important role played by the canopy cover in reducing soil erosion. On the one hand, the vegetation intercepting the rainfall (Cremaschi and Rodolfi, 1991) substantially limits the detachment of soil particles

caused by the mechanical impact of the raindrops on the soil surface. On the other hand, the vegetation indirectly improves the physical (e.g., porosity, compaction, surface selling) and chemical soil properties (organic matter). In the case of the EX-01 watershed the herbaceous cover is very low. The tree-harvesting operation, generally performed in spring and summer, exposes the soil directly to the heavy rainstorms in autumn. Thus, both the ground soil litter as well as the soil are quickly washed-out.

According to the plot experiments, the different conditions of the vegetation cover present in the wooded and harvested areas show a direct effect on the amount of outflow. HPlot-1 in an area of bare soil without any tree cover shows a run-off coefficient of 11.4 %. In contrast, HPlot-2 located in undisturbed forest conditions measured a run-off coefficient of 6.1%. In the proximity of the study area, apart from the discussed experiments, no other plot rainfall/run-off experiments were performed by other authors. However, at watershed scale (Ovito watershed), Bono and Capelli (1994) found a rather low run-off coefficient in the period from July to November compared to the winter trimester. Thus, although the rainfall/run-off plot experiments had to be interrupted during November, following Bono and Capelli (1994) higher run-off coefficients linked to an increased soil moisture regime can be confidently assumed. Other rainfall/run-off measurements at both plot and watershed scale for Italian locations (Burlando and Rosso, 2002; Bagarello and Ferro, 2004; Aucelli et al., 2006), with a similar annual precipitation pattern of the study area, indicate discharge amounts with a trend similar to the one observed at watershed scale by Bono and Capelli (1994).

Furthermore, the plot experiment clearly indicates the major influence of the vegetation cover on the generation of the overland flow in the study area. The result obtained by comprising the sediment yield of the two plots clearly shows the reducing effect of the canopy cover on the soil particle mobilization. The non-linear relationship between the plot liquid and solid yield emphasizes the effect of the rainsplash erosion on soil particle displacement.

With regard to the soil, it is a well-established concept that the soil texture plays a dominant role in the soil erodibility (Renard et al., 1997) and defines several of the other properties able to affect the soil erodibility (Knapen et al., 2007). According to the 35 top-soil samples analyzed for grain sizes, silt loam and to a lesser extent sandy loam texture classes dominate the EX-01 watershed. For all soil samples low values of clay fraction between 4 and 10% were measured. The low amount of clay fraction in the soil results in a low cohesion of the soils (Torri et al., 1997). Elustondo et al. (1990) found a close relationship between soil aggregation and organic matter associated with clay fraction. Resulting from the experiments for the K-factor (USLE, Wischmeier and Smith, 1978) silt

loam soils are amongst the most erodible soils under inter-rill and rill soil erosion processes (Knapen et al., 2007). Torri et al. (1997) also confirmed that coarse soil textures are subject to lower erodibility compared to the medium and fine soil textures. However, in addition to the soil characteristics that generally increase soil erosion further influence factions have been found in the examined watershed. For instance, an organic matter content greater than 5% for most of the experimental watershed area suggests a mitigation of the soil erosivity (Wischmeier and Smith, 1978; Lal and Elliot, 1994; Torri et al., 1997). The organic matter is found to be an important factor determining structural stability in topsoils. Soil organic matter, and especially humic substances (Knapen et al., 2007) act as a cementing agent between the mineral particles thereby increasing the aggregated stability (Govers, 1990). This, in turn, reduces the vulnerability of the soil to rainsplash and concentrated flow erosion. Furthermore, its effect on reducing the soil vulnerability depends on the clay and water content of the soil (Rapp, 1998, in Knapen et al., 2007). Finally, in the EX-01 watershed high rock fragments (Ø>2 mm) on the soil were observed. Poesen et al. (1994) suggested that the presence of a rock fragment cover at the soil surface may positively or negatively affect soil erosion by water depending on the temporal and spatial scale under consideration. However, in the EX-01 watershed after an intense phase of soil erosion, the exposure of rock fragments led to the formation of an 'erosion pavement' (Poesen et al., 1994) that was able to reduce the erosion rates, the raindrop impact effect as well as the concentrated flow.

7.4.2. HILLSLOPE MORPHOEVOLUTION

The analysis of the surface level changes obtained from the metallic stakes revealed a dominant soil mobilization in the harvested watershed. As indicated by the stakes, a net surface loss of -0.57 cm was recorded in the EX-01 watershed whereas the corresponding loss in EX-02 only added up to -0.027 cm. The more active soil particles movement regime recorded in the EX-01 watershed can fully be ascribed to the canopy cover effect which distinguishes it from the forested EX-02 watershed. It must be emphasized that no differences in the soil characteristics, the slope gradient and the slope aspect could be observed among the two watersheds at the beginning of the experiment.

The change in the individual soil surface level measured by the stakes statistically correlated with the topographical factors (i.e., LS-factor [R^2=0.097; n=60; insignificant], slope gradient [R^2=0.129; n=60; insignificant], slope length [R^2=0.195; n=60; insignificant], slope aspect [R^2=0.053; n=60; insignificant] and complex curvature[R^2=0.142; n=60; insignificant]) derived from the DEM show a very poor correlation. As observed above, the

DEM, although of good spatial resolution (5x5 m) has a quality that is still very far from sufficiently representing the micro-topographical situations of the stakes locations.

As expected, the sediment movement regime shows a strong link to the precipitation pattern. The distribution of the precipitation of the considered period is shown in Tables 8.15 and 8.16. During the quarters considered differences in the rainfall characteristics and soil surface level changes were observed. In the quarter from September to December 2008 the precipitation amount of 717.4 mm corresponds to a rainfall erosivity index (R-factor) of 1571 MJ mm h^{-1} ha^{-1}. In contrast, from January to April (2009) 430 mm rain only relate to 157.5 MJ mm h^{-1} ha^{-1}. Most stakes indicate the strongest surface level variation during the period from September to December 2008, while the surface variation of the soil was considerably lower from January to April 2009.

Furthermore, the low rainfall (144.2 mm) and the deriving low R-factor value (138.3 MJ mm h^{-1} ha^{-1}) found during the quarter from May to August 2009 coincided with the low variations of the soil surface level recorded by the stakes. During the final quarter analyzed (Sep–Dec 2010), the stakes once again show a net decrease of the soil surface although lower occurred from September–December 2008. Similar to the first quarter, during the last quarter under observation, both, rainfall (687.8 mm) and the R-factor (962.7 MJ mm h^{-1} ha^{-1}) were rather high. Still, the soil surface level variations in the investigated area clearly indicate a low relationship between soil erosion and the total monthly precipitations.

Thus, the situation described above allows a strong relationship between the soil erosion magnitude and the rain erosivity to be assumed. If the just-hypothesized increase in run-off due to the rise in soil moisture during January to May holds, this process seems to have a lower impact on soil erosion with respect to the rainfall erosivity. Accordingly, the capacity of higher overland flow to erode and transport soil particles during the January–May quarter is mitigated by the low rainfall erosivity. Evidently, the rainfall intensity plays a fundamental role in the denudation process. Heavy precipitation with frontal origin as typically occurring from September to December has a high rainfall kinetic energy, which results in high R-factor values. According to the stake measurements and further morphological indications analyzed for the study sites during this specific period, the heavy precipitations cause the detachment effect of the raindrop impact to highly influence the slope erosional processes. As observed by Torri et al. (1987), the raindrop impact on the soil in relation to a thin laminar flow on the soil can increase the soil denudation process. In contrast, when the laminar hits a certain thickness the effect of the raindrop is reduced and may even approach zero (about 3 times the raindrop diameter) (Mutcher and Young,1975). Consistently, short precipitations do not produce high overland flow values due to the

lower soil moisture in this period. Nevertheless, the thin laminar flow across the slopes combined with the high rainsplash erosivity seems to erode the soil very effectively.

The morphological and micro-morphometrical observations in the EX-01 watershed prompt the hypothesis of a greater impact of the rainsplash erosion than wash-out process. Across the entire watershed typical micromorphological forms suggesting rainsplash erosion, such as soil surface compaction, splash pedestal (Fig. 7.5) formation and the increase of the surface stoniness could be observed. Studying soil erosion processes in disturbed forested areas of south Italy, van Asch (1983) stated that the rainsplash effect has a dominant role in the uplands erosion in such environments. Moreover, this is amplified by the absence of a dense vegetation cover and the stormy nature of the precipitations. With regard to the peak in the soil surface level change, the highest erosion in the period directly following the forest-harvesting activities is in accordance with the findings of Callegari et al. (2001). However, a strong impact of soil compaction on the surface level change during this phase cannot be ruled out.

To conclude, the major influence of the canopy cover on both, run-off generation and soil erosion rates found by Sorriso-Valvo et al. (1995) in the disturbed mountain areas of Calabria could also be observed in the Central Apennine mountain areas by means of field observations and field measurements.

7.4.3. COMPARING MULTIPLE METHODS

The final operation for the EX-01 experimental watershed was the application of the RUSLE and USPED soil erosion prediction models. The average annual gross erosion rates predicted by the two models are 46.2 t ha^{-1} (RUSLE) and 55.8 t ha^{-1} (USPED). This values match to the average soil surface level change of 49 t ha^{-1} yr^{-1} recorded by the stakes. Thus, this allows to attest good performance in predicting gross soil erosion (with the C-factor setting described in the Chapter 5.1.1.2.4) in harvested areas to the RUSLE-based model. The almost bare soil, together with the rather homogeneous watershed topography permits a reliable prediction of soil erosion using these types of models. The USPED model also indicates possible areas where eroded particles may deposit. Most areas where USPED predicts sediment deposition are in accordance with the stake measurements. In contrast, in cases when at least two RUSLE factors are bigger than zero, the RUSLE-based models predict soil erosion. As a consequence, RUSLE predicted soil losses for all locations where the stakes indicated a sediment accumulation. In fact, Warren et al. (2005) noted this limitation by comparing the RUSLE and USPED outcomes with soil erosion and deposition measured via the Cesium-137 method. The

confirmed shortfall of the RUSLE model leads to the suggestion that the USPED model would be the preferred choice for soil erosion prediction in the given research context.

In the case of the EX-01 watershed, a good qualitative as well quantitative soil loss prediction of the models was observed. If compared to the map of soil erosion features (Fig. 7.6), model results satisfactorily indicate the spatial distribution and intensity of soil erosion. However, the application of the metallic stake technique prevented a quantification of the sediment amount that reached the watershed outlet in the observed period, i.e., the net erosion. The geomorphological information acquired (deposit forms on the stream, low footslopes deposition) can only roughly suggest high values of net erosion.

CHAPTER 8

Past and Present Dynamics of Human-induced Soil Erosion in a Sensitive Area of the Turano Watershed

8. PAST AND PRESENT DYNAMICS OF HUMAN-INDUCED SOIL EROSION IN A SENSITIVE AREA OF THE TURANO WATERSHED

The application of soil erosion prediction models and fieldwork measurements indicates that the sector with pelitic-arenaceous substratum is prone to high soil erosion when affected by anthropogenic disturbance. The aim of this part of the study is to find evidence to identify past soil erosion processes induced by human beings in a selected area of the Turano watershed that is presently prone to human-induced soil erosion. In order to gain information about both, long-term soil erosion and the paleoenvironmental conditions of the study site, three drilling cores (available at Freie Universität Berlin, Holzmann, 2010) excavated in alluvial sediments were examined.

8.1. STUDY SITE

The study area is shown in Figure 8.1 (UTM coordinates 4667980N and 347378E). It is a small watershed (2.3 km²) at the footslope of the carbonatic ridge where the village of Pietrasecca is located, in the central-eastern sector of the Turano watershed. According to the official topographic map scaled at 1:25.000 (IGMI, 1994), the watershed is called Fosso delle Rosce (called FDR in the following).

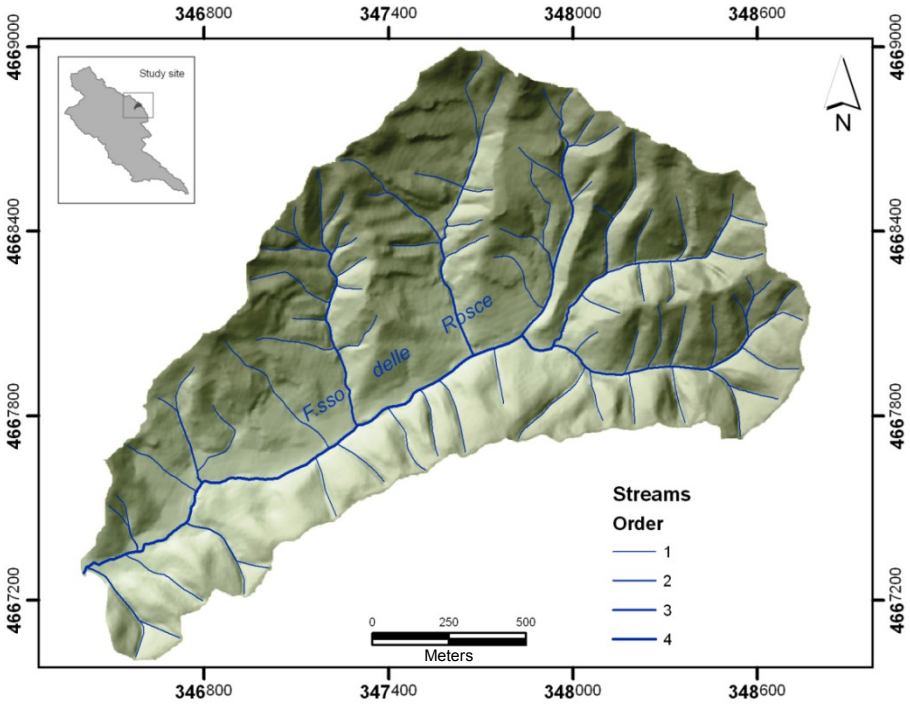

Fig. 8.1 – The study site.

This 2.5 km-long and 225 m deep watershed is incised into the middle Miocene flysch in pelitic-arenaceous facies (Carminati et al., 2007). The sandstone forms the entire bedrock of the watershed. About 0.1 km² of alluvial sediments cover the valley bottom, often

surrounded by colluvial deposits. The alluvial deposits have been indicated as Pleisto-Holocenic (Angelucci et al., 1959; Agostini, 1994). Cambisol not so well developed with a sandy loam and silt loam substrate dominate. These soils which show a yellow-brown color (7.5YR 3/2-10YR 4/4) have a depth ranging from a few centimeters (uplands) up more than 1.5 meters (Bucci, 1978). Generally, the soils within the watershed show a superficial layer rich in organic matter and an O-A-Bw-C-R sequence of the horizons (Cucchiarelli et al., 2006).

Climatically the study area is located in the temperate region (orotemperate thermotype, subhumid ombrotype) according to the bioclimatic map proposed in Fig. 4.12 (Chapter 4.2.4). The FDR watershed characterized by elevations ranging between 811 m and 1036 m a.s.l. shows an annual mean temperature around 11.3°C (Carsoli meteorological stations 1930-1983) and an annual precipitation of about 1200 mm (Carsoli meteorological stations 1921-1984). Both, air temperature and precipitation regime show a strong seasonality. In line with the climate data described in Chapter 5.2 the rainfall is heavier in winter, with the maximum in November. Erosivity of the rain (R-factor) is maximum in November.

The flat plains of the valley are only partially cultivated by small 'familiar' farming, while the rest are used for grazing cattle. Moreover, deciduous forest covers the largest part of the hills today. The forest coenosis is represented mainly by coppice trees (Abbate et al., 1994) dominated by *Quercus cerris* and *Carpinus betulus* while bush is generally *Cytisus scoparius*. The forest is subject to coppice-cutting cycles of 18-25 years resulting in high soil erosion rates as described in Chapter 3.4.1. During the period 1997-2010 about 1.17 km² were harvested, equaling 68% of the entire watershed surface.

Table 8.1 – Climate characteristics of the study site (data from Fredi and Pugliese, 1994).

Climate characteristics	Carsoli [1921-1984]
Mean annual rainfall [mm]	1172
Absolute minimum monthly rainfall [mm]	41
Absolute maximum monthly rainfall [mm]	148
Mean annual temperature [°C]	11.3
Minimum monthly temperature [°C]	9.3 (January)
Maximum monthly temperature [°C]	28.3 (August)

8.2. METHODOLOGY

8.2.1. GEOMORPHOLOGICAL AND MORPHOMETRICAL ANALYSES

Fieldwork survey and aerial photograph interpretation were performed for both the landform identification and geomorphological features mapping. The fieldwork activities were developed during April 2010 and September 2010, following the interpretation of the aerial photographs (Regione Abruzzo Volo 2007, 1:5000 scaled) carried out using a mirror stereoscope.

The topographic parameters were delineated from a DEM based on a contour line of a 1:5000-scale topographic map (CTR Abruzzo). The DEM was delineated using the Topogrid sub-module of ArcInfo 9.3 (Hutchinson, 1989) where contour lines, elevation points and the stream network (endowed of z-values) formed the base of the interpolation. Output was a DEM with a spatial resolution of 2 x 2 meters.

8.2.2. SEDIMENT EXTRACTION AND ANALYSIS

The information about depositional dynamics in the floodplain of the FDR were carried out from three cores collected during the drilling campaigns performed in Summer 2009 and April 2010.

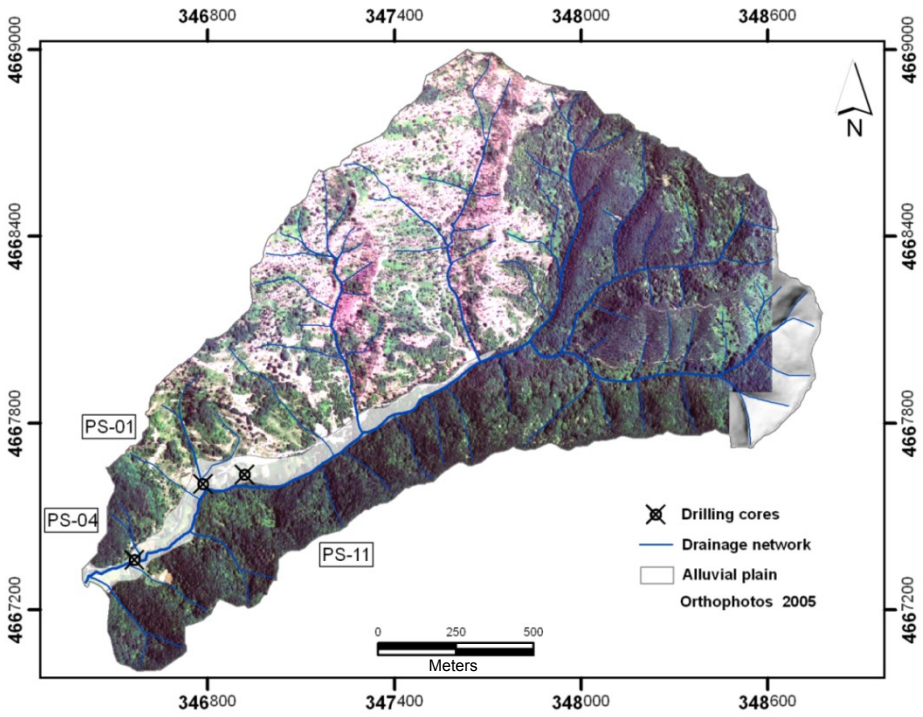

Fig. 8.2 – Drilling core locations in the FDR watershed. Ortophoto: Lazio Region 2005.

All the cores were excavated with a Wacker percussion driller and in each perforation the rock basement was reached. The total length of alluvial profile obtained is about 23 m. The sedimentological description and sampling (sampling interval ten centimeters with a

resolution of two centimeters) of the cores were carried out in the laboratories of the Department of Earth Sciences of the FU Berlin.

The loss on ignition (LOI) method (Dean, 1974) based on differential thermal analysis was used to determinate the TOC and TIC content in the samples. This methodology was preferred to the Woesthoff Carmhograph method because its results correlate well with the Woesthoff Carmhograph ones (TC, n=34 R^2=0.974; α<0.01) and the laboratory procedure is less time consuming. The TOC and TIC in the 230 samples was depleted in an oven at 550° and 880°, respectively. After each burning the samples were weighed using a Sartorius (resolution 0.0001 g) scales. The TC content is given by the sum of the TOC and TIC fractions. For the samples of the core PS-11, the magnetic susceptibility was measured by taking the mean of three measurements, each of ten centimeters, of the cores by using a magnetic susceptibility meter (MS2). Furthermore, during the cores sedimentological description some samples (n=8) for dating analysis were collected. The sediment deposition chronology was obtained from radiocarbon (14C) analysis performed in the Poznan Radiocarbon Laboratory. Finally, radiocarbon dates were calibrated using the program OxCal 4.1 from Bronk Ramsey (2010) using the calibration curve IntCal2009; r:5 atmospheric data came from Reimer et al. (2009) (Appendix J).

8.3. RESULTS

8.3.1. LANDFORM AND PRESENT-DAY MORPHODYNAMICS IN THE FDS WATERSHED

The investigated physiographic unit is mainly constituted of a flat-bottomed valley with an asymmetric profile. Slope gradients widely exceed 25°. The north-facing slopes show a greater slope gradient (on average 27.7°) than the southern ones (on average 20.1°). Both slopes are furthermore incised by V-shaped valleys. These valleys on the southern-facing slopes are characterized by a higher-order and a more gentle inclination. The total drained area is 2.5 km in length with a main stream that drains 1.8 km from east to west. The longitudinal profile of the main valley shows a very steep headwater area (22°) followed by a stream segment with moderate slope (7.9°) and a valley bottom with a low gradient (0.2°). For the FDR watershed Strahler's (1952) hypsometric curve shows a complex morphology with a concave-convex shape and the hypsometric integral (f) is equal to 0.45.

The observation of the surface hydrography illustrates a river network highly hierarchical where the hydric denudation processes have a very active role on the slopes. The drainage pattern is clearly dendritic in nature, with three third-order streams (after Strahler, 1952) draining the headwater area. The watershed's total stream network is about 20.3 km long and streams are mainly concentrated on the right hydrographic slope. The Dd (Horton, 1945) value of 8.8 suggests that the FDR is densely drained. The density of hierarchical anomaly (ga, Avena et al., 1967) is equal to 27.4. According to studies performed by Ciccacci et al. (1992) in watersheds of central Italy, a ga value above 20 might indicate the presence of intense inter-rill, rill and landslides as the main denudational processes.

Figure 8.3 shows the geomorphological map of Biasini et al. (1983) modified by the author. The already exhaustive work of Biasini et al. (1983) has been integrated and enhanced with some novel geomorphological forms mainly linked to the change of land use that the watershed has experienced in the last two decades. Comparing the present land-use map of the Ovito watershed (created for this study, Fig. 5.4 – Chapter 5.1.3.2) with the land-use map of Burri (1994) a decrease of farmland surface occurred in the FDR while the forestland and pastureland surface increased. During the field surveys signs of soil erosion that were not been present during the 1983 (Biasini et al.) survey could be recorded. At present, both inter-rill and rill processes are much more evident on the slopes. Tangible signs of widespread erosion due to sheet erosion processes are visible in the harvested forest sectors. The areas subject to rill erosion are more pronounced on the footslopes where the cattle are grazing. These processes of soil erosion are, in general, more intense

on the slopes facing south that are characterized by lower vegetation cover. Here, where the low canopy cover interacts with the steeper slopes the erosion damages are more severe. The presence of deep rills in the lower part of the slopes can be related to the increased flow shear stress exercised by a faster and more concentrated overland flow. In addition, some channeled flow erosion forms were mapped. Active stream incisions into the bedrock area are widely present in the lower-order streams across the watershed. In the case of the main stream, both forms of bank erosion along the floodplains and rock falls from the steepest slopes of the north-facing slope were mapped.

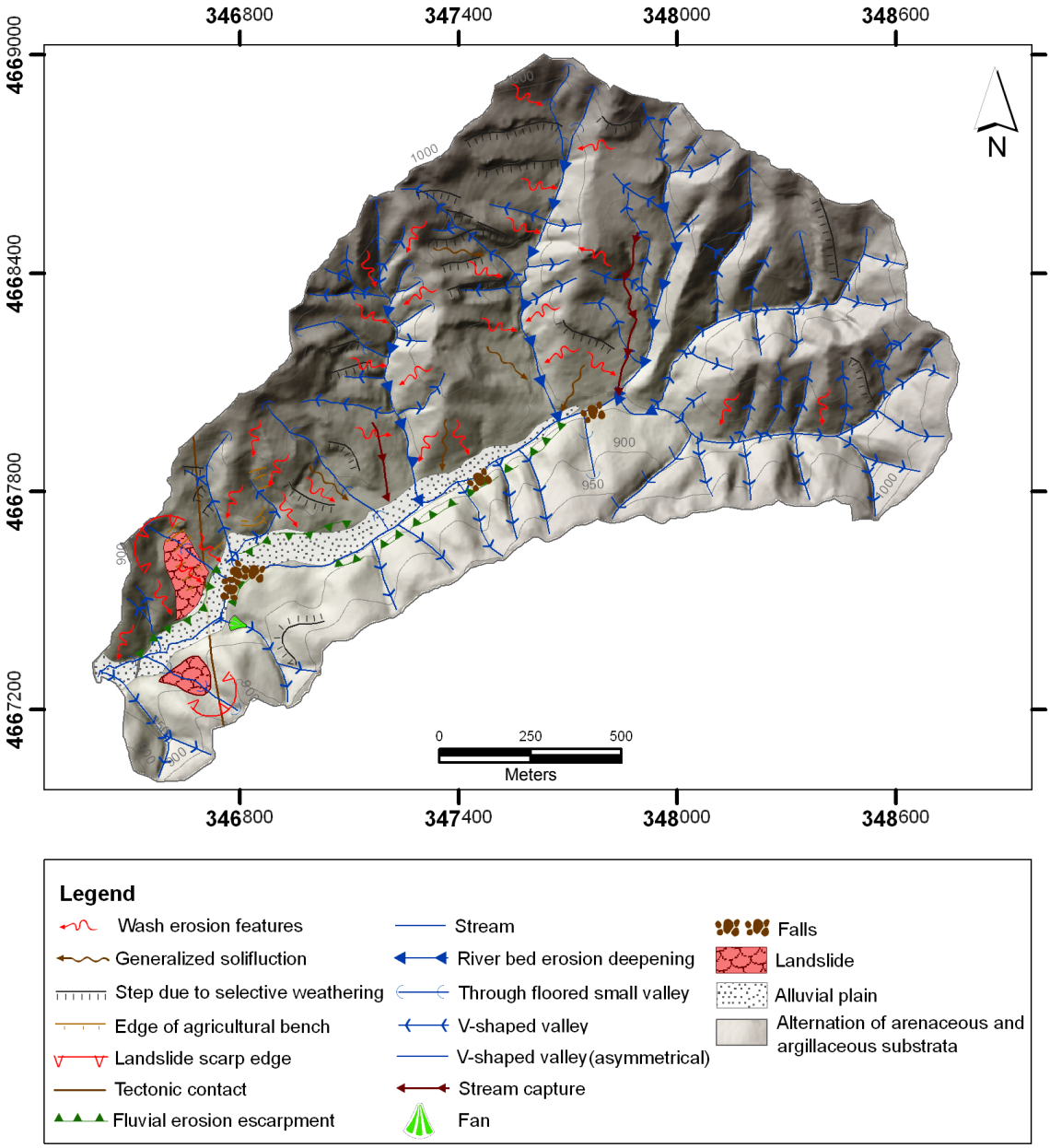

Fig. 8.3 – Geomorphological map of FDR.

The main valley bottom is largely filled with alluvial deposits (0.1 km²). While the fluvial dynamics have reshape the stream bed as described above the farming activities on the flooding surfaces have smoothed the contact area between colluvial and alluvial sediments at the foot of the slopes over the years. At the same time, soil tillage together with soil erosion processes induced a slight gradient on the originally flat surface in river stream direction. Lastly, evidence of sediment deposition due to recent flooding events could not be observed.

With regard to the forms of deposits linked to highly concentrated overland flow some small alluvial fans, often truncated by anthropogenic surface remodeling, not reported in the geomorphological maps of 1994 have been recognized.

Furthermore, insightful processes of recent stream capture were examined and mapped in the field using GPS and subsequently analyzed in a GIS environment. The stream capture processes are fully induced by humans. Suffering from the heavy machineries used to transport the wood the soil of the paths completely lost its structure. The increased run-off due to the canopy cover removal in the harvested area (Chapter 6.3.4) and the soil fragility along the paths gave rise to the linear incision processes that resulted in two gullies. These gullies grew until one reached a maximum depth and width of 75 cm and 170 cm, respectively. As illustrated in Figure 8.4 and Figure 8.5, the biggest of the two gullies, developed over about 5 years along the excavated paths used for forest-harvesting activities, started to capture the upslope running overland flow

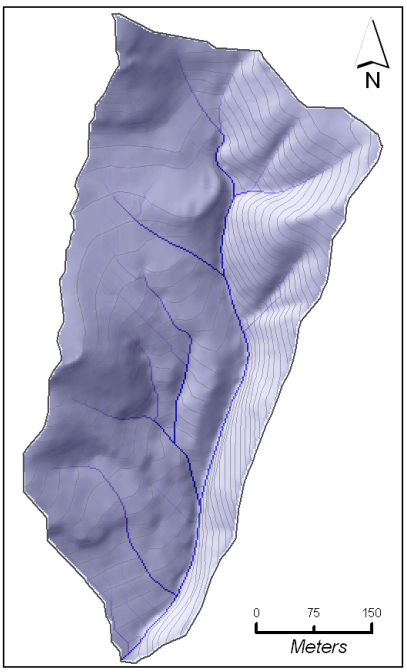

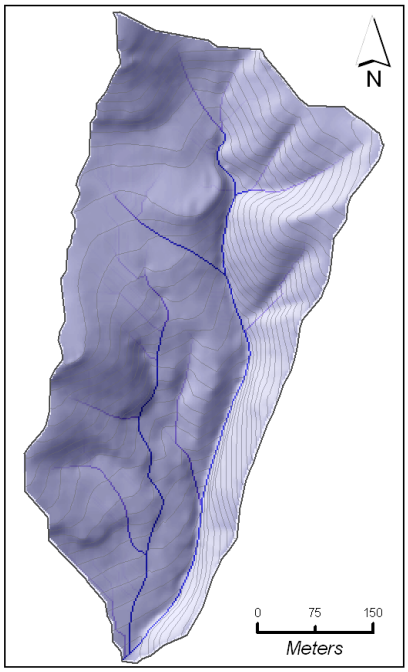

Fig. 8.4 – Drainage network FDR sub-watershed 2005. Fig. 8.5 – Drainage network FDR sub-watershed 2010.

Fig. 8.6 – Gully incision on the rock basement.

Fig. 8.7 – Gully confluence with the mainstream.

During visual interpretations of aerialphotos in the period from 2005 to 2010 approximately 14 km of paths for handling machinery were mapped (Fig. 8.8.). On average the paths are 2.5 m in width so that they cover a total area of about 3.5 ha. The presence of only two gullies despite the large number of paths may lead to the assumption that a particular slope conformation is required for their formation. However, one cannot exclude that further gullies with this morphogenic origin might be present in areas unreachable at the moment due to being highly vegetated.

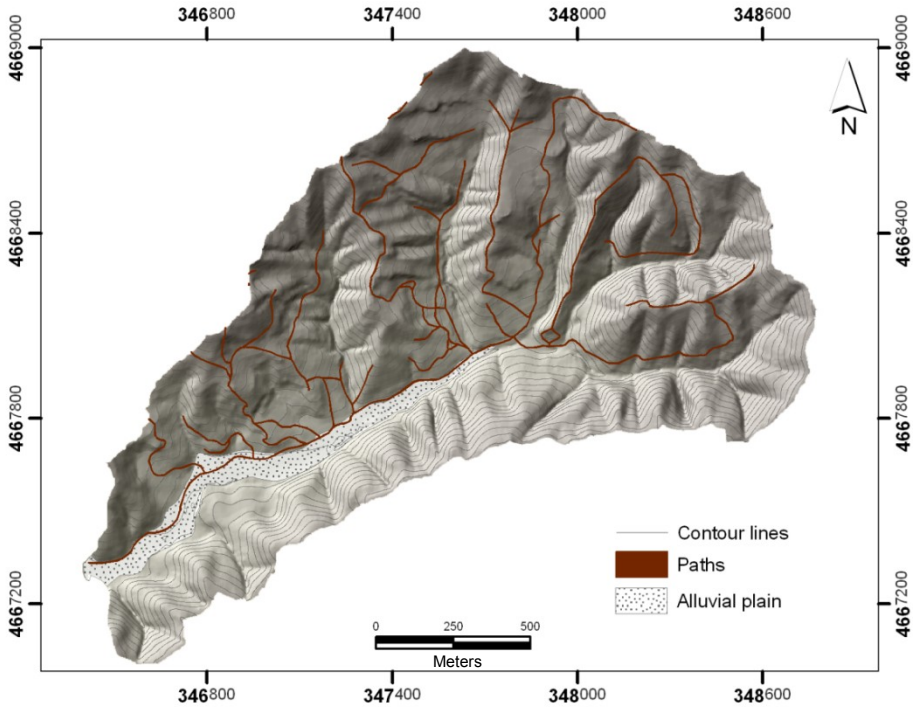

Fig. 8.8 – Paths in the FDR watershed.

Finally, some remarks about the present geomorphological situation regarding the solifluction processes and selective erosional forms need to be provided. Compared to the

solifluction forms already mapped by Biasini et al. (1983), during the surveys in the FDR no additional forms were found. Today, the solifluction forms mapped in 1983 are barely visible. However, the selective erosion forms are still clearly visible. It seems as if they are the result of the different consistencies of the torbiditic series layer.

8.3.2. SEDIMENTOLOGICAL RESULTS

The results of the sedimentological analysis and the macroscopical classification of the valley infills derived from the cores are presented in table and in a graphic format on the following pages.

The first profile considered (PS-04) represents a 500 cm-thick alluvial sequence from the lower part of the FDR watershed near the confluence with the Fosso Corvini river. In the lower part of the sequence, sandy material is prevalent, changing to prevalent silty material at 390 cm depth. Yet, further sandy layers can be observed at 275, 245 and 185 cm depth. In addition, the analysis of the core reveals rather low charcoal contents close to the bottom that tend to increase from a depth of 360 cm. The total organic carbon content is inverse proportionally related to the depth and also strongly increases at about a depth of 360 cm.

Table 8.2 – PS-04 core characteristics.

Site 1
Core code: PS-04
Location: 4667360N 346564E
Elevation: 815.7 m a.s.l.
Stream distance: 4 m
Elevation respect to stream: ≈80 cm
Water table level: ≈100 cm depth
Core depth: 500 cm
Number of main layers: 25
Min layer thickness: 1 cm
Max layer thickness: 50 cm
TOC min: 0.6%.
TOC max: 2.6%.
TOC mean: 1.5%.
TIC min: 0.1%
TIC max: 0.8%.
TIC mean: 0.2%

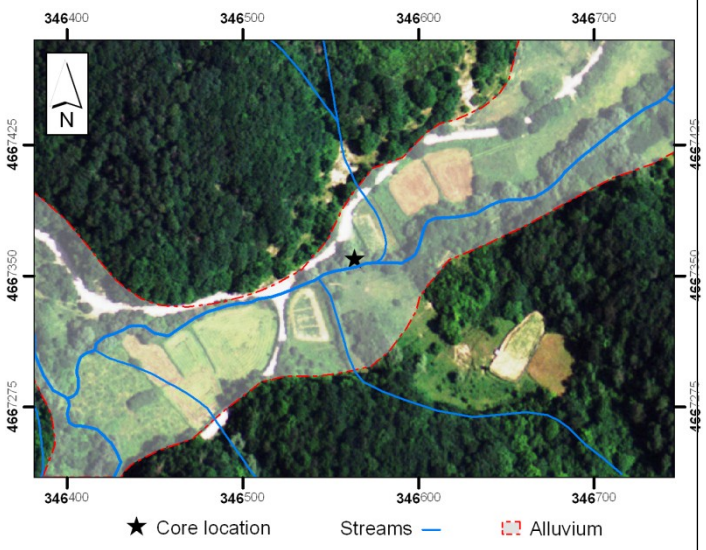

Fig. 8.9 – Drilling core PS-04 location

PS-04 Core stratigraphy

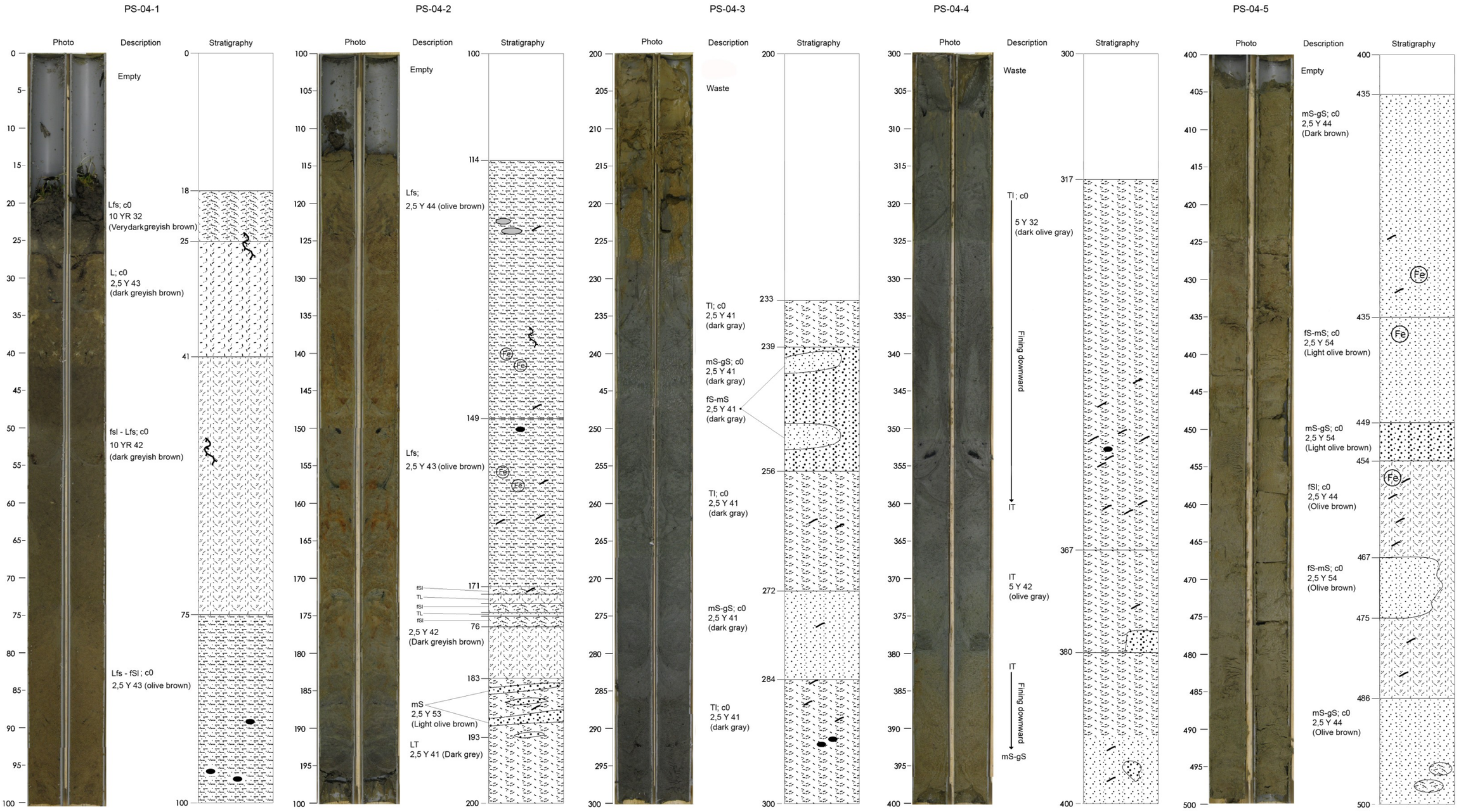

Fig. 8.10 – Core PS-04 stratigraphy

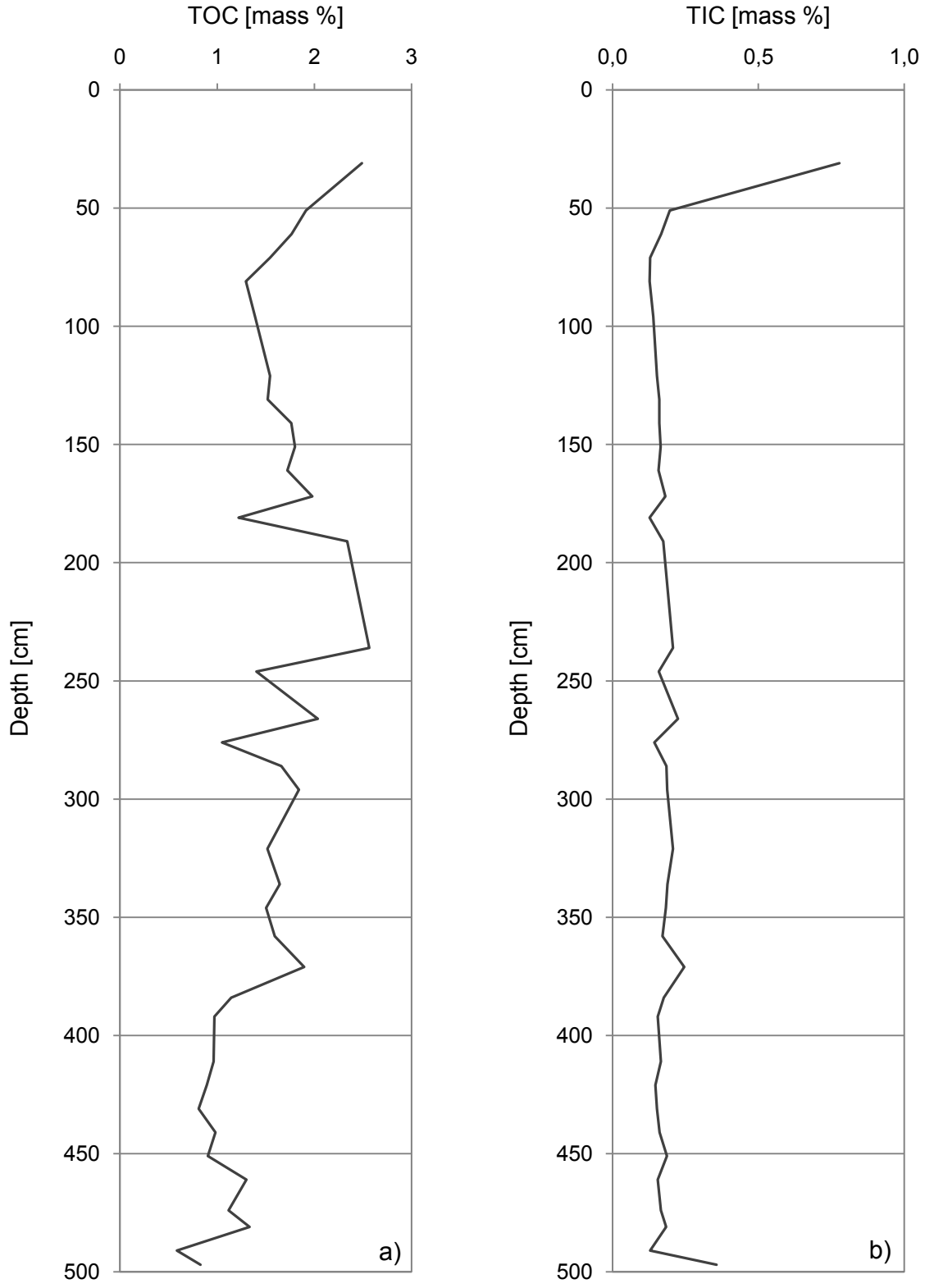

Fig. 8.11 – Organic (a) and inorganic (b) carbon content in core PS-04.

The alluvial profile PS-01 is an 800 cm-thick sequence located 330 m upstream from the location of core PS-04. Sedimentological analysis of this core was carried out directly in

the field. Results have indicated the predominance of silty sediments with intercalations of sand.

Table 8.3 - Ps-01 core characteristics.

Site 2
Core code: PS-01
Location: 4667694N 346785E
Elevation: 822.1 m a.s.l.
Stream distance: 21 m
Elevation respect to stream:≈220cm
Water table level: ≈330 cm depth
Core depth: 800 cm
Number of main layers: 33
Min layer thickness: 7 cm
Max later thickness: 200 cm
TOC min: 0.2%.
TOC max: 4.5%.
TOC mean: 1.3%.
TIC min: 0.2%
TIC max: 0.4%.
TIC mean: 0.3%

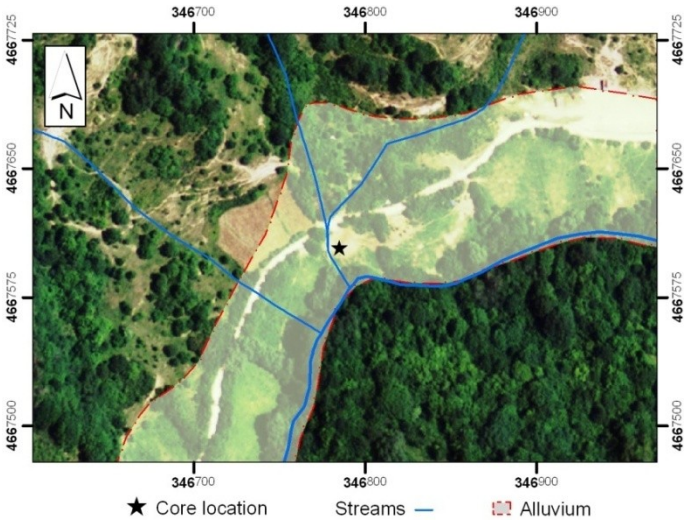

Fig. 8.12 – Drilling core PS-01 location.

PS-01 Core stratigraphy

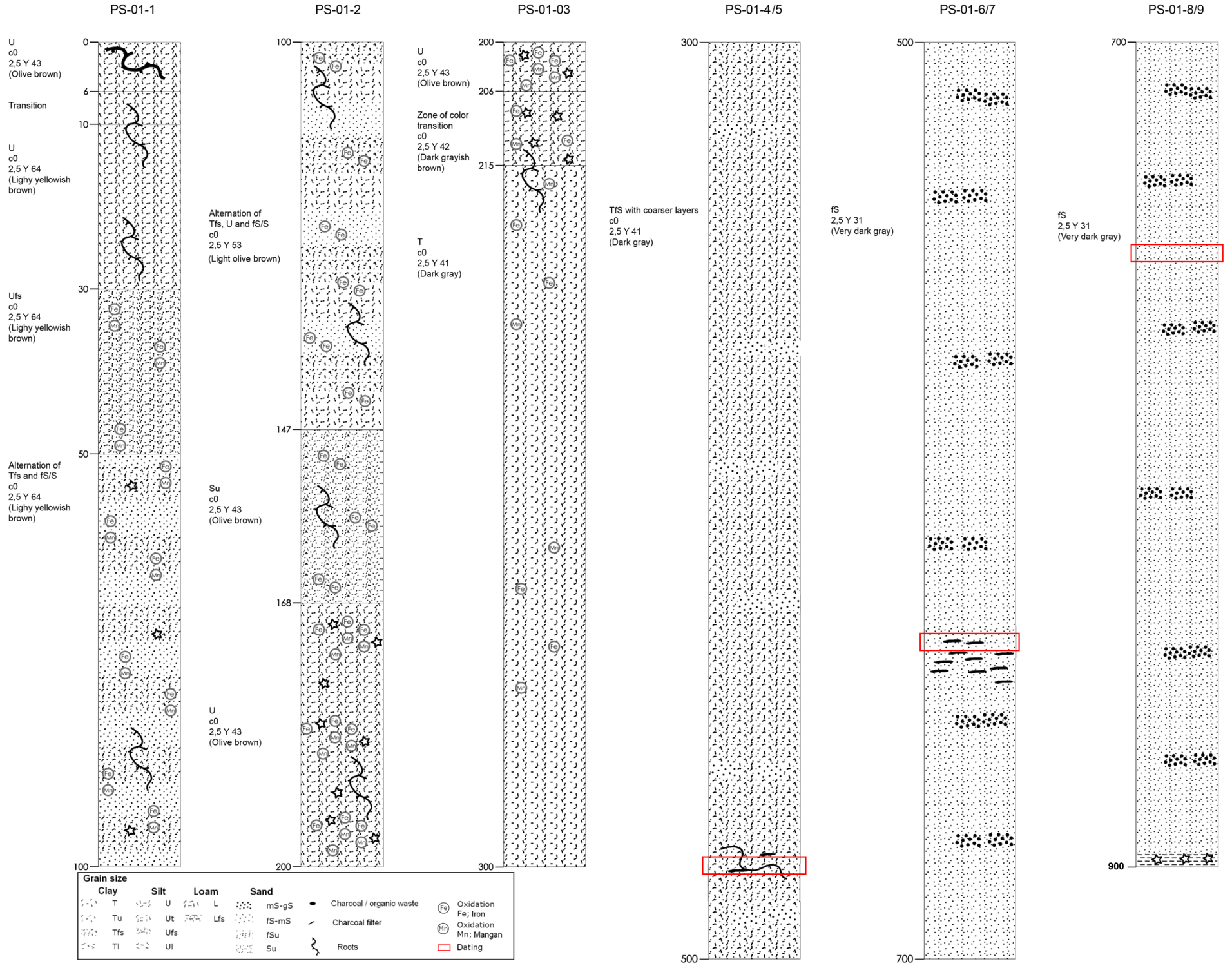

Fig. 8.13 – Core PS-01 stratigraphy.

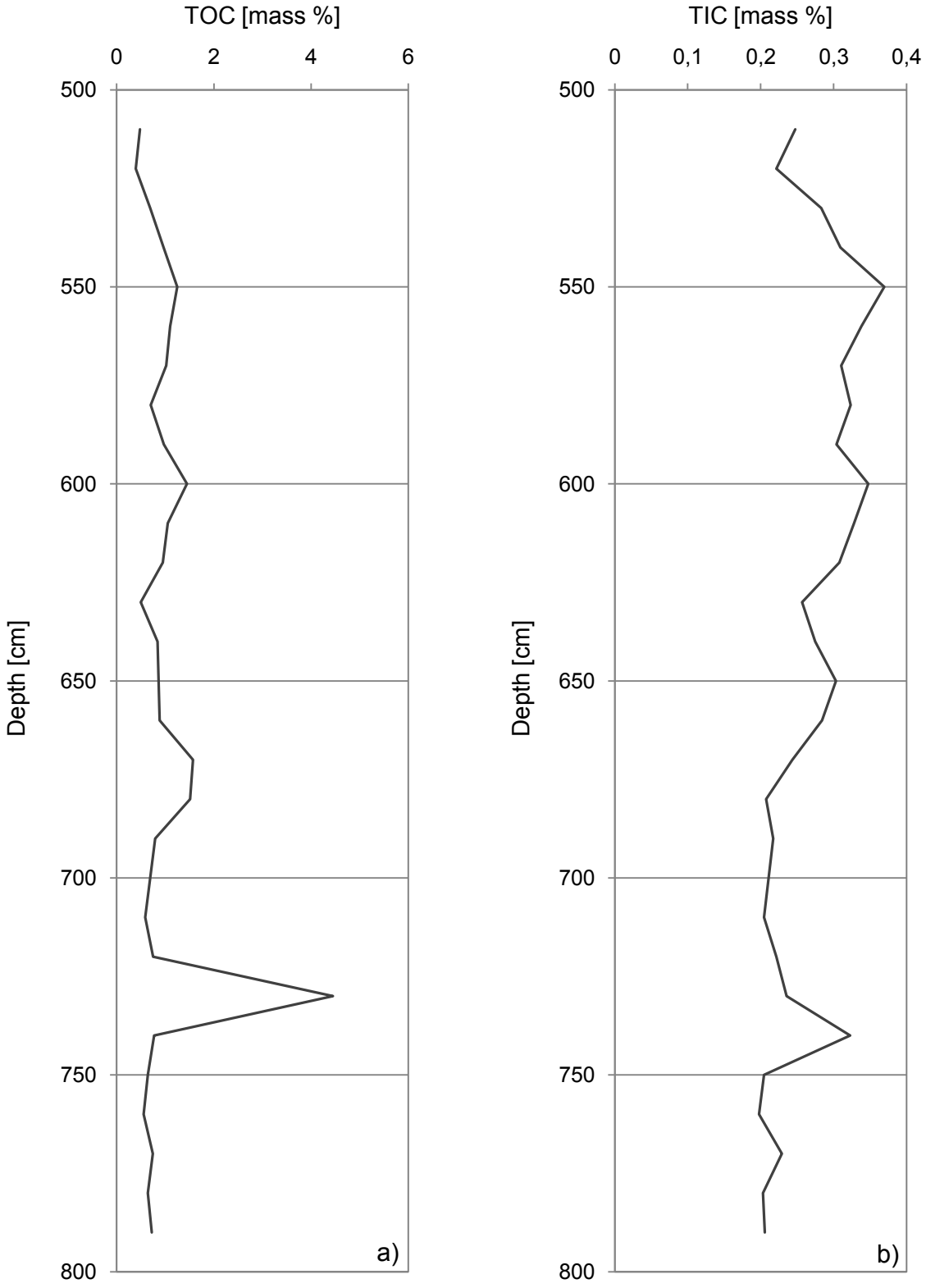

Fig. 8.14 – Organic (a) and inorganic (b) carbon content in core PS-01.

The alluvial profile PS-11 is an approximately 10 m thick sequence situated 130 m upstream from profile PS-04 and 460 m from PS-01. Here, the core also shows sequences

of silty/clayey sediments and intercalated sandy layers. A trend of fining upward sequences within these sandy layers were observed, indicating a flood origin with a selective deposition. The charcoal content is higher compared to the other two cores. Moreover, there are several layers rich in charcoal from 890 to 140 cm depth. In addition, the TOC content (average) in the PS-11 core is about 30% higher compared to the PS-01 and PS-04 cores.

Table 8.4 – PS-11 core characteristics.

Site 3
Core code: PS-011
Location: 4667634N 346917E
Elevation: 823.2 m a.s.l.
Stream distance: 23 m
Elevation respect to stream:≈250cm
Water table level: ≈230
Core depth: 1000 cm
Number of main layers: 426
Min layer thickness: 1 cm
Max later thickness: 60 cm
TOC min: 0.1%.
TOC max: 6.7%.
TOC mean: 2.1%.
TIC min: 0.1%
TIC max: 0.3%.
TIC mean: 0.2%

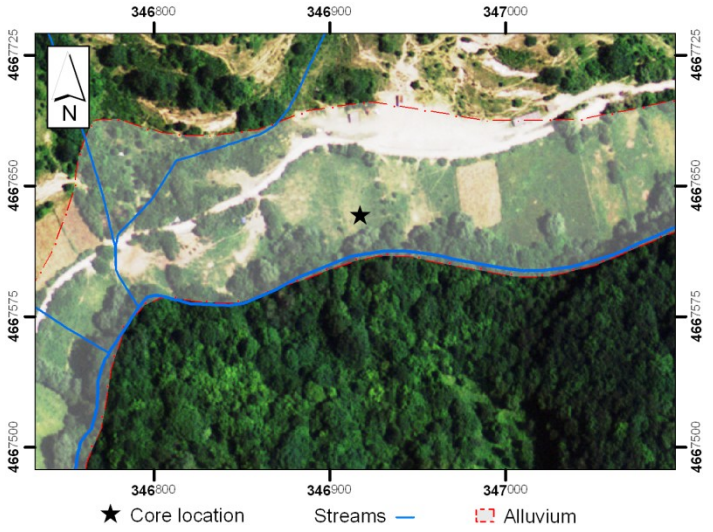

Fig. 8.15 – Drilling core PS-11 location.

PS-11 Core stratigraphy

PS-11-1

Photo

Description

Empty

Organic matter

fSu; c0
5 Y 32
(Dark olive gray)

fSu; c0
2,5 Y 44
(Olive brown)

fSu; c0
2,5 Y 54
(Light olive brown)

mS-gS; c0
2,5 Y 54

fSu; c0
2,5 Y 54

mS-g-S; c0
2,5 Y 54

fSu; c0
2,5 Y 54

Stratigraphy

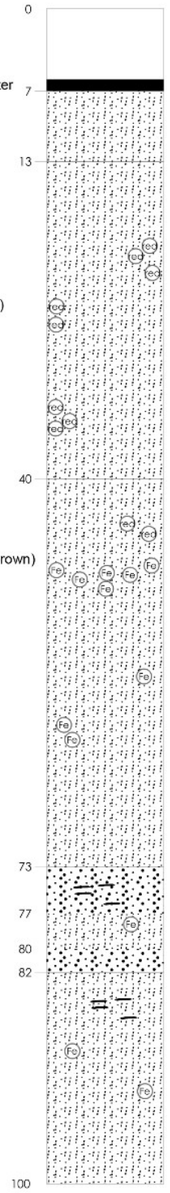

PS-11-2

Photo

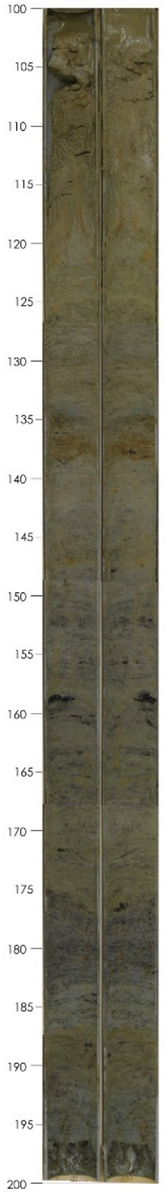

Description

Empty

fSu; c0
2,5 Y 54

fSl; c0
2,5 Y 54

mS-gS; c0
5 y 43
(Olive)

fSl; c0
2,5 Y 43
(Olve brown)

mS-gS; c0
5 y 43
(Olive)

fSl; c0
5 Y 32
(Dark olive gray)

L; c0
5 Y 41
(Dark gray)

mS-gS; c0
2,5 Y 42
(Dark graysh brown)

fS-mS; c0
5 Y 42

Stratigraphy

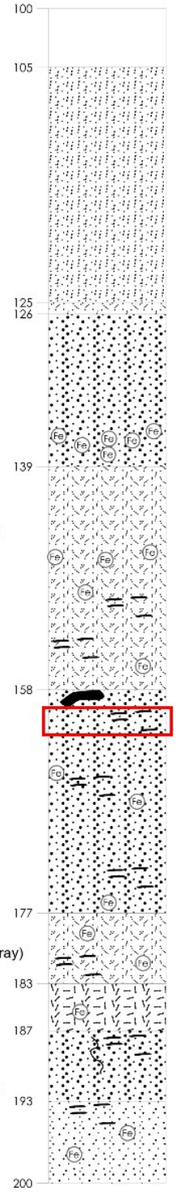

PS-11-3

Photo

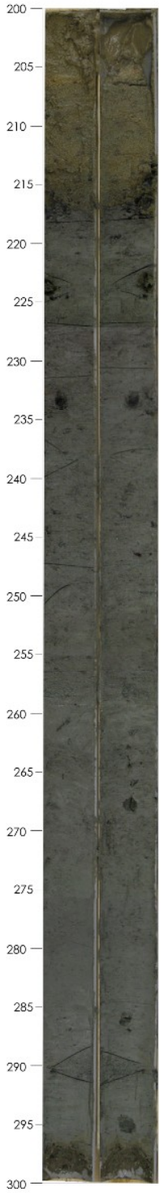

Description

Empty

Lfs; c0
5 Y 41
(Dark gray)

Lfs; c0
5 Y 31
(Very dark gray)

fSl; c0
fS-mS
5 Y 41
(Dark gray)

tTfs; c0
5 Y 41

mSl; c0
5 Y 41

Tfs; c0
5 Y 41

Tl; c0
5 Y 41

Sl
5 Y 41

Stratigraphy

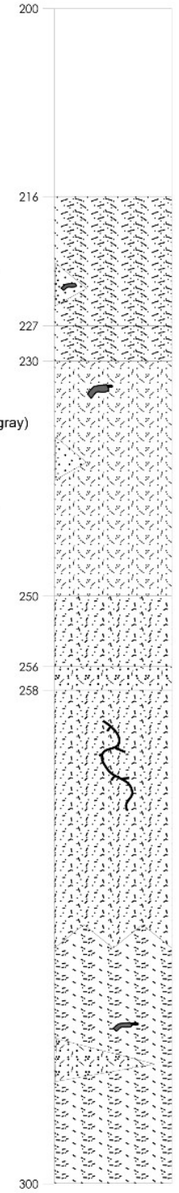

PS-11-4

Photo

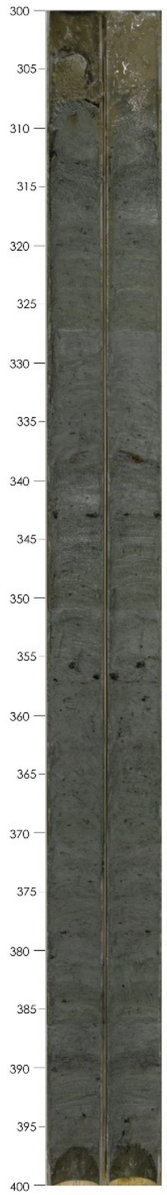

Description

Empty

1 45 GY
(Dark greenish gray)

Stratigraphy

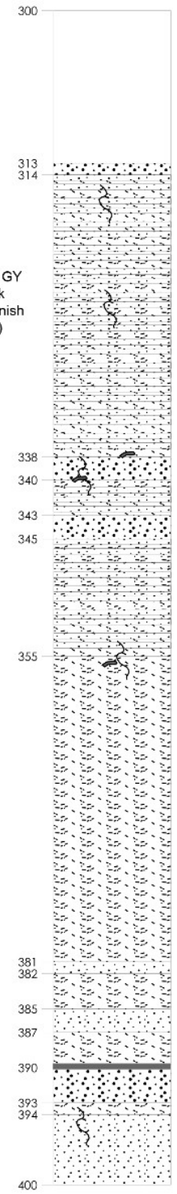

PS-11-5

Photo

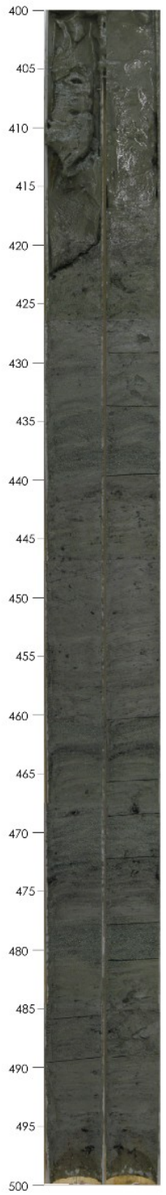

Description

Empty

Gley 1 40Y
(Dark greenish gray)

5 Y 32
(Dark olive gray)

5 Y 32
(Dark olive gray)

Stratigraphy

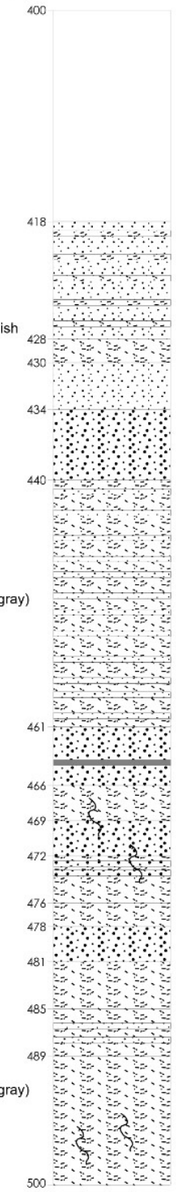

Grain size

Clay		Silt		Loam		Sand	
	T		U		L		mS-gS
	Tu		Ut		Lfs		fS-mS
	Tfs		Ufs				fSu
	Tl		Ul				Su

Charcoal / organic waste

Charcoal filter

Roots

Oxidation Fe; Iron

Oxidation Mn; Mangan

Dating

Fig. 8.1 – Core PS-11 stratigraphy (1 of 2).

PS-11 Core stratigraphy

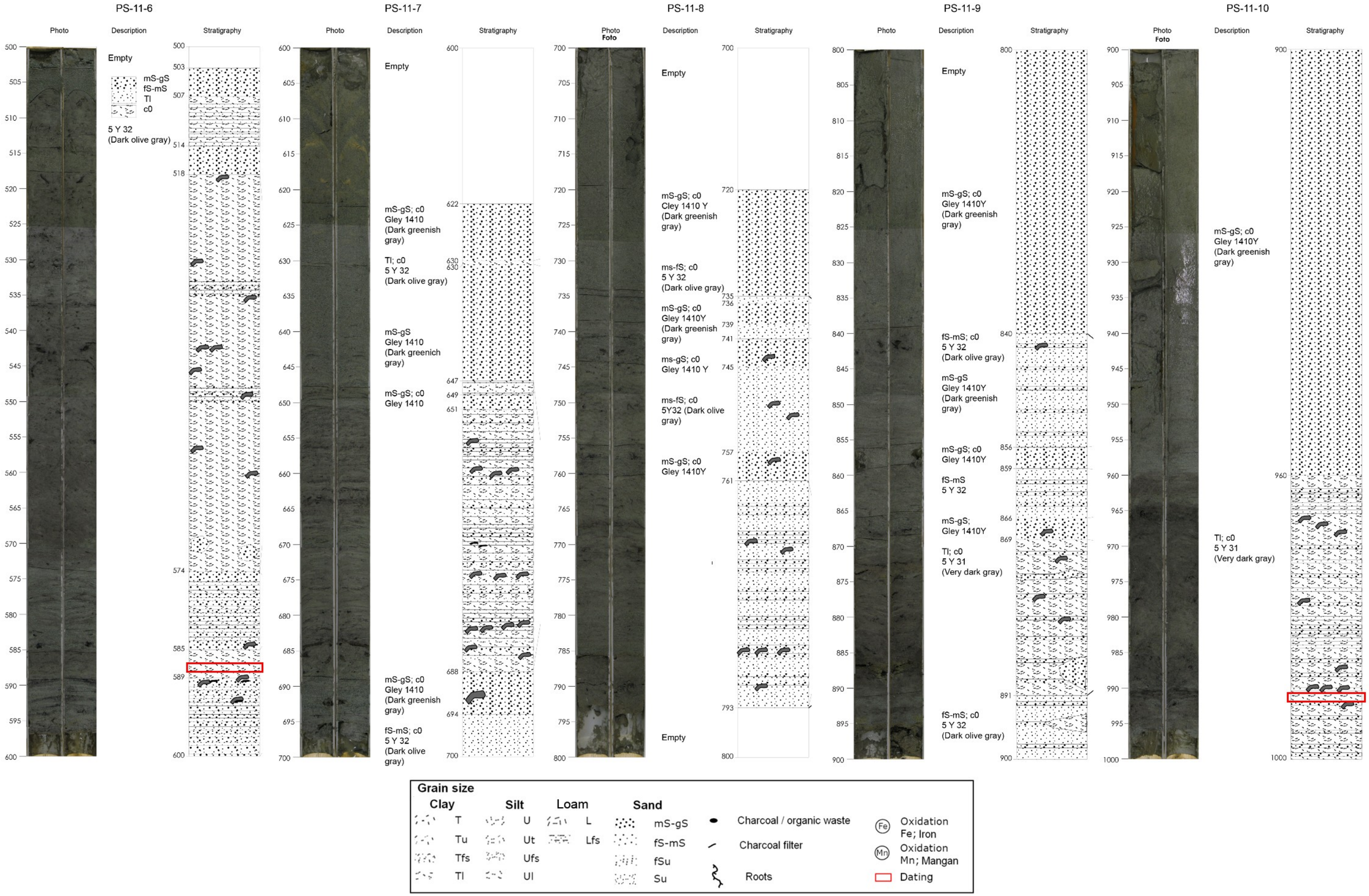

Fig. 8.1 – Core PS-11 stratigraphy (2 of 2).

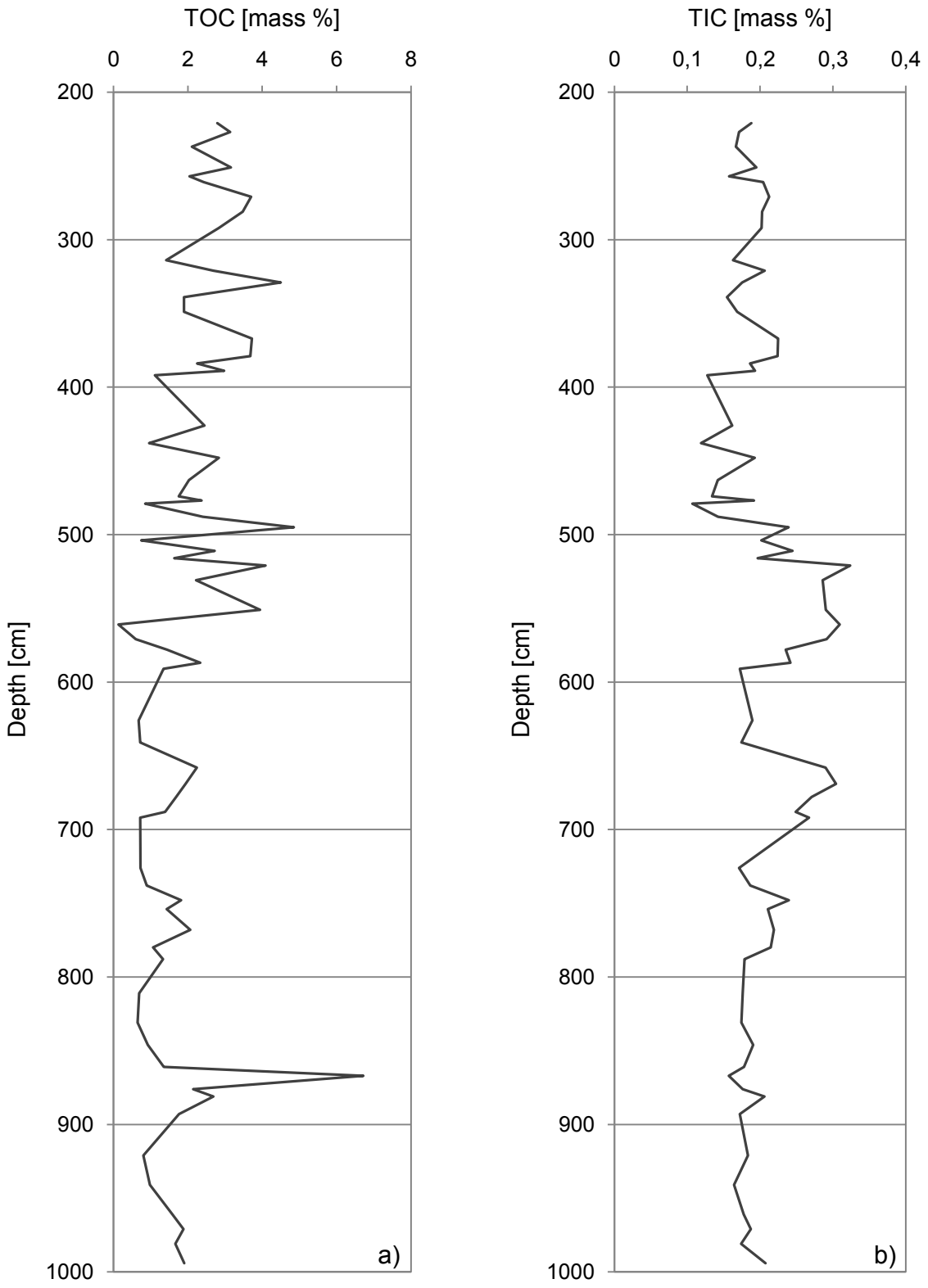

Fig. 8.17 – Organic (a) and inorganic (b) carbon content in core PS-11.

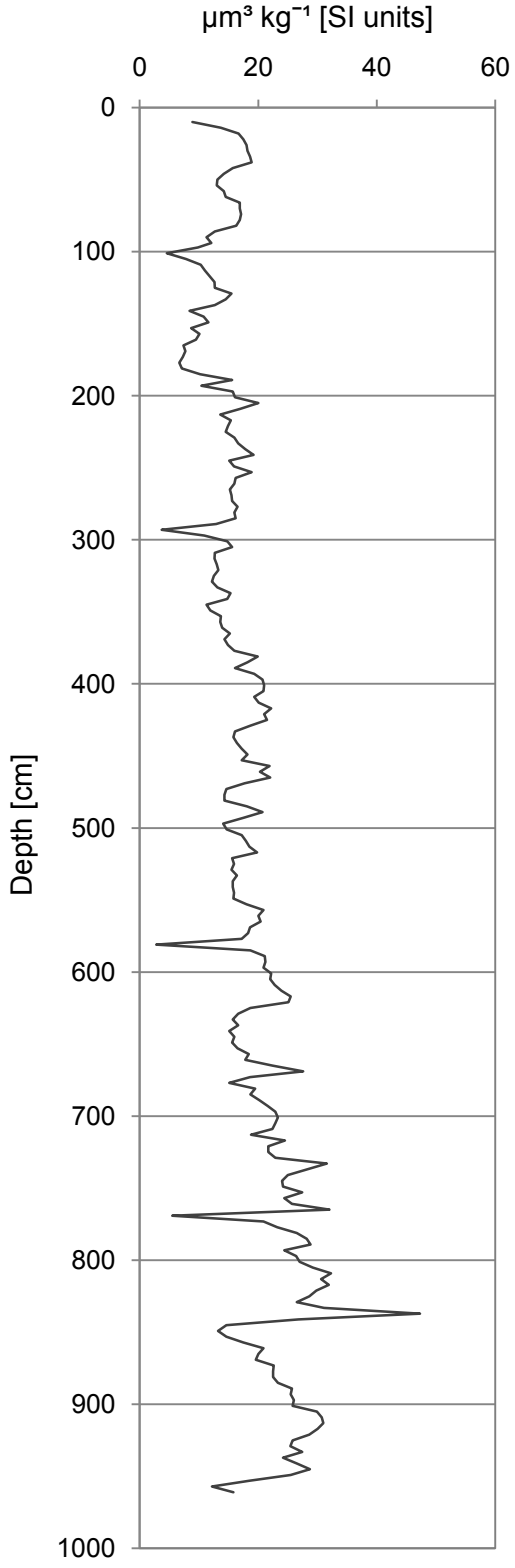

Fig. 8.18 – Magnetic susceptibility of the core PS-11.

8.3.3. AGE MODEL

To identify the chronological frame of the sediments infilling the investigated valley eight samples of organic material (mostly charcoal) were submitted to radiocarbon dating (Table 8.5). According to their alluvial genesis the sediments become younger from the bottom to the top of the profile, which is consistent with the principle of stratigraphic superimposition. The extrapolation of an age model based on linear interpolation for the core PS-11 (Fig. 8.15) shows a rather constant age-depth correlation. The PS-11 core age-depth regression can be described as:

$$Age\ [cal.yr\ AD] = -0.899 \cdot depth\ [cm] + 1464.8 \quad \text{(Eq. 8.1)}$$

The sedimentation rates of the core PS-11 obtained from Equation 9.1 range from 1.51 to 0.89 cm yr^{-1}. Accordingly, PS-11 alluvial sediments are rather young. The oldest sediments belong to the bottom of the core PS-04 dated between 202 and 2 BC.

Table 8.5 – 14C dates of the FDR.

Sample	Material	Depth	TIC	TOC	14C age	Calibrated age
		[cm]	[mass %]	[mass %]	[a BP]	[a BC/AD]
PS-01 480	Charcoal	480	-	-	960 ± 35	1017 - 1160
PS-01 632	Charcoal	632	0.3	0.5	990 ± 35	986 - 1155
PS-01 720	Charcoal	720	0.2	0.7	1390 ± 30	602 - 674
PS-04 150	Charcoal	150	0.2	1.8	780 ± 30	1212 - 1281
PS-04 470	Charcoal	470	0.2	1.1	2090 ± 35	-202 - -2
PS-11 159	Charcoal	159	0.2	2.1	600± 30	1297 - 1409
PS-11 585	Charcoal	585	0.2	2.3	1155 ± 30	778 - 971
PS-11 991	Charcoal	991	0.2	1.9	1450 ± 30	561 - 651

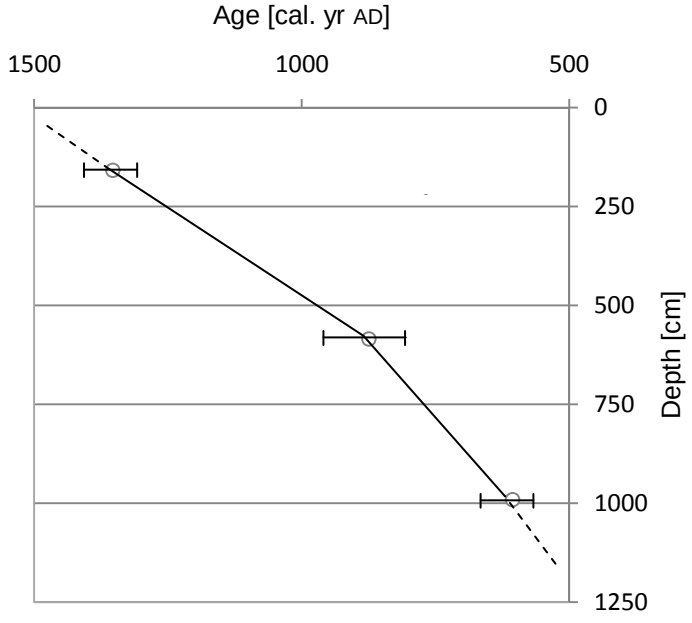

Fig. 8.19 – Age model of the core PS-11.

8.4. DISCUSSIONS

8.4.1. PRESENT DAY UPLANDS EROSIONAL PROCESSES

Studies so far performed in the pelitic-arenaceous geological sector of the Turano watershed have represented its main geomorphological aspect. The observations of the FDR watershed indicate the watershed's inclination for intense hydric erosion. This conforms to the previous geomorphological studies executed in the area (Angelucci et al., 1959; Callori di Vignale, 1981; Biasini et al., 1983; Apat, 2009). The FDR watershed displays forms of intense hillslope denudational, mass movements (i.e., earth flows, solifluction) and gully erosion. The presence of accelerated soil erosion processes is mainly linked to the alteration of the natural environment characteristics caused by the anthropogenic impact. In fact, the complete watershed surface is exploited by human beings through farming, grazing and forest-harvesting activities. The high environmental impacts resulting from these anthropogenic activities are connected to the generally high sensitivity of the area due to natural factors such as, climate pattern (Freddi and Pugliese, 1994), lithological characteristics (Agostini, 1994), hydrological behavior (Bucci, 1978; Bono and Capelli, 1994) and high soil erodibility. Their combination facilitates the slope instability (Biasini et al., 1983).

8.4.2. FDR WATERSHED EVOLUTION

The Ovito watershed, where the FDR watershed is located, is a sector of the Carseolani mountain chain that has been the object of several geological, speleological and geomorphological studies (Biasini et al., 1983; Agostini, 1994, Agnesi et al., 1994). It is situated on the Cretaceous-Miocene bland anticline (Angelucci, 1959). In its nucleus, this anticline is composed of shelf 'Rudistae limestones' (upper Cretaceous) followed in transgression by 'Bryozoa limestones' (middle Miocene) (Agostini, 1994). The carbonatic ridge (dorsale carbonatica di Pietrasecca) stretches along the typical NW-SE Apennine direction and has an important cave system (Bono and Capelli, 1994). The FDR as well as the other Ovito sub-watersheds have developed transversally (southeast of the ridge) incising the hemipelagites marls and pelitic-arenaceous flysch. The water of the watershed is completely drained by one cave of the above-mentioned karst system, the so-called 'Inghiottitoio of Ovito'. The neotectonic and geomorphological evolution evidently control the hydrography of the area. Angelucci (1959) Agostini (1994) and Sauro et al. (1994) stated the presence of different stages of the geomorphological evolution, composed of a paleovalley and two fossil hanging water sinks (i.e., the paleo-Ovito cave and the Cervo cave).

An important aspect for the evolution of the area is represented by the selective erosional processes, which constitute an important aspect for the evolution of the area because they have shaped the two predominant rock units (limestone and flysch) in different ways. The pelitic-arenaceous sector erodes much faster than the carbonatic one. However, there is not a large difference in altitude (only a few tens of meters) between the tops of the limestone and flysch relief that most likely represent the altitude level of a paleo surface. Based on morphometric analysis, Sauro et al. (1994) posited that if the mountain peaks represent geological relics of a paleo flat surface the relief should be relatively young. In fact, if the selective erosion operated for a considerably long period, the carbonate ridge would be much higher compared to the one of the flysch unit.

According to the 2x2 m DEM resolution and the elevation of the geological relics it is possible to roughly estimate 237 M m³ of sediment eroded for FDR watershed. There are evident geomorphological proofs that from the moment when the paleovalley (Vena chonca) stopped to be the Ovito outlet, the whole eroded sediment in the area started to cross the carbonatic ridge through the hypogeal karst system.

The longitudinal profiles of the FDR streams have highly been influenced by the uplift of the siliciclastic sector together with the lowering of the river network base level that resulted from the karst processes on the carbonatic ridge. These joint factors may have caused an alternation of the stream erosion and the alluvial deposition phase in the FDR watershed.

Agostini (1994), observing the Quaternary deposits in the area, noted that the alluvial deposits (in some cases terraced) indicate repeated rejuvenating and stabilization phases of the drainage network due to morphodynamic causes for the sediments of ancient cycles and anthropogenic causes (rhexistasy) for more recent cycles. Some studies, e.g., Conca di Oricola (Colica et al., 1993) Rieti Basin (Calderini et al., 1996), and Piana del Cavaliere (Barbieri et al., 1998) found the presence of Pleistocene alluvial deposits in the proximity of the FDR watershed applying 14C dating of the sediments. However, the results of the 14C dating did not reveal indications of Pleistocene alluvial deposits in the Ovito watershed. In fact, the three cores and further cores observed in the Ovito watershed (Holzmann, 2010, personal communication) consisted of Holocene, more precisely sub-Atlantic sediments.

The valley infilling sediments observed in the area consist of layered alluvium, originating from the erosion of the upland. The formation of these sediments as well as the absence of alluvial sediments dated older than sub-Atlantic can be the explained by the impact of climatic and anthropogenic factors in the area.

For central Italy, the historical fluctuation of the climate has been reconstructed by several studies (among other, Le Roy Ladurie, 1982; Magri and Follieri, 1989; Dragoni, 1996; Giraudi, 2004; Magny et al., 2007) using different techniques (i.e., lake oscillation in central Italy, pollen analyses of peat-bog, expansion and recession of ice-caps and historical data post 1000 AD). Climatic information derived from the several investigations of palaeoenvironmental proxies in Italy have recently been merged by Colacicchi and (2008) to formulate a scheme of climate variations in central Italy. According to Colacicchi and al. (2008) in central Italy within the last three millennia different periods can be distinguished: cold/rainy periods (from 900 BC to 250 BC; from 200 AD to 800 AD; from 1300 to 1850) and two warm/dry periods (from 250 BC to 200 AD; from 800 AD to 1250 AD). This climatic reconstruction is congruent with other studies in Europe (Lamb; 1995).

Regarding the anthropogenic activities in the area, past human presence can only roughly be reconstructed from the rather poor literature sources. According to the best knowledge of the author, sources about human activities in the area reveal information on: 1) The possible presence of a fortified settlement where today the town of Pietrasecca is located (Grossi, 1991). This fortified town was of Aequi origin and was assumingly inhabited since the X to IV century BC (Grossi, 1991). 2). The arrival of the Romans in the area who founded the city of Carsoli (Castrum Solis) in 299 BC (Livy, 59 BC – AD 17, cited in Giovannoni 2003). This old Roman settlement of Carsoli is located about 6 km in a SW direction with respect to FDR watershed. 3) The discovery of Roman archaeological findings in Pietrasecca (e.g., ceramics, tombstone, coins (Agostini, 1994; Agostini and Gizzi, 1994)) indicate the Roman presence in the imminent vicinity of the FDR watershed. 4) The location of Pietrasecca was under the control of noble families (Orsini and Colonna) during the period between X and XVIII century AD (De Vitis, 1985).

Crossing the information obtained by the alluvial deposits, the climatic variations and the human presence in the area the following evolution phases can be distinguished during the Holocene:

Pre-sub-Atlantic – The human impact in the FDR area can be assumed insignificant for the following reasons. Researchers have noted that during the first Iron Age (end of the X century BC) the Salto and Turano Valley were occupied by the Aequi (Giovannoni, 2003) and Sabine tribes (Strabo, V book). The Pietrasecca location was most likely occupied by one of their settlements in the area (Grossi, 1991). The carbonatic ridge of Pietrasecca offered a naturally well-protected location and the nearby rather flat plain of the Vena Cionca (paleovalley of Pietrasecca) represented an optimal area for farming. According to studies of Italian (Hughes and Thirgood, 1982) and other European locations (Kaplan et

al., 2009) there is evidence to assume there was a phase in which the European landscape was abundantly covered by woods during this period. The thermophile vegetation presently covering the Ovito watershed was most probably replaced during this period by plants which today belong to the mountain vegetation belt, such as Abies and Fagus. The spread of Fagus in central Italy caused by a drop in temperature during the Holocene period was recognized by an analysis of the lake sediments of the Lago di Vico *(*Magri and Sadori 1999), the Valle di Castiglione (Alessio et al., 1989) and the Lago Lungo (Calderoni et al., 1994). Thus, the low human impact and a dense vegetation cover may have resulted in a phase of prevailing biostasy. Relevant alluvial floods could most likely not occur due to the control of the vegetation on both, run-off generation and soil erosion processes in the uplands. Furthermore, morpho-structural aspects of the FDR and rest of the Ovito watershed could also have inhibited these alluvial floods. The fine parent materials (Bertolani et al., 1994) and soil particles could be easily transported as a suspended load in the concentrated run-off.

This hypothesis is partially proved by the flood-quiescent status of the FDR watershed in spite of the altering climatic situations during the pre-sub-Atlantic Holocene. It follows that even the wettest conditions of the Holocene did not create the conditions necessary for the formation of alluvial deposition. During this phase of biostasy, older alluvium, if present in the valley bottom at that time, could be re-eroded by the stream action.

The exploitation of the wooded vegetation in the area made by the Aequi cannot be ruled out. Still, there are indications to assume an absence of the environmental impact in the FDR watershed during the Aequi domination in the area.

Sub-Atlantic – According to the historical sources at the end of the war between the Romans and the Aequi, 304 BC, the console Publio Sempronio Sofo entered the Aequi territory and in only fifty days besieged and afterwards destroyed 31 Aequi fortresses (Giovannoni 2003). One of them could have been Pietrasecca (Grossi, 1991). Only one year later, in 303 BC (Livy, 59 BC – AD 17, cited in Giovannoni 2003) a Roman colony was founded at Alba Fucens (21 km east of Pietrasecca) which was assigned by 12,000 settlers. During 299 BC (Livy, 59 BC – AD 17, cited in Giovannoni 2003) the city of Carsoli was founded in the Turano valley, where the Romans assigned 4000 settlers. Most likely the Pietrasecca area was a territorial pertinency of Carsoli. The arrival of the Romans in the area coincided with the beginning of a climatic amelioration period that lasted from 250 BC to the III century AD (note as the climatic optimum in Roman times (Williams, 2000)). The first alluvial deposition in the FDR watershed, according to the OxCal 4.1 program (Bronk Ramsey, 2010), is dated back between 202 and 2 BC, which is during the first

stage of the 'Roman climatic optimum'. The location subject to floods is located near the watershed outlet, just a few meters in front of the confluence of the FDR River and the Fosso Corvini River. Stratigraphically, the layers observed in the core appear to be thick and composed of coarse material without charcoal. It is possible to presume a change in land use with the arrival of the Romans in the area. The change of land use could alter the watershed balance more effectively than previously done by climatic changes. In fact, the stratigraphic sequences observed in the FDR watershed did not reveal alluvial sediments of the former cold and rainy periods, 3800–2300 BC, 1600–1100 BC (Rothlisberger, cited in Calderini et al., 1998) and 900–250 BC (Colacicchi et al., 2008). Indeed, signs of alluvial sediments only start to occur during the period of climatic amelioration. Thus, with the changed pattern of land use imposed by the Romans, the area not subject to alluvial events most probably had passed from a phase of prevailing biostasy to a phase of anthropic rhexistasy. However, even if it is possible to precisely identify the beginning of an alluvial phase in the area most likely induced by humans, the specific human activities that caused it can only be hypothesized. The lack of archeological information about the land use as well as the absence of a pollen analysis of the drilling cores precisely for the study site do not allow for sufficient elements to identify with confidence the land use changes that initiated the flood phase.

However, the low number of inhabitants in the city of Carsoli during the first two centuries BC suggests a rather low demand of food that comes along with a lack of extensive farming in the area. Thus, it is possible to assume that by virtue of its geographical conformation the flat plain of the Piana del Cavaliere (very close to the Carsoli city) could be used by the Romans for agricultural purposes. This assumption is backed by some historical sources. Columella and Pliny the Elder in the I century AD (E. Pais, 1923, cited in Sciò et al., 2000) described the fertility of these areas in the Turano watershed. Ovid (43 BC – 18 AD, cited in Maialetti, 2001) mentioned the cold autumn-winter climate, inappropriate for olive farming but optimal for wheat production (during summer). On the other hand, the mountain sector of the Carseolani range with pretty steep slopes covered by coppice trees was less appealing for farming purposes. It is possible to suppose that these mountain areas could be exploited for wood and charcoal supply. The presence of logger activities in the area of Carsoli is stated in the epigraphies (C.I.L, IX; 4008, 4071, cited in Sciò et al., 2000) where the presence of *fabri tignari* (carpenters) and *dentrophori* (lambermen) has been mentioned.

According to Lamendola (2008) extensive logging was undertaken in the Roman territory between I BC and II AD. These logging activities satisfied Rome's great demand for timber

during this period of urbanization. The rapid increase in the public and private construction activities called for additional timber demand, both directly (e.g., structures and furniture) as well as indirectly (e.g., lime production). In addition, the conquest strategy of the Romans to expand across the Mediterranean area required a powerful navy, which is a further reason for the great timber need. The logging activities in the central Italy in that period were recognized by numerous historical sources (Hughes and Thirgood, 1982). The Roman writer Lucretius (I BC) commented that 'day by day they [the agriculturalists] would constrain the woods more and more to reside up the mountains until only the most inaccessible mountain areas remained wooded' (cited in Williams, 2000, addition added in brackets by Williams). Livy (59 BC - AD 17, cited in Hughes and Thirgood, 1982) described Italy during the fourth century BC as: 'In those days, the Ciminian forest was more impassable and appalling that were lately the wooded defiles of Germany' while two centuries later these forests were largely reduced. Moreover, other information about the forest clearing in central Italy can be found in Strabo (63 BC – AD 21, cited in Hughes and Thirgood, 1982). Firstly, Strabo (63 BC – AD 21, cited in Hughes and Thirgood, 1982) commented that the forested areas around Pisa were harvested to construct public and private buildings in Rome and countryside villas. For the latter, Strabo (63 BC – AD 21, cited in Williams, 2000) mentioned the clearing of the forests of Avernian in Campania which had been 'brought by the toil of man into cultivation, though in former times they were thickly covered with a wild and untrodden forest of large trees'. Furthermore, according to the historical sources the forested locations close to the sea and rivers were preferred by the Romans since they could more easily ship the material to the populated centers (Williams, 2000). For the Turano area, the navigable fluvial connection to the Tiber River represented a possible transporting way. It has been noted that the Romans used to float much of the timber down the Tiber to the city (Williams, 2000).

Thus, although the archeological evidence of forest clearing in the study site can only be indirectly proved, according to the dating of the sediments of the PS-04 drilling cores a considerable change took place in the area during the period between 202 and 2 BC. The presence of a flood-prone phase with the Roman arrival is in line with several observations made in Italy (Sauro, 1993; Lowe et al., 1994; Ayala and French, 2005; Mariotti et al., 2006) and Central Europe (Mäckel et al., 2001, 2002, 2003; Dotterweich, 2008). Moreover, it is also stated that the large forest clearing produced accelerated soil erosion processes and a substantial rise of the suspended load of the river (Stott et al., 1997). This could have had an impact on the geomorphological evolution of the deltas of the main river whose evolution is mainly controlled by the interaction of the postglacial sea-level rise, the sediment influx from drainage basins and tectonic uplifts (Funiciello, 2003; Bellotti et al.,

2004; Aguzzi et al., 2007; Rendell et al., 2007; Antonioli et al., 2009). Although it is difficult to relate the uplands erosion to the growth of the river deltas, especially taking into account the consideration made in Chapter 7.3.1 about the impact of human-induced upland erosion on the watershed's SY, some studies reported a relevant increase of the river deltas during the Roman imperial time (Bellotti et al., 1995; Bellotti et al., 2004). In the case of the Tiber River, a phase of sporadic floods (with flood events in 414 BC, 363 BC, 241 BC and 215 BC) passed over into a flood-prone phase that started during the II BC (indicated by floods in 202 BC, 193 BC, 192 BC, 189 BC, 103 BC, 54 BC, 44 BC, 27 BC, 23 BC, 22 BC, 13 BC, 5 AD, 12 AD, 15 AD, 36 AD and 69 AD) (Livy, IV; Livy, XXX; Livy, XXXV; Livy, XXXVIII; Cassius Dio, LIII, Cassius Dio, LIV). Notably, the flood-prone phase of the Tiber coincided with the emergence of the wide-ranging Italic logging (Lamendola, 2008).

As follows from the drilling core analyses, during the period from 200 BC to 500 AD floods involved only the lower sector of the FDR watershed near its outlet. Subsequently, during the period around 600–640 AD, the alluvial sector of the FDR watershed considerably extended into an upstream direction. At this stage, the floods started to deposit sediments in the location of core PS-01 and core PS-11, respectively located 330 and 460 m upstream of the core PS-04.

Core PS-01 was described and sampled in the field during summer 2009. This highly influenced the quality of its description. In contrast, PS-11 being a closed core was studied in the FU Berlin laboratories. It offered valuable insights into the stratigraphic sequence of the alluvial sediments. According to core PS-11, the alluvial sequence is finely laminated in the sector close to the rock basement at 960 to 1000 cm of depth. The charcoal at a depth of 991 cm of depth dates back to the beginning of the sedimentation at approximately 600 AD (between 551 and 651 AD). From 600 AD onwards, the alluvial plain sediments deposited until they reach a maximum measured depth of 10 m (core PS-11). During this period, from the climatic point of view, central Italy was characterized by a rainy and cold period that lasted from 200 to 800 AD, known as the 'cold medieval phase' (Pinna, 1996). There are sequences with silty/clayey sediments and intercalated sandy sequences in this part of the alluvial sequence. The sandy layers appear at regular intervals. A trend-like fining upward sequences within these sandy layers indicates a flood origin with a selective deposition. Here, moreover, some layers rich in charcoal suggest the presence of some fire events (core PS-11, depth 980 cm, 780 cm, 680 cm, 660 cm and 590 cm).

The low number of dated points along the core only allows for a rough estimation of the sediment deposition rate. Nonetheless, the accumulation rates are estimated at 1.51 cm

yr^{-1} from 600 to 870 AD and at 0.89 cm yr^{-1} from 870 to 1350 AD. Subsequently, the more recent increase in the alluvial plain is estimated at about 0.24 cm yr^{-1}. It follows that the early Middle Ages can be roughly identified as the period with maximum sediment deposition at the FDR watershed site. Unfortunately, this is also the period in which there is a gap of literature sources. However, useful indications about the alluvial deposition could be obtained by observing the sediment stratigraphy of the cores. The finely laminated layers described above stop at about 960 to 900 cm of depth where one can observe only sedimentation of coarse sand material. Alternating finely laminated layers and sandy layers run through the whole core suggesting an alternation of flood events and extraordinary flood events. The numerous thin layers in sectors along the core appear to represent new layers occurring almost annually, which suggests the persistence over time of human activities that caused the flood-prone phase of the watershed.

One can state with relatively high confidence that after the Roman arrival in the area, the FDR watershed suffered a phase of prevailing anthropic rhexistasy. The clearance of the trees led to the transition from a phase of biostasy to a phase of rhexistasy that initiated accelerated soil erosion processes similar or even more severe to those mapped at present. During the Early Middle Ages the situation had worsened and flooding events increased in frequency and magnitude. Presumably, this may have been a consequence of the increased human pressure due to a changed land-use pattern. It is likely that the area was used only for wood supply during the era of the Roman Empire. The existence of a few settlements did not involve intensive land use. In contrast, during the Middle Ages the fragmentation of the area caused by the rise of urban centers and thus their populations led to a more intensive use of mountainous areas. Along with this, the growing population size and density called for an increased food supply, too. Moreover, it is important to emphasize the changed settlement preferences in the area during the Middle Ages, with a movement trend towards the hills as the preferred settlement location, as a result of encastellation (Cristallini et al., 2002). Hence, the FDR watershed, and from the broader perspective the entire Carseolani mountain region were most likely subject to an exploitation by human beings for settlements as well as for agricultural and grazing purposes.

The abundant and permanent presence of layers rich in charcoal in core PS-11 testifies to regular events of fire in the area during the period from 600 to 1400 AD. Nevertheless, archeological sources do not provide background information to specify the reasons or purposes for these fires (e.g., to produce charcoal, to facilitate farming and grazing, accidents).

To conclude, the data available only allow for a fragmentary reconstruction of the past human impact in the area. Nevertheless, the information acquired permits to significantly enhance the insights gained during the field experiments in the EX-01 and EX-02 watersheds. Furthermore, they provide some implicit information about soil erosion processes from a long-term perspective. The transition from the biostasy to the rhexistasy anthropic phase induced erosion processes and floods that were able to accumulate vast amounts of sediments in a relatively short period of time. As a consequence, the area left a phase of pedogenesis and entered a period of soil removal. The occurrence of the flood-prone phase coincided with the establishment of the Roman rural system in the Turano watershed area. It is thus clear evidence of the area's landscape sensitivity and its susceptibility to accelerated soil erosion. In the long run, the land-cover and the land-use changes in the study site seem to be more significant in terms of erosion than with regard to climatic change.

Chapter 9

Summary and Conclusions

9. SUMMARY AND CONCLUSIONS

9.1. SUMMARY

In order to reach the research goal, the set of investigation activities in the selected watershed was carefully chosen to conform to academic standards. It comprised of 1) the analysis of the climatic conditions of the Turano watershed, 2) spatially distributed modeling of soil erosion at watershed scale, 3) the measurement of soil erosion at hillslope-scale (field monitoring) and 4) an analysis of past and present human-induced soil erosion.

The observation of the climate characteristics allowed for the identification of the spatio-temporal variations of rainfall, temperature and snowfall within the watershed under consideration. Findings of this part of the study revealed that the mean annual precipitation of 1204 mm yr^{-1} in the Turano watershed exceeds the national average (970 mm yr^{-1}). For the period from 1997 to 2005, the mean annual erosivity value of the rainstorms was estimated at about 1942 MJ mm ha^{-1} h^{-1} yr^{-1}. In autumn and the second half of spring, the rainfall erosivity is higher than during winter and summer, approaching a maximum in September and a minimum in January. With regard to the spatial distribution of the rainfall erosivity, the maximum values have been associated with the mountainous area of the Simbruini' Mountains while the minimum values were obtained for the eastern sector of the valley area of the watershed. In these Apennine watersheds, a temporary snow cover on the soil surface constitutes another factor that can spatially influence soil erosion dynamics. However, across the study period, both, the spatial distribution and the temporal persistence of snow on the soil surface have been identified as critical influencing factors. They have consequently been integrated into the soil erosion modeling approach.

The application of the RUSLE and USPED models allowed maps of the soil erosion risk in the Turano watershed to be generated. Because these two models capture the complexity of soil erosion processes through different approaches, their outcomes are naturally rather heterogeneous. The RUSLE model predicted an annual mean gross erosion value of 11 t ha^{-1} yr^{-1} whereas the USPED model estimated 3.2 t ha^{-1} yr^{-1}. However, the outcomes of both models clearly coincide in identifying the areas that are more prone to soil erosion. The values of erosion obtained from the application of the two models emphasize that the form of territorial management provokes notable increases in the predicted erosion rates in both, agricultural land as well as forestland. In the case of forestlands that are subject to forest-harvesting activities, the predicted soil erosion rates increase by about 9 times when applying the RUSLE model and by 11 times when applying the USPED model. The use of NDVI data to estimate C-factor values enables the spatial and seasonal variations of the canopy cover density to be incorporated. This can greatly improve the model's prediction

quality of soil erosion. Considering the harvested forest area and the seasonal variations of the canopy cover, this study contributes to research by going beyond the widespread assumption of homogeneous land use in forest areas that soil erosion modeling has frequently been based on.

Another aspect observed at watershed scale was the SY dynamics of this intramountain watershed. With an annual average of measured area-specific sediment yield of 32.35 t ha^{-1} yr^{-1} the Turano watershed is among the Italian watersheds with the highest SY. Comparing the SY values estimated by the models with the actually measured siltation in Turano Lake the latter appeared to be significantly higher. The lower SY values predicted by the models (11 to 40 times lower for RUSLE; 76 times lower for USPED) indicate the inappropriateness of these types of models for the quantitative estimation of the watershed SY in Apennine environments. In fact, with respect to the Turano watershed the sediments with an inter-rill and rill genesis may represent only a minority share of the total eroded sediments that reach the watershed outlet. Furthermore, the Tu index approach has been found to provide the best performance for the SY prediction in the studied watershed. The characteristics of the drainage network have turned out to directly or indirectly play an important role in determining the SY value. The study activities carried out suggest further factors such as the locally high Dd values, the geographical distribution of the lithologies, the farmlands in the proximity of the main watershed's streams, the presence of landslides and the forest harvesting, which constitute concomitant causes of the high SY value in the watershed.

Direct monitoring of the changes in the post-forest-harvesting soil surface level at watershed scale indicates that the selected area can be confidently considered a soil erosion hot spot. Indeed, the actually measured mean soil erosion rate of 49 t ha^{-1} yr^{-1} for the EX-01 watershed (1.97 ha^{-1}) has been found to exceed the measured rate in undisturbed forested EX-02 watershed (2.3 t ha^{-1} yr^{-1}) by about 21 times. The soil erosion rate measured in the EX-01 watershed is one order of magnitude higher than the gross erosion values predicted by the RUSLE (3.9 t ha^{-1} yr^{-1}) and USPED (1.49 t ha^{-1} yr^{-1}) models for forestlands. From the research findings it also follows that if the C-factor is well calibrated the RUSLE and USPED models offer relatively good results in predicting soil erosion rates in harvested forest areas. However, for this task it would also be necessary to improve the DEM resolution. In the best case, researchers are advised to base their prediction on LiDAR data.

The sensitivity to human-induced soil erosion observed in the experimental first-order watershed (EX-01) has been confirmed by the long-term soil erosion information obtained from analyzing the alluvial sequences in the FDR sub-watershed. Thereby, an evident

transition from a flood-quiescence phase to a flood-prone phase that occurred between 200 and 2 BC has been identified. The occurrence of this flood-prone phase temporarily coincides with the arrival of the Romans in the area. During the Middle Ages the alluvial deposition experienced the highest sediment deposition rate which can be assumed to constitute the environmental response to an increased human perturbation of the natural dynamics of the area. As a further contribution to the missing research in the area, this study activity observed the exploitation of the forestland (e.g., forest harvesting, charcoal production, pasture) and the change in land use (e.g., agriculture, settlements) in the past and in the present, both of which caused severe soil degradation due to soil erosion.

The overall picture gained from the research activities carried out portrays an intramountain watershed with soil erosion processes due to human activities at a moderately high level. Although the croplands are mainly located in the flat alluvial plain with a low to moderate soil erosion potential, the large use of forestland for wood supply (i.e., coppicing) and the creation of pasturelands make some specific sectors of the watershed susceptible to severe risks of soil erosion. The topographic conformation and the high rainfall erosivity that characterize this Apennine watershed result in a high soil erosion risk that in combination with the removal of the vegetation easily gives rise to the occurrence of high soil erosion rates.

Still, the environmental effects of the accelerate processes of soil erosion could be mitigated through the use of soil conservation practices that are currently neither applied nor planned for in the area. The development of adequate management strategies for the watershed, especially for the areas affected by coppicing activities and overgrazing, may considerably diminish and in some cases even prevent processes of severe soil erosion. In doing so, the environmental value of these sensitive areas would be preserved. In this context, this study provides a cognitive contribution for research in order to reach a better understanding of the soil erosion phenomenon in central Italy's forested watersheds. It may also represent a useful point of departure to develop future sustainable land use planning strategies for these environments.

9.2. CONCLUSIONS

The overall aim of this research was to investigate the spatio-temporal pattern and dynamic changes of the soil erosion risk within the selected physiographic unit by means of various sophisticated investigation techniques. This study particularly paid attention to the observation of the evolution dynamics and the magnitude of soil erosion processes resulting from silviculture activities in forested area, i.e., cyclical forest harvesting and their inherent environmental impact.

The first fundamental research question posed during the planning phase of this study raised the issue of whether researchers systematically underestimate soil erosion rates of forested, mountainous watershed hillslopes and also misjudge the suspended sediment yields in the drainage networks. The extremely low number of studies in this kind of environments, particularly in the mountainous watersheds of Central Italy, could mislead to assume an absence of soil erosion processes with relevant damaging impacts on the environment. The outcomes of the present study, however, clearly demonstrate that this hypothesis must be rejected because several indications of high soil erosion risk were identified in the selected watershed. Importantly, with 1.33 M t^{-1} yr^{-1} of annual sediment yield, which is equal to an area-specific sediment yield of 32.35 t ha^{-1} yr^{-1}, the Turano watershed is among the Italian watersheds with the highest sediment discharge. These sediment yield values significantly exceed the 1-2 t ha^{-1} yr^{-1} soil erosion considered as the tolerable soil loss threshold for some European Countries (Verheijen et al., 2009). Consequently, high values of soil erosion, in addition to being an on-site problem causing the loss of the nutrient-rich upper layers of the soil, also have a huge impact on the water quality. This eroded soil, delivered to the water bodies is a physical and chemical pollutant that can cause a very serious threat for those mountainous watersheds, such as the Turano, that are exploited for drinking-water supply and hydropower production. Secondly, the results of the applied soil erosion prediction models indicate that sizable sectors of the study area are potentially prone to severe soil erosion rates. More specifically, the areas located on rather steep slopes of the northern-central part of the watershed and exploited for grazing, wood supply and agricultural purposes are soil erosion-prone. Excluding the undisturbed forested areas as well as the other natural areas of the Turano watershed from the soil loss calculation, high average annual soil erosion rates equal to 36.1 t^{-1} yr^{-1} and 11 t^{-1} yr^{-1} were predicted according to the RUSLE and USPED modeling approach, respectively.

The second research question targeted the soil erosion processes in forested areas disturbed by human activities. The specific modeling techniques adopted to predict soil erosion for the 19 km^2 of harvested forest show that these areas potentially produce an

amount of mobilized sediment equal to 45% of the amount mobilized in the total 270 km² undisturbed forest (equal to 79,218 t yr^{-1}). The verification of the results obtained from the theoretical soil erosion model prediction by means of numerous in situ field observations confirms the accuracy of the model predictions of soil erosion values. Especially, this is true for both, the qualitative results that were validated with the mapped soil erosion features in the Ovito sub-watershed as well as the quantitative results that were validated with on-site field observations, i.e., the measurement of the soil surface level change using metallic stakes in the two first-order watersheds EX-01 and EX-02.

Finally, one can conclude that the forested areas in the Turano watershed that are subject to forest harvesting are soil erosion-prone. As a result, this leads to the proposition that the areas of the Central Apennine region with similar environmental and human dynamics are soil erosion-prone too. The high soil erosion rates observed in the Turano watershed during the field measurements and the information gained from the past soil erosion dynamics evidently identifies these areas as soil erosion hot-spots. In addition, the extensive and systematic logging carried out over the centuries, starting with the Roman arrival in the area (299 BC), drastically altered the sediment yield of the watershed. In fact, the high erosion rates on the uplands of the past have assumingly mobilized huge amounts of sediments that were deposited in the dense drainage network of the Turano watershed and in its proximities. Thus, during high river flow events there is a re-entrainment of these sediment particles within or close to the drainage network which are transported and subsequently deposited in the Turano Lake. Although the forest harvesting impact, by itself, can hardly justify the high sediment yield obtained for the Turano River, this study nevertheless sheds light on the adequacy of using sediment yield data to re-calibrate models such as the RUSLE and WaTEM/SEDEM (van Rompaey et al., 2003) for the prediction of present upland soil erosion. This study therefore provides fruitful insights as these models currently result in a substantial overestimation of real upland erosion rates when applied in Italy. Hence, given the presented findings of this study, one could at least partly ascribe the overestimation to inappropriate use if sediment yields for re-calibration of the models without considering alternative sediment sources within the Italian watersheds, e.g., disturbed forestland, bank erosion with consequent bank failure and channel shifting, badlands and occurrence and type of mass movements.

9.3. FUTURE RESEARCH

This thesis provides valuable research intelligence about soil erosion within a narrowly defined area. Drawing on these in-depth insights, studies on the impact of forest-harvesting activities with the aim to enlarge the study area to the whole Italian country need to be pursued. The experience gained by means of the Turano watershed case study, which can be considered as a pilot area, can be used as a basis to develop a study methodology for the assessment of soil erosion risk in Italian forestlands. To do that, it is recommended to delineate the actual forest body of the country in a first step. Through a modeling approach, similar to the one used for the Turano watershed, the potentially soil erosion due to both forest harvesting and wild fires will be predicted across the entire country in a subsequent step. The proposed research undertaking should include a data set stretching at least over 20 years of observations as this period can be considered as adequately representing the entire cycle of forest coppicing.

Chapter 10

References

10. REFERENCES

'A'

Abbate, G., Frattaroli, A. R., Pace, L., (1994). 'Memoria illustrativa alla carta della vegetazione dell'area di Pietrasecca (scala 1:10.000).' In Ezio Burri editor, L'area carsica di Pietrasecca (Carsoli, Abruzzo). Studio multidisciplinare, Chieti. Istituto Italiano di Speleologia Memoria 5, pp. 159-164. (in Italian)

Accordi, G., Carbone, F., Civitelli, G., Corda, L., De Rita, D., Esu, D., Funiciello, R., Kostakis, T., Mariotti, G., Sposato, A., (1988). 'Note illustrative della carta delle litofacies del Lazio–Abruzzo ed aree limitrofe.' C.N.R., Prog. Fin. Geodinamica, Quad. della Ric. Scient., 114, pp. 223. (in Italian)

Accordi, G., and Carbone, F., (1986). 'Editors, Lithofacies map of Latium-Abruzzi and neighbouring areas. Scale 1:250,000.' Quad. Ric. Sci. 114.

Agassi, M., (1995). 'Soil erosion, conservation and rehabilitation'. Edited by Menachem Agassi. Marcel Dekker: New York.

Agnesi, V., Cappodonia, C., Conoscenti, C., Di Maggio, C., Marker, M., Rotigliano, E., (2006). 'Valutazione dell'erosione del suolo nel bacino del fiume San Leonardo (Sicilia centro-occidentale, Italia).' In Atti del Convegno Conclusivo del Progetto : Erosione dei suoli in ambiente mediterraneo: valutazione diretta e indiretta in aree sperimentali e bacini idrografici, pp. 13-27. (in Italian)

Agostini, S., (1994). 'Grotta del Cervo: archeologia e paleontologia.' Memorie dell'Istituto Italiano di Speleologia, 2, pp. 125-126. (in italian)

Agostini, S., and Gizzi, E., (1994). 'I reperti archeologici della grotta del Cervo (Abruzzo – Italia Centrale).' Memorie dell'Istituto Italiano di Speleologia, 2, pp. 127-134. (in italian)

Agostini, S., and Rossi, A., (1986). 'Il carsismo dei monti Carsiolani.' Proc. 9th Int. Speleol. Congr., Barcelona, pp. 199-202. (in Italian)

Agostini, S., (1994). 'Caratteri geologici e strutturali dell'anticlinale e del bacino di Pietrasecca (AQ) – Abruzzo.' Mem. Ist. Ital. Speleol., 2, pp. 13-21. (in Italian)

Agritec, (2004). "Piano preliminare di assetto della Riserva dei Monti Navegna e Cervia". Regione Lazio: Lazio. (in Italian)

Aguzzi, M., Amorosi, A., Colalongo, M.L., Ricci Lucchi, M., Rossi, V., Sarti, G., and Vaiani, S.C., (2007). 'Late Quaternary climatic evolution of the Arno coastal plain (Western Tuscany, Italy) from subsurface data.' Sedimentary Geology, 202, pp. 211-229.

AIA - Italian aerobiology association. 'Köppen Italian climate.' Online source available: http://www.ilpolline.it/clima-italia [Accessed May 2009].

Aksoy, H., Kavvas.H.L., (2005). 'A review of hillslope and watershed scale erosion and sediment transport models'. CATENA, 64, pp. 247-271.

Alessio, M., Allegri, L., Bella, F., Calderoni, G., Cortesi, C., Dai Pra, G., De Rita, D., Esu, D., Follieri, M., Improta, S., Magri, D., Narcisi, B., Petrone, V., and Sadori, L. (1989). '14C dating, geochemical features, faunistic and pollen analyses of the uppermost 10 m core from Valle di Castiglione (Rome, Italy).' Geologica Romana, 25, pp. 287-308.

Amore, E., Modica, C., Nearing, M.A., Santoro V.C., (2004). 'Scale effect in USLE and WEPP application for soil erosion computation from three Sicilian basins.' Journal of Hydrology, 293, pp. 100-114.

Anderson, B., and Potts, D.F., (1987). 'Suspended sediment and turbidity following road construction and logging in western Montana'. Southern Journal of Applied Forestry, 23, pp. 229-233.

Anderson S.P., Dietrich W.E., Montgomery D.R., Torres R., Conrad M.E., Loague K., (1997). 'Subsurface flow paths in a steep, unchanneled patterns.' Oikos, 49, pp. 340-346.

Angelucci, A., Chimenti, M., Pasquini, G.,. (1959). 'Nota preliminare su alcune ricerche geologiche e geomorfologiche nella grotta di attraversamento di Pietrasecca (M. Carseolani) e nel suo bacino di alimentazione.' Boll. Soc. Geol. Italiana, 79, pp. 1-14. (in Italian)

Antonioli, F., Ferranti, L., Fontana, A., Amorosi, A, Bondesan, A., BRAITENBERG C., Dutton, A., Fontolan, Gm, Furlani, S., Lambeck, K., Mastronuzzi, G., Monaco, C., Spada, Gm, and Stocchi, P., (2009). 'Holocene relative sea-level changes and vertical movements along the Italian and Istrian coastlines.' Quaternary International, 206, pp. 102-133.

APAT, AA.VV. (2002). 'Atlante delle opere di sistemazione dei versanti.' Manuali e linee guida 10/2002, Dipartimento difesa del suolo. (in Italian).

APAT, (2009). 'Annuario dei dati ambientali.' Online source available: http://annuario.apat.it/ [Accessed May 2009]. (in Italian)

APAT, AA.VV (2009). 'Carta geomorfologia d'Italia, Foglio 368 - Tagliacozzo.' Scale 1:50.000. APAT ed.

APAT - Chiarini E., D'Orefice M., Graciotti R.., La Posta E., Papasodaro F. (2008). 'Geomorphological map 367 – Tagliacozzo.'

Archydro ,(2010). Online source available: http://www.crwr.utexas.edu/gis/gishydro06/ Groundwater/ ArcHydro Groundwater ESRIUC2006.htm). [Accesses December 1998].

Ariathurai, R., Arulanandan, K., (1978). 'Erosion rates of cohesive soils.' Journal of the Hydraulics Division Proceedings of the ASCE, 104, pp. 279–283.

Arnáez, J., Larrea, V., Ortigosa, L., (2004). 'Surface runoff and soil erosion on unpaved forest roads from rainfall simulation tests in northeastern Spain.' CATENA, 57, pp. 1-14.

Arnold, J.G., Williams, J.R., (1995). 'SWAT – Soil and Water Assessment Tool'. Draft Users Manual, I. Temple, TX.

Arnoldus, H.M.J., (1977). 'Methodology used to determine the maximum potential average annual soil loss due to sheet and rill erosion in Morocco.' FAO Soils Bull, 34, pp. 39-51.

Arnoldus, H.M.J., (1980). 'An approximation of the rainfall factor in the USLE.' In M. DeBoodt and D. Gabriels, Editors, Assessment of Erosion, John Wiley & Sons: Chichester, pp. 127-132.

ARSAA - Cucchiarelli I., Paolanti M., Rivieccio, R, Santucci, S., (2006). 'Atlante dei suoli. Carta dei suoli della Regione Abruzzo a scala 250.000.' ARSSA Aruzzo, pp.247.

Aucelli, P. C., De Angelis A., Colombo C., Palumbo g., Scarciglia F., and Rosskopf C. M., (2006). 'La stazione sperimentale per la misura dell'erosione del suolo di Morgiapietravalle (Molise , Italia): Primi risultati sperimentali.' Atti del Convegno Conclusivo (PRIN/COFIN 2002): Erosione idrica in ambiente mediterraneo, valutazione diretta e indiretta in aree sperimentali e bacini idrografici, a cura di G. Rodolfi: Firenze, 17 Dicembre 2004, pp. 105-124. (in Italian)

Avena, G.C., Giuliano, G., Lupia Palmieri, E., (1967). 'Sulla valutazione quantitativa della gerarchizzazione ed evoluzione dei reticoli fluviali.' Boll. Soc. Geol. It., 86, pp. 781-796.

Avena, G. C., Lupia Palmieri, E., (1969). 'Analisi geomorfica quantitativa, in «Idrologia dell'alto bacino del Liri (Appennino Centrale)».' Geologica Romana, 8, pp.319-378. (in Italian)

Avesani S., (2009). Online sourcwe: www.sabinaonline.biz/territorio/valledelturano.htm [Accessed May 2009].

Avolio, S., Ciancio, O., Grinovero, C., Iovino, F., Mirabella, A., Raglione, M., Sfalanga, M., Torri, D., (1980). 'Effetti del tipo di bosco sull'entità dell'erosione in unità idrologiche della Calabria - modelli erosivi'. Annali Istituto Sperimentale Selvicoltura, 11, pp. 45-131. (in Italian)

Ayala, G., and French, C., (2005). 'Erosion modelling of past land use practices in the Fiume di Sotto di Troina river valley, North-Central Sicily.' Geoarchaeology, 20, pp. 149-167.

Ayres, Q., (1936). 'Soil Erosion and its Control'. MeGraw-Hill Book Company, Inc: New York.

'B'

Bagarello, V., Ferro, V., and Giordano, G., (1991).'Contributo alla valutazione del fronte di deflusso di Williams e del coefficiente di resa solida per alcuni bacini idrografici siciliani.' Rivista di ingegneria agraria, 4. (in Italian)

Bagarello, V., and Ferro, V., (2004). 'Plot-scale measurement of soil erosion at the experimental area of Sparacia (southern Italy).' Hydrological Processes, 18, pp. 141-157.

Bagarello, V., Ferro, V.,Giordano, G., Mannocchi, F., Pampalone, V., Todisco, F., Vergni, L., (2011). 'Effect of plot size on measured soil loss for two Italian experimental sites.' Biosystems Engineering, 108, pp. 18-27.

Bagnouls, F., Gaussen, H., (1953). 'Saison sache et indexe xerothermique.' Bulletin Sociètè Historique Naturalistic de Tolouse, pp. 3-30.

Baihua Fu, Lachlan, Newham, T.H., and Ramos-Scharrón, C.E., (2010). 'A review of surface erosion and sediment delivery models for unsealed roads'. Environmental Modelling & Software, 25, pp. 1-14.

Barbieri, M., D'Orefice, M., Raciotti, R., (1998). 'Datazione radiometrica di un deposito colluviale in un conoide situato nel settore meridionale della Piana del Cavaliere (Appennino Lazioale-Abruzzese).' Geog. Fis. Del Quat., 21, pp. 267-269. (in Italian)

Bartole, R., (1995). 'The North Tyrrhenian–Northern Apennines postcollisional system: constraints for a geodynamic model.' Terra Nova, 7, pp. 7-30.

Basso, F., (1995). 'Difesa del Suolo e Tutela dell'Ambiente.' Pitagora (Ed.): Bologna, pp.486.

Baumler, R., Zech, W., (1997). 'Atmospheric deposition and impact of forest thinning on the throughfall of mountain forest ecosystems in the Bavarian Alps'. Forest Ecology and Management, 95, pp. 243-251.

Bazzoffi, P., Baldassarre, G., Vacca, S., (1996). 'Validation of PISA2 model for automatic assessment of reservoir sedimentation'. In: Albertson, M. (Ed.), Proceedings of the International Conference on Reservoir Sedimentation. Colorado State Univ., pp. 519-528.

Beasley, D.B., Huggins, L.F., Monke, E.J., (1980). 'ANSWERS: a model for watershed planning'. Transactions of the ASAE, pp. 938-944.

Bell, M., Boardman, J., (1992). 'Past and present soil erosion – archeological and geographical perspectives'. Oxbow Monograph, 22: Oxford.

Bellotti, P., Milli, S., Tortora, P., and Valeri P., (1995). 'Physical stratigraphy and sedimentology of the LatePleistocene-Holocene Tiber Delta depositional sequence.' Sedimentology, 42, pp. 617-634.

Bellotti, P., Caputo, C., Davoli, L., Evangelista, C., Garzanti, E., Pugliese F., and Valeri, P., (2004). 'Morpho-sedimentary characteristics and Holocene evolution of the emergent part of the Ombrone River delta (southern Tuscany).' Geomorphology, 61, pp. 71-90.

Bernacca, E., (1972). 'La previsione del tempo e i climi della Terra di'Italia.' Monograph published by Casa Editrice La Scuola: Brescia, pp. 88. (in Italian)

Bertolani, M., Lugli, S., and Rossi, A., (1994). 'Studio petrografico delle grotte di attraversamento di Pietrasecca (L'Aquila- Italia Centrale).' Mem. Ist. Ital. Speleol., 2, pp. 71-83.

Beven, K.J., Kirkby, M.J., (1979). 'A physically-based variable contributing area model of basin hydrology.' Hydrological Sciences Bulletin, 24, pp. 43-69.

Beven, K.J., (2001). 'Rainfall-Runoff Modelling'. The Primer, Wiley: Chichester.

Biasini, A., Buonasorte, G., Fredi, P., Lupia Palmieri, P., (1983). 'Bacino dell'Ovito – Pietrasecca. Carta tematica in scala 1:15.000 e 1:25.000.' Istituto di Geologia e Paleontologia – Università di Roma, Multigrafica Editrice: Rome. (in Italian)

Bigi, S., Calamita, F., Cello, G., Centamore, E., Deiana, G., Paltrinieri, W., Ridolfi, M., (1996). 'Evoluzione messiniano-pliocenica del sistema catena-avanfossa nell'area marchigiano-abruzzese esterna.' Studi Geologici Camerti, Volume Speciale, 1, pp. 29-35. (in Italian)

Bigi, S., Costa Pisani, P. (2005). 'From a deformed Peri-Tethyan carbonate platform to a fold-and-thrust-del: an example from the Central Apennines (Italy).' Journal of Structural Geology, 27, pp.523-539 Bizzini, F., Caruano, R.,, and Collana, P., (2009). 'The silting problem for resevoirs of Italian large dams.' Commision Internationale Des Grands Barrager. Brasilia, May 2009. Online source: http://www.itcold.it/data/q89-r12_5.pdf [Accessed Febrary 2011].

Blasi, C., (1993). 'Carta del fitoclima del Lazio (regionalizzazione).' Regione Lazio, Ass. Agricoltura-Foreste Caccia e Pesca, Usi civili; Università 'La Sapienza' - Roma - Dip. Biologia Vegetale. (in italian).

Blasi, C., (1996). 'Il fitoclima d'Italia.' Plant Biosystem. 130, pp. 166-176. (in Italian)

Boardman, J., Ligneau, L., De Roo, A.P.J., Vandaele, K., (1994). 'Flooding of property by runoff from agricultural land in northwestern Europe'. Geomorphology, 10**,** pp. 183-196.

Boardman, J., (2006). 'Soil erosion science: reflections on the limitations of current approaches'. Catena, 68, pp.73-86.

Boardman, J., and Poesen, J., (2006). 'Soil Erosion in Europe'. Wiley: Chichester, pp. 878.

Bochet, E., Poesen, J., and Rubio, J. L., (2006). 'Runoff and soil loss under individual plants of a semi-arid Mediterranean shrubland: influence of plant morphology and rainfall intensity'. Earth Surface Processes and Landforms Earth Surf. Process. Landforms, 31, pp. 536–549.

Bono, P., Capelli, G., (1994). 'Idrologia sotterranea e di superficie dei monti Carseolani (Italia Centrale).' Istituto Italiano di Speleologia. Memoria, 5,pp. 23-45. (in Italian)

Borghetti, M., Magnani, F., (2009). 'Controllo dell'uso dell'acqua nei sistemi forestali'. Atti del III Congresso Nazionale di Selvicoltura, Taormina, 15-19 Ottobre 2008.

Bosch, J.M., Hewlett J.D., (1982). 'A review of catchment experiments to determine the effects of vegetation changes on water yield and evaporation'. Journal of Hydrology, 55, pp. 3-23.

Bradford, J.M., Huang, C., (1993). 'Comparison of interill soil loss for laboratory and field procedures.' Soil Technology, 6, pp. 145-156.

Bronk Ramsey, C., (2010). http://c14.arch.ox.ac.uk/oxcalhelp/hlp_contents.html

Brown , L.C. and Foster, G.R., (1987). 'Storm erosivity using idealized intensity distributions.' Transaction of the ASAE, 30, pp. 379-386.

Brown, E., Lu Zhang, McMahon, T.A., Western, A.W., Vertessy, R.A., (2005). 'A review of paired catchment studies for determining changes in water yield resulting from alterations in vegetation'. Journal of Hydrology, 310, pp. 28-61.

Brunori, C.A., Oliveri, S., Luzi, Zilioli, L., and Eugenio (1998). 'GIS and remote sensing techniques integration aimed forthe evaluation of the Esino catchment impact on coastalwater quality.' Editors: Cecchi, Giovanna. Zilioli, Eugenio; Istituto di Ricerca sul Rischio Sismico/CNR (Italy). Online source: http://dx.doi.org/10.1117/12.332731 [Accessed December 2010].

Bryan, R.B., and Poesen, J., (1989). 'Laboratory experiments on the influence of slope length on runoff, percolation and rill development.' Earth Surface Processes and Landforms, 14, pp. 211-231.

Bryan, R. B., (2000). 'Soil erodibility and processes of water erosion on hillslope.' Geomorphology, 32, pp. 385-415.

Bucci M., (1978). 'Studio idrogeologico ed idrografico dei bacini rappresentativi dell'Ovito (Pietrasecca) e di Camposecco (Pereto) anni 1976-77-78.' Diploma thesis. La Sapienza University. Rome. (in Italian)

Burch, G.J., Bath, R.K., Moore, I.D., and O'Loughlin, E.M., (1987). 'Comparative hydrological behaviour of forested and cleared catchments in southeastern Australia', Journal of Hydrology, 90, pp. 19-42.

Burlando, P., and Rosso, R., (2002). 'Effects of transient climate change on basin hydrology. Precipitation scenarios for the Arno River, central Italy.' Hydrological Processes, 16, pp. 1151-1175.

'C'

Candela, A., Ciraolo, G., Noto, L., and Santoro, M., (2006). Stima dell'erosione idrica in due bacini siciliani mediante tecniche GIS. Online source: http://surplus.unipa.it/oa/handle/10447/19345 [Accessed Febrary 2009]. (in Italian)

Calderini, G., Calderoni, G., Cavinato, G.P., Gliozzi, E., and Paccara, P., (1998). 'The upper Quaternary sedimentary sequence at the Rieti Basin (central Italy): A record of sedimentation response to climatic changes.' Palaeogeography, Palaeoclimatology, Palaeoecology, 140, pp. 97-111.

Calderoni, G., Carrara, C., Ferreli, L., Follieri, M., Gliozzi, E., Magri, D., Narcisi, B., Parlotto, M., Sadori, and L., Serva, L., (1994). 'Palaeoenvironmental, palaeoclimatic and chronological interpretations of a late Quaternary sediment core from Piana di Rieti (central Apennines, Italy).' Geologia, 56, pp. 43-72

Callegari, G., Iovino F., Mendicino, V., Veltri A., (2001). 'Hydrological balance and soil erosion in Eucalyptus coppices (Eucalyptus occidentalis, Endl.)'. Proceedings of the

International Conference: Eucalyptus in the Mediterranean basin: perspectives and new utilization. Centro Promozione Pubblicità: Florence, p. 283-290.

Callori di Vignale, C. 1981. 'Studio idrogeologico e idrologico dei bacini rappresentativi dell'Ovito (Pietrasecca) e Camposecco (Pereto).' Thesis. Università degli Studi di Roma la Sapienza. Facoltà di Scienze Matematiche Fisiche e Naturali. Rome. (in Italian)

Campo, J., Andreu, V., Gimeno-García, E., González O., and Rubio, J.L., (2006). 'Occurrence of soil erosion after repeated experimental fires in a Mediterranean environment'. Geomorphology, 82, pp. 376-387.

Cantore, V., Iovino, F., and Puglisi, S., (1994). 'Influenza della forma di governo sui deflussi liquidi e solidi in piantagioni di eucalitti'. L'Italia Forestale e Montana, 5, pp. 463-477. (in Italian)

Caporali E., Tartaglia V., (2002). 'Analisi multivariata della variabilità spaziale delle piogge indice.' 28° Convegno di Idraulica e Costruzioni idrauliche: Potenza, pp. 16-19 Online source:
http://difa.unibas.it/jFM/laboratori/CostrIdr/SitoConvegno2008/articoliPDF/PDF[Accessed 2010].

Capolongo, D., Pennetta, L., Piccarreta, M., Fallacara G., and Boenzi, F., (2008). 'Spatial and temporal variations in soil erosion anddeposition due to land-levelling in a semi-arid areaof Basilicata (Southern Italy).' Earth Surf. Process. Landforms, 33, pp. 364-379.

Capolongo, D., Diodato, N., Mannaerts, C.M., Piccarreta, M., and Strobl, R.O., (2008b). 'Analyzing temporal changes in climate erosivity using a simplified rainfall erosivity model in Basilicata (southern Italy).' Journal of Hydrology, 356, pp. 119-130.

CARG, (2010). 'Geological maps.' Online: http://www.isprambiente.gov.it/MEDIA/carg/lazio.html

Carminati, E., Corda, L., Mariotti, G., Brandano, M. (2007). 'Tectonic control on the architecture of a Miocene carbonate ramp in the Central Apennines (Italy): Insights from facies and backstripping analyses.' Sedimentary Geology, 198, pp. 233-253.

Carrozzoni P. (1986). 'Collepiccolo e la Valle del Turano.' Stampato a cura della Comunità montana Turano. Editrice Il Velino. Rieti. (in Italian)

Castiglioni, G.B., (1933). 'Osservazioni sui calanchi appenninici'. Boll.Soc. Geol. It., 52.

Castiglioni, G.B., (1986). 'Geomorfologia.' Utet: Torino, pp. 436.

Cavinato, G.P., De Celles, P.G., (1999). 'Extensional basins in the tectonically bimodal central Apennines fold–thrust belt, Italy: response to corner flow above a subducting slab in retrograde motion.' Geology, 27, pp. 955-958.

Ceccarelli, T., Giordano, F., Luise, A., Perini, L., Salvati, L., (2006). 'La vulnerabilità alla desertificazione in Italia: raccolta, analisi, confronto e verifica delle procedure cartografiche di mappatura e degli indicatori a scala nazionale e locale'. APAT, CRA UCEA, Manuali e linee guida 40/2006, ISBN – 88-448-02010-4. (in Italian)

Centamore, E., Ciccacci, S., Del Monte, M., Fredi P., and Lupia Palmieri, E., (1996). 'Morphological and morphometric approach to the study of the structural arrangement of northeastern Abruzzo (central Italy).' Geomorphology, **16,** pp. 127-137.

Cerdan, O., Souchère, V., Lecomte, V., Couturier A., and Le Bissonnais, Y., (2002). 'Incorporating soil surface crusting processes in an expert-based runoff model: STREAM (Sealing and Transfer by Runoff and Erosion related to Agricultural Management)'. Catena, 46, pp. 189-205.

Cerdan, O., Poesen, J., Govers, G., Saby, N., Le Bissonnais, Y., Gobin, A., Vacca, A., Quinton, J., Auerswald, K., Klik, A., Kwaad, F.P.M., and Roxo, M.J., (2007). 'Sheet and Rill Erosion'. In: J. Boardman and J. Poesen, Editors, Soil Erosion in Europe, Wiley: Chichester, pp. 501-513.

Cerdan, O., Govers, G., Le Bissonnais, Y., Van Oost, K., Poesen, J., Saby, N., Gobin, A., Vacca, A., Quinton, J., Auerswald, K., Klik, A., Kwaad, F.J.P.M., Raclot, D., Ionita, I., Rejman, J., Rousseva, S., Muxart, T., Roxo, M.J., Dostal. T., (2010). 'Rates and spatial variations of soil erosion in Europe: A study based on erosion plot data.' Geomorphology, 122, pp. 167-177.

Cernusca, A., Bahn, M., Chemini, C., Graber, W., Siegwolf, R., Tappeiner, U., and Tenhunen, J., (1998). 'ECOMONT: a combined approach of field measurements and process-based modelling for assessing effects of land-use changes in mountain landscapes.' Ecological Modelling, 113, pp. 167-178.

Chapline, W. R., (1929). 'Erosion on rangeland'. Jou. Am. Soc. Agron., 21, pp. 423-429.

Chisci, G., (1986). 'Influence of change in Land use and management on the acceleration of land degradation phenomena in Apennine hilly areas.' In G. Chisci and Morgan R.P.C. – Soil erosion in the European Community: Balkema.

Chisci, G., Bazzoffi, P., (1995). 'Fruttiviticoltura di collina, limitazione dell'erosione edell'inquina-mento.' Interventi agrobiologici. Agricoltura, 10, pp. 41-45.

Ciampalini, R., and Torri, D., (1998). 'Detachment of soil particles by shallow flow: Sampling methodology and observations'. Catena, 32, pp. 37-53.

Ciabatti, M., (1982). 'Elementi di idrologia superficiale.' Libreria Universitaria Editrice: Bologna. Ciancio O., Corona P., (2000). 'Risorse forestali italiane e prospettive di sviluppo'. Accademia delle Scienze: Roma. (in Italian)

Ciancio. O., and Nocentini. S., (2004). 'Il bosco ceduo. Selvicoltura Assestamento Gestione'. Accademia Italiana di Scienze Forestali. Florence, pp. 721. (in Italian)

Ciancio O., Iovino F., Menguzzato A., Nicolaci A., Nocentini S., (2006). 'Structure and growth of a small group selection forest of calabrian pine in Southern Italy: A hypothesis for continuous cover forestry based on traditional silviculture'. Forest Ecology and Management, 224, pp. 229-234.

Ciccacci, S., Fredi, P., and Lupia Palmieri, E. (1977). 'Rapporti fra trasporto solido e parametri climatici e geomorfici in alcuni bacini idrografici italiani.' Workshop 'Misura del trasporto solido al fondo nei corsi d'acqua', Consiglio Nazionale delle Ricerche: Florence. (in Italian)

Ciccacci, S., Fredi, P., Lupia Palmieri, E., Pugliese, F., (1980). 'Contributo dell'analisi geomorfica quantitativa alla valutazione dell'entità dell'erosione nei bacini fluviali.' Boll. Soc. Geol. It., 99, pp. 455-516. (in Italian)

Ciccacci, S., D'Alessandro, L., Fredi, P., (1983). 'Sulla valutazione indiretta dell'interrimento nei bacini lacustri: il lago artificiale di Scandarello (Rieti)'. Atti XXIII Congr. Geogr. It., Catania, pp. 37-52. (in Italian)

Ciccacci, S., Fredi, P., Lupia Palmieri, E., Salvini, F., (1986). 'An approach to the quantitative analysis of the relations between drainage pattern and fracture trend.' In Intemational Geomorphology, volume Part II, pp. 49-68.

Ciccacci, S., D'Alessandro, L., Fredi, P., and Lupia Palmieri, E., (1988). 'Contributo dell'analisi geomorfica quantitativa allo studio dei processi di denudazione nel bacino idrografico del torrente Paglia (contribution of the quantitative geomorphic analysis to the

study of denudation processes in the Paglia stream catchment, Toscana, Italy).' Suppl Geogr Fis Dinam Quat., 1, pp. 171-188. (in Italian)

Ciccacci, S., D'Alessandro, L., Fredi, P., Lupia Palmieri, E., (1992). 'Relation between morphometric characteristics and denudation processes in some drainage basins of Italy.' Zeit. Geomorph. N. F., 36, pp. 53-67.

Ciccacci, S., Delm Monte, M., Lupia Palmieri, E., and Salvatore M.C., (2006). 'Entità dei processi di denudazione e variazioni morfologiche recenti nell'area di radiocofani (Toscana Meridionale).' Atti del Convegno Conclusivo (PRIN/COFIN 2002): Erosione idrica in ambiente mediterraneo, valutazione diretta e indiretta in aree sperimentali e bacini idrografici, a cura di G. Rodolfi: Florence, pp. 29-64. (in Italian)

Colacicchi, R., Bizzarri, R., (2008). 'Correlation between environmental evolution, hystorical settlement and cultural heritage upgrading in Valle Umbra (central Italy).' Geogr. Fis. Dinam. Quat., 31, pp. 107-118.

Colica, A., Lorenzoni, P., Magaldi, D., and Raglione, M., (1995). 'Geologia del quaternario e lineazioni nella conca tettonica tra Oricola e Carsoli in provincia dell'Aquila.' Boll. Serv. Geol. D'Italia, 112, pp. 49-58. (in Italian)

Cooke, R.U., and Doornkamp, J.C., (1974). 'Geomorphology in Environmental Management.' Clarendon: Oxford.

Corda, L., Esu, D., Katsakis, T., and Mariotti, G., (1986). 'Marine and continental syn-postorogenic sequances.' In Accordi et al., CNR, Quaderni de 'La Ricerca Scientidica' 144, pp. 223.

Corda, L., Brandano, M., (2003). 'Aphotic zone carbonate production on a Miocene ramp, Central Apennines, Italy.' Sedimentary Geology, 161, pp. 55-70.

Cremaschi, M., Rodolfi, G. (1991). 'Il suolo – Pedologia nelle scienze della terra e nella valutazione del territorio.' Nuova Italia Scientifica (NSI): Roma. (in Italian)

Cristallini, C., Calabri, E., Castiglia, G., Bonifazzi A., (2002). 'La tenuta regionale di Sala.' Regione Lazio. Rubbettino editore: Lazio. (in Italian)

Croke, J., Hairsine, P., and Fogarty, P., (2001). 'Soil recovery from track construction and harvesting changes in surface infiltration, erosion, and delivery rates with time'. Forest Ecology and Management, 143, pp. 3-12.

Cucchiarelli, I., Paolanti M., Rivieccio, R, Santucci, S., (2006). 'Atlante dei suoli. Carta dei suoli della Regione Abruzzo a scala 250.000.' ARSSA Aruzzo, pp. 247. (in Italian)

'D'

De Asis, A.M., Omasa, K., (2007). 'Estimation of vegetation parameter for modeling soil erosion using linear Spectral Mixture Analysis of Landsat ETM data.' ISPRS Journal of Photogrammetry and Remote Sensing, 62, pp. 309.324.

De Jong, S.M., Brouwer, L.C., Riezebos, H. T. (1998). 'Erosion hazard assessment in the Peyne catchment, France.' Working paper DeMon-2 Project. Dept. Physical Geography: Utrecht University.

De Meo, M., (2006).'Tecniche costruttive murarie medioevali: La Sabina.' L'Erma di Bretschneider. Roma. (in Italian)

De Moor, J.J.W., Kasse, C., van Balen, R., Vandenberghe, J.,Wallinga, J., (2008). 'Human and climate impact on catchment development during the Holocene - Geul River, the Netherlands'. Geomorphology, 98, pp. 316-339.

De Philippis, A., (1970). 'La copertura forestale e la difesa del suolo'. Diploma thesis. Istituto di Tecnica e Propaganda Agraria, Rome. (in Italian)

De Ploey, J., (1977). 'Some experimental data on slopewash and wind action with reference to Quaternary morphogenesis in Belgium.' Earth Surface Processes, 2, pp. 101-116.

De Roo, A.P.J., Offermans, R.J.E., Cremers, N.H.D.T., (1996). 'LISEM: a single-event physically based hydrological and soil erosion model for drainage basins. II: sensitivity analysis, validation and application'. Hydrol. Proc., 10, pp. 1119-1126.

De Vecchis, G., (2004). 'Un futuro possibile per la montagna italiana.' Kappa: Rome. (in Italian)

De Vente, J., Poesen, J., (2005). 'Predicting soil erosion and sediment yield at the basin scale: scale issues and semi-quantitative models'. Earth-Sci. Rev., 71, pp. 95-125.

De Vente, J., Poesen, J., Bazzoffi, P., Van Rompaey, A., and Verstraeten, G., (2006). 'Predicting catchment sediment yield in Mediterranean environments: the importance of sediment sources and connectivity in Italian drainage basins.' Earth Surface Processes and Landforms, 31, pp. 1017-1034.

De Vente, J., Poesen, J., Arabkhedri, M., and Verstraeten G., (2007). 'The sediment delivery problem revisited.' Progress in Physical Geography, 31, pp. 155-178.

De Vitis, F., (1985). 'Centri storici minori: considerazioni urbanistiche ed architettoniche, in Architettura e Arte nella Marsica, 1984-1985.' I. Architettura, Sop Beni Amb. Arch. Stor. Abruzzo, Marcello Ferri ed., L'Aquila, pp.48. (in Italian)

Di Lisio, A., Aucelli, P.P.C., and Russo , F., (2010). 'Analisi morfometrica ed elaborazione in automatico di dati geomorfologici delVallone Grande del Fiume Biferno (Molise, Italia).' Online source: http://www.gitonline.eu/pdf_sanleo/poster/Di%20Lisio.pdf (in Italian)

Del Monte, M., (1996). 'Rapporti tra caratteristiche morfometriche e processi di denudazione nel bacino idrografico del torrente Calandrella (Basilicata).' Geol. Rom., 32, pp. 151-165. (in Italian)

Del Monte, M., Fredi, P., Lupia Palmieri, E., and Marini, R., (2002). 'Contribution of quantitative geomorphic analysis to the evaluation of geomorphological hazards.' In Applied Geomorphology: Theory and Practice, Allison R.J. (ed.): J. Wiley & Sons, pp. 335-358.

Del Monte, M., Fredi, P., Lupia Palmieri E., and Marini R., (2002). 'Contribution of quantitative geomorphic analysis to the evaluation of geomorphological hazards.' In R. Allison, Ed., Applied Geomorphology: Theory and Practice,Wiley: Chichester, pp. 335-358.

Del Monte, M. (2003). 'Caratteristiche morfometriche e morfodinamiche dell'alto bacino del Fiume Orcia (Toscana meridionale).' Atti del XXVIII Congresso Geografico Italiano: Rome, pp. 1938-1975. (in Italian)

Della Seta, M., Del Monte, M., Fredi, P. and Palmieri, E.L., (2007). 'Direct and indirect evaluation of denudation rates in Central Italy.' Catena, 71, pp. 21-30.

Della Seta, M., Del Monte, M., Fredi, P. and Lupia Palmieri, E., (2009). 'Space-time variability of denudation rates at the catchment and hillslope scales on the Tyrrhenian Side of Central Italy.' Geomorphology, 107, pp. 161-177.

Dean, W. E. Jr., (1974). 'Determination of carbonate and organic matter in calcareous sediments and sedimentary rocks by loss on ignition: Comparison with other methods.' J. Sed. Petrol., 44, pp. 242–248.

Dennis, M., Rorke, F., Bryan, B., (1982). 'The relationship of soil loss by interrill erosion to slope gradient.' CATENA, 38, pp. 211-222.

Desmet, P.J.J., and Govers, G., (1996). 'A GIS procedure for automatically calculating the USLE LS factor on topographically complex landscape units.' Journal of Soil and Water Conservation, 51, pp. 427-433.

Diodato, N., (2004). 'Estimating RUSLE's rainfall factor in the part of Italy with a Mediterranean rainfall regime'. Hydrology and Earth Sciences, 8, pp. 103-107.

Dissmeyer, G.E., and Foster. G.R., (1984). 'A guide for predicting sheet and rill erosion on forest land'. USDA Forest Service, State Priv. For. Tech. Publ. R8-TP-6, pp. 40.

Doglioni, C., (1991). 'A proposal for the kinematic modelling of Wdipping subductions; possible applications to the Tyrrhenian-Apennines system.' Terra Nova, 3, pp. 423-434.

Dotterweich, M., (2008). 'The history of soil erosion and fluvial deposits in small catchments of central Europe: Deciphering the long-term interaction between humans and the environment - A review.' Geomorphology, 101, pp. 192-208.

Dragoni, W., (1996). 'Response of some Hydrogeological Systems in Central Italy to climatic variations.' In A.N. Angelakis & A.S. Issar (Eds.), «Diachronic Climatic Impact on Water Resources». NATO ASI Series, Vol. 1, 36, Springer Verlag, Berlin-Heidelberg, pp. 193-212.

Dramis, F., and Gentili, B., (1977). 'I parametri F (Frequenza di drenaggio) e D (Densità di drenaggio) e le loro variazioni in funzione della scala di rappresentazione cartografica.' Bollettino della Società Geologica Italiana, 96, pp. 637-651. (in Italian)

Dubayah, R., and Rich, P.M., (1995). 'Topographic solar radiation models for GIS.' Int. J Geographical Information Systems, 9, pp. 405-419.

Ducci, D., (1999). 'The spatial variability of climatic data in the Hydrogeologic budgets.' Proceedings of International Conference on 'ModelCARE 1999', II, pp. 673-678.

Dunne, T., (1978). 'Field studies of hillslope flow processes'. In M. J . Kirkby (ed.), Hillslope Hydrology. John Wiley and Sons: Chichester, pp. 227-293.

Dunne, T., and Leopold, L.B., (1978). 'Water in Environmental Planning.' Freeman: San Francisco, pp. 818.

'E'

EEA- CORINE, (1992). 'Soil erosion risk and important land resources in the southern regions of the European Community'. Final report EUR 13233-EN, European Environment Agency.

Edeso, J. M., Merino, A., Gonzalez, M.J., and Marauri, P., (1999). 'Soil erosion under different harvesting managements in steep forestlands from northern Spain'. Land Degradation and Development, 10, pp. 79-88.

Ellison, WD., (1945). 'Some effects of raindrops and surface flow on soil erosion and infiltration'. Transactions of American Geophysics Union, 26, pp. 415–429.

Elustondo, J., Angers, D.A., Laverdière, M.R. and N'dayegamiye, A., (1990). 'Influence de la culture de maïs et de la prairie sur l'agrégation et la matière organique de sept sols de Québec.' Can. J. Soil Sci., 70, pp. 395-403.

Engel, B., Mohtar, R., (1999). 'Estimating soil erosion using RUSLE (Revised Universal Soil Loss Equation) and the ArcviewGIS.' Purdue University.

ENVCO, 2010- ENVCO – Environmental Equipment. Online Source: www.envcoglobal. com /catalog/product/infiltrometer/mini-disk-infiltrometer.html [Accessed June 2009].

Eurostat, (2009). Online source: http://epp.eurostat.ec.europa.eu/portal/page/portal/ agriculture/ introduction [Accessed Febrary 2011].

Ewen, J., Parkin, G., O'Connell, P.E., (2000). 'SHETRAN: a coupled surface/subsurface modelling system for 3D water flow and sediment and solute transport in river basins'. ASCE J. Hydrol. Eng., 5, pp. 250-258.

'F'

Falace, M., (2007). 'Contributo alla valutazione del dissesto idrogeologico nel bacino sperimentale Bonis: stima dell'incertezza spaziale del fattore di erodibilità del suolo K'. PhD Thesys. (in Italian)

Fanelli, M., Fanelli, M., Niccolai, C., (2000). 'La creazione di riserve idriche tramite sbarramenti: implicazioni ambientali e finanziarie'. INGENIERÍA DEL AGUA, 7, pp. 14-25. (in Italian)

Faniran, A., (1968). 'The index of drainage intensity: a provisional new drainage factor.' Aust. J. Sci., 3, pp. 328-330.

FAO, (1976). 'A Framework for Land Evaluation'. FAO Soils Bulletin No. 32. FAO, Rome. FAO, (1993). 'Field measurement of soil erosion and runoff'. Soils Bulletin No. 68, Ed. Rome: N. W. Hudson.

FAO, (1998). 'World reference base for soil resources.' World Soil Resources Rep. 84, Rome.

Farabegoli, E., and Agostini, C., (2000). 'Identification of calanco, a badland landform in the northern Apennines, Italy.' Earth Surf. Process. Landforms, 25, pp. 307-318.

Farifteh, J., and Soeters, R., (2006). 'Origin of biancane and calanchi in East Aliano, southern Italy'. Geomorphology, 77, pp. 142-152.

Favis-Mortlock, D., Boardman, J., Bell, M., (1997). 'Modeling long-term atrophogenic erosion of a loess cover: South Downs'. Holocene, 7, pp. 79-89.

Fazzini, M., (1997). 'Analisi Statistica delle principalicaratteristichemeteoclimatichedella Regione Marcheanche in funzione di alcuni parametrigeografici e geomorfologici.' Thesis, Università di Camerino. (in Italian)

Felix-Henningsen, P., Morgan, R.P.C., Mushala, H.M., Richson, R.J., and Scholten, T., (1997). 'Soil erosion in Swaziland: A synthesis.' Soil Technology, 11, pp. 319-329.

Ferrari, E., Iovino, F., Veltri, A., (2004). 'Bosco e ciclo dell'acqua: aspetti metodologici ed applicativi'. In Tecniche per la difesa dall'inquinamento, Editoriale Bios: Cosenza, pp. 645-660.

Ferrari, R., Pasqui, M., Bottai, L., Esposito, S., and Di Giuseppe E., (2005). 'Assessment of soil erosion estimate based on a high temporal resolution rainfall dataset.' In Proc. 7th European Conference on Applications of Meteorology (ECAM), 12-16 September 2005: Utrecht.

Ferro, V., Porto P., Tusa, G., (1998). 'Testing a distributed approach for modelling sediment delivery.' Hydrological Sciences Journal, 43, pp. 425-442.

Ferro, V., Di Stefano, C., Minacapilli, M., and Santoro, M., (2003). 'Calibrating the SEDD model for Sicilian ungauged basins.' In Erosion prediction inungauged basins: integrating methods and techniques, De Boer D, Froehlich W, Mizuyama T, Pietroniro A (eds). IAHS Publication 279: Sapporo, pp. 151-161.

Flanagan, D.C., Livingston, J., (1995). 'USDA WEPP: Hillslope profile and watershed model documentation'. NSERL Report No. 11. USDA-ARS National Soil Erosion Research Laboratory: West Lafayette.

Fournier, F., (1960). 'Climat et erosion.' Presses Universitaires de France, Paris. Ferrari' R., Pasqui' M., Bottai' L., Esposito' S., Di Giuseppe' E.' (2005). 'Assessment of soil erosion estimate based on a hightemporal resolution rainfall dataset.' In Proc. 7th European Conference on Applications of Meteorology (ECAM): Utrecht, pp. 12-16.

Foster, G.R., and L.D. Meyer, (1972). 'A closed-form soil erosion equation for upland areas'. In: Shen, H.W. (Ed.), Sedimentation Symposium in Honor Prof. H.A. Einstein. Colorado State University: Fort Collins, pp. 1-19.

Foster, G.R., Lane, L.J., Nowlin, J.D., Laflen, J.M., Young, R.A., (1981). 'Estimating erosion and sediment yield on field-sized areas'. Transactions of the ASAE, pp. 1253-1262.

Foster, I.D.L., Mighall, T.M., Wotton, C., Owens P.M., and Walling, D.E., (2000). 'Evidence for Mediaeval soil erosion in theSouth Hams region of Devon, UK'. The Holocene, 10, pp. 261-271.

Foster, G.R., (1982). 'Modeling erosion process. In Hydrologic Modeling of Small Watersheds'. C.T. Hann, ed., ASAE Monograph, 5: St. Joseph, pp. 298-379.

Foster, I. D. L., (1995). 'Lake and reservoir bottom sediments as a source of soil erosion and sediment transport data in the UK'. In Sediment and Water Quality in River Catchment Systems, I. D. L. Foster, A. M. Gurnell and B. W. Webb, eds: Chichester, pp. 265-283.

Foster, G.R, Yoder, D.C., Weesis, D.A., McCool, D.C., McGregor, K.G., and Bingner, R.D., (2003). 'User's guide (Draft January 2003)–Revised Universal Soil Loss Equation Version 2 (RUSLE2).' USDA-ARS: Washington.

Frattini, P., Crosta, G.B., Fusi, N., Dal Negro, P., (2004). 'Shallow landslides in pyroclastic soils: a distributed modeling approach for hazard assessment'. Eng Geol, 73, pp. 277-295.

Freddi, P., and Pugliese, F., (1994). 'Inquadramento geografico dell'erea di Pietrasecca (Abruzzo – Italia Cantrale).' In Ezio Burri editor, L'area carsica di Pietrasecca (Carsoli, Abruzzo). Studio multidisciplinare, Chieti. Istituto Italiano di Speleologia Memoria 5, pp. 7-12. (in Italian)

Fritschen, L.J., Simpson, J.R., (1985). 'Evapotranspiration from forests: measurement and modeling'. In The forest-atmosphere interaction, Hutchison and Hicks eds. Reidel Publishing Co.:Boston, pp. 293-308.

Fu, P., and Rich, P.M., (2002). 'A geometric solar radiation model with applications in agriculture and forestry.' Comput. Electron. Agr., 37, pp. 25-35.

Funiciello, R., Giordano, G., and De Rita, D., (2003). 'The Albano maar lake (Colli Albani Volcano, Italy): recent volcanic activity and evidence of pre-Roman age catastrophic lahar events.' Journal of Volcanology and Geothermal Research, 123, pp. 43-61.

'G'

Galadini, F., Messina, P., Giaccio, P., Sposato, A., (2003). 'Early uplift history Abruzzi Apennines (central Italy): available geomorphological constraints.' Quaternary International, 101-102, pp. 125-135.

Galadini, F., Messina, P., (2004). 'Early–Middle Pleistocene eastward migration of the Abruzzi Apennine (central Italy) extensional domain.' Journal of Geodynamics, 37, pp. 57-81.

Garcìa-Ruiz, J.M., Arnàez, J., Beguerìa, S., Seeger, M., Martì-Bono, C., Regüès, D., Lana-Renault, N., White, S., (2005). 'Runoff generation in an intensively disturbed, abandoned farmland catchment, Central Spanish Pyrenees'. Catena, 59, pp. 79-92.

Garfì, G., Veltri, A., Callegari, G., Iovino, F., (2006). 'Effetti della ceduazione sulle perdite di suolo in popolamenti di castagno della Catena Costiera Cosentina (Calabria)'. L'Italia Forestale e Montana, 61, pp. 507-531. (in Italian)

Gatto, W.L., Halvorson, J.J, DK McCool, AJ Palazzo, A.J., (2001). 'Effects of freeze-thaw cycling on soil erosion'. In Landscape erosion and evolution modeling. Edited by Harmon R., S., and Doe II W.,w.: New York, pp. 29-55.

Gioia, D., Martino, C., and Schiattarella, M., (2011). 'Long- to short-term denudation rates in the southernApennines: geomorphological markers and chronologicalconstraints.' Geologica Carpathica, 62, pp.missing.

Giovannoni, M.T., (2003). 'Gli Equi. Notizie sull'origine, sugli insediamenti e sulle guerre contro Roma.' AEQUA,14, pp.10-15. http://www.aequa.org/Autori.asp [Accessed Jun 2010] (in Italian).

Giraud, C., (2004). 'Le oscillazioni di livello del Lago di Mezzano (Valentano – VT): Variazioni climatiche ed influenza antropica.' Il Quaternario-Italian Journal of Quaternary Science, 17, pp. 221-230. (in Italian)

Gobin, A. and Govers, G., 2003. 'Pan-European Soil Risk Erosion Assessment.' Contract no. QLK5-CT-1999- 01323. Third Annual Report (1 Apr '02 - 1 Apr '03). Laboratory for Experimental Geomorphology. Katholieke Universiteit Leuven: School of Geography. University of Leeds. Estacion Experimental de Zonas Aridas, Almeria Consejo Superior de Investigaciones Cientificas. Unité de Science du Sol, Orléans Institut National de la Recherche Agronomique European Soil Bureau. Environment Institute DG - Joint Research Centre, Ispra. Agricultural University of Athens. International Soil Reference and Information Centre Wageningen University and Research Centre, Rome, Italy, pp. 145.

Gomi, T., R.D. Moore, and M.A. Hassan. (2005). 'Suspended Sediment Dynamics in Small Forest Streams on the Pacific Northwest'. Journal of the American Water Resources Association (JAWRA), 41, pp. 877-898.

Goovaerts, P., (2000). 'Geostatistical approaches for incorporating elevation into the spatial interpolation of rainfall.' Journal of Hydrology, 228, pp. 113-129.

Govers, G., Everaert, W., Poesen, J., Rauws, G., De Ploey, J., and Lautridou, J.P., (1990). 'A long-flume study of the dynamic factors affecting the resistance of a loamy soil to concentrated flow erosion.' Earth Surface Processes and Landforms, 15, pp. 313-328.

Govers, G., Poesen, J., Goossens D., and Christensen, B.T.. (2004). 'Soil erosion-processes, damages and countermeasures'. In P. Schjonning and S. Elmholt, Ers, Managing Soil Quality, Challenges in Modern Agriculture, CABI Publishing: Wallingford, pp. 199-217.

Grah, R.F., Wilson, C.C., (1944). 'Some components of rainfall interception'. Journal of Forestry, 42, pp. 890-898.

Grauso, S., Fattoruso, G., Crocetti, C., and Montanari, A., (2007). 'A spatially distributed analysis of erosionsusceptibility and sediment yield in ariver basin by means of geomorphicparameters and regression relationships.' Hydrol. Earth Syst. Sci. Discuss., 4, pp. 627-654.

Grauso, B., Pagano, A., Fattoruso, G., De bonis, P., Onori, P., Regina, P., and Tebano, C., (2008). 'Relations between climatic–geomorphological parameters and sediment yield in a

mediterranean semi-arid area (Sicily, southern Italy).' Environmental Geology, 54, pp. 219-234.

Grauso, S., Fattoruso, G., Crocetti, C., and Montanari, A., (2008b). 'Estimating the suspended sediment yield in a river network by means of geomorphic parameters and regression relationships.' Hydrology and Earth System Sciences, 12, pp. 177-191.

Gravelius, H., (1914). 'Grundrifi der gesamten Gewâsserkunde.' Band 1: hlufikunde (Compendium of Hydrology. vol. 1, Goschen: Berlin. (in german)

Green, T.R., Beavis, S.G., Dietrich, C.R., and Jakeman, A.J., (1999). 'Relating stream-bank erosion to in-stream transport of suspended sediment'. Hydrological Processes, 13, pp. 777-787.

Grimm, M., Jones, R. and Montanarella, L., (2002). 'Soil Erosion Risk in Europe. European Soil Bureau.' Institute for Environment and Sustainability JRC Ispra. European Comission. Joint Research Centre: Rome.

Grimm, M., Jones, R.J.A., Rusco E., and Montanarella, L., (2003). 'Soil Erosion Risk in Italy: A Revised USLE Approach.' European Soil Bureau Research Report vol. 11 (2003) EUR 19022 EN

Grossi, G., (1991). 'Topografia antica della Marsica (Aequi-Marsi e Volsci): quindici anni di ricerche, 1974-1989.' Atti del Convegno di Archeologia 'Il Fucino e le aree limitrofe nell'antichità', Archeo Club D'Italia – Sezione Marsica, Avezzano, pp. 199-237. (in Italian)

Gucinski, H., Furniss, M.J., Ziemer, R.R., Brookes, M. (2001). 'Forest roads: a synthesis of scientific information'. Gen. Techn. Rep. PNW-GTR-509, US Department of Agriculture, Forest Service, pp. 103.

Gueguen, E., Doglioni, C., Fernandez, M., (1998). 'On the post 25 Ma geodynamic evolution of the western Mediterranean.' Tectonophysics, 298, pp. 259–269.

Guidi, G., Manetti, M.C., (1994). 'Ricerche sull'evoluzione naturale di soprassuoli forestali a Quercus cerris L. e Fagus sylvatica L. nell'Appennino meridionale. Secondo contributo - osservazioni su alcuni fattori della produttività e del microclima in due aree protette.' Ann. Ist. Sper. Selv. XXIII, pp. 201-223. (in Italian)

Guy, B.T., Dickinson, W.T., Rudra, R.P., (1987).' The roles of rainfall and runoff in the sediment transport capacity of inter-rill flow'. Am. Soc. Agric. Eng., 1, pp. 86-100.

Gutteridge, L., Haskins, K., and Davey, D., (1991). 'Integrated Quantity/Quality Modelling-Stage 3', Gutteridge Haskins and Davey, for Department of Water Resources: Sydney, pp. 102.

'H'

Haan, C.T., Barfield, B.J., and Hayes.J.C., (1994). 'Design Hydrology and Sedimentlogy for Small Catchments'. Academic Press: New York.

Hadley, R.F., Schumm, S.A., (1961). 'Sediment sources and drainage basin characteristics in upper Cheyenne River Basin.' U.S. Geological Survey

Hanley, N., Faichney, R., Munro, A., Shortle, J.S., (1998). 'Economic and environmental modelling for pollution control in an estuary'. Journal of Environmental Management, 52, pp. 211-225.

Harden, C.P., (2001). 'Soil erosion and sustainable mountain development. Experiments, observations, and recommendations from the Ecuadorian Andes'. Mountain Research and Development, 21, pp. 77-83.

Harmon, R.S., and Doe, W.W.III, (2001). 'Landscape Erosion and Evolution Modeling', Springer: Verlag, pp. 535.

Held, R., and Clawson, M., (1965). 'Soil Conservation in Perspective', John Hopkins University Press, Baltimore.

Herrero, J., and Pérez-Coveta, O., (2005). 'Soil salinity changes over 24 years in a Mediterranean irrigated district'. Geoderma, 125, pp. 287-308.

Hewlett, J.D., Hibbert, A.R., (1961). 'Increase in water yield after several types of forest cutting'. IAHS AISH, 6, pp. 5-17.

Hill, J. and Schütt, B. (2000). 'Mapping complex patterns of erosion and stability in dry Mediterranean ecosystems.' Remote Sensing of Environment, 74. pp. 557-659.

Hoffmann, T., Erkens, G., Cohen, K.M., Houben, P., Seidel, J., and Dikau, R., (2007). 'Holocene floodplain sediment storage and hillslope erosion within the Rhine catchment'. The Holocene, 17, pp. 105-118.

Hornbeck, J.W., (1975). 'Moderating the impact of contemporary forest cutting on hydrologic and nutrient cycles', IAHS-AISH Publication, 117, pp. 423-433.

Horton, R.E., (1933). 'The role of infiltration in the hydrologic cycle'. Trans. Am. Geophys. Union, 14, pp. 446–460.

Horton, R.,E., (1945). 'Erosional development of streams and their drainage basins. Hydrophysical approach to quantitative morphology.' Geol. Soc. Am. Bull., 56(, pp.275-370.

Huang, J., Lacey, S.T., and Ryan, P.J., (1996). 'Impact of forest harvesting on the hydraulic properties of surface soil.' Soil Science, 161, pp. 79-86.

Hudson, N.W., (1993). 'Field measurement of soil erosion and runoff.' FAO Soils Bull., 68, pp. 139.

Hudson, N. W. (1995). 'Soil Conservation'. BT Batsford Limited: London.

Hughes J.D., and Thirgood, J., (1982). 'Deforestation, erosion, and forest management in ancient Greece and Rome', Journal of Forest History, 26, pp. 60-75.

Hutchinson, M.F., (1989). 'A new procedure for gridding elevation and stream line data with automatic removal of spurious pits.' Journal of Hydrology, 106, pp. 211-232.

Hydrographic and Oceanographic Institute of Rome. (2009). Online source: www.idrografico.roma.it/default.aspx [Accessed Jul.-Nov. 2009].

Hynes, H.B.N, (1972). 'The ecology of running water.' Liverpool University Press, pp.24.

'I'

IGMI, (1994). 'Fogli 358, 367 and 376.'Topographical maps, IGMI: Florence.

INRA - Le Bissonnais, Y. and Daroussin, J. (2001). 'A pedotransfer rule for estimating soil crusting and its use in assessing the risk of soil erosion'. Technical Report INRA: Orléans.

Iovino, F., Puglisi, S., (1991). 'L'aménagement des reboisements de protection'. Un cas d'étude. 10th World Forestry Congress, Paris.

Iovino F., Veltri A., (2004). 'Gestione del bosco e impatto sulle risorse idriche'. In Gestione dei Sistemi Forestali e Risorse Idriche. Quaderni di Idrotecnica, Editoriale Bios,17, pp. 29-43. (in Italian)

Iovino, F., (2009). 'Ruolo della selvicoltura nella conservazione del suolo'. In Ciancio O., Atti del Terzo Congresso Nazionale di Selvicoltura (Taormina, 16-19 Ottobre 2008). Accademia Italiana di Scienze Forestali, Firenze. Volume I, pp. 425-436.

Iovino, F., Borghetti, M., Veltri, A., (2009b). 'Foreste e ciclo dell'acqua'. Forest@, 6, pp. 256-273. (in Italian)

Iovino, F., Marchetti, M., (2010). 'Selvicoltura: conversazione del suolo, risorse idriche, lotta alla desertificazione.' Italian Journal of Forest and Mountain Environments, pp. 121-30. (in Italian)

IPCC- Nakicenovic, N., Alcamo, J., Davis, G., et al. IPCC (Intergovernmental Panel on Climate Change), (2000). 'Special report on emission scenarios, Intergovernmental Panel on Climate Change.' Cambridge University Press: Cambridge, pp. 599.

ISTAT, (2002). 'Annuario Statistico Italiano", Year 2002. (in Italian)

ISTAT, (2005). 14° 'Censimento generale della popolazione e delle Abitazioni, 2005'. (in Italian)

ISPRA, (2010). Online GIS source: http://www.mais.sinanet.isprambiente.it/ost/ [Accessed 2010]

'J'

Jetten, V., de Roo, A., and Favis-Mortlock D., (1999). 'Evaluation of field-scale and catchment-scale soil erosion models.' CATENA, 37, Issues 3-4, pp. 521-541.

Jetten, V., and Favis-Mortlock, D., (2006). 'Modelling soil erosion in Europe'. In J. Boardman and J. Poesen, Editors, Soil Erosion in Europe, Wiley: pp. 696-716.

Johnson, M.G., and Beschta, R.L., (1980).' Logging, infiltration capacity, and surface erodibility in western Oregon'. J. For., 78, pp. 334-33.

Johanson, R.C., Imhoff, J.C., Davis, H.H., (1980). 'Users Manual for the Hydrologic Simulation Program-Fortran (HSPF) version No. 5.0.' EPA-600/9-80-105. US EPA Environmental Research Laboratory: Athens.

Jones, R.J.A., Le Bissonnais, Y., Bazzoffi, P., Sanchez Diaz, J., Düwel, O., Loj, G., Øygarden, L., Prasuhn, V., Rydell, B., Strauss, P., Berenyi Uveges, J., Vandekerckhove, L., Yordanov, Y., (2004). 'Nature and extent of soil erosion in Europe.' In: Van-Camp, L., Bujarrabal, B., Gentile, A.-R., Jones, R.J.A., Montanarella, L., Olazabal, C., Selvaradjou, S.-K. (Eds.), Reports of the Technical Working Groups Established Under the Thematic Strategy for Soil Protection. Volume II Erosion. EUR 21319 EN/2. Office for Official Publications of the European Communities, Luxembourg, pp. 145-185.

Jones, R.J.A., Le Bas, C., Kozak, J., Düwel, O., King, D., 2006. Identifying risk areas for soilerosion in Europe. In: Eckelmann, W., et al. (Ed.), 'Common Criteria for RiskIdentification According to Soil Threats, European Soil Bureau Research Report20, EUR 22185 EN.' Office for Official Publications of the European Communities,Luxembourg, pp. 23-33.

Jordán, L., Martínez-Zavala, L., (2008). 'Soil loss and runoff rates on unpaved forest roads in southern Spain after simulated rainfall.' Forest Ecology and Management, 255, pp. 913-919.

Julien, P.Y. and Simmons, D.B., 1985. 'Sediment transport capacity of overland flow'. Transactions of ASAE, 28, pp.755-762.

'K'

Kaplan, J.O., Krumhardt, K.M., and Zimmermann, N., (2009). 'The prehistoric and preindustrial deforestation of Europe.' Quaternary Science Reviews, 28, pp. 27-28.

Keim, R. F. and Shoenholtz, S.H., (1999). 'Functions and effectiveness of silvicultural streamside management zones in loessial bluff forests'. Forest Ecology and Management, 118, pp. 197-209.

Kinnell, P.I.A., (1985). 'The influence of flow discharge on sediment concentrations in raindrop induced flow transport'. Aust. J. Soil Res., 26, pp. 575-582.

Kinnell, P.I.A., (1990). 'The mechanics of raindrop induced flow transport.' Aust. J. Soil. Res. 28, pp. 497-516.

Kinnell, P.I.A., (2000). 'AGNPS-UM: applying the USLE-M within the agricultural non point source pollution model.' Environmental Modellingand Software, 15, pp. 331-341.

Kinnell, P.I.A., (2007). 'Runoff dependent erosivity and slope length factors suitable for modeling annual erosion using the Universal Soil Loss Equation.' Hydrol Process, 21, pp. 2681-2689

Kinnell, P.I.A., (2008). 'Sediment delivery from hill slopes and the Universal Soil Loss Equation: Some perceptions and misconceptions.' Hydrological Processes, 22, pp. 3168-3175.

Kirkby, M.J., (1985). 'Hillslope hydrology'. In Anderson, M.G. and Burt, T.P., ers, Hydrologicalforecasting. Wiley: Chichester, pp. 37-75.

Kirkby, M. J., and Cox, N. J., (1995). 'A climatic index for soil erosion potential (CSEP) including seasonal and vegetation factors.' Catena, 25, pp. 333-352.

Kirkby, J.M., Le Bissonais, Y., Coulthard, T.J., Daroussin, J., McMahon M.D., (2000). 'The development of land quality indicators for soil degradation by water erosion Agriculture.' Ecosystems and Environment, 81, pp. 125-135.

Knapen, a., Poesen, J., Govers, G., Gyssels, G., and Nachtergaele, J., (2007). 'Resistance of soils to concentrated flow erosion: A review Original Research Article'. Earth-Science Reviews, 80, pp. 75-109.

Knapp, B.J., (1978). 'Infiltration and storage of soil water'. In Hillslope Hydrology Ed. MJ Kirkby. Wiley: Chichester, pp. 43-72.

Kort, J.,Collins, M., and Ditsch, D., (1998). 'A review of soil erosion potential associated with biomass crops'. Biomass and Bioenergy, 14, pp. 351-360.

Kosmas, C., Danalatos, N., Cammeraat, L.H., Chabart, M., Diamantopoulos, J., Farand, R., Gutierrez, L., Jacob, A., Marques, H., Martinez-Fernandez, J., Mizara, A., Moustakas, N., Nicolau, J.M., Oliveros, C., Pinna, G., Puddu, R., Puigdefabregas, J., Roxo, M., Simao, A., Stamou, G., Tomasi, N., Usai, D. and Vacca, A., (1997). 'The effect of land use on runoff and soil erosion rates under Mediterranean conditions'. Catena 29, pp. 45-59.

'L'

Lal, R., (1990). 'Soil Erosion in the Tropics: Principles and Management '. McGraw-Hill: New York.

Lal, R., Elliott, W., (1994).'Erodibility and erosivity.' In: Lal, R. (Ed.), Soil Erosion Research Methods. St. Lucie Press: Delray Beach, pp. 181-208.

Lal, R., (2001). 'Soil degradation by erosion.' Land Degradation & Development, 12, 519-539.

Lal, R., (2003). 'Soil erosion and the global carbon budget'. Environment International, 29, pp. 437-450.

Lamb, H.H., (1995). 'Climate, history and modern world (2nd edn).' Routledge: London.

Lamendola, F., (2008). 'Le flotte dell'antico Mediterraneo distrussero le foreste causando alluvioni e malaria.' Arrianna ed. Online source: http://www.ariannaeditrice.it/articolo.php ?id_articolo=18501 [accessed Februry 2011].

Lang, A., (2003). 'Phases of soil erosion-derived colluviation in the loess hills of South Germany.' Catena, 51, pp. 209-221.

Lang A., and Bork H.R., (2006). 'Past soil erosion in Europe'. In J. Boardman and J. Poesen, Editors, Soil Erosion in Europe, Wiley: Chichester, pp. 465-476.

Lang, A., Hönscheidt, S., (1999). 'Age and source of colluvial sediments at Vaihingen–Enz, Germany.' CATENA, 38, pp. 89-107.

Lazzari, M., and Schiattarella, M., (2010). 'Estimating Long to Short-Term Erosion Rates of Fluvial vs Mass Movement Processes: An Example from the Axial Zone of the Southern Italian Apennines.' Ital. J. Agron. / Riv. Agron., 3, pp. 57-66.

Le Bissonnais, Y., Bruno, J.F., Cerdan, O., Couturier, A., Elyakime, B., Fox D., Lebrun, P., Martin, P, Morschel, J., Papy, F., Souchère, V., (2003). 'Maltrise de l'èrosion hydrique des sols cultivès: phénomènes physiques et dispositifs d'action'. Programme GESSOL, Report Final.

Le Bissonnais, Y., and Singer, M.J., (1992). 'Crusting, runoff and erosion response to soil water content and successive rainfalls.' Soil Sci. Soc. Am. J. 56, pp. 1898–1903.

Leprun, J.C., (1981). 'A erosão, a conservaçao e o manejo do solo no Nordeste Brasileiro.' Recife: Ministério do Interior. SUDENE, Brasil.

Le Roy Ladurie, E., (1982). 'Tempo di festa, tempo di carestia, Storia del clima dall'anno 1000.' Einaudi paperbacks, 138, Einaudi: Torino, pp. 449. (in Italian)

Littleboy, M., Silburn, M.D., Freebairn, D.M., Woodruff, D.R., Hammer, G.L., Leslie, J.K., 1992. 'Impact of soil erosion on production in cropping systems'. I. Development and validation of a simulation model.' Australian Journal of Soil Research, 30, pp. 757-774.

Llorens, P., Gallart, F., (2000). 'A simplified method for forest water storage capacity measurement.' Journal of Hydrology, 240, pp. 131-144.

Lombardi F., Neto and. Moldenhauer, W.C., (1992). 'Erosividade da chuva: sua distribuicão e relacão com perdas de solo em Campinas.' SP, Bragantia, 51, pp. 189-196. (in Italian)

Lo, S.A., El-Swaify, Dangler, E.W., and Shinshiro, L., (1985). 'Effectiveness of EI_{30} as an erosivity index in Hawaii.' In S.A. El-Swaify, W.C. Moldenhauer and A. Lo, Editors, Soil Erosion and Conservation, Soil Conservation Society of America, Ankeny, pp. 384-392.

Lorenzoni, P., Magaldi, D., Raglione, M., (1995). 'Rilevamento cartografico e valutazione ingegneristica dei suoli della Conca intramontana di Oricola e Carsoli in provincia dell'Aquila.' Quaderni di scienze del suolo, 6, pp. 33-80. (in Italian)

Loureiro N., S., Coutinho M., A., (2001). 'A new procedure to estimate the RUSLE EI30 index, based on monthly rainfall data and applied to the Algarve region, Portugal.' Journal of Hydrology, 250, pp. 12-18.

Lowe, J.J., Branch, N., Watson, C., (1994). 'The chronology of human disturbance of the vegetation of the Northern Apennines during the Holocene.' Monografie di "Natura Bresciana", 20, pp. 169-187.

Lupia Palmieri, E., Ciccacci, S., Civitelli, G., Corda, L., D'Alessandro, L., Del Monte M., Fredi, P., Pugliese, F., (1995). 'Geomorfologia quantitativa e morfodinamica del territorio abruzzese: il bacino idrografico del fiume Sinello (quantitative geomorphology and morphodynamics in the abruzzo: the Sinello river basin, southern Italy).' Geogr Fis Dinam Quat, 18, pp. 31-46.

'M'

Mäckel, R., Friedmann, A., Seidel, J., Schneider, R., (2001). 'Natural and anthropogenic changes in the palaeoecosystem of theBlack Forest and Upper Rhine Lowlands since the Bronze Ag.e' Regensburger Beiträge zur Prähistorischen Archäologie 7, pp. 143-160.

Mäckel, R., Schneider, R., Friedmann, A., Seidel, J., (2002).' Environmental changes and human impact on the relief development in the Upper Rhine Valley and Black Forest (South-West-Germany) during the Holocene.' Zeitschrift für Geomorphologie,N.F. Supplementband 128, pp. 31-45.

Mäckel, R., Schneider, R., Seidel, J., (2003). 'Anthropogenic impact on the landscape of Southern Badenia (Germany) during the Holocene — documented by colluvial and alluvial sediments'. Archaeometry, 45, pp. 487-501.

Macklin, M.G., Passmore, D.G., Stevenson, A.C., Cowley, D.C., Edwards, D.N., and O'Brian, C.F., (1991). 'Holocene alluviation and land-use change on Callaly Moor, Northumberland, England.' Journal of Quaternary Science, 6, pp. 225-232.

Magri, D., and Follieri, M., (1989). 'Caratteri della biostratigrafia pollinica dell'Olocene in Italia centrale.' Memorie della Società Geologica Italiana, 42, pp. 147-153. (in Italian)

Magny, M., de Beaulieu, J.L., Drescher-Schneider, R., Vannière, B., Walter-Simonnet, A.V., and Miras, Y., (2007). 'Holocene climate changes in the central Mediterranean as recorded by lake-level fluctuations at Lake Accesa (Tuscany, Italy).' Quaternary Science Reviews, 26, pp.1736-1758.

Magri, D., Sadori, L., (1999). 'Late Pleistocene and Holocene pollen stratigraphy at Lago diVico, central Italy.' Veget Hist Archaeobot, 8, pp. 247-260.

Maialetti, S., (2000). 'Qualche notizia inedita sull'antica città di Carsioli.' Aequa, 2, pp. 7-12. http://www.aequa.org/Autori.asp [Accessed May 2010]. (in Italian)

Maner, S.B., **(**1958). 'Factors affecting sediment delivery rates in the Red Hills physiographic area'. Transactions of the American Geophysical Union, 39, pp. 669-75.

Marini, R., (1995). 'Contributo della geomorfologia quantitativa alla valutazione della pericolosità geomorfologica.' PhD Thesis, Università degli Studi di Roma "La Sapienza", Rome.

Mariotti Lippi, M., Bellini, C., Trinci, C., Benvenuti, M., Pallecchi, P., and Sagri, M., (2006). 'Pollen analysis of the ship site of Pisa San Rossore, Tuscany, Italy: the implications for catastrophic hydrological events and climatic change during the late Holocene.' Veget Hist Archaeobot. DOI 10.1007/s00334-006-0070-x

Märker, M., Angeli, L., Bottai, L., Costantini, R., Ferrari, R., Innocenti, L., and Siciliano, G., (2008). 'Assessment of land degradation susceptibility by scenario analysis: A case study in Southern Tuscany.' Italy. Geomorphology, 93, pp. 120-129.

Marchetti, R., (1993). Ecologia applicata. SITE, Città Studi: Milano, pp.309-311.

Marchi, E., Piegai, F., (2001). 'Sistemi di utilizzazione forestale a basso impatto ambientale.' L'Italia Forestale e Montana, 56, pp. 477-490. (in Italian)

Marks, S. D. and Rutt, G. P. (1997). 'Fluvial sediment inputs to upland gravel bed rivers draining forested catchments: potential ecological impacts.' Hydrology and Earth System Sciences,1 , pp. 499-508

Martino, S., Moscatelli, M., Scarascia Mugnozza G. (2004). 'Quaternary mass movements controlled by a structurally complex setting in the central Apennines (Italy).' Engineering Geology, 72, pp. 33-55.

Massaro, M.E., Russo, M., and Zuppetta, A., (1996). 'Analisi indiretta dell'entità dell'erosione nel bacino del fiume Tammaro.' Geogr. Fis. Dinam. Quatern., 19, pp. 381-394. (in Italian)

Meeus, J., Van der Ploeg, J.D., Wijermans, M. (1988). 'Changing agricultural landscapes in Europe: continuity, deterioration or rupture?' IFLA Conference 1988. International Federation of Landscape Architects: Rotterdam.

Megahan, W.F., Seyedbagheri, K.A., Mosko, T.L. and Ketcheson, G.L., (1986). 'Construction phase sediment budget for forest roads on granitic slopes in Idaho'. In Drainage Basin Sediment Delivery, ed. R.F. Handley, International Association of Hydrologic Scientific Publications, pp. 31-39.

Melchiorri, F. (1987). 'Evoluzione geologica plio-pleistocenica della media-alta valle del Turano.' Unpubbliched Thesis, University of Rome 'La Sapienza': Rome. (in Italian)

Mitas, L., Mitasova, H., (1998). 'Distributed soil erosion simulation for effective erosion prevention.' Water Resour. Res., 34, pp. 505-516.

Mitasova, H., Hofierka, J., Zlocha, M. and Iverson, L.R., (1996). 'Modeling topographic potential for erosion and deposition using GIS'. International Journal of Geographical Information Science, 10, pp. 629-641

Mitasova, H., (1997). 'GIS Tools for Erosion/Deposition Modelling and Multidimensional Visualization. Part IV: Process based Erosion Simulation.' Geographic Modelling and Systems Laboratory, University of Illinois: Illinois.

Mitasova, H., (1999). 'Terrain Modelling and Soil Erosion Simulation.' Geographic Modelling and Systems Laboratory, University of Illinois, Illinois. Online source: http://skagit.meas.ncsu. edu/~helena/gmslab/erosion/usped.html [Accessed December 2009].

Montgomery, D.R., (2007). 'Soil erosion and agricultural sustainability.' Proceedings of the National Academy of Sciences of the United States of America, 104, pp. 268-272.

Moore, I.D., Burch, G. J., (1986). 'Physical basis of the length-slope factor in the universal soil loss equation.' Soil Science Society of America Journal 50, pp. 1294-1298.

Moore, D.C. and Singer, M.J. (1990). 'Crust formation effects on soil erosion processes'. Soil Science Society of America Journal, 54, pp. 15-28.

Moretti, S., Rodolfi, G., (2000). 'A typical 'calanchi' landscape on the Eastern Apennine margin (Atri, Central Italy): geomorphological features and evolution.' CATENA, 40, pp. 217-228.

Morgan, R.P.C. (1978). 'Field studies of rainsplash erosion.' Earth Surface Processes, 3, pp. 295-299.

Morgan, R.P.C., Morgan, D.D.V. and Finney, H.J., (1984). 'A predictive model for the assessment of erosion risk'. Journal of Agricultural Engineering Research, 30, pp.245-253.

Morgan, R.P.C. (1992). 'Soil Erosion in the Northern Countries of the European Community.' EIW Workshop: Elaboration of a Framework of a Code of Good Agricultural Practices, Brussels, 21-22 May 1992.

Morgan, R.P.C., (1996). 'Soil erosion and conservation'. Longman: London, pp. 297.

Morgan, R.P.C., Quinton, J.N., Smith, R.E., Govers, G., Poesen, J.W.A., Auerswald, K., Chisci, G., Torri, D., Styczen, M.E., (1998). 'The European Soil Erosion Model (EUROSEM): a dynamic approach for predicting sediment transport from fields and small catchments.' Earth Surf. Process. Landf. 23, pp.527-544.

Morgan, R.P.C., (2005). 'Soil Erosion and Conservation.' Blackwell Publishing, p. 299.

Morris, G.L. and Fan, J., (1998). 'Reservoir sedimentation handbook: design and management of dams, reservoirs and watersheds for sustainable use.' McGraw-Hill, pp.848.

Moscatelli, M., Milli, S., Stanzione, O., Marini, M., Gennari, G., and Vallone, G., (2004). 'Depositi torbiditici del Massiniano inferiore dell'Appenino Centrale: bacini del Salto-Tragliacozzo e della Laga (Lazio, Abruzzo, Marche).' II Congress GeoSed, 25-28 Sep.: Rome. (in Italian)

Moss, A.J., (1988). 'The effects of flow-velocity variations on rain-driven transportation and the role of raindrop impact in the movement of solids.' Aust. J. Soil Res., 26, pp. 443-450.

Murakami, S., Tsuboyama, Y., Shimizu, T., Fujieda, M., and Noguchi, S., (2000). 'Variation of evapotranspiration with stand age and climate in a small Japanese forested catchment.' Journal of Hydrology, 227, pp. 114-127.

Murphy G., Jackson R.J., (1989). 'Water regime changes resulting from soil disturbance through mechanisation of forest operations.' ECE/ILO/FAO Joint Committee on forest working techniques and training of forest workers: Louvan-la-Neuve.

Mutchler, C. K., and Young, R.A., (1975). 'Soil detachment by raindrops.' In Proc.Sediment Yield Workshop, Oxford, MS. USDA Rep. ARS-S-40, pp. 113-117.

'N'

Nearing, M.A., Foster, G.R., Lane, L.J., Finkner, S.C., (1989). 'A process-based soil erosion model for USDA-water erosion prediction project technology.' Transactions of the ASAE, 32, pp. 1587-1593.

Nearing, M.A., Lane, L.J., and Lopes, V.L., (1994). 'Modelling Soil Erosion.' In Lal, R. (Ed.). Soil Erosion Research Methods, pp. 127-156.

Newson, M. D., (1980). 'The erosion of drainage ditches and its effect on bedload yields in mid-Wales.' Earth Surface Processes and Landforms, 5, pp. 275-290.

Nichols, M.H. and Renard, K.G., (1999). 'Sediment yield from semi-arid watersheds.' Agricultural Research Service, Southwest Watershed Research Center: Tucson.

Norton, D., Shainberg, I., Cihacek, L. and Edwards, J.H., (1999). 'Erosion and soil chemical properties.' In Lal, R., Editor. Soil Quality and Soil Erosion, CRC Press: Boca Raton, pp. 39-56.

Novotny, V., and Olem, H., (1994). 'Water Quality: Prevention, Identification, and Management of Diffuse Pollution.' Van Nostrand Reinhold: New York

'O'

O'Callaghan, J., and Mark, D., (1984). 'The extraction of drainage networks from digital elevation data.' Computer Vision, Graphics and Image Processing, 28, pp. 328-344. Ochumba, P. B. O., (1990). 'Massive fish kills within the Nyanza Gulf of Lake Victoria, Kenya.' Hydrobiologia, 208, pp. 93-99.

Oldeman, L.R., Hakkeling, R.T.A., and Sombroek, W.G., (1991). 'World map of the status of human-induced soil degradation, An Explanatory Note (Global Assessment of Soil Degradation GLASOD).' Work. Pap. 90/07, ISRIC: Wageningen.

Oldeman, L.R., (1994). 'The global extent of soil degradation.' In: Greenland, D.J. and Szabolcs, I., Editors, 1994. Soil resilience and sustainable land use, CAB International: Wallingford, pp. 99-118.

Oljienink, J., (1988). 'Present and future estimates of evapotraspiration and runoff for Europe.' Working Paper WP/88037, IIASA.

Oliveira, R.C., and Medina, B.F., (1990). 'A erosividade das chuvas em Manaus (AM).' Revista Brasileira de Ciência do Solo, 14, pp. 235-239.

Olson, G.W., (1981). 'Archeology: Lesson on future soil use.' J. Soil Water Conservation. 36 pp.261-26. Opie, J., (2000). 'Ogallala: Water for a Dry Land'. University of Nebraska Press: Lincoln.

Osterkamp, W.R., and Toy, T.J., (1997). 'Geomorphic considerations for erosion prediction.' Environmental Geology, 29, pp. 152-57.

Øverland, H., (1990). 'Einfluss der Landnutzung auf Hochwasserabfluss und Schwebstofftransport.' Institut fur Wasserwesen, Universitat der Bundeswehr Munchen, Report 35/1990.

'P'

Parsons, A.J., Wainwright, J., Brazier, R.E. and Powell, D.M. (2006). 'Is sediment delivery a fallacy?' Earth Surface Processes and Landforms, 31, pp.1325-28.

Passerini, G., (1937). 'Influenza delle immersioni degli strati e influenza dell'orientamento dei versanti sulla degradazione delle argille plioceniche.' Boll. Soc. Geol. It., 56. (in Italian)

Patric, J.H., (2002). 'Forest Erosion Rates.' Online source: www.syllabus.syr.edu/ esf/rdbriggs/ for345/erosion.htm. [Accessed May 2008].

Patrick, J. H. (1976). "Soil erosion in the eastern forest." Journal of Forestry, October, 1976, pp. 671-677.

Pelacani, S., Märker, M., and Rodolfi, G., 'Simulation of soil erosion and deposition in a changing land use: A modelling approach to implement the support practice factor.' Geomorphology, 99, pp. 329-340.

Pérez-Peña, J.V, Azañón J.M., Azor A. (2009). 'CalHypso: An ArcGIS extension tocalculate hypsometric curves and their statistical moments. Applications todrainage basin analysis in SE Spain.' Computers and Geosciences, 35, pp.1214-1223.

PESERA - Gobin, A., Govers, G., Kirkby, M.J., Le Bissonnais, Y., Kosmas, C., Puidefabrecas, J. Van Lynden, G. and Jones R.J.A. (1999). 'PESERA Project Technical Annex.' Contract No.: QLKS-CT-1999-01323, European Commission: Luxembourg.

Pierce, W.E., Larson, and K.H., (1986). 'Field Estimates of C Factors: How Good Are They and How Do They Affect Calculations of Erosion?' Soil conservation: assessing the national resources inventoryDi National Research Council (U.S.). Board on Agriculture. Committee on Conservation Needs and Opportunities, pp. 63-85.

Pimentel, D.C., and Kounang, N., (1998). 'Ecology of soil erosion in ecosystems.' Ecosystems, 1, pp. 416-426.

PNC, 2010. Portale Cartografico Nazionale. Online source: http://www.pcn.minambiente.it/ mdSearch/ [Accessed January 2010].

Pinna, M., (1996). 'Le Variazioni del Clima - Dall'Ultima grande glaciazione alle prospettive per il XXI Secolo.' FrancoAngeli: Milano, pp. 214. (in Italian)

Poesen, J., and Lavee, H., (1994). 'Rock fragments in topsoils: significance and processes.' Catena, 23, pp. 1-28.

Poesen, J.W.A., Hooke, J.M., (1997). 'Erosion, flooding and channel management in Mediterranean environments of southern Europe.' Physical Geography, 21, pp. 157-199.

Poesen, J., Nachtergaele, J., Verstraeten, G. and Valentin, C., (2003). 'Gully erosion and environmental change: Importance and research needs.' Catena, 50, pp. 91-113.

Poesen, J., Vanwalleghem, T., De Vente, J., Knapen, A., Verstraeten, G., and Martinez-Casasnova, J.A., (2006). 'Gully erosion in Europe.' In: Boardman, J., Poesen, J. (Eds.), Soil Erosion in Europe. Wiley: Chichester, pp. 515-536.

Porto, P., Walling, D.E., Tamburino, V., Callegari G. (2003). 'Relating caesium-137 and soil loss from cultivated land.' CATENA, 53, pp.303-326

Porto, P., Walling, D.E., Callegari, G., (2005). 'Investigating sediment sources within a small catchment in southern Italy. Sediment Budgets.' (Proceedings of symposium S1 held during the Seventh IAHS ScientificAssemblyat FozdoIguaçu, Brazil,April 2005), 291. IAHS Publ., pp. 113-122.

Porto, P., Walling, D.E., Callegari, G., (2009). 'Investigating the effects of afforestation on soil erosion and sediment mobilisation in two small catchments in Southern Italy.' CATENA, 79, pp. 81-188.

Pratesi, C.A., (2007). 'Il marketing del made in italy, nuovi scenari e competitività.' Franco Angeli: Milano. (in Italian)

Predhomme, C., (1999). 'Mapping a Statistic Extreme Rainfall in a Mountain Region.' In Phys. Chem. Earth (B), 24, pp. 79-84.

PRIN/COFIN 2002-2006. 'Erosione idrica in ambiente mediterraneo: valutazione diretta e indiretta in aree sperimentali e bacini idrografici.' Rodolfi G (Ed.). Atti del Convegno Conclusivo del Progetto MIUR-COFIN 2002, Firenze 2004, pp. 13-27. (in Italian)

Prosser, I.P., Young, B., Rustomji, P., Hughes, A., Moran, C., (2001). 'A model of river sediment budgets as an element of river health assessment.' In Proceedings of the International Congress on Modelling and Simulation (MODSIM'2001), December 10-13, pp. 861–866.

'R'

Raffy, J., (1982). 'Orogenèse et dislocations quateraires du versat terrhénien des Abruzzes (Italie cental).' Revue de Géographie physique, Paris, 23, pp. 55-72.

Ramrath, A., Zolitschka, B., Wulf, S., Negendank, J.F.W., (1999). 'Late Pleistocene climatic variations as recorded in two Italian maar lakes (Lago di Mezzano, Lago Grande di Monticchio).' Quaternary Science Reviews, 18, pp. 977-992.

Ramrath, A., Sadori, L., Negendank, J.F.W., (2000). 'Sediments from Lago di Mezzano, central Italy: a record of late Glacial/Holocene climatic variations and anthropogenic impact.' The Holocene, 10, pp. 87-95.

Rapetti, F., Salvetti, A., and Soagnolo, M., (2006). 'Climatologia e idrologia del bacino del torrente Roglio (Val d'Era - Toscana).' Atti del Convegno Conclusivo (PRIN/COFIN 2002): Erosione idrica in ambiente mediterraneo, valutazione diretta e indiretta in aree sperimentali e bacini idrografici, a cura di G. Rodolfi: Florence, pp.105-124. (in Italian)

Rapp, I., (1998). 'Effects of soil properties and experimental conditions on the rill erodibilities of selected soils.' Ph.D. Thesis, Faculty of Biological and Agricultural Sciences, University of Pretoria, South Africa.

Reich, P., Eswaran, H., and Beinroth, F., (2000). 'Global dimensions of vulnerability to wind and water erosion.' USDA, Washington.

Reid, L.M. and Dunne, T., (1984). 'Sediment production from forest road surfaces.' Water Resources Research 20 11, pp. 1753-1761.

Reimer, P.J., Baillie, M.G.L., Bard, E. Bayliss, A., Beck, J.W., Blackwell, P.G., Bronk Ramsey, C., Buck, C.E., Burr, G.S. Edwards, R.L., Friedrich, M., Grootes, P.M., Guilderson, T.P., Hajdas, I., Heaton, T.J., Hogg, A.G., Hughen, K.A., Kaiser, K.F., Kromer, B., McCormac, F.G., Manning, S.W., Reimer, RR.W., Richards, D.A., Southon, J.R., Talamo, S., Turney, C.S.M., van der Plicht, J., and Weyhenmeyer, C.E., 'IntCal09 and Marine09 radiocarbon age calibration curves, 0–50,000 years cal BP.' Radiocarbon, 51, pp. 1111-1150.

Renard, K.G., and Ferreira, V.A., (1993). 'RUSLE model description and database sensitivity.' J. Environ. Qual., 22, pp. 458-466.

Renard, G., Foster, G.R., Weesies, G.A., and Porter, J.P., (1991). 'RUSLE-Revised universal soil loss equation.' Journal of Soil and Water Conseruation. 46, 30-33.

Renard K.G., Freimund J.R. (1994). 'Using monthly precipitation data to estimate the Rfactor in the RUSLE.' Journal of Hydrology, 157, pp. 287-306.

Renard, K.G., Foster, G.R., Weesies, G.A., McCool, D.K., and Yoder, D.C., (1997). 'Predicting Soil Erosion by Water: A Guide to Conservation Planning with the Revised Universal Soil Loss Equation (RUSLE).' Agriculture Handbook N.703, U.S. Department of Agriculture Research Service, Washington, pp.348.

Rendell, H. M., Claridge, A.J., and Clarke, M.L., (2007). 'Late Holocene Mediterranean coastal change along the Tiber Delta andRoman occupation of the Laurentine shore, central Italy.' Quaternary Geochronology, 2, pp.83-88.

Richards, J.A., (1992). 'Remote Sensing Digital Image Analysis.' Springer-Verlag:Cambridge.

Richter G. (Hrsg.) (1998): Bodenerosion. Analyse und Bilanz eines Umweltproblems. Darmstadt.

Rieti Province, (2002). 'Turano: per un diverso sviluppo delle valli interne.' Progetto di territorio. www.provincia.rieti.it/downloads/Prog_Turano.pdf [Accessed April 2009]. (in Italian)

Righini, G., Costantini, E. A.C., Sulli, L., (2001). 'La banca dati delle regioni pedologiche italiane.' Boll. Soc. It. Scienza del Suolo, 50, pp. 261-271. (in Italian)

Riserva Naturale dei Monti Cervia e Navegna. Online source: www.navegnacervia.it/flora.php [Accessed September 2008]

Rivas-Martines, S., (2004). 'Global bioclimatica (clasificaciòn Bioblicatica de la Tierra).'Nueva version. Online source: www.globalbioclimatics.org/book/publications [Accessed May 2009].

Roberts J (1983). 'Forest transpiration: a conservative hydrological process?' Journal of Hydrology, 66, pp. 133-141.

Robichaud, P. R., and Waldrop, T.A., (1994). A comparison of surface runoff and sediment yields from low- and high-severity site preparation burns.' Water Resources Bulletin, 30,pp. 27-34.

Rodolfi G., Zanchi, C., 2002. 'Climate Change Related to Erosion and Desertification: 1. Mediterranean Europe. In: Sidle R.C., Environmental change and geomorphic hazards in forests.' IUFRO Research Series, CABI Publishing, pp. 67-86.

Rodolfi G., (2006). 'Erosione idrica del suolo in ambiente Mediterraneo: valutazione diretta e indiretta in aree campione e bacini idrografici.' In Rodolfi G (ed) Atti del Convegno Conclusivo del Progetto MIUR-COFIN 2002 Erosione idrica in ambiente mediterraneo: valutazione diretta e indiretta in aree sperimentali e bacini idrografici. Firenze, pp. 13-27. (In Italian)

Romero-Díaz, A., Martínez Lloris, M., Belmonte Serrato, F., (2004). 'The construction of dikes of hydrological correction as policy to retain the erosion and to avoid the silting up of dams in the Segura basin (Spain).' In Faz, A., Ortiz, R., García, G. (Eds.), Fourth International Conference on Land Degradation. Cartagena.

Romero-Díaz, F. Alonso-Sarriá and M. Martínez-Lloris, (2007) 'Erosion rates obtained from check-dam sedimentation (SE Spain). A multi-method comparison'. Catena, 71, pp. 172-178.

Rommens, T., Verstraeten, G., Poesen, J., Govers, G., Van Rompaey, A., Peeters, I., Lang, A.,(2005). 'Soil erosion and sediment deposition in the Belgian loess belt during the Holocene: establishing a sediment budget for a small agricultural catchment.' The Holocene, 15, pp. 1032-1043.

Rommens , T., Verstraeten, G., Bogman, P., Peeters, I., Poesen, J., Govers, J., Van Rompaey, A., Lang, A., (2006). 'Holocene alluvial sediment storage in a small river catchment in the loess area of central Belgium.' Geomorphology, 77, pp. 187-201.

Rose, C.W., Williams, J.R., Sander, G.C., and Barry, D.A., (1983). 'A mathematical model of soil erosion and deposition processes. 1. Theory for a plane element.' Soil Science Society of America Journal, 47, pp. 991-995.

Rothlisberger, F., (1986). '10000 Jahre Gletschergeschichte der Erde.' Sauerlander Aarau: Frankfurt.

Rozanov, B.G., (1990). 'Human impacts on the evolution of soils under various ecological conditions of world.' In Trans. of 14th ICSS, Plenary lecture. Int. Soc. Soil Sci.: Kyoto, pp. 53-62.

Rufino, R.L., Biscaia, R.C.M., and Herten, G.H., (1993). 'Determinacão do potencial erosivo da chuva do estado do Parana,.'Revista Brasileira de Ciência do Solo, 17, pp. 439-444.

'S'

Saavedra, C.,(2005). 'Estimating spatial patterns of soil erosion and deposition in the Andean region using geo-information techniques. A case study in Cochabamba,' Bolivia. Doctoral dissertation. UNESCO-IHE and Wageningen University (WUR).

Sadori, L., Giraudi, C., Petitti, P., Ramrath, A., 'Human impact at Lago di Mezzano (central Italy) during the Bronze Age: a multidisciplinary approach.' Quaternary International, 113, pp. 5-17

Salsotto, A., Dana, A., (1980). 'Utilità della vegetazione forestale contro il dissesto idrogeologico.' Dissesti, Torrenti e Boschi Regione Piemonte – Assessorato Agricoltura e Foreste - II Edizione: Torino. (in Italian)

Sanders, D.W., (1992). 'Soil Conservation: Strategies and Policies'. In Soil Conservation for Survival, Eds. Talo K., and Humi, H., Soil and Water Conservation Society, World Association of Soil and Water Conservation: Ankeny.

Sauro, U., (1993). 'Human impact on the karst of the Venetian Fore-Alps.' Italy. Environmental Geology, 21, pp. 115-121.

Sbarra, P., (2004). 'Contributo della geomorfologia quantitativa alla caratterizzazione morfologica e morfodinamica di alcuni paesaggi italiani.' Thesis, Università degli Studi di Roma La Sapienza. Facoltà di Scienze Matematiche, Fisiche e Naturali, Rome. Pp. 213. (in Italian)

Sciò, M., Toti, M.E., Meuti, M., (2000). 'L'incastellamento del carseolano nei secoli X e XI.' Municipality of Pereto. www.pereto.info [Accessed July 2009]. (in Italian)

Scheffer, M., Carpenter, S., Foley, J.A., Folke, C., and Walker, B., (2001). 'Catastrophic shifts in ecosystems.' Nature, 413, pp. 591-596. (in Italian)

Scherr, S.J., Yadav, Land S., (1996). 'Degradation in the developing world: implications for food, agriculture and the environment to 2020.' IFPRI, Food,Agric. and the Environment Discussion Paper 14: Washington, pp. 36.

Schmidt, J., von Werner M., and Michael, A., (1996). 'EROSION 2D/3D. Ein Computermodell zur Simulation der Bodenerosion durch Wasser.' Hrsg.: Sächsische Landesanstalt für Landwirtschaft, Dresden and Sächsisches Landesamt für Umwelt und Geologie: Freiberg.

Schumm, S.,A., (1956) . 'Evolution of drainage systems and slopes in Badlands at Perth Amboy, New Jersey', Geol. Soc. Am. Bull., 67, pp. 597-646.

Schumm, S.A., (1963). 'Sinuosity of alluvial rivers on the great plains.' Geol. Soc. Am. Bull., 74, pp. 1089-1100.

Schütt, B., (2000). 'Holocene paleohydrology of playa lakes in northern and central Spain: a reconstruction based on the mineral composition of lacustrine sediments.' Quaternary International, 73-74, pp. 7-27

Shaoshan An, Fenli Zheng, Feng Zhang, Scott Van Pelt, Ute Hamer and Franz Makeschin. (2008). 'Soil quality degradation processes along a deforestation chronosequence in the Ziwuling area, China.' Catena, 75, pp. 248-256.

Sharma, P.P., (1996). 'Interrill erosion'. In:Agassi, M. (ed.). Soil Erosion, Conservation and Rehabilitation. Marcel Dekker, Inc., USA.

Shirazi, M.A., and Boersma, L., (1984). 'A unifying quantitative analysis of soil texture.' Soil Sci. Soc. Am. J.,48, pp. 142-147.

Sibbesen, E., (1995). 'Phosphorus, nitrogen and carbon in particlesize fractions of soils and sediments.' In Correl, A. (Ed.), Surface runoff, erosion and loss of phosphorus at two agricultural soils in Denmark, plot studies 1989–1992, SPreport No. 11, pp. 135-148.

Singh, D., Herlin, I., Berroir, J.P., Silva, E.F. and Simoes-Meirelles, P., (2004). 'An approach to correlate NDVI with soil colour for erosion process using NOAA/AVHRR data.' Advances in Space Research, 33, pp. 328-332.

Sirvent, J., Desir, G., Gutierrez, M., Sancho, C., and Benito, G., (1997). 'Erosion rates in badland areas recorded by collectors, erosion pins and profilometer techniques (Ebro Basin, NE-Spain).' Geomorphology, 18, pp. 61-75.

Smith, K,G, (1950). 'Standards for grading texture of erosional topography.' Am. J. Sci., 248, pp. 655-668.

Smith, R.E., (1981). 'A kinematic model for surface mine sediment yield.' Transactions of the ASAE, pp.1508-1514.

Smith, H.G., Dragovich, D., (2008). 'Post-fire hillslope erosion response in a sub-alpine environment, south-eastern Australia.' CATENA, 73, pp. 274-285.

Soil Taxonomy, (1998). 'Keys to soil taxonomy.' 8th ed. Department of Agriculture, Natural Resources Conservation Service, Soil Survey Staff, Washington DC, pp. 326.

Sommella, P., (1998). 'Italia antica.' L'urbanistica romana, Rome.

Sorrentino, G., (2001).' Indagine regionale sulla stima dell'aggressività della pioggia nello studio dell'erosione idrica.' Thesis, Università degli Studi della Calabria, Facoltà di Ingegneria: Cosenza. (in Italian)

Sorriso-Valvo, M., Bryan, R.B., Yair, A., Iovino, F. and Antronico, L., (1995). 'Impact of afforestation on hydrological response and sediment production in a small Calabrian catchment.' Catena, 25, pp. 89-104.

Strabo, (63 BC – AD 21). 'The Geography.' Book number V. Online: http://penelope. uchicago.edu/Thayer/E/Roman/Texts/Strabo/5C*.html [accessed June 2009]

Stednick, J.D., (1996). 'Monitoring the effects of timber harvest on annual water yield.' Journal of Hydrology, 176, pp. 79.95.

Stefanini, G., (1921). 'Le balze di Volterra e le forme del suolo nei terreni pliocenici.' In: Marinelli O., Guida per l'escursione scientifica e storica dell'VIII Congresso Geografico Italiano.

Stock, J. and Montgomery, D.R., (1999). 'Geologic constraints on bedrock river incision using the stream power law.' Journal of Geophysical Research, 104, pp. 4983-4993.

Stoneman, G.L., (1993). 'Hydrological response to thinning a small jarrah (Eucalyptus marginata) forest catchment.' Journal of Hydrology, 150, pp. 393-407.

Stott, T. A., Ferguson, R. I., Johnson, R. C. and Newson, M. D. (1986). 'Sediment budgets in forested and unforested basins in upland Scotland.' In Drainage Basin Sediment Delivery (R. F. Hadley, ed.), International Association of Hydrological Sciences Publication, 159, pp. 57-68.

Stott, A., (1997). 'Comparison of stream bank erosion processes on forested and moorland streams in the Balquhidder catchments.' Earth Surface Processes and Landforms 22, pp. 383-400.

Stott, T., G., Leeks, S., Marks, and Sawyer, A., (2001). 'Environmentally Sensitive Plot-Scale Timber Harvesting: Impact on Suspended Sediment.' Bedload and Bank Erosion Dynamics. Journal of Environmental Management, 63, pp. 3-25.

Strahler, A.,N., (1957). 'Quantitative analysis of watershed geomorphology.' Trans Am Geophys Union, 38, pp. 913-920.

Strahler, A.N., (1964). 'Quantitative geomorphology of drainage basin and channel networks.' In Chow VT (ed) Handbook of applied hydrology. McGraw Hill Book Co.: New York, pp. 4-76

Stringer, L.C., (2008). 'Reviewing the International Year of Deserts and Desertification 2006: What contribution towards combating global desertification and implementing the United Nations Convention to Combat Desertification?' Journal of Arid Environments, 72, pp. 2065-207.

Strunk, H., (2003). 'Soil degradation and overland flow as causes of gully erosion on mountain pastures and in forests.' Catena, 50, pp. 185-198.

Susmel, L., (1968). 'Sull'azione regimante e antierosiva della foresta.' In Atti del Convegno "Le scienze della natura di fronte agli eventi idrogeologici.' Accademia dei Lincei, Rome, pp. 301-402. (in Italian)

Swanson, F.J., and Dyrness, C.T., (1975).' Impact of clear-cutting and road construction on soil erosion by landslides in the western Cascade Range, Oregon.' Geology, 3, pp. 393-396.

Swanston, D. N., (1991). 'Natural Processes.' In W. R. Meehan (ed.). Influences of Forest and Rangeland Management on Salmonid Fishes and Their Habitat: Special Publication 19, Bethesda, American Fisheries Society: Bethesda, pp. 139-180.

Symeonakis, E., (2001). 'Soil Erosion Modelling over Sub-Saharan Africa Using Remote Sensing and Geographical Information Systems.' PhD Dissertation Thesis, University of London: London.

'T'

Tague, C. and Band, L., (2001). 'Simulating the impact of road construction and forest harvesting on hydrological response.' Earth Surface Processes and Landforms, 26, pp.131-151.

Takei, A., Kobaski, S., and Fukushima, Y., (1981). 'Erosion and sediment transport measurement in a weathered granite mountain area.' In Erosion and Sediment Transport Measurement, Proceedings of the Florence Symposium, IAHS Publ. no. 133. pp. 493-502.

Tamburino, V., Barbagallo, S. and Vella, P. (1990). 'Evaluation of sediment deposition in Sicilian artificial reservoirs.' In Sinniger, R.O. and Monbaron, M., editors, Hydrology in mountainous regions II: artificial reservoirs, water and slopes, Lausanne: IAHS publication, 194, pp. 113-20.

Taylor, M.P., Macklinm, M.G., and Hudson-Edwards, K., (2000). 'River sedimentation and fluvial response to Holocene environmental change in the Yorkshire Ouse Basin, northern England.' The Holocene, 10, pp. 201-212.

Teklehaimanot, Z., Jarvis, P.G., Ledger, D.C., (1991). 'Rainfall interception and boundary layer conductance in relation to tree spacing.' Journal of Hydrology, 123, pp. 261-278.

Teklehaimanot, G., (2003). 'Use of simple field tests and revised MMF model for assessing soil erosion: case study Lom Kao Area, Thailand.' ITC-MSC Thesis.

Terranova, O., Antronico, L., Coscarelli, R., Iaquinta, P., (2009). 'Soil erosion risk scenarios in the Mediterranean environment using RUSLE and GIS: An application model for Calabria (southern Italy).' Geomorphology, 3-4, pp. 228-245.

Thiemann, S., (2006). 'Detection and assessment of erosion risk in the wareshed of Bilate river.' Southern Ethiopian Rift valley. Doctoral dissertation. Freie Universität Berlin.

Thornes, J.B., (1990). 'Vegetation and Erosion: Processes and Environments.' Wiley, Chichester: London.

Tokunaga, E., (1984). 'Ordering of divide segments and law of divide segments numbers.' Transactions. Japanese Geomorphological Union 5, pp. 71-77.

Tokunaga, E., (2000). 'Dimension of a channel network and space-filling properties of its basin.' Transactions, Japanese Geomorphological Union 21, pp. 431-499.

Tonelli, W., (2007). 'Stato vegetazionale dei bacini e protezione fornita dalla vegetazione.' In Piano di tutela delle acque. Regione Lazio. (in Italian)

Torri, D., and Poesen, J., (1992). 'The effect of soil surface slope on raindrop detachment.' Catena, 19, pp. 561-578.

Torri, D., and Bryan, R.B., (1997). 'Micropiping processes and biancane evolution in Southeast Tuscany, Italy.' Geomorphology, 20, pp. 219-235.

Torri, D., Pouse, J., and Borselli, L., (1997). 'Predictability and ucertainty of the erodibility factor using a global data set.' Catena, 31, pp. 1-22.

Toubert, P., (1993). 'Les structures du Latium medieval, I, II.' Rome.

'U'

UNFCCC, (1997). 'Kyoto Protocol to the United Nations Framework Convention on Climate Change.' UNFCC: Bonn.

UNCCD, (1994). 'United Nations Convention to Combat Desertification: The Convention. Part I. Introduction. Article 1. p5.' UN: Bonn.

UNFCD, (1996). 'United Nations framework convention to combat desertification'. Bonn, Germany.

UNCED, (1992). 'Agenda 21: programme of action for sustainable development, rio declaration on environment and development, statement of principles. Final text of agreement negotiated by governments at the United Nations Conference on Environment and Development (UNCED).' 3 – 14 June 1992, Rio de Janeiro, Brazil, UNDP: New York.

U.S Geological Survey, (2009). Omline source: http://www.usgs.gov/ [Accessed Febrary 2009].

USLE - Grimm, M., Jones, R.J.A. and Montanarella. L. (2002). 'Soil erosion risk assessment in Europe using USLE and a K-factor modified by susceptibility to surface crusting.' Technical Report, European Soil Bureau JRC: Ispra, pp.38.

USDA – Bennett, H.H. and Chapline, W.R., (1928). 'Soil erosion: a national menace.' U.S. Dept. of Agriculture Circular vol. 33, U.S. Government Printing Office: Washington.

USDA. (1975). 'Sediment sources, Yield, and Delivery Ratios.' National Engineering Handbook, Section 3 Sedimentation.

Soil Survey Division Staff, (1993). 'Soil survey manual.'. Soil Conservation Service, U.S. Department of Agriculture Handbook 18. Online: http://soils.usda.gov/technical/manual/

USDA, (2010). Online source: http://soils.usda.gov/technical/handbook/images/Part618 exhibit8_hi.jpg [Accessed June 2010].

'V'

Van der Knijff, J.M., Jones, R.J.A., Montanarella, L. (1999). 'Soil erosion risk assessment in Italy.' European Soil Bureau. EUR 19044 EN, pp. 52.

Van der Knijff, J.M., Jones, R.J.A., and Montanarella, L. (2002). 'Soil Erosion Risk Assessment in Italy.' In J.L. Rubio, R.P.C Morgan, S. Asins and V. Andreu (eds). Proceedings of the third International Congress Man and Soil at the Third Millennium. Geoforma Ediciones, Logrono. pp.1903-1913.

Van Dijk, A.I.J.M., Bruijnzeel, L.A., Rosewell, C.J., (2002).' Rainfall intensity–kinetic energy relationship: a critical literature appraisal.' Journal of Hydrology, 261, pp. 1-23.

Van Rompaey, A, Verstaeten, G., Van Oost, K., Govers G., and Poesen, J., (2001). 'Modelling mean annual sediment yield using a distributed approach.' Earth Surface Process Landforms, 26, pp. 1221-1236.

Van Rompaey, A.J.J., Bazzoffi, P., Jones, R.J.A, Montanarella, L., and Govers, G., (2003). 'Validation of Soil Erosion Risk Assessments in Italy. 'European Soil Bureau Research

Report No.12, EUR 20676 EN., Office for Official Publications of the European Communities: Luxembourg, pp. 25.

Van Rompaey, A.J.J., Krasa, J., Dostal, T. and Govers, G., (2003b). 'Modelling sediment supply to rivers and reservoirs in Eastern Europe during and after collectivization period.' Hydrobiologia, 494, pp. 169-176.

Van Rompaey, A.J.J., Bazzoffi, P., Jones, R.J.A. and Montanarella, L., 2005. 'Modelling sediment yields in Italian catchments'. Geomorphology, 65, pp.157-169.

Valentin, C., Rajot, J.L., and Mitja, D., (2004). 'Responses of soil crusting, runoff and erosion to fallowing in the sub-humid and semi-arid regions of West Africa, Agriculture.' Ecosystems and Environment, 104, pp. 287-302.

Vanoni, V.A., (1975). 'Sedimentation Engineering.' Manual and Report No. 54. American Society of Civil Engineers: New York.

Van Oost, G. Govers, O. Cerdan, D. Thauré, A. Van Rompaey, A. Steegen, J. Nachtergaele, I. Takken, J. Poesen, (2005). 'Spatially distributed data for erosion model calibration and validation: The Ganspoel and Kinderveld datasets.' CATENA, 61, pp. 105-121.

Verheijen, F.G.A., Jones, R.J.A., Rickson, R.J., Smith, C.J., (2009). 'Tolerable versus actual soil erosion rates in Europe.' Earth-Science Reviews, 94, pp. 23-38.

Verstraeten, G., and Poesen, J., (1999). 'The nature of small-scale flooding, muddy floods and retention pond sedimentation in central Belgium.' Geomorphology, 29, pp. 275-292

Vertessey, R.A., Watson, F.G.R., Rahman, J.M., Cuddy, S.D., Seaton, S.P., Chiew, F.H., Scanlon, P.J., Marston, F.M., Lymbuner, L., Jeanelle, S., Verbunt, M., (2001). 'New software to aid water quality management in the catchments and waterways of the south-east Queensland region.' In Proceedings of the Third Australian Stream Management Conference, August 27-29, pp. 611-616.

Viney, N.R., Sivapalan, M., (1999). 'A conceptual model of sediment transport: application to the Avon River Basin in Western Australia.' Hydrological Processes, 13, pp. 727-743.

Vittorini, V., (1977). 'Osservazioni sulle origini e sul ruolo di due forme di erosione nelle argille: calanchi e biancane.' Boll. Soc. Geogr. Ital., 6, pp. 25-54. (in Italian)

Viviroli and R. Weingartner, R., (2004). 'The hydrological significance of mountains: from regional to global scale.' Hydrology and Earth System Sciences **8**, pp. 1016-1029

Vrieling, A., (2006). 'Satellite remote sensing for water erosion assessment: A review.' CATENA, 65, pp. 2-18.

'W'

Walker, P.H., Kinnell, P.I.A., Green, P., (1978). 'Transport of a noncohesive sandy mixture in rainfall and runoff experiments.' Soil Sci. Soc. Am. J., 42, pp.793-801.

Wallace, J. S., (1997). 'Evaporation and radiation interception by neighbouring plants.' Quarterly Journal of the Royal Meteorological Society, 123, pp. 1885-1905.

Walling, D.E., (1983). 'The sediment delivery problem.' Journal of Hydrology, 65, pp.209-37.

Walling, D.E., and Quine, T.A., (1990). 'Calibration of caesium-137 measurements toprovide quantitative erosion rate data.' Land Degradation and Rehabilitation, 2,161-175.

Walling, D.E., Russel, M.A., Hodgkinson, R.A., Zhang, Y., (2002). 'Establishing sediment budgets for two small lowland agricultural catchments in the UK.' Catena, 47, pp. 323–353.

Walling, D.E., and Fang, D., (2003). 'Recent trends in the suspended sediment loads of the world's rivers.' Global and Planetary Change, 39, pp. 111-126.

Walter, M.T., Mehta, V.K., Marrone, A.M., Boll, J., Marchant, P.G., Steenhuis, T.S., and Walter, M.F., (2003). 'Simple estimation of prevalence of Hortonian flow in New York City watersheds.' J. Hydrol. Eng., 8, pp. 214-218.

Warren, S.D., Mitasova, H., Hohmann, M.G., Landsberger, S., Iskander F.Y., Ruzycki, T.S., and Senseman, G.M. (2005). 'Validation of a 3-D enhancement of the Universal Soil Loss Equation for prediction of soil erosion abd sediment deposition.' Catena, 64, pp. 281-296.

Wemple, B.C., Jones, J.A. and Grant, G.E., (1996). 'Channel network extension by logging roads in two basins, Western Cascades, Oregon.' Water Resources Research Bulletin, 32, pp. 1195-1207.

Wemple, B.C., Swanson, F.J. and Jones, J.A., (2001). 'Forest road and geomorphic process interactions, Cascade Range, Oregon.' Earth Surface Processes and Landforms, 26, pp. 191-204.

Wenner, C.G. , (1981). 'Soil Conservation in Kenya: Especially in Small-Scale Farming in High Potential Areas Using Labour Intensive Methods (rev. 7th ed.).' Ministry of Agriculture, Nairobi: 230 pp.

Verheijen, F.G.A., Jones, R.J.A., Rickson, R.J., and Smith, C.J. (2009). 'Tolerable versus actual soil erosion rates in Europe.' Earth-Science Reviews, 94, pp. 23-38.

Wicks, J. M. and Bathurst, J. C., (1996). 'SHESED: a physically based, distributed erosion and sediment yield component for the SHE hydrological modelling system.' J. Hydrol., 175, pp. 213-238.

Williams, J. R. (1975). 'Sediment-yield prediction with universal equation using runoff energy factor, in: Present and prospective technology for predicting sediment yield and sources,' ARS.S-40, U.S. Gov. Print. Office, Washington, pp. 244–252.

Williams, J.R., Jones, C.A., Dyke, P.T., (1984). 'A modelling approach to determining the relationship between erosion and soil productivity.' Transactions of the ASAE, 27, pp. 129-144.

Williams M., (2000). 'Dark ages and dark areas: global deforestation in the deep past.' Journal of Historical Geography, 26, pp. 28-46

Wischmeier, W.H., (1958). 'A rainfall erosion index for a universal soil-loss equation.' Soil Sci. Soc. Am. Proc., 23, pp. 246-249.

Wischmeier, W.H., Johnson, C.B., Cross, V. (1971). 'A soil erodibility nomograph for farmland and construction sites.' Journal of Soil and Water Conservation, 26, pp. 189-193.

Wischmeier , W.H., and Mannering, M., (1969). 'Relation of soil properties to its erodibility.' Soil Sci. Soc. Am. Proc., 33, pp. 131-137.

Wischmeier, W.H., and Smith, D.D., (1978). 'Predicting rainfall erosion losses.' Agriculture Handbook, n. 537, Agriculture Research Service, US Department of Agriculture: Washington, pp. 55.

'Y'

Young, R.A., Onstad, C.A., Bosch, D.D., Anderson, W.P., (1989). 'AGNPS: a nonpoint-source pollution model for evaluating agricultural watersheds.' Journal of Soil and Water Conservation, pp. 168-173.

Yu, B., Rose, C.W., Cielsiolka, C.A.A., Coughlan, K.J., Fentie, B., (1997). 'Towards a framework for runoff and soil loss prediction using GUEST technology'. Australian Journal of Soil Research, 35, pp. 1191-1212.

'Z'

Zamboni, M., (2007). 'Analisi dei processi di erosione delsuolo nel bacino del fiume Tusciano.' Thesis, Università degli studi di Napoli Federico II. Polo delle Scienze e delle Tecnologie C.I.R.A.M. Napoli, pp. 173. (in Italian)

Zanchi, C., (1993). 'Aspetti dell'erosione dei suoli nei ambienti del bacino del Mediterraneo, in montagna ed in collina'. Atti del Convegno La difesa del suolo in ambiente mediterraneo, Cala Gonone, 12-14 June 1991, ERSAT, Cagliari, pp. 57-69. (in Italian)

Zanchi, C., and Giordani, C., (1995). 'Elementi di conservazione del suolo.' Pàtron Editore: Bologna. (in Italian)

Zhang, R., (1997). 'Determination of soil sorptivity and hydraulic conductivity from the disk infiltrometer.' Soil Sci. Soc. Am. J., 61, pp. 1024-1030.

Zhou, P., Luukkanen, O., Tokola, T., and Nieminen. J., (2008). 'Effect of vegetation cover on soil erosion in a mountainous watershed.' Catena, 75, pp. 319-325.

Zolitschka, B., (1998). 'A 14,000year sediment yield record from western Germany based on annually laminated lake sediments.' Geomorphology, 22, pp. 1-17.

Chapter 11

APPENDICES

11. APPENDICES

APPENDIX A – Lithotypes present in the Turano watershed

Lithotypes characteristics:

Code	Lithotype	Surface [%]	Period
1	Alluvial deposits	5.8	Holocene
2	Scree	2.8	Holocene
3	Colluvial and eluvial deposits	2.9	Holocene
4	Landslide	0.6	Holocene
5	Fans	0.6	Holocene
6	Conglomerates	2.3	Pleistocene
7	Breccias	0.1	middle Pleistocene
8	Conglomerates	0.1	Late Pliocene
9	Conglomerates	0.02	middle Pleistocene
10	Vulcan ash	1.5	middle Pleistocene
11	Gray clay and sandy clay	2.3	Pleistocene
11.1	Silty clay	0.02	Pleistocene
12	Moraines	0.7	Pleistocene
13	Pelitic-arenaceous turbidites	1.3	Messinian
14	Arenaceous turbidites	4.4	Messinian
15	Turbidites predominantly arenaceous	15.7	Messinian
16	Breccias arenites	3	Tortonian–Messinian
17	Pelitic-arenaceous strata	1.5	Tortonian–Messinian
18	Alternations of clay and marl with thin layers of fine sandstones and siltstones	2.3	Serravallian–Messinian
19	Alternation of marl, limestone and marl clay	10.4	Bordigalian–Langhian
20	Briozoa and litotamni limestones	14.1	Langhian–Serravallian
21	Alternations of fine calcarenites and marls	0.9	Aquitanian–Burdigalian
22	Calcarenites	0.8	Rupelian–Aquitanian
23	Marl, marly limestone	1.3	Priabonian–Rupelian
24	Calciruditi brownish	1.5	Danian–Priabonian
25	Micritic limestones	0.4	Ypresian–Rupelian
26	Limestone and secondarily dolomitic limestone	10.5	Turonian–Campanian
27	White limestone	1.3	Campanian–Maastrichtian
28	Limestone and dolomitic limestone	0.1	Albian–Cenomanian
29	Limestone and dolomitic limestone	4.8	Aptian–Cenomanian
30	White limestone	3.3	Valamginian–Barremian
31	White limestone, sometimes dolomitic	2.6	Berriasian–Barremian
32	Calcilutitis	0.1	Aalenian–Bajocian
33	Calcilutitis	0.005	Pliensbachian–Toarcian
34	Crystalline dolomite	0.009	Sinemurian–Toarciano (?)

APPENDIX B – Geomorphological units

Turano geomorphological units:

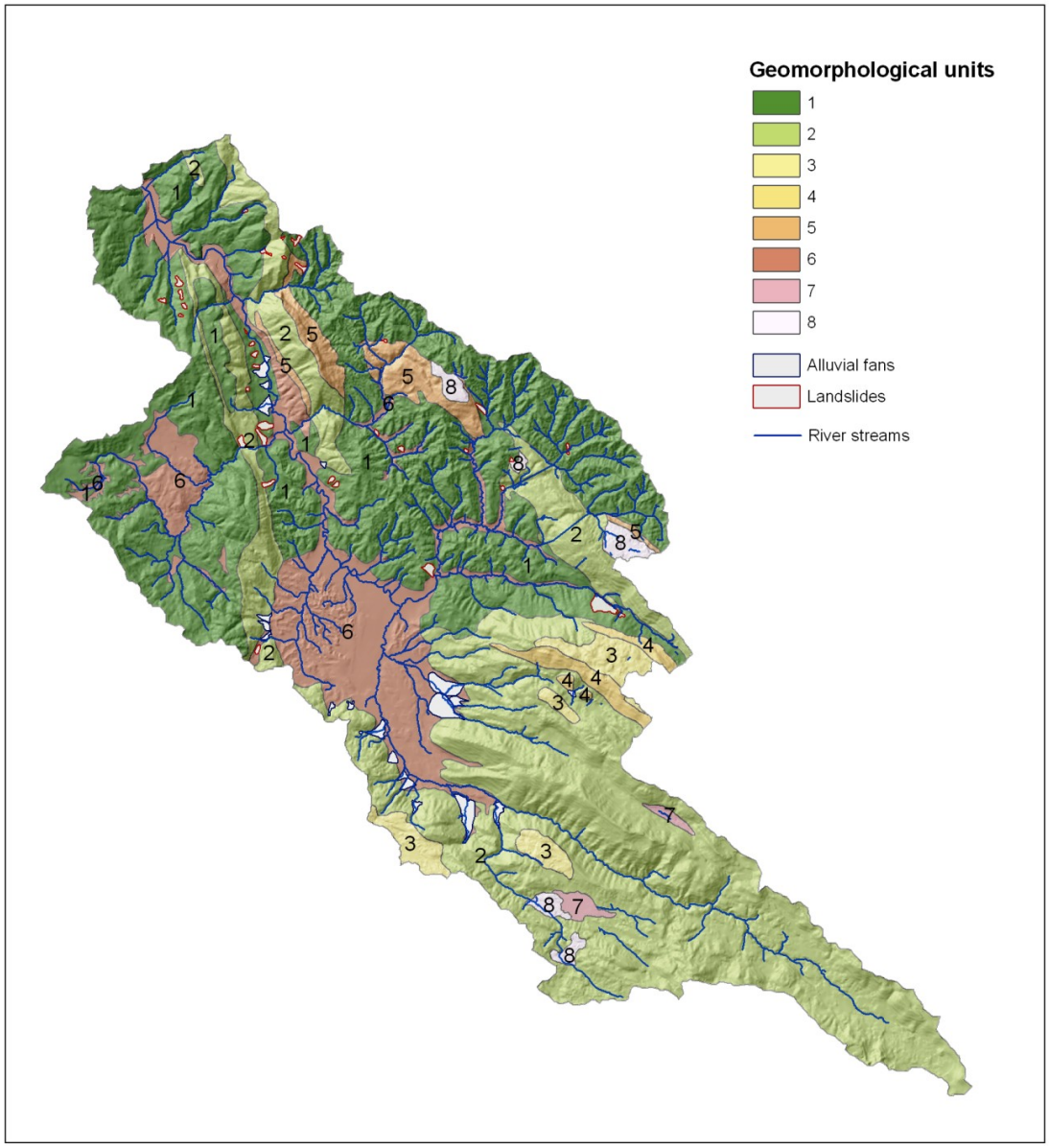

- (1) Areas lying on terrigenous rocks mainly shaped by fluvio-denudative processes and gravitative processes where the lithotypes are more argillaceous.
- (2) Carbonate slopes shaped by karst processes and fluvio-denudative processes with their respective deposits.
- (3) Carbonate highlands and paleo-surfaces primarily interested by karst processes.
- (4) Tectonic and denudate slopes (or fault slopes).
- (5) Tectonic gravitational slopes.
- (6) Deposits of intramontaneous basins or valley bottoms.
- (7) Doline karst system.
- (8) Structural surface interested by karst processes.

APPENDIX C – Regional climate

Characteristics of the central Italy meteorological station:

Stations	Elevation	Years	Rainfall
	[m a.s.l.]	[yrs]	[mean]
Ancona Falconara	10	30	777
Aquila	737	47	721.7
Ardea	37	45	859.3
Ascoli Piceno	166	30	1031
Bracciano	288	49	1034.2
camerino	664	30	1042
Campotosto	1430	46	1056.7
Castel del Monte	1300	47	885.5
Castel di Sangro	805	45	974.4
Civitavecchia	6	48	621.7
Colonna	350	30	983
Fabriano	357	30	1026
Fermo	280	30	1164
Ficulle	437	45	916.8
Filettino	1062	36	1542.0
Foligno	235	21	921.1
Fumone	780	30	942
Gaeta	50	30	678
Giuliano di Roma	363	27	1069.4
Guardiagrele	577	46	924.2
Isola Sacra	4	47	775.4
Ladispoli	5	45	744.1
Latina	12	49	900.3
Lenola	470	57	1096.4
Leonessa	974	49	1456.9
Licenza	478	49	1474.9
Macerata	342	30	789
Nereto	163	47	751.0
Norcia	604	32	864.0
Viterbo	327	48	795.2

Stations	Elevatio	Years	Rainfall
	[m a.s.l.]	[yrs]	[mean]
Ortona	68	47	705.4
Orvieto	315	47	770.7
Palena	767	48	995.6
Palmoli	650	45	729.7
Penne	438	48	850.4
Pereto	800	46	1034.3
Perugia	493	50	809.5
Pescara	5	47	694.3
Pescasseroli	1150	46	1550.5
Pescocostanzo	1395	43	961.8
Popoli	260	47	722.9
Posticciola	540	51	1026.0
Riano	102	41	1107.4
Rieti	402	40	1081.8
Rocca di	1329	46	1021.9
Roma Macao	55	52	808.5
Scanno	1030	46	1104.7
Scerni	287	57	625.9
Scurcola Mars	730	46	895.3
Sella di Corvo	990	41	1397.9
Spoleto	317	50	977.6
Subiaco	511	52	1212.8
Sutri	291	35	1071.3
Tarquinia	145	43	646.3
Teramo	300	48	785.5
Terracina	2	48	945.8
Todi	411	52	812.4
Tuscania	166	46	822.4
Velletri	352	42	1193.7
Viterbo	327	48	795.2

Annual average rainfall versus elevation:

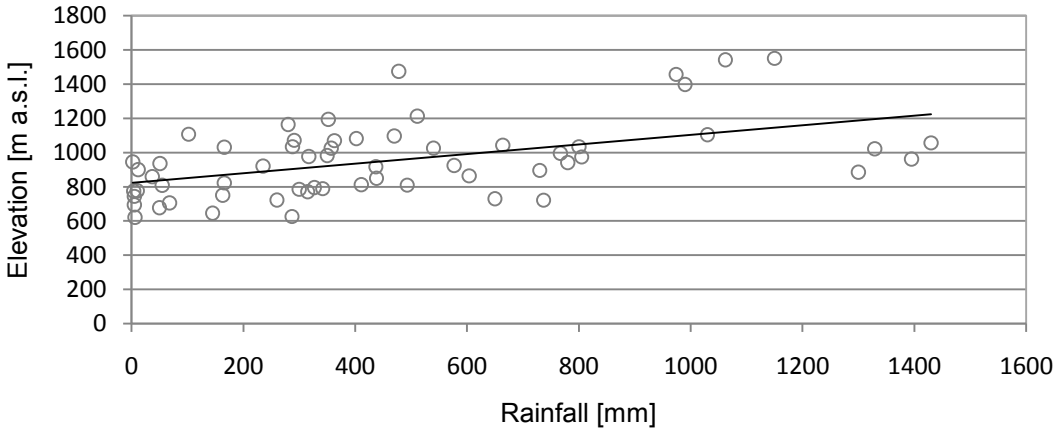

Spline interpolation of the annual rainfall values:

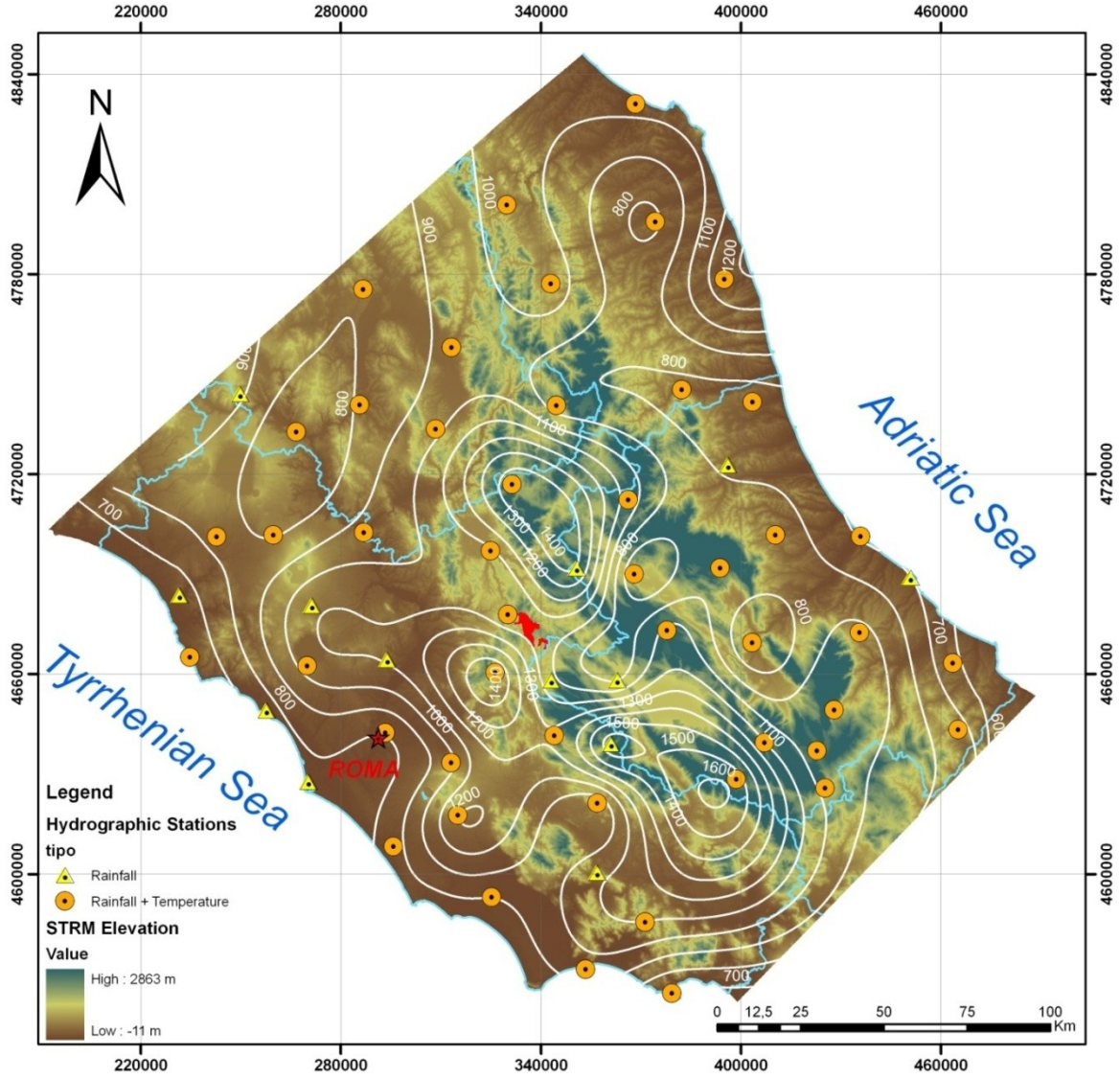

APPENDIX D – Analysis of the climate anomalies

Temperature

Posticciola meteorological station:

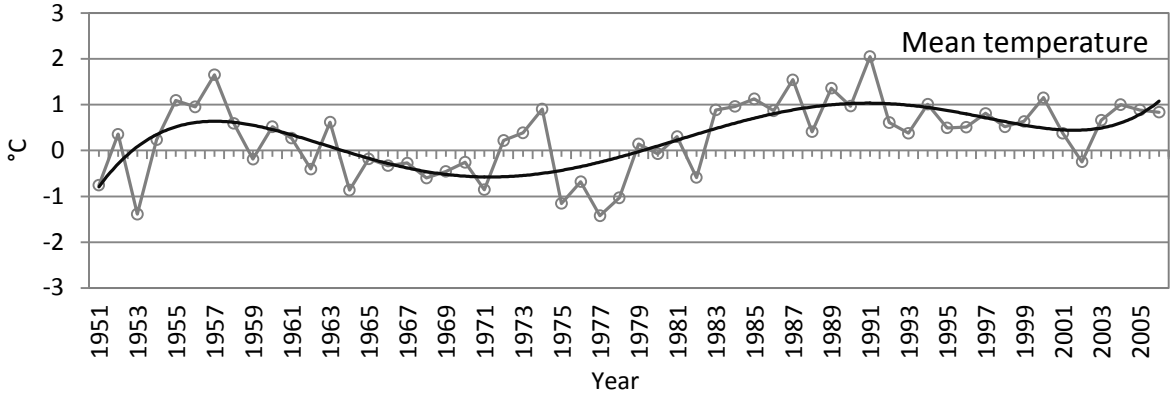

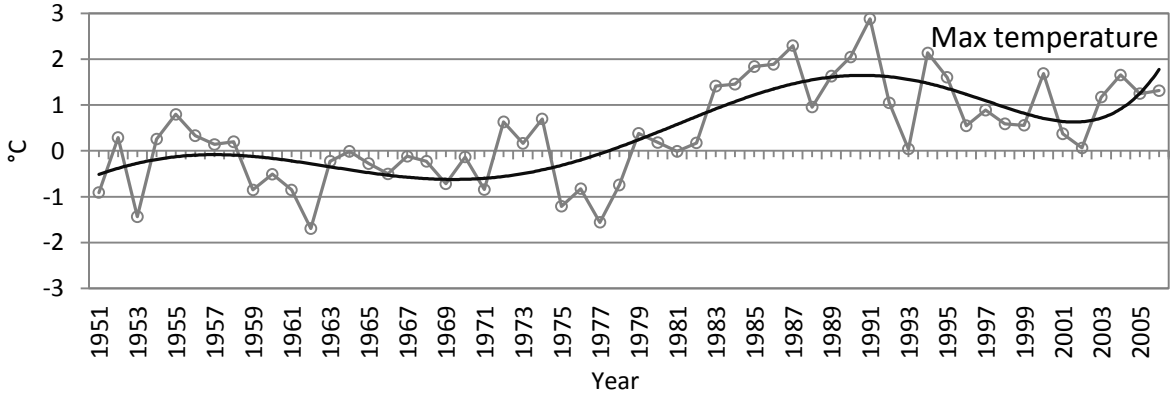

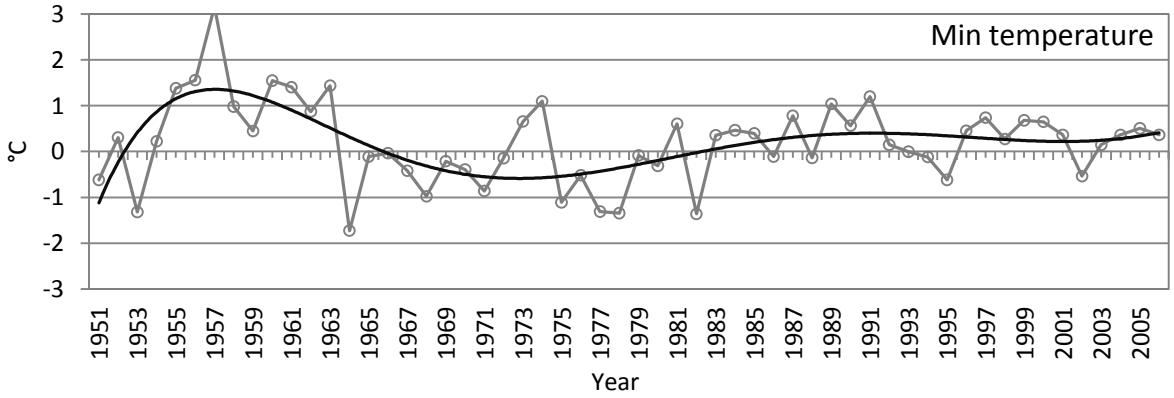

	T Mean	TMax	TMin
Annual	0.378 (α<0.01)	0.608 (α<0.01)	0.058 (α>0.05)
Winter	0.415 (α<0.01)	0.019 (α>0.05)	0.607 (α<0.01)
Spring	0.170 (α<0.01)	0.119 (α>0.05)	0.425 (α<0.01)
Summer	0.017 (α>0.05)	0.133 (α>0.05)	0.087 (α>0.05)
Autumn	0.279 (α>0.05)	-0.008 (α>0.05)	0.491 (α<0.01)

Linear correlation coefficient (R^2)

Subiaco meteorological station:

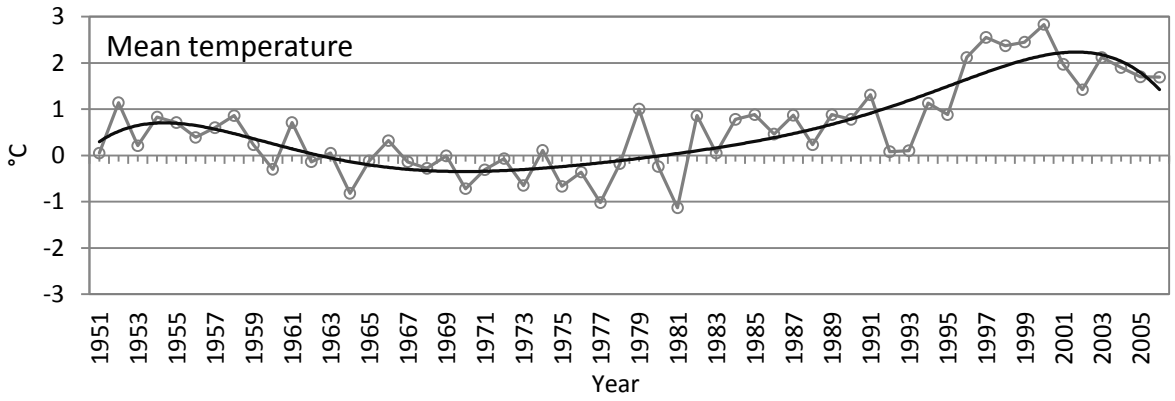

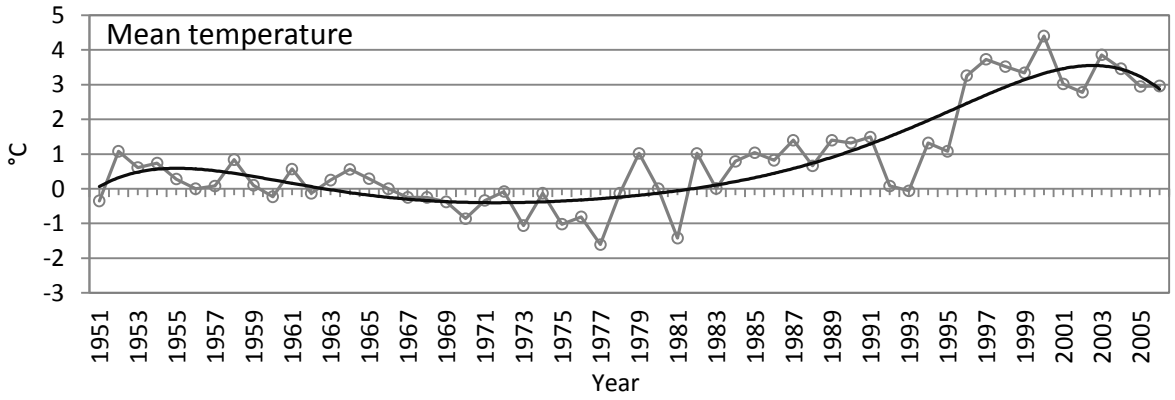

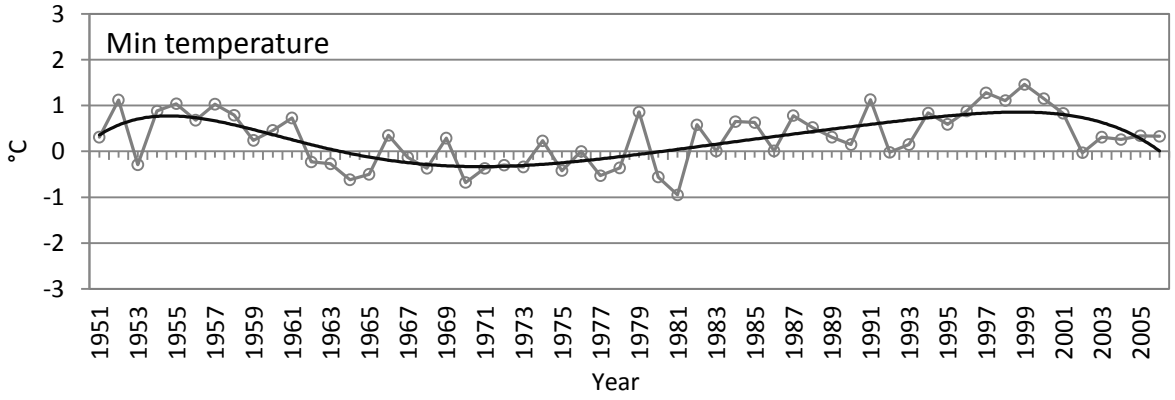

	T Mean	TMax	TMin
Annual	0.597 (α<0.01)	0.680 (α<0.01)	0.205 (α>0.05)
Winter	0.345 (α<0.05)	0.485 (α<0.01)	0.038 (α>0.05)
Spring	0.239 (α>0.05)	0.274 (α>0.05)	0.075 (α>0.05)
Summer	0.296 (α<0.05)	0.354 (α<0.05)	0.171 (α>0.05)
Autumn	0.424 (α<0.01)	0.550 (α<0.01)	0.207 (α>0.05)

Linear correlation coefficient (R^2)

Temperature range

Posticciola meteorological station:

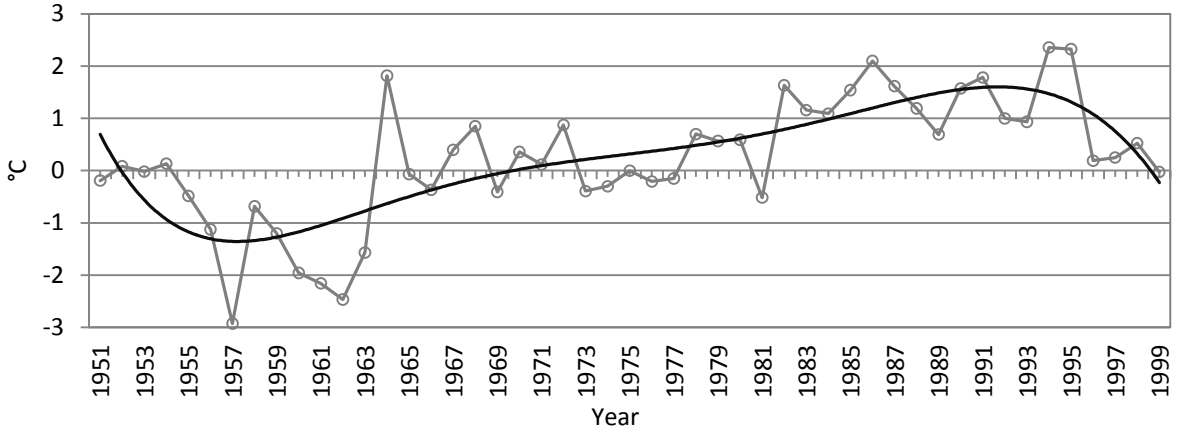

Subiaco meteorological station:

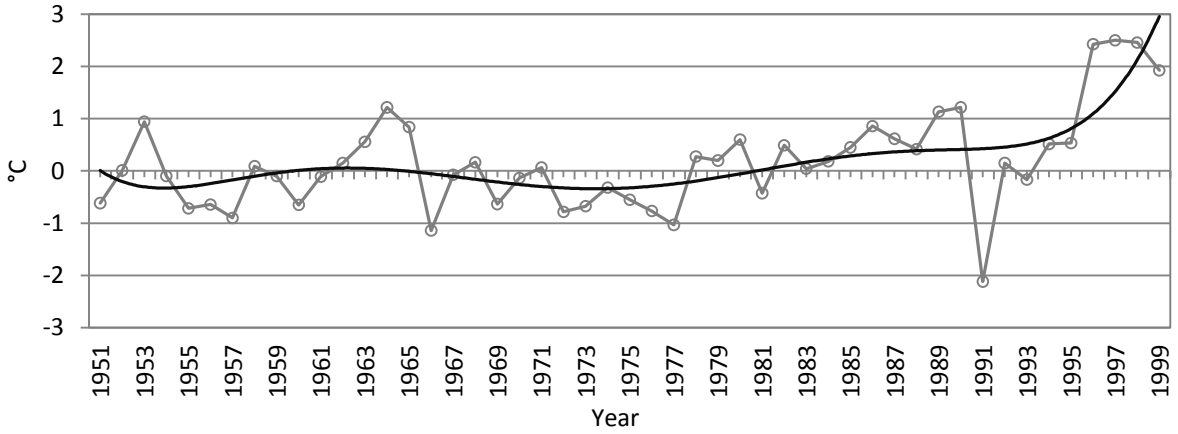

	Temperature range
Posticciola	0.626 (α<0.01)
Subiaco	0.467 (α<0.01)

Linear correlation coefficient (R^2)

Rainfall

Posticciola meteorological station:

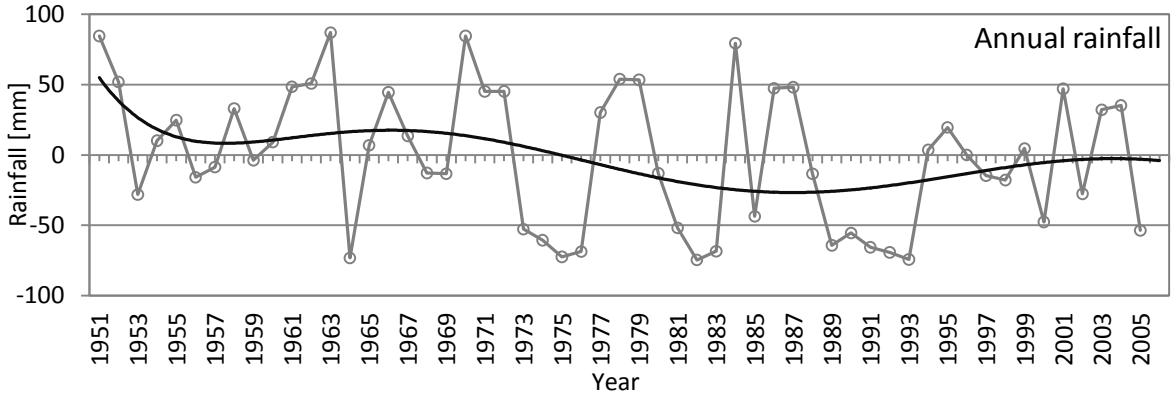

Subiaco meteorological station:

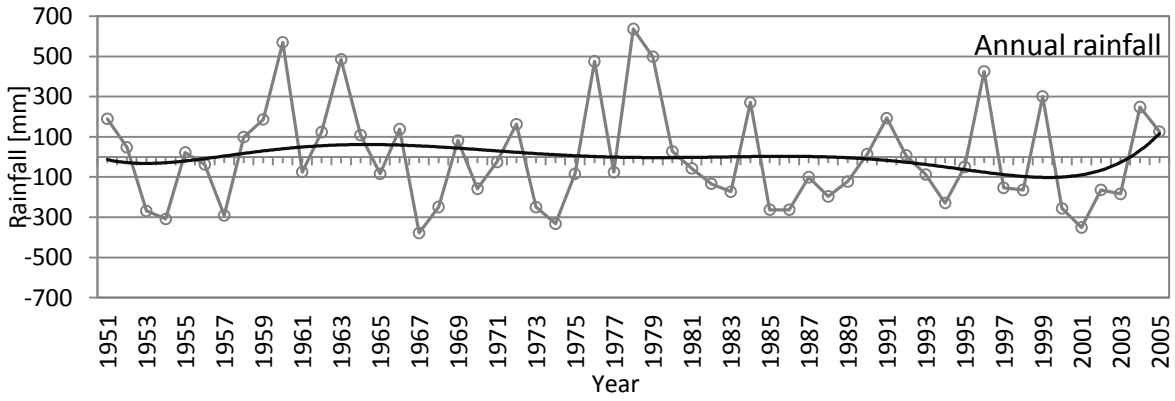

	Posticciola	Subiaco
Annual	-0.276 (α<0.05)	-0.0.86 (α>0.05)
Winter	-0.223 (α>0.05)	-0.204 (α>0.05)
Spring	-0.144 (α>0.05)	-0.056 (α>0.05)
Summer	0.023 (α>0.05)	-0.079 (α>0.05)
Autumn	0.168 (α>0.05)	0.158 (α>0.05)

Linear correlation coefficient (R^2)

Rainfall intensity

Posticciola meteorological station:

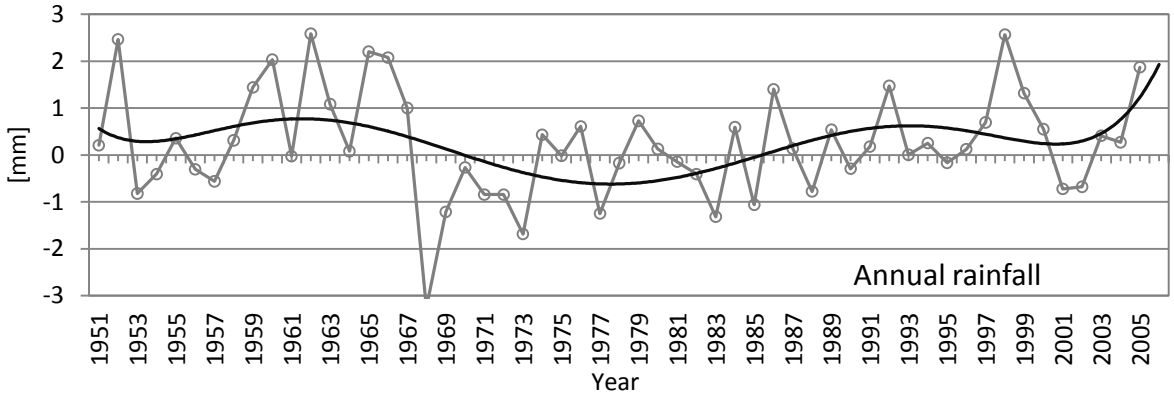

Subiaco meteorological station:

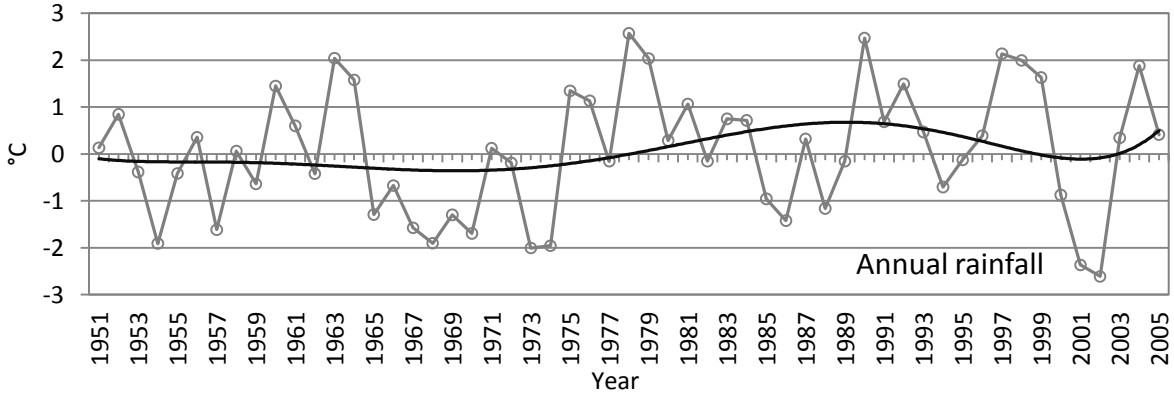

	Temperature range
Posticciola	0.002 (α>0.05)
Subiaco	0.160 (α>0.05)

Linear correlation coefficient (R^2)

APPENDIX E – C-FACTOR TEST

RUSLE C-factor estimation according to some methods present in literature:

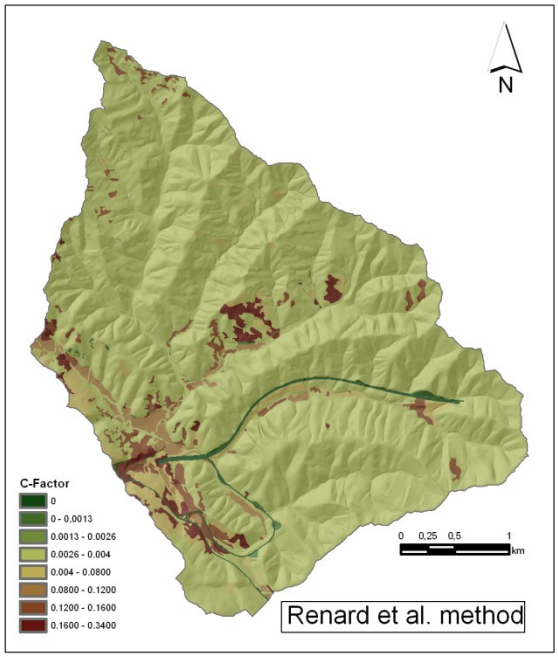

C-Factor characteristics

Average value: 0.0167 Min value: 0
St. Dev. value: 0.0570 Max value: 0.34

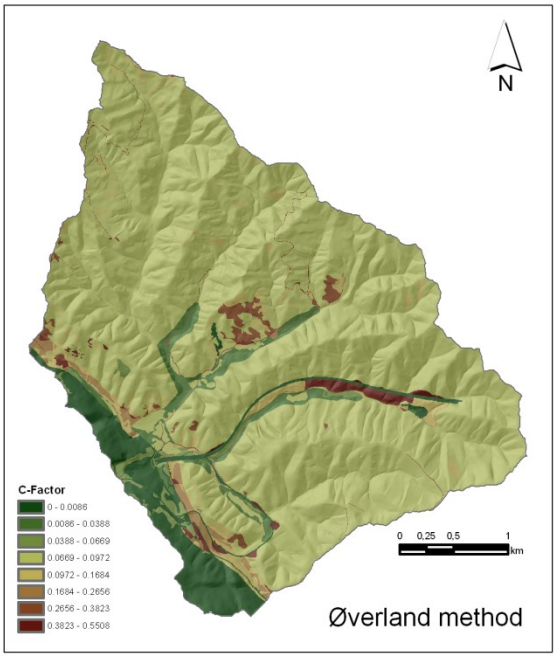

C-Factor characteristics

Average value: 0.0859 Min value: 0
St. Dev. value: 0.0629 Max value: 0.55

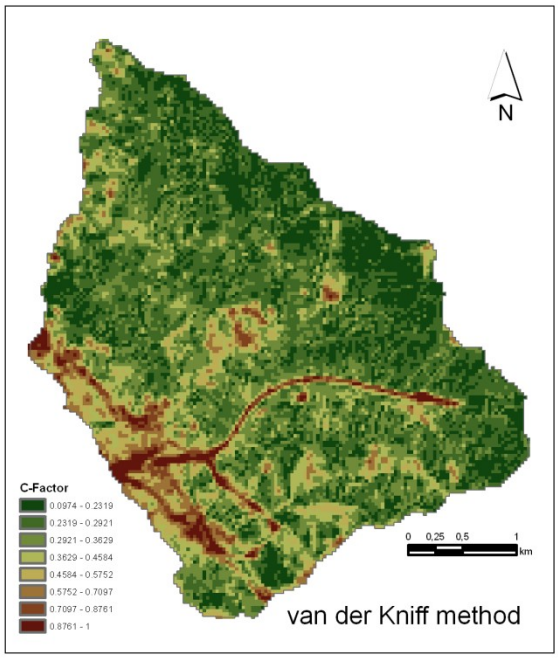

C-Factor characteristics

Average value: 0.3412 Min value: 0.0974
St. Dev. value: 0.1611 Max value: 1

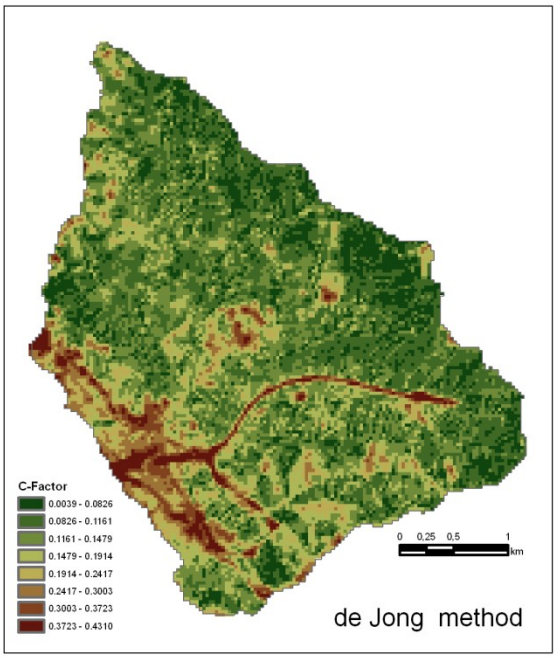

C-Factor characteristics

Average value: 0.1448 Min value: 0.0039
St. Dev. value: 0.0751 Max value: 0.43

RUSLE C-factor estimation according to the method shown in Fig.5.2 (Chapter 5.1.1.2.4)

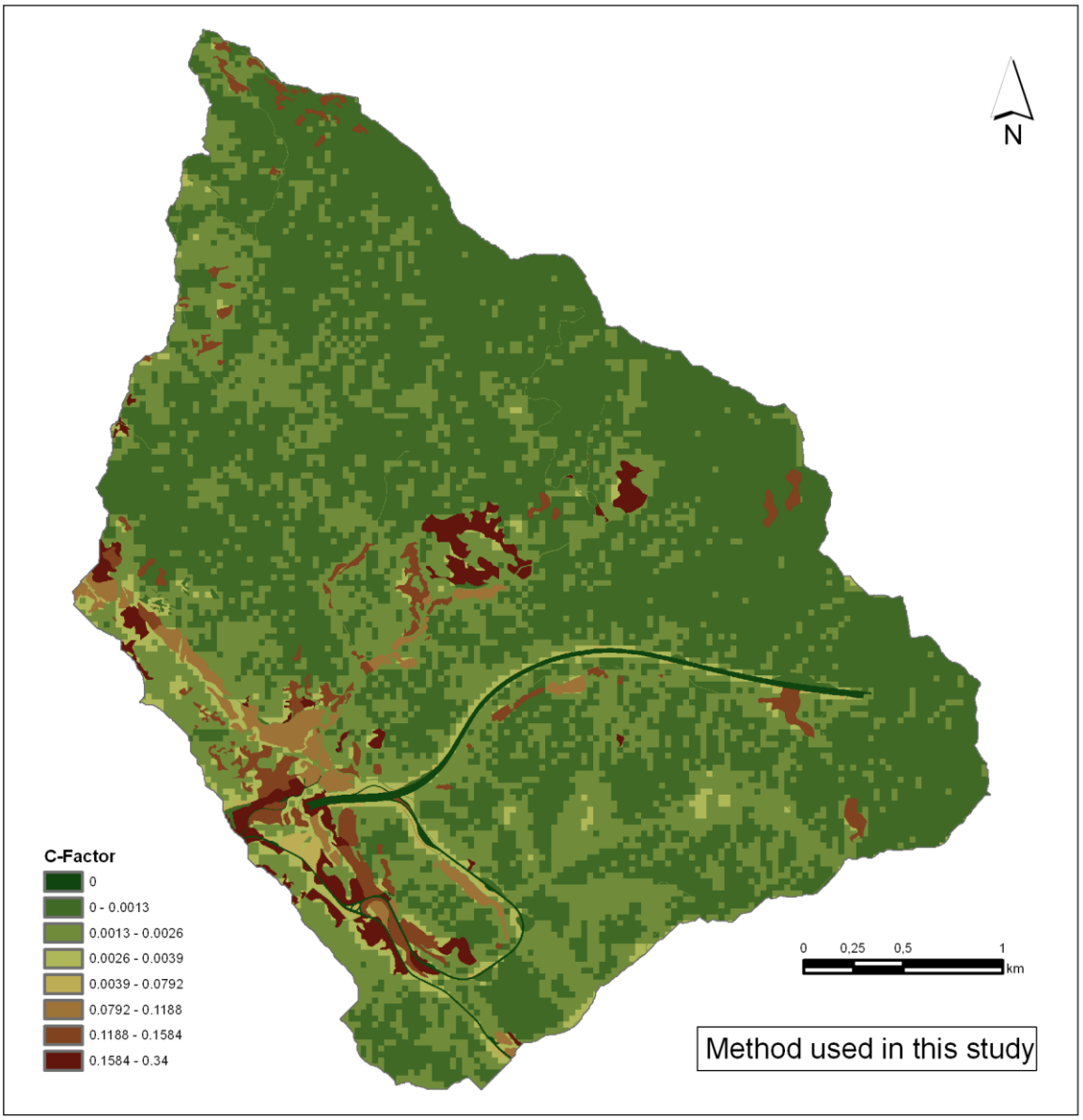

C-Factor characteristics

Average value: 0.0146 Min value: 0
St. Dev. value: 0.0570 Max value: 0.34

APPENDIX F – USPED scheme

ArcGis operations:

Step 1 – First input parameters: DEM, K, C

Step 2 - Calculate the first order derivatives from the DEM
- 2.1. Slope
- 2.2. Aspect

Step 3 - Calculate the second order derivatives from the DEM
- 3.1. FlowAcc

Step 4 – Building SFlowTopo layer with the Raster Calculator:
- 4.1. [FlowAcc] * resolution * **Sin**([Slope] * 0.01745) Prevailing inter-rill erosion

Step 5 - Building the qsx layer with the Raster Calculator:
- 5.1. [SFlowTopo] * [K] * [C] * [R] * **Cos**((([Aspect] * (-1)) + 450) * .01745)

Step 6 - Building the qsy layer with the Raster Calculator:
- 6.1. [SFlowTopo] * [K] * [C] * [R] * **Sin**((([Aspect] * (-1)) + 450) * .01745)

Step 7 – Calculate the first order derivatives from the Qsx
- 7.1. Qsx_Slope
- 7.2. Qsx_Aspect

Step 8 – Calculate the first order derivatives from the Qsy
- 8.1. Qsy_Slope
- 8.2. Qsy_Aspect

Step 9 - Building the qsx_dx layer with the Raster Calculator:
- 9.1. Cos((([qsx_aspect] * (-1)) + 450) * .01745) * Tan([qsx_slope] * .01745)

Step 10 - Building the qsy_dy layer with the Raster Calculator:
- 10.1. Sin((([qsy_aspect] * (-1)) + 450) * .01745) * Tan([qsy_slope] * .01745)

Step 11 – Building the erdep layer with the Raster Calculator:
- 11.1. ([qsx_dx] + [qsy_dy]) * 10 - For prevailing inter-rill erosion

The letters K, C, R refers to RUSLE K-factor, C-factor and R-factor, respectively.

APPENDIX G – Rainfall erosivity

Characteristics of the R-factor in the Turano watershed (values result from the predicted Rmonthly):

	Jan	Feb	Mar	Apr	May	Jun	Jul	Agu	Sep	Oct	Nov	Dec
	[MJ mm h⁻¹ ha⁻¹ month⁻¹]											
R-factor mean	77	92	99	147	205	127	106	138	330	344	161	117
R-factor max	125	136	134	180	232	185	218	199	399	417	250	165
R-factor min	44	53	78	117	174	100	72	50	245	289	116	67

Rainstorm erosivity values from 1998 to 2007 for Posticciola:

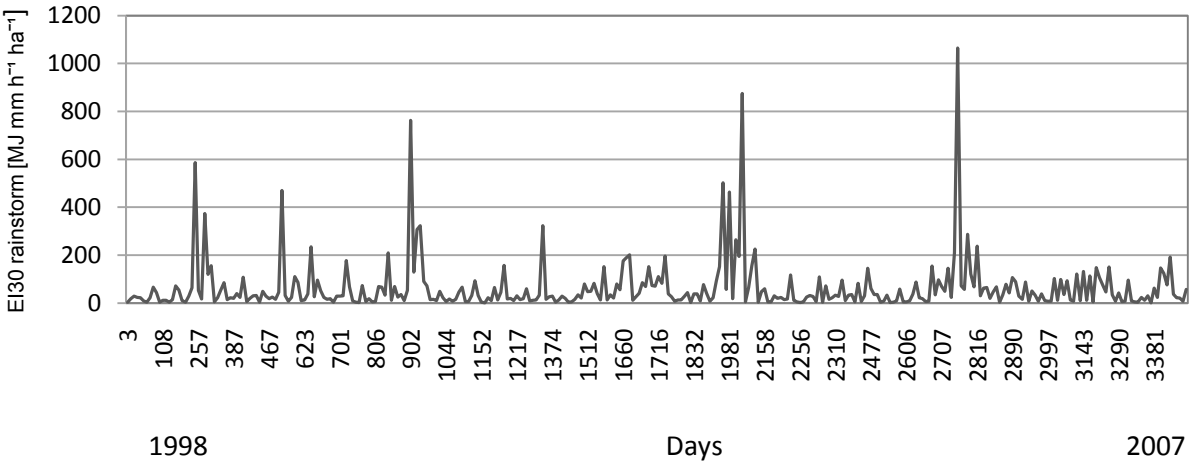

Annual distribution of average monthly rainfall and R-factor for Posticciola (1998-2007):

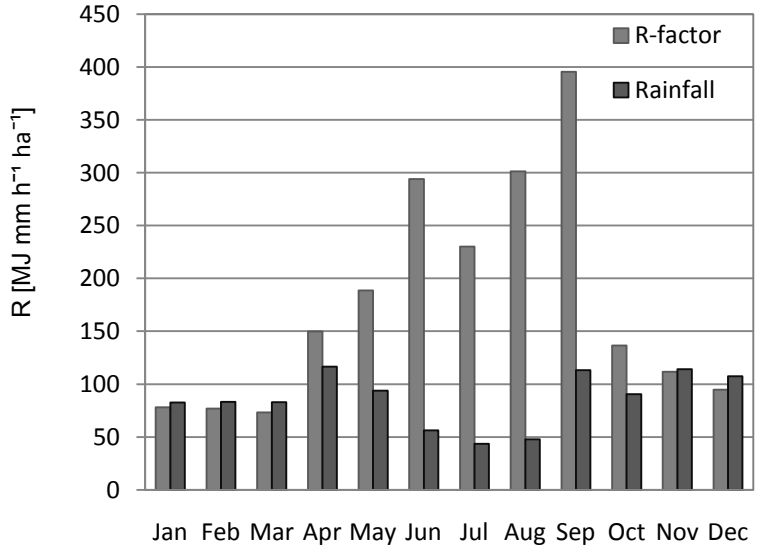

Measured and estimated rainfall erosivity for the Posticciola and Arsoli locations (the values shown in the table represent the total R-factor from October 1997 to September 2005 divided by seasons):

	Calibration data sets *(Posticciola)*		Validation dataset (Arsoli)	
	Rainstorm R	Estimated R	Rainstorm R	Estimated R
	[MJ mm h^{-1} ha^{-1}]	[MJ mm h^{-1} ha^{-1}]	[MJ mm h^{-1} ha^{-1}]	[MJ mm h^{-1} ha^{-1}]
Winter	2523.0	2524.5	1578.8	1212.1
Spring	2680.3	2678.3	1479.2	1061.7
Summer	3406.7	3692.8	1146.1	1389.1
Autumn	5830.7	5830.3	3158.2	2699.5

Comparison of the R-Factor results of the equations tested in Chapter 6:

Method	Annual
	[MJ mm h^{-1} ha^{-1} yr^{-1}]
Renard et al. (1997)	2663
Ruffino et al. (1993)	5712
Oliveira (1988)	985
Leprun (1981)	522
Lombardi et al. (1992)	6641
Renard e Freimund (1994)	4837
Ferrari et al. (2005) linear	4010
Ferrari et al. (2005) exponential	3788
Arnould (1980)	440
Arnoulds (1997)	428
Lo et al. (1985)	4541
Van der Knijff (1999)	1678

Appendix H – Measured and predicted Area-specific sediment yield (SSY in t ha^{-1} yr^{-1}) for 21 Italian drainage basins. (Van Rompaey et al. 2003):

Watershed	Measured SY	Predicted SY	Predicted Erosion	SDR
	[t ha^{-1} yr^{-1}]	[t ha^{-1} yr^{-1}]	[t ha^{-1} yr^{-1}]	[-]
Ancipa	5.6	7.8	54.3	0.14
Barcis	5.2	5.2	55	0.09
Castello	3.7	6.5	18.4	0.35
Cignana	0	5.8	8.5	0.68
Desueri	16.8	9.8	37.2	0.26
Flumendosa	0.9	2.8	44.8	0.06
Gammauta	1.6	3	16.7	0.18
Lavagnina	4.1	9.6	111.1	0.09
Letino	0.5	4.3	38.2	0.11
Mignano	12.8	20.6	108.8	0.19
Mulargia	10.3	6.4	20.9	0.31
Placemoulin	2.3	4.8	12.1	0.4
Ponte Fontanella	6.7	9	33.5	0.27
Pozzillo	19.6	19.2	144.5	0.13
Prizzi	5.7	4.7	32.6	0.14
Rochemolles	0.1	3.1	13.6	0.23
Santa Luce	9.2	10.7	44.1	0.24
Scalere	0.9	7.3	73	0.1
Scandarella	4.9	7.8	37.9	0.21
Serra di Corvo	1.9	4	15.4	0.26
Suviana	3.8	4	49.4	0.08
Torre Crosis	1.2	5.5	66.6	0.08

APPENDIX I – Soil surface change measured by the metallic stakes:

Prifile 1	Jan 2009	apr-09	Jul 2009	Jan 2010
	[cm]	[cm]	[cm]	[cm]
P-1/1	4.5	4.3	4.7	7
P-1/2	-1.5	-1.7	-1.8	-2.1
P-1/3	-1.3	-1.5	-1.6	-2.5
P-1/4	1.4	1.4	1.4	3
P-1/5	-0.5	-0.6	-0.5	-1.5
P-1/6	-1.1	-0.9	-0.9	-0.7
P-1/7	-0.3	-0.7	-0.8	-0.7
P-1/8	3	3.2	3.5	2.9
P-1/9	-1.4	-1.2	-0.9	0.7
P-1/10	-0.5	-0.4	-0.5	-0.9
P-1/11	2.3	2.4	2.2	1.7
P-1/12	-3.6	-5	-5.6	-7.1
P-1/13	-0.9	-0.4	-0.5	-0.8
P-1/14	-1.5	-1.6	-1.7	-1.8
P-1/15	-1.3	-1.5	-1.5	-1.8

Profile 2	Jan 2009	apr-09	Jul 2009	Jan 2010
	[cm]	[cm]	[cm]	[cm]
P-2/1	-0.9	-1.3	-1.4	-1.9
P-2/2	-0.8	-0.4	-0.4	-0.5
P-2/3	-0.4	-0.5	-0.6	-0.8
P-2/4	-1.6	-1.7	-1.9	-2.1
P-2/5	-0.5	-0.7	-0.5	-0.4
P-2/6	-1.7	-1.7	-1.8	-1.9
P-2/7	-	-0.4	-0.5	-0.9
P-2/8	-	-0.2	-0.3	-1.1
P-2/9	-2.5	-2.3	-2	-3
P-2/10	-3.1	-3	-3	-2.7
P-2/11	0.7	0.9	1	1.7

V-shaped	Jan 2009	apr-09	Jul 2009	Jan 2010
	[cm]	[cm]	[cm]	[cm]
PV-1	0.5	0.4	0.5	0.3
PV-2	0.8	0.8	0.9	0.7
PV-3	0.7	1.1	1.1	1
PV-4	-0.6	-0.2	-0.2	-0.2
PV-5	1.1	1	1.1	0.7
PV-6	-0.4	0.5	0.6	0.8
PV-7	0.2	0.3	0.3	0.2
PV-8	1.4	2.1	2	2.3

Plot-1	Jan 2009	apr-09	Jul 2009	Jan 2010
	[cm]	[cm]	[cm]	[cm]
Plot-1/1	-2.5	4	4.1	4.7
Plot-1/2	-0.5	-	-	
Plot-1/3	-0.4	-0.8	-1	-1.1
Plot-1/4	0	-0.2	-0.3	-0.5
Plot-1/5	-0.2	-0.3	-0.3	-0.5
Plot-1/6	0.4	-2	-1.5	-1.9
Plot-1/7	0.3	2	2.1	-2.3
Plot-1/8	-2	-1.9	-1.8	-1.9
Plot-1/9	-0.6	-0.8	-0.9	-1
Plot-1/10	0	-0.9	-1.1	-2
Plot-1/11	-0.2	-0.5	-0.5	-0.7
Plot-1/12	-0.2	0	0	0.1
Plot-1/13	-4.8	-4.2	-4	-3.3
Plot-1/14	0.2	0.6	0.5	0.6
Plot-1/15	-3.8	-5	-4	-4
Plot-1/16	-1.8	-2.4	-2.5	-3
Plot-1/17	-2.4	-2.4	-2.4	-2.2
Plot-1/18	0	0	-0.2	-0.5
Plot-1/19	8	7.3	7.1	4.9
Plot-1/20	-6	-6.2	-6	-6
Plot-1/21	-1.5	-2.1	-1.7	-1.3
Plot-1/22	-5.5	-5	-4.5	-4.3
Plot-1/23	3	3.1	3	3.3
Plot-1/24	-0.4	-0.4	-0.4	-0.8
Plot-1/25	0	-0.1	-0.1	-0.3
Plot-1/26	0.5	0.8	3	3.5

Free-stak.	Jan 2009	apr-09	Jul 2009	Jan 2010
	[cm]	[cm]	[cm]	[cm]
Free-1	-0.3	-0.4	-0.5	-0.8
Free-2	-2	-2	-2.5	-2.4
Free-3	-0.2	-0.3	-0.3	-0.3
Free-4	-1.6	-1.5	-1.4	-1.7
Free-5	0.2	0.2	0.3	0.2
Free-6	-0.3	0.9	1	1.4
Free-7	-0.4	-0.6	-0.5	-0.8
Free-8	0.1	0.2	0.2	0.5
Free-9	-1.4	-1.7	-1.8	-1.5
Free-10	0.5	-0.4	-0.5	-0.9

Plot-2	Jan 2009	apr-09	Jul 2009	Jan 2010
	[cm]	[cm]	[cm]	[cm]
Plot-2/1	0.2	0.2	0.2	0.2
Plot-2/2	0	-0.1	-0.1	-0.3
Plot-2/3	0.1	0.1	0	0
Plot-2/4	-0.1	-0.1	-0.1	-0.3
Plot-2/5	-0.1	-0.1	-0.1	-0.2
Plot-2/6	0.3	0.3	0.3	0.2
Plot-2/7	0	0	0	0.1
Plot-2/8	-0.2	-0.3	-0.3	-0.5
Plot-2/9	0	0.1	0	0
Plot-2/10	0.5	0.4	0.4	0.3
Plot-2/11	0	0	0.1	0.1
Plot-2/12	-0.1	-0.2	-0.2	0.2
Plot-2/13	-0.2	-0.1	-0.2	-0.3
Plot-2/14	-0.1	0	0	0.1
Plot-2/15	0.1	0.1	0.1	0

APPENDIX J – Calibrated date

Core PS-04

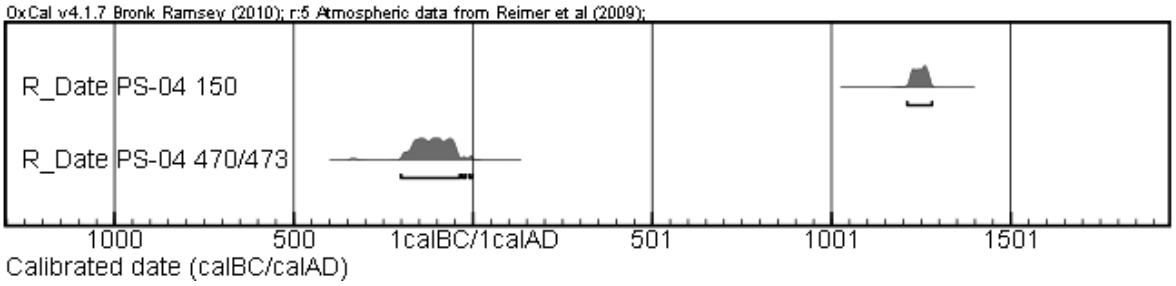

Core PS-01

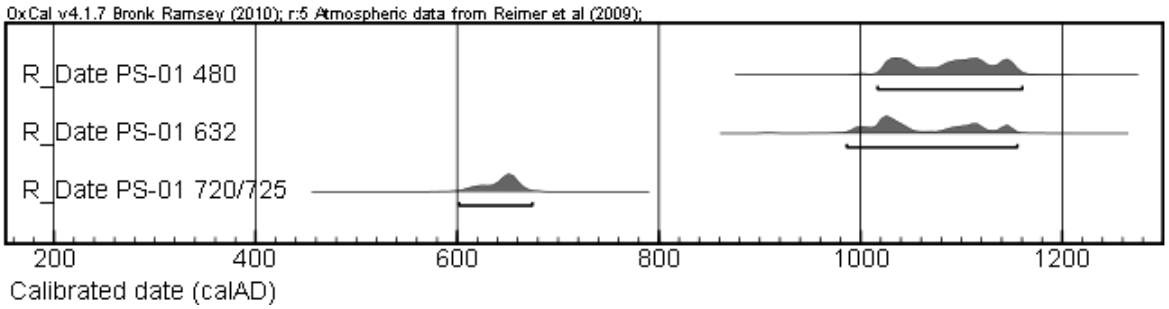

Core PS-11

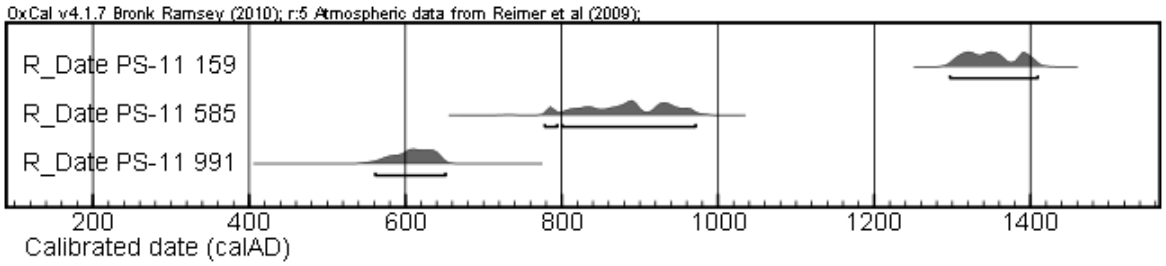

APPENDIX K – Soil erosion risk classes and geomorphometric characteristics of the Turano sub-watersheds.

APPENDIX L – Average annual soil loss maps (RUSLE and USPED models, period 1997-2005)

See the CD attached.

ERKLÄRUNG

Hiermit erkläre ich, dass ich die Dissertation ‘Risk Assessment of Human-induced Accelerated Soil Erosion Processes in the Intermountain Watersheds of Central Italy. A Case Study of the Upper Turano Watershed (Latium-Abruzzi)’ selbständig angefertigt und keine anderen als die von mir angegebenen Quellen und Hilfsmittel verwendet habe.

Ich erkläre weiterhin, dass die Dissertation bisher nicht in dieser oder anderer Form in einem anderen Prüfungsverfahren vorgelegen hat.

Berlin, 6 Juni 2011.

_____

(Pasquale Borrelli)